USGS
science for a changing world

Prepared in cooperation with Juab, Millard, Salt Lake, Tooele, and Utah Counties

Hydrology and Numerical Simulation of Groundwater Movement and Heat Transport in Snake Valley and Surrounding Areas, Juab, Millard, and Beaver Counties, Utah, and White Pine and Lincoln Counties, Nevada

Scientific Investigations Report 2014–5103

U.S. Department of the Interior
U.S. Geological Survey

Cover photograph: Looking west towards Wheeler Peak, Great Basin National Park, May 2010. Photograph by Melissa Masbruch, U.S. Geological Survey.

Hydrology and Numerical Simulation of Groundwater Movement and Heat Transport in Snake Valley and Surrounding Areas, Juab, Millard, and Beaver Counties, Utah, and White Pine and Lincoln Counties, Nevada

By Melissa D. Masbruch, Philip M. Gardner, and Lynette E. Brooks

Prepared in cooperation with Juab, Millard, Salt Lake, Tooele, and Utah Counties

Scientific Investigations Report 2014–5103

U.S. Department of the Interior
U.S. Geological Survey

U.S. Department of the Interior
SALLY JEWELL, Secretary

U.S. Geological Survey
Suzette M. Kimball, Acting Director

U.S. Geological Survey, Reston, Virginia: 2014

Suggested citation:
Masbruch, M.D., Gardner, P.M., and Brooks, L.E., 2014, Hydrology and numerical simulation of groundwater movement and heat transport in Snake Valley and surrounding areas, Juab, Millard, and Beaver Counties, Utah, and White Pine and Lincoln Counties, Nevada: U.S. Geological Survey Scientific Investigations Report 2014-5103, 108 p. *http://dx.doi.org/10.3133/sir20145103*.

ISSN 2328-0328 (online)

Contents

Figures

Tables

Conversion Factors and Datums

Inch/Pound to SI

Multiply	By	To obtain
	Length	
inch (in)	25.4	millimeter (mm)
foot (ft)	0.3048	meter (m)
mile (mi)	1.609	kilometer (km)
	Area	
acre	0.004047	square kilometer (km^2)
square mile (mi^2)	2.590	square kilometer (km^2)
	Volume	
cubic foot (ft^3)	0.02832	cubic meter (m^3)
acre-foot (acre-ft)	1,233	cubic meter (m^3)
	Flow rate	
acre-foot per year (acre-ft/yr)	1,233	cubic meter per year (m^3/yr)
foot per second (ft/s)	0.3048	meter per second (m/s)
foot per day (ft/d)	0.3048	meter per day (m/d)
foot per year (ft/yr)	0.3048	meter per year (m/yr)
cubic foot per second (ft^3/s)	0.02832	cubic meter per second (m^3/s)
cubic foot per day (ft^3/d)	0.02832	cubic meter per day (m^3/d)
inch per day (in/d)	25.4	millimeter per day (mm/d)
	Mass	
pound, avoirdupois (lb)	0.4536	kilogram (kg)
	Density	
pound per cubic foot (lb/ft^3)	16.02	kilogram per cubic meter (kg/m^3)
	Energy	
kilowatthour (kWh)	3,600,000	joule (J)
	Hydraulic conductivity	
foot per day (ft/d)	0.3048	meter per day (m/d)

SI to Inch/Pound

Multiply	By	To obtain
	Length	
millimeter (mm)	0.03937	inch (in)
meter (m)	3.281	foot (ft)
kilometer (km)	0.6214	mile (mi)
	Area	
square kilometer (km^2)	247.1	acre
square kilometer (km^2)	0.3861	square mile (mi^2)
	Volume	
cubic meter (m^3)	35.31	cubic foot (ft^3)
cubic meter (m^3)	0.0008107	acre-foot (acre-ft)
	Flow rate	
cubic meter per year (m^3/yr)	0.000811	acre-foot per year (acre-ft/yr)
meter per second (m/s)	3.281	foot per second (ft/s)
meter per day (m/d)	3.281	foot per day (ft/d)
meter per year (m/yr)	3.281	foot per year (ft/yr)
cubic meter per second (m^3/s)	35.31	cubic foot per second (ft^3/s)
cubic meter per day (m^3/d)	35.31	cubic foot per day (ft^3/d)
millimeter per day (mm/d)	0.03937	inch per day (in/d)
	Mass	
kilogram (kg)	2.205	pound avoirdupois (lb)

Multiply	By	To obtain
	Density	
kilogram per cubic meter (kg/m^3)	0.06242	pound per cubic foot (lb/ft^3)
	Energy	
joule (J)	0.0000002	kilowatthour (kWh)
	Hydraulic conductivity	
meter per day (m/d)	3.281	foot per day (ft/d)

Temperature in degrees Celsius (°C), degrees Fahrenheit (°F), and Kelvin (K) may be converted using the following equations:

Temp °F=(1.8 temp °C)+32

Temp °C=(temp °F-32)/1.8

Temp °F=(1.8 temp K)-459.67

Temp °C=temp K-273.15

A watt (W) is a unit of power and is equal to 1 Joule per second (J/s).

A joule (J) is a unit of energy and is equal to 1 kilogram·meters squared/seconds squared (kg·m^2/s^2).

Temperature gradients are reported in change in temperature, in degrees Celsius, per kilometer of depth (°C/km).

Heat flow is reported as the number of milliwatts (mW) per square meter (mW/m^2).

Vertical coordinate information is referenced to the National Geodetic Vertical Datum of 1929 (NGVD 29).

Horizontal coordinate information is referenced to the North American Datum of 1983 (NAD 83).

Altitude, as used in this report, refers to distance above the vertical datum.

*Transmissivity: The standard unit for transmissivity is cubic foot per day per square foot times foot of aquifer thickness [(ft^3/d)/ft^2]ft or [(m^3/d)/m^2]m. In this report, the mathematically reduced form, foot squared per day (ft^2/d) or meters squared per day (m^2/d), is used for convenience.

Hydrology and Numerical Simulation of Groundwater Movement and Heat Transport in Snake Valley and Surrounding Areas, Juab, Millard, and Beaver Counties, Utah, and White Pine and Lincoln Counties, Nevada

By Melissa D. Masbruch, Philip M. Gardner, and Lynette E. Brooks

Abstract

Snake Valley and surrounding areas, along the Utah-Nevada state border, are part of the Great Basin carbonate and alluvial aquifer system. The groundwater system in the study area consists of water in unconsolidated deposits in basins and water in consolidated rock underlying the basins and in the adjacent mountain blocks. Most recharge occurs from precipitation on the mountain blocks and most discharge occurs from the lower altitude basin-fill deposits mainly as evapotranspiration, springflow, and well withdrawals.

The Snake Valley area regional groundwater system was simulated using a three-dimensional model incorporating both groundwater flow and heat transport. The model was constructed with MODFLOW-2000, a version of the U.S. Geological Survey's groundwater flow model, and MT3DMS, a transport model that simulates advection, dispersion, and chemical reactions of solutes or heat in groundwater systems. Observations of groundwater discharge by evapotranspiration, springflow, mountain stream base flow, and well withdrawals; groundwater-level altitudes; and groundwater temperatures were used to calibrate the model. Parameter values estimated by regression analyses were reasonable and within the range of expected values.

This study represents one of the first regional modeling efforts to include calibration to groundwater temperature data. The inclusion of temperature observations reduced parameter uncertainty, in some cases quite significantly, over using just water-level altitude and discharge observations. Of the 39 parameters used to simulate horizontal hydraulic conductivity, uncertainty on 11 of these parameters was reduced to one order of magnitude or less. Other significant reductions in parameter uncertainty occurred in parameters representing the vertical anisotropy ratio, drain and river conductance, recharge rates, and well withdrawal rates.

The model provides a good representation of the groundwater system. Simulated water-level altitudes range over almost 2,000 meters (m); 98 percent of the simulated values of water-level altitudes in wells are within 30 m of observed water-level altitudes, and 58 percent of them are within 12 m. Nineteen of 20 simulated discharges are within 30 percent of observed discharge. Eighty-one percent of the simulated values of groundwater temperatures in wells are within 2 degrees Celsius (°C) of the observed values, and 55 percent of them are within 0.75 °C. The numerical model represents a more robust quantification of groundwater budget components than previous studies because the model integrates all components of the groundwater budget. The model also incorporates new data including (1) a detailed hydrogeologic framework, and (2) more observations, including several new water-level altitudes throughout the study area, several new measurements of spring discharge within Snake Valley which had not previously been monitored, and groundwater temperature data. Uncertainty in the estimates of subsurface flow are less than those of previous studies because the model balanced recharge and discharge across the entire simulated area, not just in each hydrographic area, and because of the large dataset of observations (water-level altitudes, discharge, and temperatures) used to calibrate the model and the resulting transmissivity distribution.

Groundwater recharge from precipitation and unconsumed irrigation in Snake Valley is 160,000 acre-feet per year (acre-ft/yr), which is within the range of previous estimates. Subsurface inflow from southern Spring Valley to southern Snake Valley is 13,000 acre-ft/yr and is within the range of previous estimates; subsurface inflow from Spring Valley to Snake Valley north of the Snake Range, however, is only 2,200 acre-ft/yr, which is much less than has been previously estimated. Groundwater discharge from groundwater evapotranspiration and springs is 100,000 acre-ft/yr, and discharge to mountain streams is 3,300 acre-ft/yr; these are within the range of previous estimates. Current well withdrawals are 28,000 acre-ft/yr. Subsurface outflow from Snake Valley moves into Pine Valley (2,000 acre-ft/yr), Wah Wah Valley (23 acre-ft/yr), Tule Valley (33,000 acre-ft/yr), Fish Springs Flat (790 acre-ft/yr), and outside of the study area towards

Great Salt Lake Desert (8,400 acre-ft/yr); these outflows, totaling about 44,000 acre-ft/yr, are within the range of previous estimates.

The subsurface flow amounts indicate the degree of connectivity between hydrographic areas within the study area. The simulated transmissivity and locations of natural discharge, however, provide a better estimate of the effect of groundwater withdrawals on groundwater resources than does the amount and direction of subsurface flow between hydrographic areas. The distribution of simulated transmissivity throughout the study area includes many areas of high transmissivity within and between hydrographic areas. Increased well withdrawals within these high transmissivity areas will likely affect a large part of the study area, resulting in declining groundwater levels, as well as leading to a decrease in natural discharge to springs and evapotranspiration.

Introduction

Snake Valley is a sparsely populated basin located along the Utah-Nevada border in the eastern Great Basin Physiographic Province described by Fenneman (1931). The study area (fig. 1), which covers approximately 21,000 km^2, is part of the Great Basin carbonate and alluvial aquifer system (GBCAAS), which comprises aquifers and confining units in unconsolidated basin-fill and volcanic deposits, carbonate, and other bedrock units (Heilweil and others, 2011). In some areas of the GBCAAS, aquifers are hydraulically connected between basins. In other areas, interbasin groundwater flow is impeded by mountain ranges that consist of less permeable rock. The basins in this study area approximately coincide with the southern half of the Great Salt Lake Desert regional groundwater flow system as defined by Harrill and others (1988). These basins are divided on the basis of hydrographic area (HA) boundaries (Harrill and others, 1988), which generally coincide with topographic basin divides. The study area consists of three partial HAs: Spring Valley, Dugway-Government Creek Valley, and Sevier Desert; and five complete HAs: Snake Valley, Fish Springs Flat, Tule Valley, Pine Valley, and Wah Wah Valley (fig. 1).

The study area is characterized by north-south trending mountain ranges and basins that range in altitude from over 3,950 m in the highest peaks of the Snake Range to less than 1,350 m in the basin floors at the southern end of the Great Salt Lake Desert (fig. 1). Climatic conditions range from temperate in the high-altitude Snake and Deep Creek Ranges to semiarid and arid across much of the rest of the study area. Annual precipitation varies from about 150 mm in the low altitudes of northernmost Snake Valley to about 760 mm in the highest altitudes of the Snake and Deep Creek Ranges, based on 30-yr average PRISM (Parameter-Elevation Regressions on Independent Slopes Model) precipitation data (Daly and others, 1994, 2008). The majority of precipitation occurs during the winter months, often as snow that accumulates in the mountains. Most groundwater in the valleys in the study area is derived from snowmelt and rainfall above altitudes of 1,800 m where precipitation amounts generally exceed losses from evapotranspiration (Hood and Rush, 1965).

The local economy is dominated by irrigated agriculture and ranching. Very few perennial streams flow into the basins and those that do are fully appropriated. Total annual withdrawal of groundwater in Snake Valley was approximately 17,500 acre-ft/yr in 2010 (Burden and others, 2011), nearly all of which was used to irrigate approximately 9,200 acres of land (Welch and others, 2007).

The Southern Nevada Water Authority (SNWA) has proposed developing unappropriated groundwater resources in Snake Valley and adjacent basins in eastern Nevada in order to supply the growing urban population of Las Vegas, Nevada. SNWA proposes to pump groundwater from five valleys in eastern Nevada using a network of 144 to 174 wells, up to 680 km of collector pipelines, and approximately 500 km of main and lateral pipelines to deliver water to Las Vegas, located more than 400 km to the south of Baker, Nevada (Southern Nevada Water Authority, 2011). SNWA plans to develop up to 185,000 acre-ft/yr of its existing water rights and applications in Spring, Snake, Cave, Dry Lake, and Delamar Valleys in eastern Nevada. A ruling was issued on March 22, 2012, granting SNWA water rights for 61,100 acre-ft/yr of groundwater from Spring Valley, located immediately to the west of Snake Valley (fig. 1). Furthermore, SNWA holds applications for approximately 50,700 acre-ft/yr of groundwater in Snake Valley.

Because of the magnitude of the SNWA groundwater development project and the possible interconnected nature of groundwater basins in the region, groundwater users and managers in Utah are concerned about declining groundwater levels and springflows in western Utah that could result from the proposed groundwater withdrawals. To address these concerns, the U.S. Geological Survey (USGS), in cooperation with Juab, Millard, Salt Lake, Tooele, and Utah Counties, conducted this study with the objectives of (1) understanding the links between basin-fill and carbonate aquifer systems, and the movement of groundwater within and between basins in the Snake Valley and surrounding area; (2) quantifying uncertainties in key components of the regional flow system, including aquifer properties, interbasin flow rates, and recharge rates and locations; and (3) evaluating the value of subsurface temperature data in constraining regional groundwater flow models. This study lays the foundation for future studies and will provide a baseline that can be used to assess the effects of future groundwater withdrawals on groundwater resources in the Snake Valley area.

The purpose of this report is to describe the groundwater hydrology of the Snake Valley area and to present the construction, calibration, and results of a numerical simulation of the groundwater system. A numerical groundwater flow and heat transport model was developed to simulate groundwater flow and heat transport in the Snake Valley area, and to test the conceptual understanding of the groundwater system.

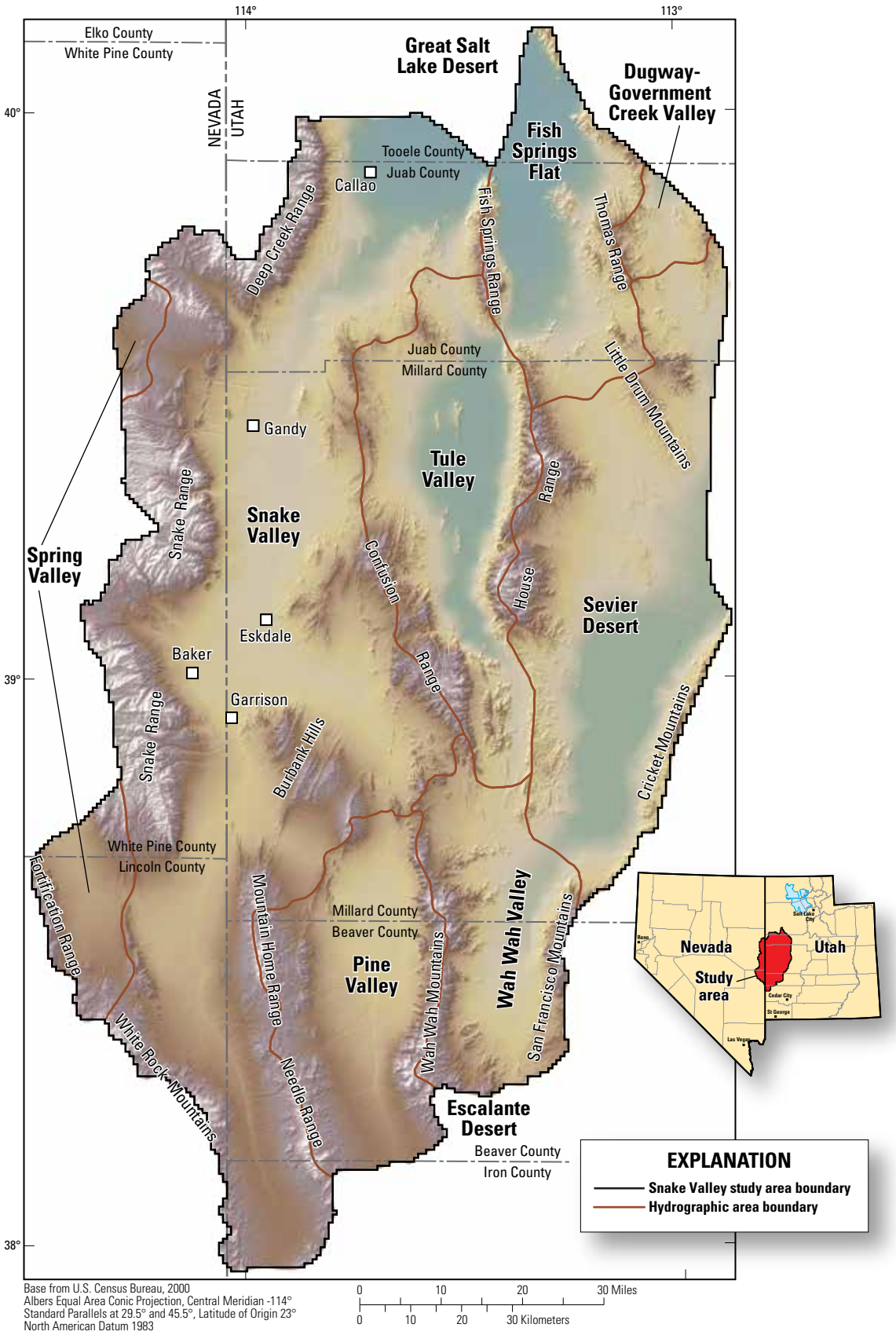

Figure 1. Location of the Snake Valley study area, Utah and Nevada.

A more complete understanding of the groundwater system and groundwater budget can aid in effective management of groundwater resources. Information from a number of previous and current investigations was compiled to conceptualize and quantify hydrologic and thermal components of the groundwater system, and to provide hydraulic and thermal properties and observation data used in the calibration of the numerical groundwater model. It was beyond the scope of the current study to develop a transient groundwater model to simulate increased groundwater withdrawals. The groundwater model developed in this study, however, can be used as a tool in future studies to assess long-term effects of groundwater withdrawals and to guide the collection of additional data that will lead to better predictions of the reduction of groundwater discharge to springs and declining water levels if increased well withdrawals were occurring.

Previous Studies

Early evaluations of the groundwater system in the study area were published by Hood and Rush (1965), Stephens (1974, 1976, 1977), Bolke and Sumsion (1978), Stephens and Sumsion (1978), and Wilberg (1991). These reconnaissance studies provide general descriptions of groundwater resources and chemical quality. Gates and Kruer (1981) summarized some of these earlier studies and compiled their data to better evaluate the southern Great Salt Lake Desert as an integrated groundwater flow system. Gates and Kruer (1981) looked at potential pathways for interbasin groundwater flow and at the source of water discharging from the Fish Springs complex. Although their study provided interpretations on the locations and amounts of interbasin flow from a thorough assessment of existing and new information, these estimates were based on sparse hydrologic data.

During the 1980s, the USGS Regional Aquifer-System Analysis (RASA) Program assessed the nation's major aquifer systems and, as part of this effort, delineated major aquifer systems in the Great Basin (GB) and evaluated regional flow in the carbonate-rock province of the Great Basin (Harrill and Prudic, 1998). The Great Basin RASA study included hydrogeology (Plume and Carlton, 1988), geochemistry (Thomas and others, 1996), hydrology (Thomas and others, 1986; Harrill and others, 1988), and a numerical groundwater flow model (Prudic and others, 1995) for a large geographic area that encompasses the Snake Valley study area. The results of the RASA studies form the basis of most subsequent conceptualizations of groundwater flow in the Great Basin.

Kirby and Hurlow (2005) revisited the hydrogeology of the Snake Valley area with the goal of assessing the potential impacts of the proposed SNWA groundwater development project on groundwater resources in Utah using an existing, basin-scale geologic framework and numerical groundwater flow model. Their conclusion, that the current understanding of geology and hydrology for the area was insufficient, prompted the Utah State Legislature to fund the establishment of a long-term groundwater monitoring network in the Snake Valley area. This network includes wells and springflow gaging in Snake Valley, and wells in Tule Valley and Fish Springs Flat where water levels and discharge are monitored continuously (Utah Geological Survey, 2009).

A more recent regional investigation, the Basin and Range carbonate-rock aquifer system (BARCAS) study was completed by the USGS and the Desert Research Institute in support of federal legislation to investigate the groundwater flow system underlying White Pine County and adjacent counties in Nevada and Utah. The BARCAS study developed potentiometric-surface maps showing groundwater flow directions in both alluvial and carbonate-rock aquifers, derived new groundwater budget estimates, and assessed interbasin groundwater flow using a combination of basin-boundary geology, hydraulic head data, and geochemistry. The results of the BARCAS study are available in a summary report (Welch and others, 2007 and references therein).

A comprehensive summary of hydrologic data for the entire GBCAAS was recently published that presents an updated conceptual model of groundwater flow for a 110,000 mi^2 area predominantly in eastern Nevada and western Utah (Heilweil and Brooks, 2011). This study was part of a national water census program summarizing groundwater availability on regional scales across the United States. The large area of the GBCAAS study completely encompasses Snake Valley and the surrounding areas investigated in the present study. In addition to providing a summary and compilation of data collected from numerous sources, the GBCAAS report also includes (1) a new hydrogeologic framework created by extracting and combining information from a variety of datasets, (2) a regional potentiometric-surface map for the entire study area, and (3) groundwater budget estimates compiled for 165 individual HAs and 17 regional groundwater flow systems.

To assess the hydrologic effects of developing groundwater in Snake Valley, Halford and Plume (2011), in cooperation with the National Park Service, refined and recalibrated the Great Basin RASA numerical model (Prudic and others, 1995) in Spring and Snake Valleys. A variant of this model was used to estimate potential effects of groundwater development on water levels, groundwater evapotranspiration, and spring discharges around the southern Snake Range. Four development scenarios were investigated and results are presented as maps of drawdown and groundwater capture, and time series of drawdowns and discharges from selected wells, springs, and control volumes. Results of the study show that (1) simulated drawdown was attenuated where groundwater discharge could be captured; (2) capture rates of groundwater discharge in Snake Valley were generally less than 1 ft/yr, but locally could be as great as 3 ft/yr; and (3) simulated drawdowns of greater than 1 ft propagated outside of Spring and Snake Valleys after 200 years of pumping in all scenarios.

Hydrogeologic Setting

The groundwater system in the study area consists of water in unconsolidated deposits in the basins and water in consolidated rock underlying the basins and in the adjacent mountain blocks. The consolidated rock and basin-fill aquifers are well connected hydraulically (Gardner and others, 2011; Sweetkind and others, 2011b), with most of the recharge occurring in the consolidated-rock mountain blocks and most of the discharge occurring within the lower altitude basin-fill deposits.

Within the study area, groundwater divides do not coincide with surface-water divides in many areas. For example, along the western boundary, the groundwater divide diverges from the topographic/surface-water divide in the southern Snake Range and actually occurs within the basin in southern Spring Valley (Gardner and others, 2011). Similarly, in the eastern part of the study area, groundwater flow from the east, west, and south converges in the Tule Valley and Sevier Desert HAs, and flows north towards Fish Springs (Gates, 1987; Prudic and others, 1995; Gardner and others, 2011). This is characteristic of many areas within the Great Basin, where interbasin groundwater flow can occur between basins.

Hydrogeologic Framework

As part of the GBCAAS study, a three-dimensional hydrogeologic framework of the eastern Great Basin was constructed (Cederberg and others, 2011; Sweetkind and others, 2011a). The GBCAAS study area is inclusive of the current study area; therefore, this same hydrogeologic framework, with a few refinements (discussed below) was used in the current study. The framework was constructed using data from a variety of sources, including geologic maps and cross sections, drill-hole data, geophysical models, and stratigraphic surfaces created for other three-dimensional hydrogeologic frameworks within the GBCAAS study area. The framework was developed using a 1-mi^2 grid cell size.

In the hydrogeologic framework developed for the GBCAAS study, the consolidated pre-Cenozoic-age rocks, Cenozoic-age sediments, and igneous rocks in the study area were subdivided into nine hydrogeologic units (HGUs) (Sweetkind and others, 2011a). An HGU has considerable lateral extent and reasonably distinct physical characteristics that may be used to infer the capacity of a sediment or rock to transmit water. The definition of HGUs is important in conceptualizing the hydrogeologic system, construction of a geologic framework for describing the groundwater flow system, and use in numerical groundwater flow models.

Of the nine HGUs defined in the hydrogeologic framework developed for the GBCAAS, seven exist in the current study area (figs. 2 and 3). The HGUs that exist in the current study area are (1) a non-carbonate confining unit (NCCU) representing low- to moderate-permeability Precambrian-age siliciclastic formations as well as intrusive igneous rocks that are locally exposed in mountain ranges, and underlie parts of the study area; (2) a lower carbonate aquifer unit (LCAU) representing a thick succession of predominantly high- to moderate-permeability Cambrian through Devonian-age carbonate rocks that are locally exposed in the mountain ranges, and present beneath most of the valleys within the study area; (3) an upper siliciclastic confining unit (USCU) representing low-permeability Mississippian-age siliciclastic rocks, predominantly shales, that are limited in extent within the study area; (4) an upper carbonate aquifer unit (UCAU) representing a thick succession of low- to high-permeability Pennsylvanian- and Permian-age carbonate rocks that are locally exposed in the mountain ranges and exist beneath some of the valleys within the study area; (5) a volcanic unit (VU) representing large volumes of low- to high-permeability Cenozoic-age volcanic rocks that are locally exposed in the mountain ranges and exist beneath some of the valleys within the study area; (6) a lower basin-fill aquifer unit (LBFAU) representing the lower (deepest) one-third of the Cenozoic-age basin-fill sediments, including moderate- to high-permeability volcanic rocks buried within the basin fill and consolidated older basin-fill sediments; and (7) an upper basin-fill aquifer unit (UBFAU) representing the upper (shallowest) two-thirds of the Cenozoic-age basin-fill sediments, including a wide variety of low- to moderate-permeability basin-fill sediments (Sweetkind and others, 2011a).

After the construction of the GBCAAS hydrogeologic framework, lithologic information from newly installed wells in Snake Valley and adjacent areas, as part of the Utah Geological Survey's (UGS) Snake Valley groundwater monitoring-well project, was used to refine the hydrogeologic framework in the study area. The following changes were made to the GBCAAS framework (Donald Sweetkind, U.S. Geological Survey, written commun., July 2010):

1. UGS well PW04B (USGS site number 383452114023402), located in volcanics (VU) on the east side of Hamlin (southern Snake) Valley, intercepted the VU at a depth consistent with the GBCAAS framework altitude. The UGS well, however, was still in VU at a depth of 299 m, whereas in the GBCAAS framework, the altitude of the contact between the VU and UCAU was at a depth of only 97 m. The altitude of the top of all Paleozoic-age units (UCAU, USCU, LCAU, and NCCU), therefore, was adjusted down by approximately 250 m in this area; for example, the top of the UCAU was adjusted from an altitude of 1,793 m to 1,543 m. Altitudes for all HGUs in a 3- by 5-grid cell area around the wellbore were similarly adjusted by hand to smooth out this correction.

2. UGS well PW02B (USGS site number 384651114025102), located in carbonates (UCAU) just north of Needle Point Spring in southern Snake Valley, intercepted the UCAU at a depth of 6.7 m. In the GBCAAS framework, however, the top of the UCAU was at a depth of 181 m. The framework in this area was adjusted by raising the altitude of the top of the UCAU by 175 m, thereby thickening the unit. This adjustment was carried northward in three grid cells, which essentially define the structural culmination of the Needle Point Anticline in this area.

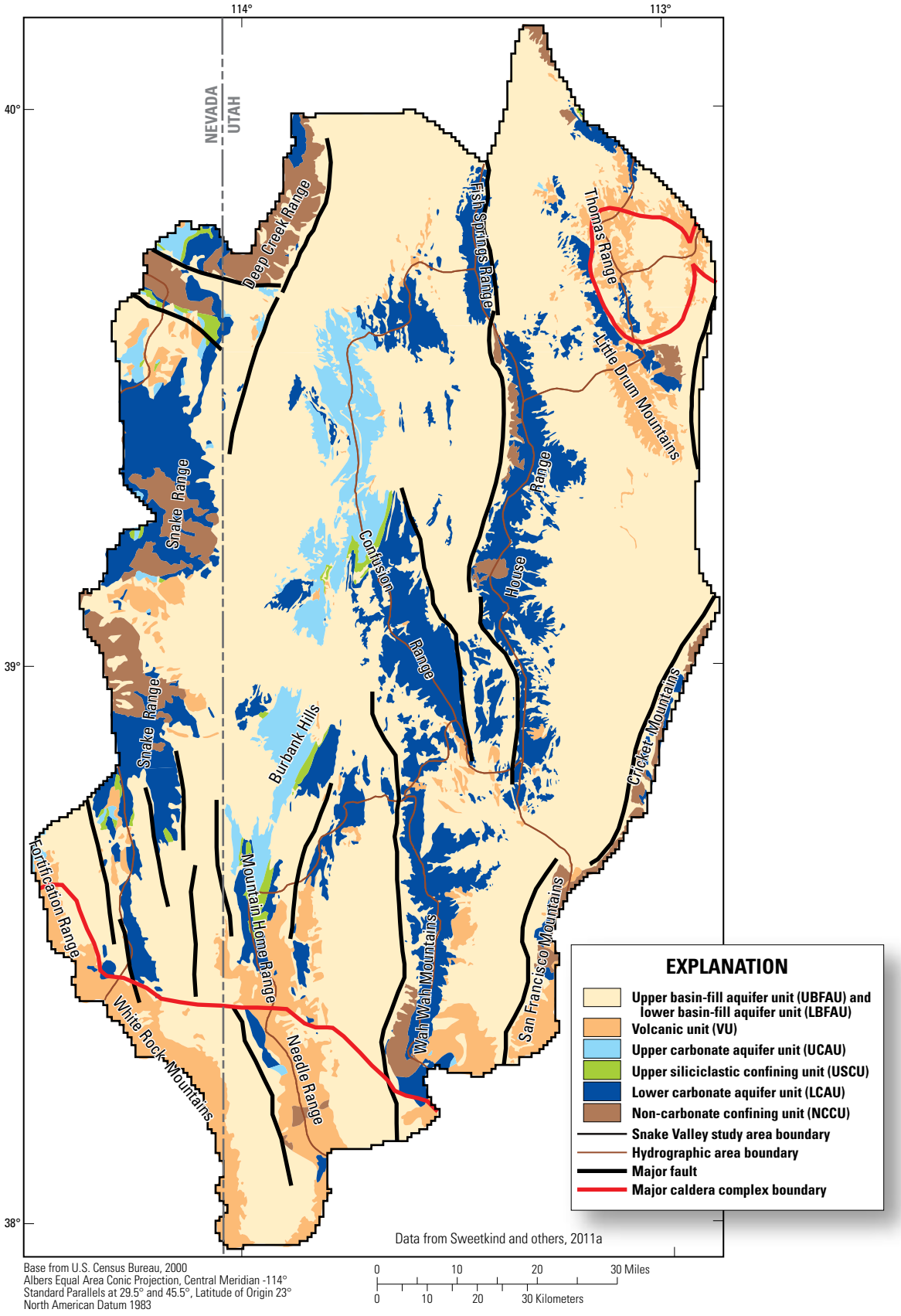

Figure 2. Surficial extent of hydrogeologic units and prominent structural features in the Snake Valley study area, Utah and Nevada.

3. UGS well PW07B (USGS site number 390143113533002), located in basin-fill deposits south of Eskdale in Snake Valley, bottomed in basin-fill deposits (UBFAU/LBFAU) at an altitude of 1,105 m. In the GBCAAS framework, however, the base of the basin-fill units was at an altitude of 1,254 m. The framework in this area was adjusted by lowering the altitude of the bottom of the basin-fill units (LBFAU) by 200 m. The altitude of the tops of the underlying Paleozoic-age units (UCAU, USCU, LCAU, and NCCU) was not adjusted; therefore, the UCAU in this area was thinned by 200 m. This adjustment was made for three grid cells in this area.

4. UGS well PW19C (USGS site number 393803113161602), located in carbonates in southern Fish Springs Flat, intercepted Cambrian-age limestone (LCAU) at a depth consistent with the GBCAAS framework altitude. In the GBCAAS framework, however, the LCAU had zero thickness in a relatively broad area in northeastern Tule Valley and in southwestern Fish Springs Flat. Consequently, the framework in this area was adjusted by lowering the altitude of the top of the NCCU by 500 m, thereby increasing the thickness of the LCAU to 500 m. This increased thickness of the LCAU is based on the exposed thickness of Cambrian-age limestone in the House Range between Fish Springs Flat and Tule Valley.

Hydrogeologic Unit Hydraulic Properties

Hydraulic properties describe the ability of a groundwater system to transmit and store water. The distribution of these properties in the study area is variable and depends on the depositional environment of sediments in the basin-fill aquifer and confining units, and on the degree of structural deformation, fracturing, and (or) chemical dissolution in the bedrock aquifers and confining units.

Sweetkind and others (2011a) estimated thickness and hydraulic properties of the HGUs in the GBCAAS study area (table 1). These were taken from studies by Belcher and others (2001, 2002) that analyzed and compiled estimates of

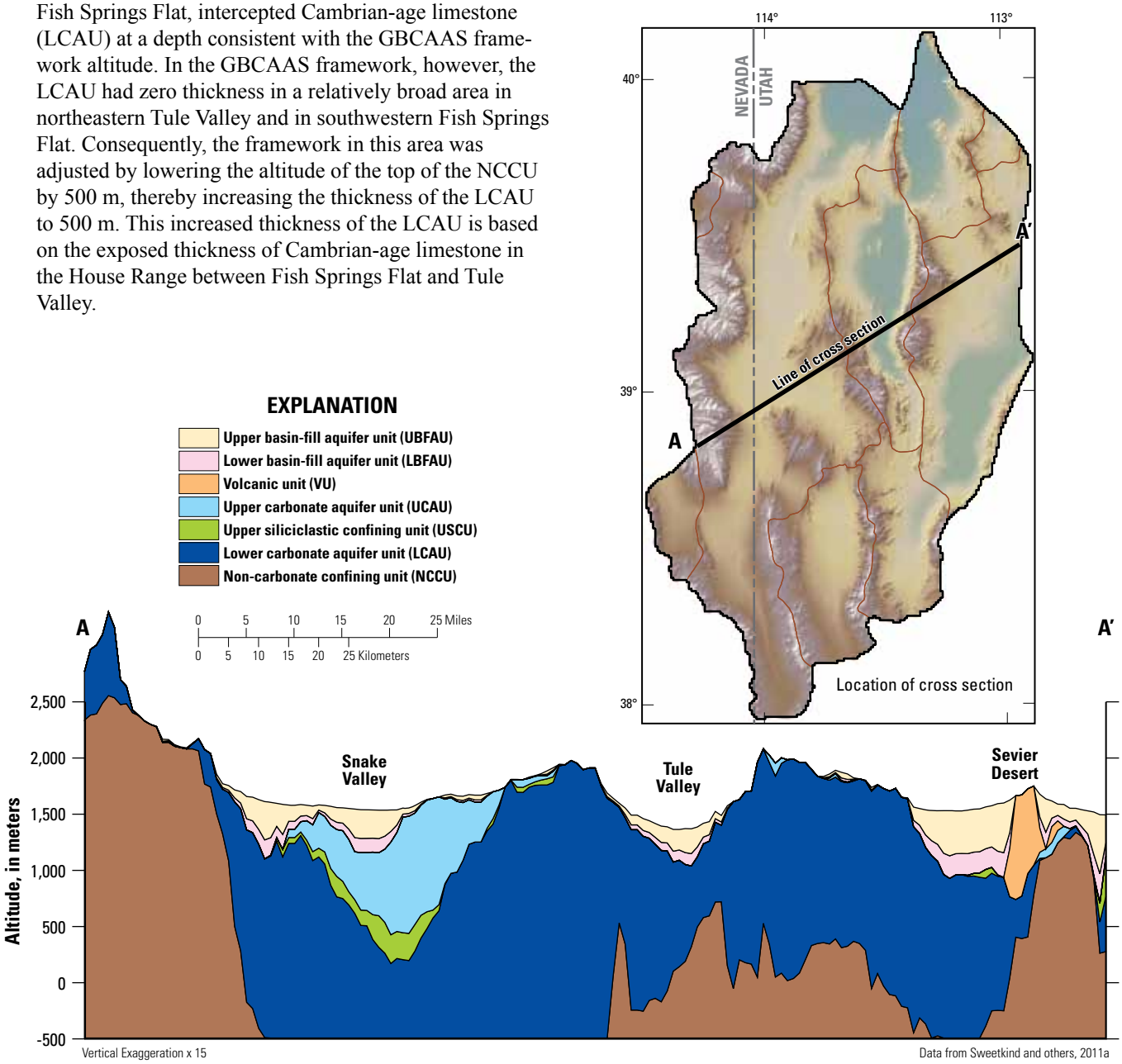

Figure 3. Cross section across central part of the Snake Valley study area in Utah and Nevada, showing hydrogeologic units.

Table 1. Hydraulic properties of hydrogeologic units in the Great Basin carbonate and alluvial aquifer system study area.

[Modified from Belcher and others, 2001, 2002, and Sweetkind and others, 2011a. **Abbreviations:** UBFAU, upper basin-fill aquifer unit; LBFAU, lower basin-fill aquifer unit; LCAU, lower carbonate aquifer unit; NCCU, non-carbonate confining unit; UCAU, upper carbonate aquifer unit; USCU, upper siliciclastic confining unit; VU, volcanic unit; >, greater than; NC, not calculated]

Major hydrogeologic unit	Hydrogeologic unit abbreviation	Maximum unit thickness (meters)	Hydraulic conductivity (meters per day)			
			Arithmetic mean	Geometric mean	Minimum	Maximum
Cenozoic basin-fill sediments	UBFAU and LBFAU	11,000	9	1	0.00003	131
Cenozoic volcanic rock	VU	1,000 (>3,900 in calderas)	6	0.9	0.01	55
Upper Paleozoic carbonate rock	UCAU	7,300	19	0.1	0.00009	319
Upper Paleozoic siliciclastic confining rock	USCU	>1,500	0.1	0.02	0.00003	0.9
Lower Paleozoic carbonate rock	LCAU	5,000	52	1	0.003	824
Non-carbonate confining rock	NCCU	NC	0.2	0.002	0.00000002	5

Table 2. Summary of estimates of aquifer properties from results of aquifer tests in Spring and Snake Valleys, Utah and Nevada.

[Data from *http://nevada.usgs.gov/water/AquiferTests/aqtests.htm* accessed on 9/4/2012. **Abbreviations:** NR, not reported; NC, not calculated; 3-D, three-dimensional]

Well identifier	Principal aquifer	Thickness (meters)	Average hydraulic conductivity (meters per day)	Average transmissivity (meters squared per day)	Type of test	Analysis method
(C-20-19)19dcd-1	Basin fill	610	0.6	680	Multiple-well pumping	3-D, numerical model
NDOW Well	Basin fill	NR	NC	28	Single-well pumping	Cooper-Jacob
Baker Creek	Basin fill	NR	8.1	84	Multiple-well pumping	3-D, numerical model
Big Springs NW	Basin fill	NR	NC	930	Single-well pumping	Cooper-Jacob
Big Springs SW	Carbonate rocks	NR	NC	370	Single-well pumping	Cooper-Jacob
Needle Point	Carbonate rocks	305	11.0	1,070	Multiple-well pumping	3-D, numerical model
184W101	Carbonate rocks	610	1.6	970	Multiple-well pumping	3-D, numerical model

transmissivity, hydraulic conductivity, storage coefficients, and anisotropy ratios for HGUs within the Death Valley regional groundwater flow system.

Additionally, the USGS Nevada Water Science Center (NVWSC) has conducted seven recent aquifer tests in Snake and Spring Valleys. These include both single and multiple pumping well tests in the basin-fill and carbonate aquifers that were analyzed by a variety of methods including the Cooper-Jacob method (Cooper and Jacob, 1946) and three-dimensional numerical simulations (accessed on September 4, 2012, at *http://nevada.usgs.gov/water/AquiferTests/aqtests.htm*). Results from these aquifer tests are summarized in table 2.

Occurrence and Movement of Groundwater

Groundwater recharge occurs mostly from the infiltration of precipitation at high altitudes (Welch and others, 2007; San Juan and others, 2010; Masbruch and others, 2011). Much of this recharge occurs in the form of snowmelt. Additional, but limited, recharge occurs from the infiltration of runoff from precipitation near the mountain front, and infiltration along stream channels (Hevesi and others, 2003; Flint and Flint, 2007a, b; Flint and others, 2011; Masbruch and others, 2011). There also may be recharge from applied irrigation; however, most of this applied water likely evaporates or is consumptively used by crops before reaching the water table. Groundwater moves from areas of recharge to springs and streams in the mountains; and to evapotranspiration areas, springs, and wells in the basins.

As part of this study, Gardner and others (2011) published a potentiometric map of Snake Valley and the surrounding areas in the southern Great Salt Lake Desert groundwater flow system. This map shows potentiometric contours based on water levels measured during the spring of 2010 from 190 wells finished in consolidated rock and basin fill. The water-level contours are used to refine conceptual pathways of intrabasin and interbasin groundwater flow. An evaluation of vertical and horizontal hydraulic gradients indicates that (1) aquifers within the consolidated rock and unconsolidated basin fill are generally hydraulically well connected and often act as a single aquifer unit; (2) a groundwater divide exists in southern Spring Valley where groundwater moving from the mountainous recharge areas on both sides of the valley diverges toward the north and south; (3) groundwater flow in Snake Valley is primarily north-northeastward, and that eastward interbasin flow out of Snake Valley may be restricted by steeply dipping, northeast trending, siliciclastic rocks extending from the Mountain Home Range as far north as the Confusion Range

(fig. 2); (4) groundwater flow is generally northward through Pine and Wah Wah Valleys, and westward through Sevier Desert toward Tule Valley where a nearly flat hydraulic gradient exists for more than 80 km from south to north; more recently collected water-level data in Pine Valley, however, indicate that groundwater in Pine Valley may follow a more easterly direction (Philip Gardner, U.S. Geological Survey, oral commun., March 2012); and (5) there is some groundwater flow out of the study area towards the Great Salt Lake Desert to the north and west from Snake Valley and Fish Springs Flat.

Conceptual Groundwater Budget

Development of a groundwater budget is important in understanding the occurrence and movement of groundwater in the flow system, and in evaluating the balance between flow into and flow out of the system. The primary components of the groundwater budget are recharge from precipitation (including direct infiltration and infiltration of runoff at lower altitudes), infiltration of mountain stream base flow, and infiltration of unconsumed irrigation; and discharge to evapotranspiration (ETg), springs, mountain streams, and well withdrawals. Recharge or discharge as subsurface (lateral) flow into or out of an HA or the study area across its boundary also may be occurring.

The current study considers all forms of recharge to and discharge from the groundwater system, including the surrounding mountains. This is illustrated by considering the fate of recharge from direct infiltration of mountain precipitation and subsurface inflow from adjacent areas to permeable consolidated rock of the mountain block (fig. 4, R1 and R3). Part of this recharge moves directly through the subsurface from the mountain block into the adjacent unconsolidated basin fill. Another part of this recharge becomes groundwater discharge to mountain streams and springs (fig. 4, D1). A fraction of this mountain-block groundwater discharge is consumptively lost as evapotranspiration, both in the mountains and as this water enters the valley in streams, and a fraction of the remaining water in the streams, combined with surface-water runoff becomes recharge to the unconsolidated basin fill (fig. 4, R2). This water ultimately discharges in the valley lowlands as evapotranspiration or to basin-fill springs (fig. 4, D2 and D3), wells (fig. 4, D4), or subsurface outflow (fig. 4, D5).

A conceptual groundwater budget for the current study was developed using estimates compiled from previous studies, as well as newer data that has been collected in the study area. Annual recharge and discharge have been previously estimated for parts of the study area and published in numerous reports (table 3). Each of these reports provide estimates for some or all water-budget components within a portion of an HA, an entire HA, or multiple HAs. Many of these previous estimates were used in the current study groundwater budget as it was beyond the scope of the current study to make updated measurements of all of the primary components of the groundwater budget. This conceptual groundwater budget was then further tested using a numerical groundwater flow model (see "Regional Groundwater Budget" section under "Model Evaluation" in this report). Groundwater budgets for this study were developed at the HA and study area scales.

Recharge

Precipitation within the study area is the primary source of groundwater recharge. The majority of precipitation comes as winter snowfall on the mountain ranges, with lesser amounts falling as rain. Infiltration of precipitation and snowmelt within the mountain block provides (1) discharge to mountain springs and base flow to mountain streams; (2) discharge to ETg, springs, and wells in the adjacent basin; and (3) flow which follows deeper and longer flow paths to regional discharge locations, including large springs and areas of ETg, in basins not adjacent to the mountain block. The majority of groundwater recharge within the study area occurs in the higher altitude mountain ranges as direct infiltration of precipitation (in-place recharge).

During the 1960s and 1970s, the USGS, in cooperation with the States of Utah and Nevada, completed a series of reconnaissance studies to evaluate the groundwater resources in these states. Generally, these studies developed groundwater budgets focused on the basin-fill (valley) portion of each HA where groundwater was being developed as a resource. Estimates of recharge from precipitation presented in these reports were based on a method developed by Maxey and Eakin (1949), which was calibrated to estimated groundwater discharge in the valleys, and provided estimates of "net" recharge to the unconsolidated basin-fill aquifer based on precipitation zones. These earlier methods did not consider groundwater discharge within the mountain block such as stream base flow and spring discharge, nor the subsequent recharge of part of this water as infiltration of runoff to unconsolidated basin-fill deposits.

In recent years, a new class of spatially distributed recharge estimation techniques utilizing water-balance methods have been developed that provide estimates for "total" recharge from precipitation in a watershed or HA (Leavesley and others, 1983; Hevesi and others, 2003; Flint and Flint, 2007a, b; Flint and others, 2011; Masbruch and others, 2011). Because these newer estimates include the partial loss of in-place recharge as groundwater discharge in the mountains to streams and springs, not considered in the earlier Maxey-Eakin method of estimating recharge, these newer spatially distributed recharge methods often yield higher recharge estimates. Consequently, these newer spatially distributed recharge estimates may cause over-appropriations of water rights if the consumptive losses of groundwater discharge in the mountains are not also considered.

Precipitation

A regional-scale water-balance method, known as the Basin Characterization Model (BCM; Flint and Flint, 2007a) developed for the GBCAAS study, was used to provide estimates

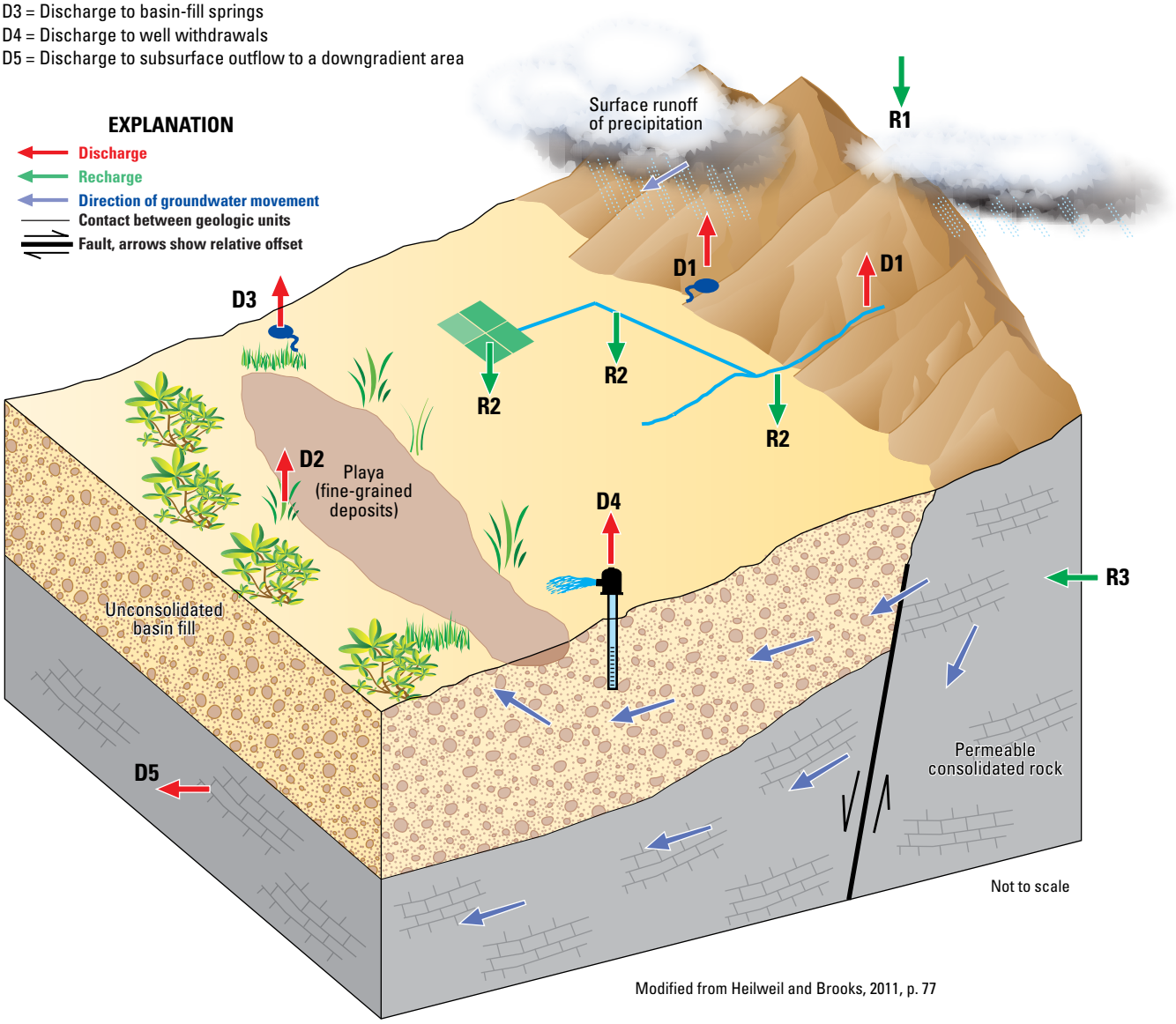

Figure 4. Conceptualization of groundwater budget components and budget calculation for the Snake Valley study area, Utah and Nevada.

of annual recharge from direct infiltration of precipitation (in-place recharge) and runoff. The BCM is a distributed-parameter water-balance accounting model used to identify areas having climatic and geologic conditions that allow for precipitation to become potential in-place recharge or runoff, and to provide estimates of each (Flint and others, 2011; Masbruch and others, 2011). BCM in-place recharge is calculated as the volume of water per time that percolates through the soil zone past the root zone and becomes net infiltration to consolidated rock or unconsolidated deposits. Runoff is the volume of water per time that runs off the surface, and may (1) infiltrate the subsurface, (2) undergo evapotranspiration further downslope, or (3) become streamflow that can, in turn, recharge the unconsolidated deposits from infiltration beneath the stream channels, irrigation canals, and (or) fields irrigated with surface water (Masbruch and others, 2011, p. 79). The

Table 3. Current study conceptual and ranges of previously reported groundwater budget estimates for hydrographic areas and the Snake Valley study area, Utah and Nevada.

[All estimates in acre-feet per year rounded to two significant figures. **Abbreviations:** HA, hydrographic area; —, no data; NE, not estimated]

	Conceptual	Previous studies
Spring Valley (HA 184)[1]		
Recharge		
Direct infiltration of precipitation (in-place recharge)	15,000	
Infiltration of runoff (includes unconsumed surface-water irrigation)	930	—
Mountain stream base flow	0	
Unconsumed irrigation from well withdrawals	0	—
Subsurface inflow	NE	—
Discharge		
Groundwater evapotranspiration + springs	0	—
Mountain streams	0	—
Well withdrawals	0	—
Subsurface outflow	NE	[2,3,4,5,6,7,8]4,000 to 49,000
Northern Spring Valley to Snake Valley	NE	[5]16,000
Southern Spring Valley to Snake Valley	NE	[2,3,4,5,6,7,8]4,000 to 33,000
Snake Valley (HA 254)		
Recharge		
Direct infiltration of precipitation (in-place recharge)	150,000	
Infiltration of runoff (includes unconsumed surface-water irrigation)	6,900	[2,3,5,9,10]99,000 to 160,000
Mountain stream base flow	360	
Unconsumed irrigation from well withdrawals	[11] 2,200	[12,13]3,300
Subsurface inflow	NE	[2,3,4,5,6,7,8]4,000 to 49,000
From Northern Spring Valley	NE	[5]16,000
From Southern Spring Valley	NE	[2,3,4,5,6,7,8]4,000 to 33,000
Discharge		
Groundwater evapotranspiration + springs	120,000	[2,3,5,14]64,000 to 130,000
Mountain streams	3,600	[14]2,800
Well withdrawals	[11] 22,000	[12,13]11,000
Subsurface outflow	NE	[2,3,4,5,7]25,000 to 43,000
To Tule Valley	NE	[2,3,4]15,000 to 42,000
To Fish Springs Flat	NE	[4]0
To outside of study area	NE	[2,4,5]10,000 to 29,000

Table 3. Current study conceptual and ranges of previously reported groundwater budget estimates for hydrographic areas and the Snake Valley study area, Utah and Nevada.—Continued

[All estimates in acre-feet per year rounded to two significant figures. **Abbreviations:** HA, hydrographic area; —, no data; NE, not estimated]

	Conceptual	Previous studies
Pine Valley (HA 255)		
Recharge		
Direct infiltration of precipitation (in-place recharge)	26,000	
Infiltration of runoff (includes unconsumed surface-water irrigation)	960	[3,9,10,15]21,000 to 27,000
Mountain stream base flow	0	
Unconsumed irrigation from well withdrawals	0	—
Subsurface inflow	NE	—
Discharge		
Groundwater evapotranspiration + springs	0	[3,14,15]0
Mountain streams	0	[3,14,15]0
Well withdrawals	0	[16]5
Subsurface outflow	NE	[3,4,15,17]3,000 to 14,000
To Wah Wah Valley	NE	[4,15,17]3,000 to 14,000
To Tule Valley	NE	[3]14,000
Wah Wah Valley (HA 256)		
Recharge		
Direct infiltration of precipitation (in-place recharge)	5,500	
Infiltration of runoff (includes unconsumed surface-water irrigation)	450	[3,9,10,18]6,000 to 7,000
Mountain stream base flow	0	
Unconsumed irrigation from well withdrawals	0	—
Subsurface inflow	NE	[4,15,17]3,000 to 14,000
From Snake Valley	NE	—
From Pine Valley	NE	[4,15,17]3,000 to 14,000
Discharge		
Groundwater evapotranspiration + springs	740	[3,14,17]1,400 to 1,500
Mountain streams	0	[3,14,17]0
Well withdrawals	0	[19]110
Subsurface outflow	NE	[3,4]8,500
To Tule Valley	NE	[3,4]8,500

BCM does not track or route runoff. For a more complete description of the BCM developed for the GBCAAS study, see Flint and others (2011) and Masbruch and others (2011).

Streamflow at the mountain front also includes base flow. This water originates as in-place recharge in the mountains and then discharges to mountain streams. Similar to runoff, a portion of this base flow subsequently recharges the basin-fill deposits as infiltration beneath stream channels, irrigation canals, or fields irrigated with surface water (Masbruch and others, 2011, p. 79).

Total groundwater recharge from precipitation is calculated as the sum of the BCM in-place recharge, recharge from runoff that infiltrates the subsurface, and a fraction of mountain stream base flow that also infiltrates the subsurface. In-place recharge is calculated at the location as it occurs in the BCM. Because the BCM does not route runoff, runoff that originates at higher altitudes was redistributed to areas along the mountain front that contain unconsolidated basin-fill material with a slope of 5 to 10 percent; in this way, recharge from upland runoff was accounted for where the streams enter the valleys. The amount of runoff that infiltrates the subsurface is typically

Table 3. Current study conceptual and ranges of previously reported groundwater budget estimates for hydrographic areas and the Snake Valley study area, Utah and Nevada.—Continued

[All estimates in acre-feet per year rounded to two significant figures. **Abbreviations:** HA, hydrographic area; —, no data; NE, not estimated]

	Conceptual	Previous studies
Tule Valley (HA 257)		
Recharge		
Direct infiltration of precipitation (in-place recharge)	13,000	[3,9,10,18]7,600 to 13,000
Infiltration of runoff (includes unconsumed surface-water irrigation)	320	
Mountain stream base flow	0	
Unconsumed irrigation from well withdrawals	0	—
Subsurface inflow	NE	[2,3,4,18,20]15,000 to 50,000
From Snake Valley	NE	[2,3,4]15,000 to 42,000
From Wah Wah Valley	NE	[3,4,18]8,500 to 32,000
From Sevier Desert	NE	[4]9,000
Discharge		
Groundwater evapotranspiration + springs	39,000	[3,14,18]24,000 to 56,000
Mountain streams	0	[3,14,18]0
Well withdrawals	0	—
Subsurface outflow	NE	[4,21]27,000 to 31,000
To Fish Springs Flat	NE	[4]27,000
Fish Springs Flat (HA 258)		
Recharge		
Direct infiltration of precipitation (in-place recharge)	1,500	[3,9,10,21]1,600 to 4,000
Infiltration of runoff (includes unconsumed surface-water irrigation)	150	
Mountain stream base flow	0	
Unconsumed irrigation from well withdrawals	0	—
Subsurface inflow	NE	[3,4,21]27,000 to 31,000
From Snake Valley	NE	[4]0
From Tule Valley	NE	[4]27,000
From Sevier Desert	NE	[4]0
Discharge		
Groundwater evapotranspiration + springs	34,000	[3,14,21]34,000 to 35,000
Mountain streams	0	[3,14,21]0
Well withdrawals	0	—
Subsurface outflow	NE	[3,4]100 to 1,000
To outside of study area	NE	[4]1,000
Dugway-Government Creek Valley (HA 259)[1]		
Recharge		
Direct infiltration of precipitation (in-place recharge)	200	—
Infiltration of runoff (includes unconsumed surface-water irrigation)	110	
Mountain stream base flow	0	
Unconsumed irrigation from well withdrawals	0	—
Subsurface inflow	NE	—
Discharge		
Groundwater evapotranspiration + springs	0	—
Mountain streams	0	—
Well withdrawals	0	—
Subsurface outflow	NE	—

Table 3. Current study conceptual and ranges of previously reported groundwater budget estimates for hydrographic areas and the Snake Valley study area, Utah and Nevada.—Continued

[All estimates in acre-feet per year rounded to two significant figures. **Abbreviations:** HA, hydrographic area; —, no data; NE, not estimated]

	Conceptual	Previous studies
Sevier Desert (HA 287)[1]		
Recharge		
Direct infiltration of precipitation (in-place recharge)	8,500	—
Infiltration of runoff (includes unconsumed surface-water irrigation)	1,600	
Mountain stream base flow	0	
Unconsumed irrigation from well withdrawals	0	—
Subsurface inflow	NE	—
Discharge		
Groundwater evapotranspiration + springs	8,600	[22]8,600
Mountain streams	0	—
Well withdrawals	0	—
Subsurface outflow	NE	[4,20]8,800 to 9,000
To Tule Valley	NE	[4]9,000
To Fish Srings Flat	NE	[4]0
Study area total		
Recharge		
Direct infiltration of precipitation (in-place recharge)	220,000	—
Infiltration of runoff (includes unconsumed surface-water irrigation)	11,000	
Mountain stream base flow	360	
Unconsumed irrigation from well withdrawals	2,200	—
Subsurface inflow	NE	—
Discharge		
Groundwater evapotranspiration + springs	200,000	—
Mountain streams	3,600	—
Well withdrawals	22,000	—
Subsurface outflow	NE	—

[1]Partial HA; estimates only for portion of HA within study area.
[2]Hood and Rush, 1965.
[3]Gates and Kruer, 1981.
[4]Harrill and others, 1988.
[5]Welch and others, 2007.
[6]Rush and Kazmi, 1965.
[7]Scott and others, 1971.
[8]Nichols, 2000.
[9]Harrill and Prudic, 1998.
[10]Masbruch, 2011a.
[11]Estimate for the year 2009.
[12]Masbruch, 2011b.
[13]Estimate for the year 2000.
[14]Masbruch, 2011c.
[15]Stephens, 1976.
[16]Estimate for the year 1976.
[17]Stephens, 1974.
[18]Stephens, 1977.
[19]Estimate for the year 1974.
[20]Holmes, 1984.
[21]Bolke and Sumsion, 1978.
[22]Wilberg, 1991.

calculated as a percentage of the total BCM runoff. For this study, it was assumed that 10 percent of the total runoff infiltrates the subsurface (Masbruch and others, 2011, p. 86); this includes recharge from the infiltration of unconsumed surface-water irrigation. Likewise, it was also assumed that 10 percent of the mountain stream base flow infiltrates the subsurface and becomes recharge (Masbruch and others, 2011, p. 92); this recharge is also distributed in areas along the mountain front that contain unconsolidated basin-fill material with a slope of 5 to 10 percent. The other 90 percent of runoff and mountain stream base flow is assumed to be consumptively lost to evapotranspiration before it can infiltrate into the aquifer (Hevesi and others, 2003; San Juan and others, 2010; Masbruch and others, 2011). Estimates of recharge from precipitation (in-place recharge plus recharge from runoff (including unconsumed surface-water irrigation) plus recharge from mountain stream base flow) for each HA and the study area are given in table 3 and conceptual recharge rates are shown on figure 5.

Unconsumed Irrigation from Well Withdrawals

Most well withdrawals in the study area are used for irrigation, and these wells are located exclusively within Snake Valley. It is assumed that part of these withdrawals recharges the aquifer system as infiltration of unconsumed irrigation water applied to fields. Irrigation return flow studies in the Amargosa Desert, CA (Stonestrom and others, 2003) and the Milford Area, UT (Susong, 1995) show that recharge from irrigation on sprinkler-irrigated fields ranges from 8 to 16 percent of the applied irrigation. Because most of the fields in Snake Valley are sprinkler irrigated, it was assumed that 10 percent of the applied irrigation groundwater recharged back into the aquifer system (table 3).

Subsurface Inflow

The potentiometric-surface map for the study area (Gardner and others, 2011) indicates that groundwater may enter and leave the study area via subsurface inflow and outflow along some parts of the study-area boundary. Subsurface flow may also occur between HAs within the study area. Previous studies have estimated subsurface flow by a variety of methods, and with little to no indication of the uncertainties on these estimates. These estimates can vary widely due to differences in the methods used to calculate them (table 3). Rather than predefining a conceptual estimate of subsurface flow, the calibrated groundwater flow model developed in this study was used to estimate subsurface inflow into the study area and between HAs within the study area. By allowing the groundwater model to predict estimates of subsurface flow, uncertainties on this estimate could be calculated. These estimates and associated uncertainties are discussed in the "Regional Groundwater Budget" section under "Model Evaluation" in this report.

Discharge

Discharge from the groundwater system occurs by evapotranspiration (ETg), as discharge to springs, as discharge to mountain streams (base flow), as well withdrawals, and as subsurface outflow to neighboring basins (fig. 6). The majority of discharge within the study area occurs as ETg.

Groundwater Evapotranspiration

Discharge to ETg (table 3) is based on estimates from previous studies (Stephens, 1977; Bolke and Sumsion, 1978; Gates and Kruer, 1981; Wilberg, 1991; Welch and others, 2007). In these studies, ETg was estimated using a volumetric calculation of ETg from major areas of phreatophytic vegetation. In some studies, discharge to springs was indirectly accounted for in the ETg estimate as these studies assumed that all spring discharge from the basin fill was ultimately consumed through evapotranspiration.

For Snake Valley, the previously reported ETg (Welch and others, 2007) was estimated for predevelopment conditions and includes discharge to springs; these contributing springs, however, were not identified in the report. In the current study, it was assumed that springs within 1 mi of an ETg area contributed to this previous ETg estimate. The previous ETg estimate for Snake Valley, therefore, was reduced by the amount of estimated spring discharge located within 1 mi of the ETg areas, and this spring discharge was accounted for separately (see "Spring Discharge" section of this report). Additionally, in the current study, representative long-term well withdrawals within Snake Valley are also being simulated, so the amount of groundwater available for ETg is reduced compared to predevelopment conditions. Previously reported ETg for Snake Valley, therefore, was further reduced by an amount equaling 90 percent of the total well withdrawals within each area (excluding the 10 percent that is assumed to recharge the aquifer from irrigation return flow).

Spring Discharge

Groundwater discharge to springs (table 3) is based on estimates from previous studies (Hood and Rush, 1965; Stephens, 1974; Bolke and Sumsion, 1978; Elliott and others, 2006), data from the USGS National Water Information System (NWIS) database (Mathey, 1998), or data collected by the UGS as part of their Snake Valley groundwater monitoring project (Lucy Jordan, Utah Geological Survey, written commun., August 2010). The majority of these springs are located in Snake Valley except for Wah Wah Springs, located in Wah Wah Valley; and Fish Springs, an area spring located in Fish Springs Flat.

Base flow to Mountain Streams

Groundwater discharge that provides base flow to mountain streams (table 3) is based on estimates from previous studies (Elliott and others, 2006; Masbruch and others, 2011). There

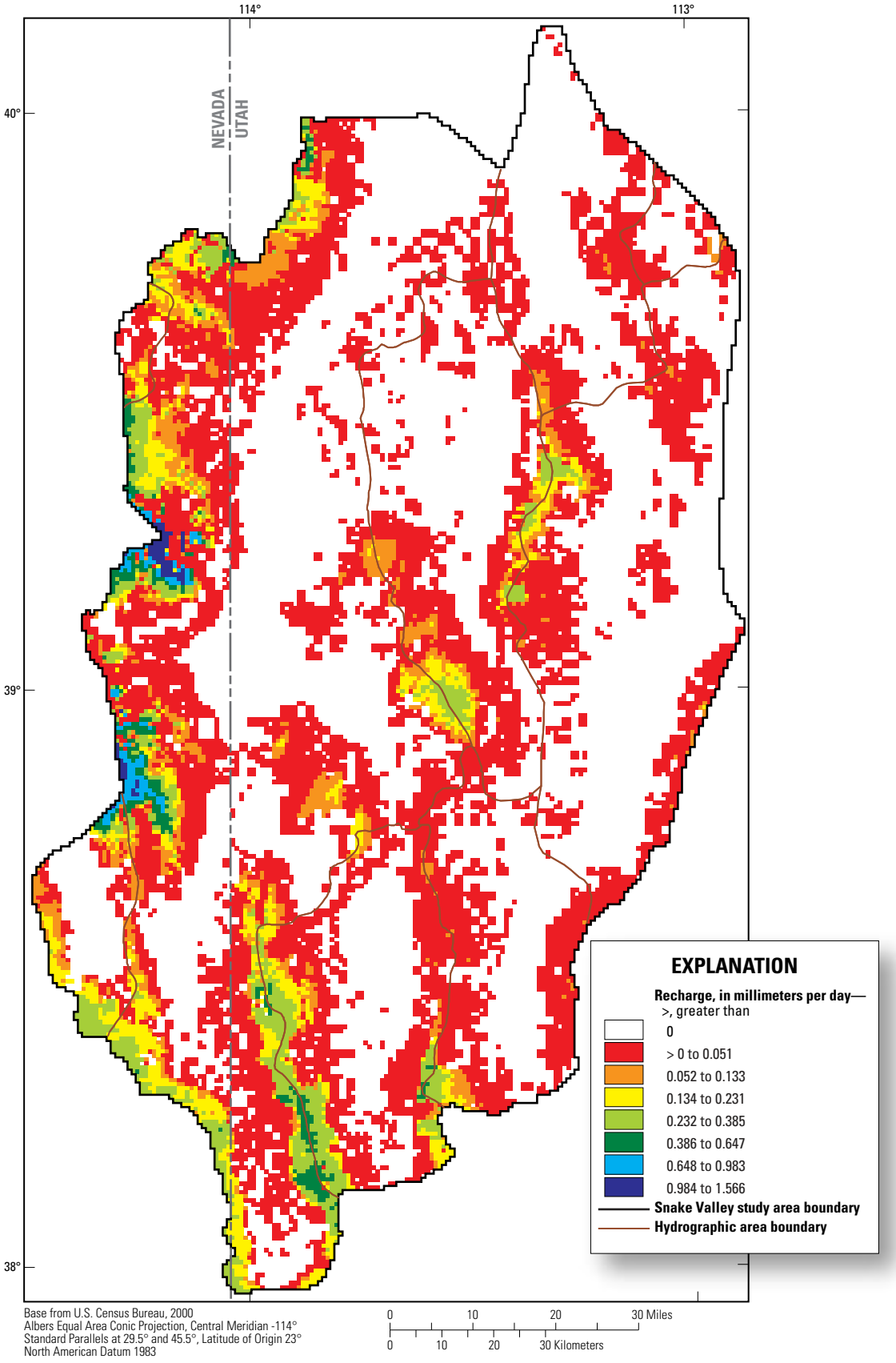

Figure 5. Conceptual rate of recharge from precipitation (in-place recharge plus recharge from runoff (including unconsumed surface-water irrigation) plus recharge from mountain stream baseflow) in the Snake Valley study area, Utah and Nevada.

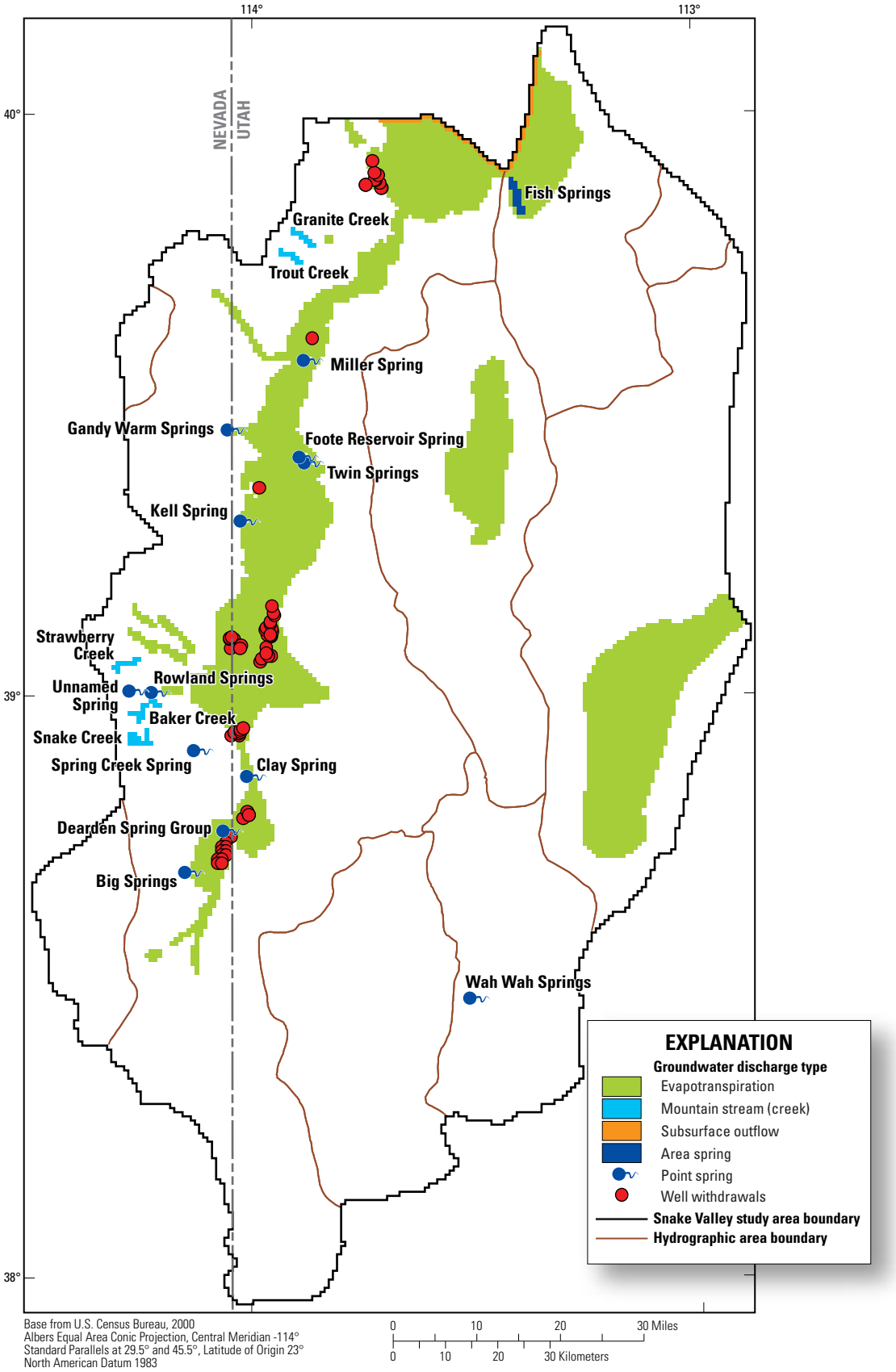

Figure 6. Locations and types of discharge in the Snake Valley study area, Utah and Nevada.

are five perennial mountain streams within the study area that had been measured previously: Granite and Trout Creeks on the east side of the Deep Creek Range; and Strawberry, Baker, and Snake Creek on the east side of the southern Snake Range. These measurements are based on the minimum mean daily discharge or are instantaneous low-flow measurements and, therefore, represent the minimum amount of groundwater discharge to mountain streams. Elliott and others (2006) also measured discharge in Lehman Creek, and these measurements indicated that the majority of base flow in Lehman Creek is supplied by Unnamed Spring and Rowland Springs. Because discharge to these springs is already accounted for in this study (see "Spring Discharge" section above), groundwater discharge to Lehman Creek is not included in this estimate.

Well Withdrawals

Groundwater withdrawals in the study area are used for irrigation, industrial use, public and domestic supply, and stock watering. Significant groundwater withdrawals from wells only occur in Snake Valley (table 3). Annual withdrawals from pumped irrigation wells in the Utah portion of the valley (fig. 7) were estimated from flow measurements and corresponding power-consumption records for individual wells for the year 2009 as part of the statewide groundwater use monitoring program (Burden and others, 2010).

There are no historical estimates of well withdrawals for the Nevada side of the HA. Well withdrawals for a large number of center pivots just to the east of Big Springs in Nevada, therefore, were estimated by assuming one well per pivot (for a total of 11 wells), and withdrawals equaling an average irrigation application rate of 3 ft/yr (Welch and others, 2007) applied over the surface area supplied by each pivot (Welborn and Moreo, 2007).

In recent years, well withdrawals for irrigation in the unconsolidated basin fill have increased, especially in the southern part of Snake Valley. The source of water for these well withdrawals is partially from groundwater in storage, but is also from capturing of natural discharge. One such example of this is Needle Point Springs in southern Snake Valley, which was a watering source for stock and wild horses; water levels in the vicinity of the spring, however, have declined so that the spring is no longer flowing (Paul Summers, Bureau of Land Management, written commun., March 2013). Increasing well withdrawals within Snake Valley will likely continue to affect the groundwater system by removing more groundwater from storage, resulting in declining groundwater levels, as well as leading to a decrease in natural discharge to springs and evapotranspiration within the basin.

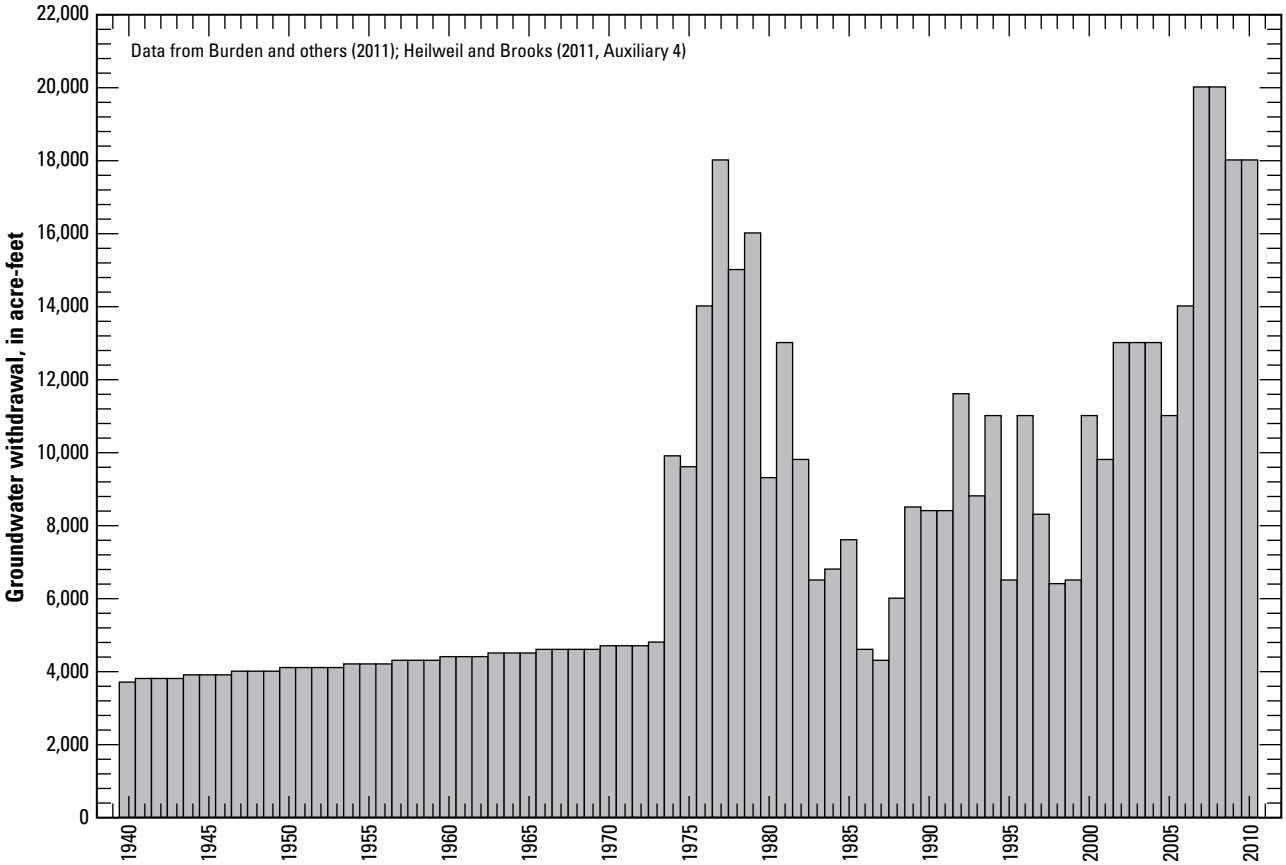

Figure 7. Estimated total annual groundwater withdrawals from wells in the Utah portion of Snake Valley, 1940–2010.

Subsurface Outflow

Similar to subsurface inflow, subsurface outflow from the study area and between HAs within the study area was estimated using the calibrated groundwater flow model (see the "Subsurface Inflow" section above). These estimates and associated uncertainties are discussed in the "Regional Groundwater Budget" section under "Model Evaluation" in this report.

Water-Level Fluctuations

Water levels in wells fluctuate in response to imbalances between groundwater recharge and discharge and are driven by both natural and anthropogenic processes. Gardner and others (2011) present multiple-year water-level hydrographs for 32 wells completed in the basin fill in Snake Valley and the surrounding valleys, showing that patterns of water-level fluctuation are distinctly different across the study area. Hydrographs from three of these wells (figs. 8 and 9) illustrate three types of water-level fluctuations that are characteristic of Snake Valley and the surrounding areas.

In the eastern half of the study area, including Tule Valley, Pine Valley, Wah Wah Valley, Fish Springs Flat, and Sevier Desert, water-level fluctuations are minimal, varying by less than about 2 ft over the period of record (for example, fig. 9, USGS site number 393933113214801). These steady water levels are likely due to a combination of low recharge rates in the nearby mountains and negligible groundwater pumping in these valleys.

Conversely, water levels in wells in the western part of the study area, namely Spring Valley and Snake Valley, experience notably more fluctuation. Many of the wells in these valleys are located close to high-altitude mountainous areas that receive substantial winter precipitation and groundwater recharge. Water levels in these wells clearly respond to annual recharge or to multiple-year periods of above- or below-average precipitation. Wells located close to the Snake and Deep Creek Ranges (for example, fig. 9, USGS site number 391322114000001) show water-level fluctuations of 10 to 20 ft over periods of only a few years. The sudden water-level rise of nearly 15 ft at the end of the record for USGS site number 391322114000001 occurred between March and June of 2010, coincident with the timing of snowmelt.

Water levels in several wells located near agricultural pumping centers (for example, fig. 9, USGS site number 390629113560301) appear to be influenced by pumping. Water levels in these areas rose in response to a period of above-average precipitation during the mid-1980s (Wilkowske and others, 2003) and most reached a maximum around the late 1980s to early 1990s. Since that time, water levels in these areas have declined steadily and show little to no recovery during subsequent periods of above-average precipitation (for example, 1996–98 and 2004–05). These water-level declines are most likely caused by groundwater withdrawal used for irrigation.

Groundwater Temperatures and Heat Flow

Within the Earth's crust, temperatures generally increase with depth (geothermal gradient). If groundwater flows are large enough, they can redistribute heat within the subsurface both vertically and laterally and alter the natural, conductive geothermal gradient of the area. These changes in the geothermal gradient and distribution of heat flow, and associated groundwater temperatures, can be used to assess the magnitude of groundwater flow in an area (Bredehoeft and Papadopulos, 1965; Cartwright, 1970; Smith and Chapman, 1983; Manning and Solomon, 2005).

Figure 10 shows a conceptualization of how groundwater flow may perturb the conductive geothermal gradient and laterally redistribute heat in terrain with high topographic relief. In areas of groundwater recharge (A on fig. 10), groundwater temperatures tend to be cooler and will depress the natural (conductive) geothermal gradient as this cold water enters the subsurface. The amount of depression of the geothermal gradient is proportional to the velocity at which the groundwater is flowing. This produces an area of lower than expected heat flow at the surface. Essentially, in these areas, the groundwater is removing heat from the subsurface. As the groundwater moves laterally away from the recharge area, it carries this extra heat energy with it and begins to warm as it moves towards the discharge area (B on fig. 10). In areas of groundwater discharge (C on fig. 10), groundwater temperatures tend to be warmer and will raise the natural (conductive) geothermal gradient as warm water at depth is brought to the surface or as any heat that was removed in the recharge area is delivered to the discharge location. This produces an area of higher than expected heat flow at the surface.

Vertical temperature logs (temperature vs. depth) have recently been collected from 23 wells in the Snake Valley area (Blackett, 2011) as part of the UGS Snake Valley groundwater monitoring project. Temperatures in these wells were measured at depths up to 500 m at intervals of 5 to 20 m using a high-precision thermistor probe and temperature-logging equipment (Blackett, 2011). The thermistor was lowered into the well at regular depth intervals, and temperature measurements at each depth were recorded once thermal equilibration was reached (typically 12 minutes for air and less than 1 minute for water). To ensure that temperatures were not being affected by local perturbations of flow due to well withdrawals, logs were only collected within wells that were not being actively pumped.

The temperature log data (Blackett, 2011) indicate an active groundwater flow system that is removing heat from the southern part of the study area and potentially redistributing it to the northern part of the study area. Typical conductive geothermal gradients for the Great Basin are approximately 30 °C/km, which correspond to a heat flow value of approximately 90 mW/m^2. Figure 11 shows the distribution of thermal gradients (Blackett, 2011) below the water table calculated from the logged wells within the Snake Valley study area. Thermal gradients in the southern part of Snake Valley are

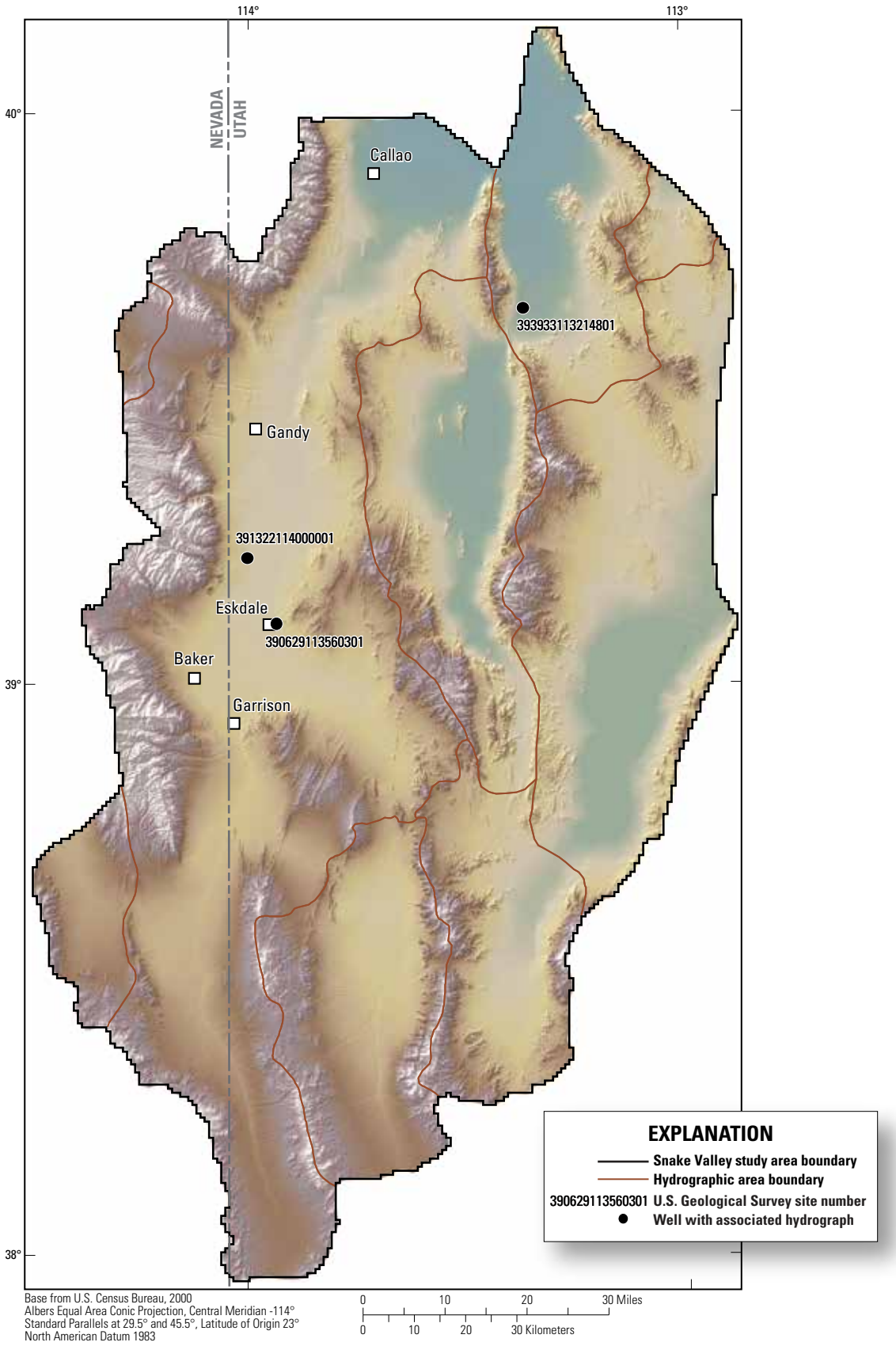

Figure 8. Location of three wells with multiple-year water-level records in the Snake Valley study area, Utah and Nevada.

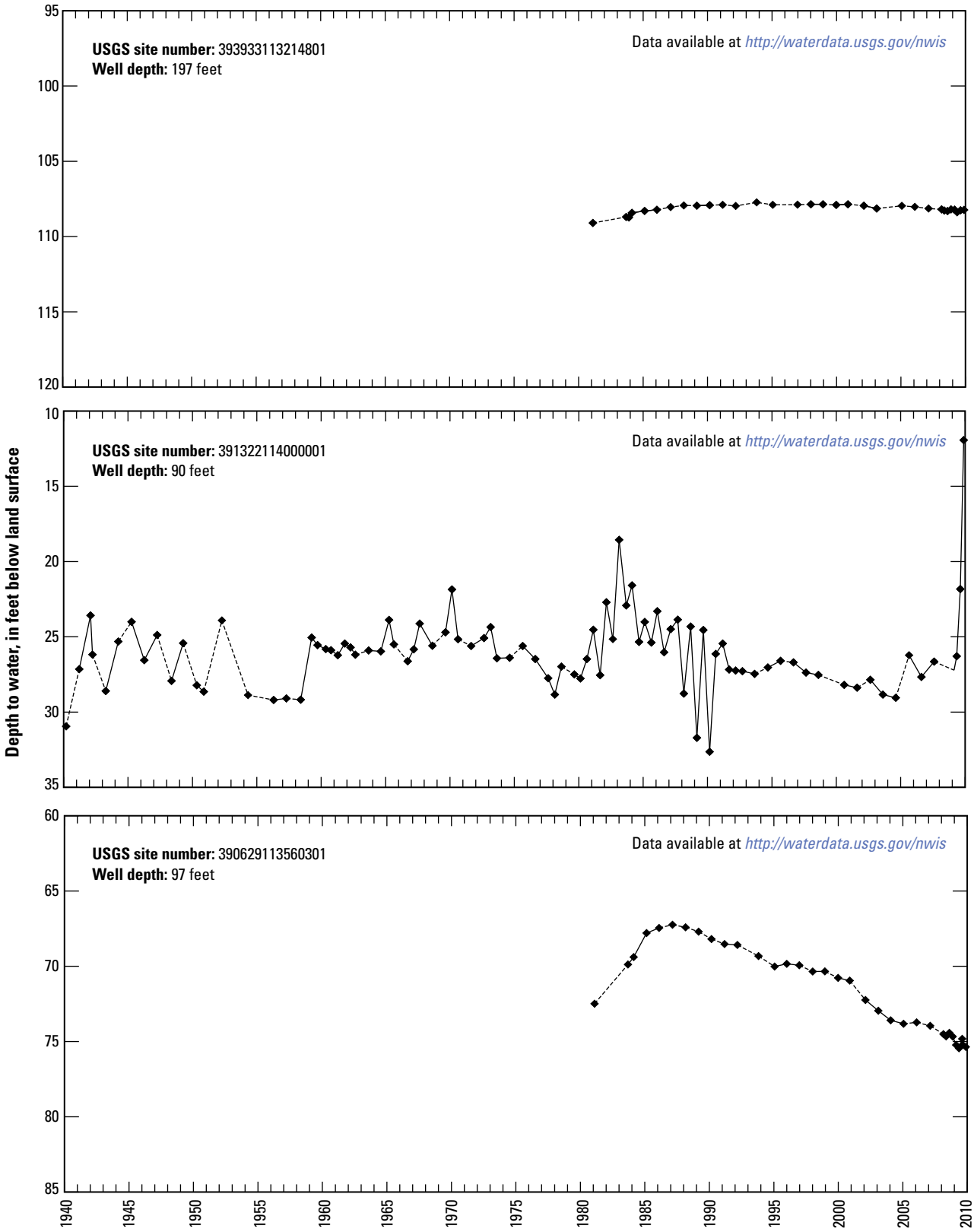

Figure 9. Multiple-year water-level hydrographs for three wells in the Snake Valley study area, Utah and Nevada.

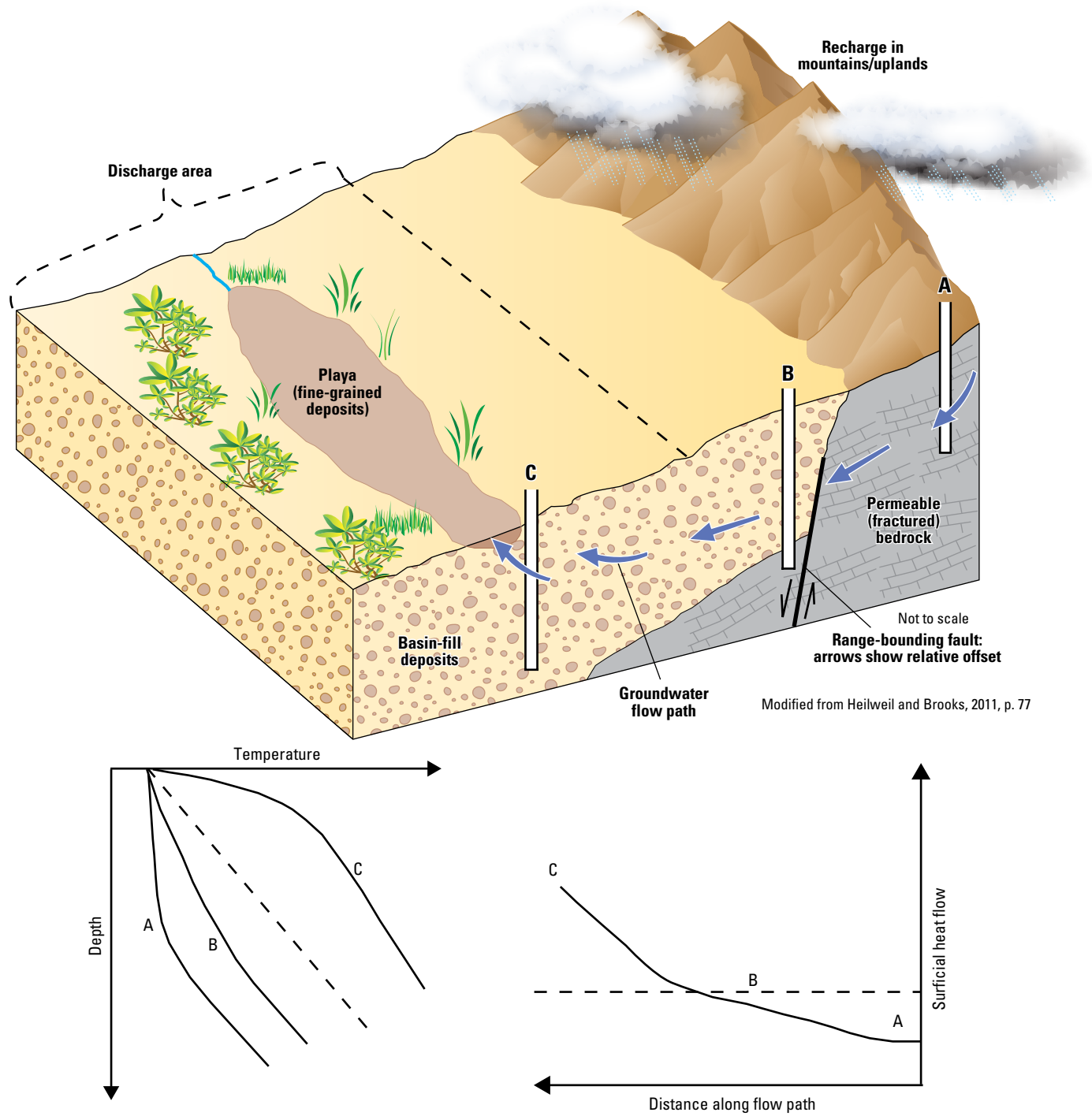

Figure 10. Conceptualization of groundwater flow in the Basin and Range and effects on geothermal gradients and surficial-heat flow. Letters in bottom figures correspond to wells A, B, and C in top figure. Background Basin and Range geothermal gradients (30 degrees Celsius per kilometer) and heat flow (90 milliwatts per meters squared) are shown by dashed lines in bottom figures.

lower than typical Basin and Range geothermal gradients, with the majority ranging between 10 and 20 °C/km, corresponding to heat flow values of 30 to 60 mW/m^2. In the northern part of the study area thermal gradients are generally higher than typical Basin and Range geothermal gradients, with temperature logs from three wells indicating gradients between 44 and 86 °C/km, corresponding to heat flow values ranging from 132 to 258 mW/m^2. Shallow thermal gradients in a well near Fish Springs, a regional discharge location in the northern part of the study area, are as high as 320 °C/km. Additionally, spring temperatures in the northern part of Snake Valley and at Fish Springs are much higher than ambient surface temperatures of approximately 12 to 13 °C, suggesting that heat is being redistributed laterally or vertically to these discharge points as well.

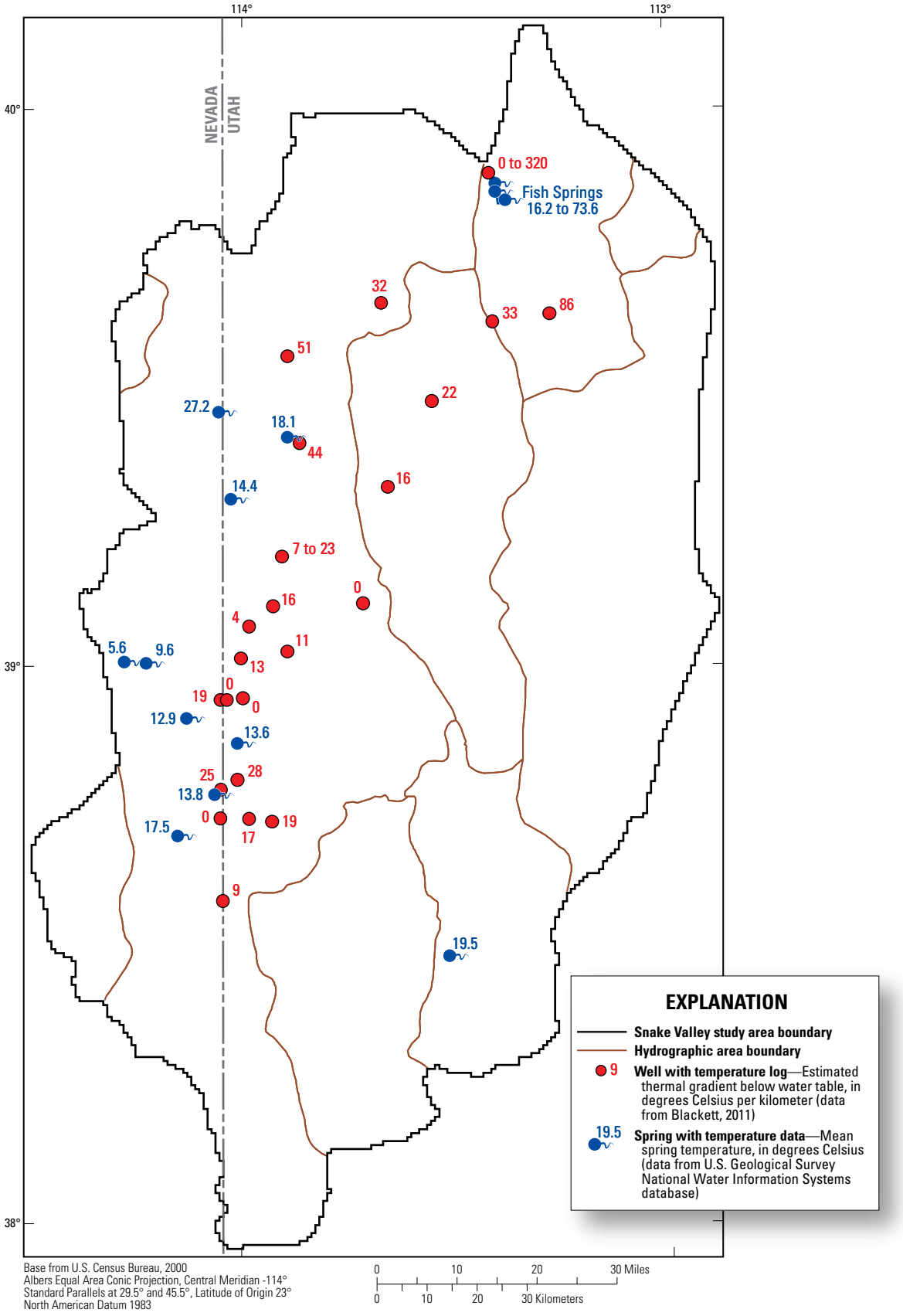

Figure 11. Location of wells with temperature logs and associated estimated thermal gradients, and springs with temperature data in the Snake Valley study area, Utah and Nevada.

Numerical Simulation of Groundwater Flow and Heat Transport

A steady-state numerical groundwater flow and heat transport model was developed to simulate groundwater flow and heat transport in the Snake Valley area, with the specific purpose of testing the conceptual model and developing a better understanding of the groundwater budget and the groundwater system. The model allows for the simulation of groundwater flow and heat transport through the groundwater system in consolidated rock and unconsolidated basin fill. The advantage of simulating both groundwater flow and heat transport is that the groundwater temperatures are additional observations besides water levels and discharge that can be used to assess model performance and constrain model parameters, thereby improving how the model represents the groundwater flow system. Development of the model included compilation and examination of water-level, streamflow, springflow, evapotranspiration, groundwater withdrawal, and temperature data, and estimation of the spatial distribution of recharge, discharge, hydraulic conductivity, and thermal properties. The "Model Construction" section discusses the details of discretization, boundary conditions, and model parameters. The "Model Calibration" section discusses how the model was changed to match observed data, and the "Model Evaluation" section discusses how adequately the model simulates the groundwater system.

Model Construction

Construction of the groundwater flow and heat transport model required (1) discretization of the groundwater system, including establishment of the model grid and boundaries; (2) assignment of boundary conditions including recharge and discharge, water-table temperatures, and basal heat flux; and (3) assignment of material properties such as hydraulic conductivity and thermal conductivity. Given the amount and complexity of the input data, it is impractical to present or reference all required information to reconstruct the model from the information presented in this report. A copy of the model and associated data sets can be obtained from the USGS Utah Water Science Center, Salt Lake City, Utah.

The model described in this report uses parameters (Harbaugh and others, 2000) to define much of the input data. A parameter is a single value that is given a name and determines the value of a variable in the finite-difference groundwater flow or heat transport equations (Harbaugh and others, 2000). When parameters are used, the data value for a cell is calculated as the product of the parameter value, which might apply to many cells and can be described using zones, and a cell multiplier defined using multiplier arrays, which applies only to that cell (Harbaugh and others, 2000). Sensitivity analysis (Hill and others, 2000) was used to assess the relative importance of various parameters in the model and guide model construction and calibration.

Numerical Model Selection

The USGS three-dimensional groundwater flow model program MODFLOW-2000 was used to simulate groundwater flow in the Snake Valley study area (Harbaugh and others, 2000; Hill and others, 2000). MODFLOW-2000 is a block-centered finite-difference code that solves the groundwater flow equation at the center of each model cell. Flow area and gradient through the cell represent the average area and gradient of groundwater flow through the cell.

The transport code MT3DMS, developed by Zheng and Wang (1999) and Zheng (2010), was used to simulate heat transport in the Snake Valley area. MT3DMS is a three-dimensional, finite-difference, multi-species transport model that simulates advection, dispersion, and chemical reactions of solutes in groundwater systems. For the advective component, MT3DMS uses the cell-by-cell flows computed by MODFLOW as input to determine advective transport through the model. Because the advection-dispersion equation governing solute transport and the conduction-advection equation governing heat transport have fundamentally the same form, heat can be treated as a solute. Modifications of inputs to the transport equation to simulate heat follow those suggested by Langevin and others (2008, p. 7–11).

The modeling codes used in this study to simulate groundwater flow and heat transport are not fully coupled; that is, the flow model does not take into account density and viscosity changes resulting from changes in groundwater temperature. Preliminary simulations of viscosity effects due to groundwater temperature showed that these effects were equivalent to changing the hydraulic conductivity of the hydrogeologic units used in the model by a factor of only two or three. This is well within the uncertainty in hydraulic conductivity, which spans at least 1 to 2 orders of magnitude. Additionally, the density of the groundwater would only vary up to 4 percent over the expected range of simulated temperatures. It was concluded, therefore, that a fully coupled groundwater flow and heat transport model likely would not simulate groundwater flow and heat transport with any additional accuracy, and a fully-coupled model was not required.

UCODE_2005 (Poeter and others, 2005) was used to perform sensitivity analysis, calibration (including parameter estimation through nonlinear regression), and uncertainty evaluation. Although MODFLOW-2000 contains the methods for these analyses (Hill and others, 2000), UCODE_2005 has the ability to handle parameters for multiple process input models, such as MODFLOW-2000 and MT3DMS, and runs the necessary sensitivity, calibration, and uncertainty analyses using all parameters for each input model simultaneously.

Grid Definition

The north-south-oriented grid for the model consists of 310 rows, 175 columns, and 7 layers, for a total of 379,750 cells with a constant grid-cell spacing of 804.65 m (0.5 mi). Finite-difference methods require that the model grid be constructed for the bounding rectangle of the model domain (fig. 12). The

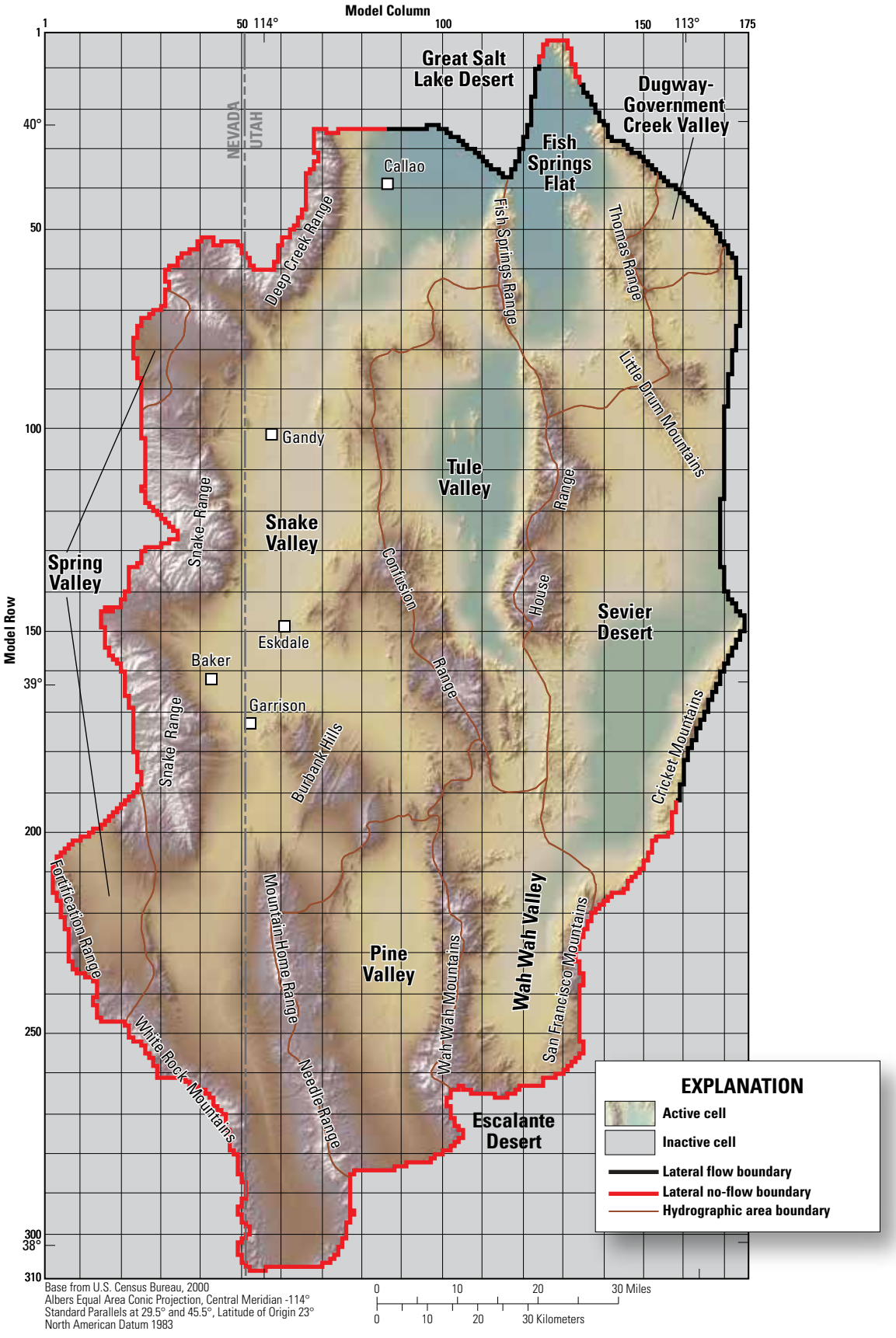

Figure 12. Location of model grid for the Snake Valley study area, Utah and Nevada.

boundary of active cells delineates the lateral boundaries of the simulated groundwater system. This boundary generally coincides with a groundwater divide along the western boundary and surface-water divides on the southern and northern boundaries.

The model uses seven layers to simulate groundwater flow and heat transport in the Snake Valley study area (fig. 13). The layers range in thickness from 5 m to more than 2,750 m (table 4 and fig. 13) and the altitude of the bottom of layer 7 is at -500 m. Model layer thicknesses generally increase with depth, allowing for greater resolution at the top of the model where more hydrologic, geologic, and thermal data are available.

All model layers were assigned as confined layers in MODFLOW-2000. The top of the groundwater system is actually unconfined, but simulating layer 1 as unconfined caused numerical instability. Simulating layer 1 as confined is a reasonable approximation if the top of the model is close to the simulated water levels in layer 1 (Faunt and others, 2011). The top of layer 1 was originally set at land surface (USGS National Elevation Dataset (NED), U.S. Geological Survey EROS Data Center, 1999); during calibration, however, it was updated to be closer to the simulated heads in layer 1. In a few isolated areas, the simulated heads in layer 1 are above land surface. These areas are generally in mountain ranges with low-permeability rocks, and discharge areas. This is expected for discharge areas, as the driving head for groundwater to discharge in ETg areas and at springs would need to be above land surface. In the mountain ranges, however, this is not a realistic condition and most likely is a result of inaccuracies produced by grid discretization and (or) uncertainties in hydrologic parameters within the mountain block. A number of these grid cells where water levels are above land surface in the mountains occur adjacent to, or within, stream channels that are not captured with the large grid cell size, or were not identified in previous studies as measured river channels.

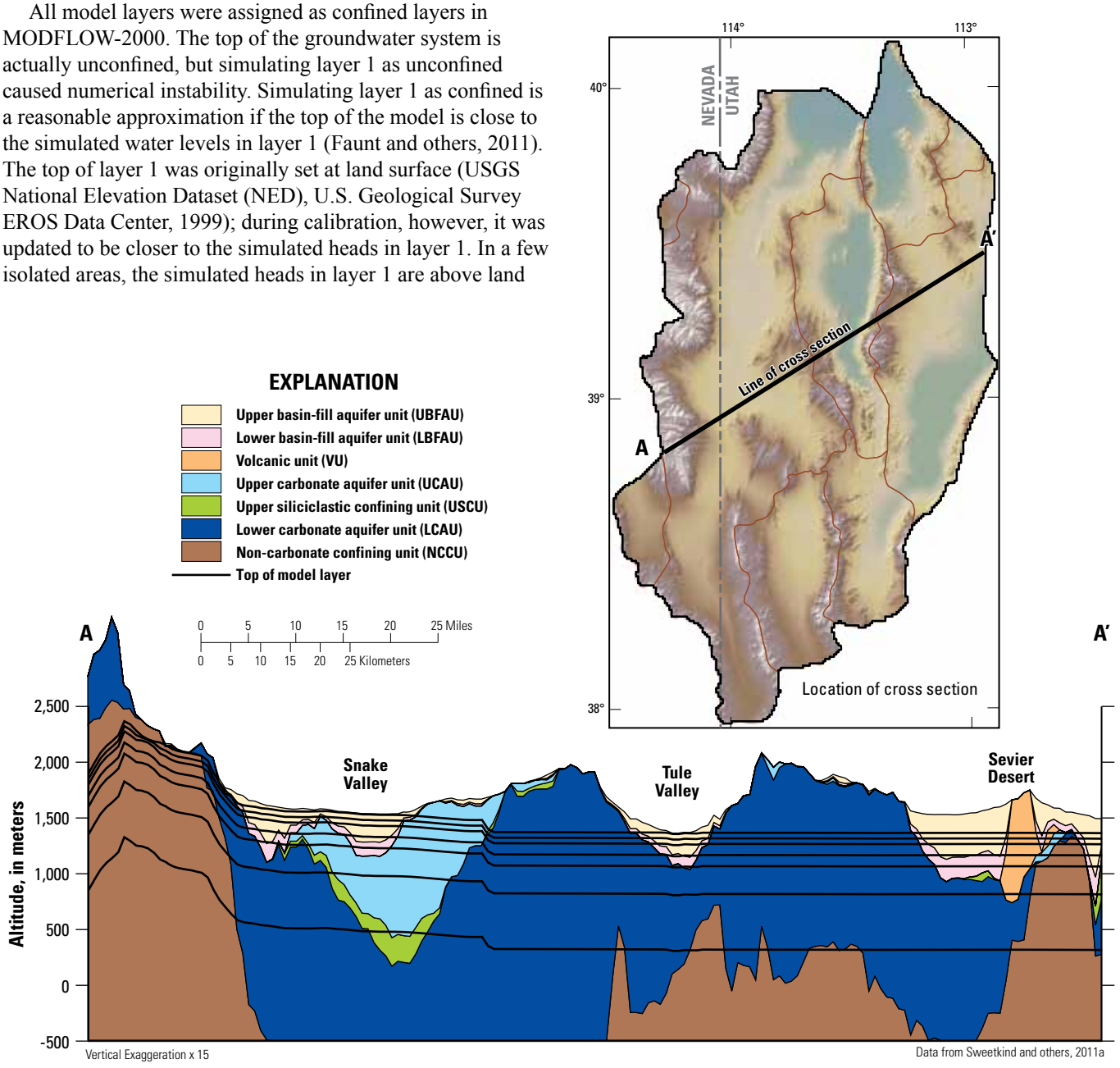

Figure 13. Northeast-trending cross section across the Snake Valley study area model domain showing hydrogeologic units and subsurface configuration of model layers.

Table 4. Thickness and depth to top of each layer in the Snake Valley area groundwater model.

Model layer	Layer thickness (meters)	Minimum depth to top of layer (meters)
1	5 to 349	0
2	5 to 50	5
3	5 to 100	10
4	5 to 100	15
5	195 to 250	20
6	500	215
7	746 to 2,754	715

Discharge within these cells, therefore, is not simulated in the model, resulting in higher water-level altitudes within these cells.

Flow Model Boundary Conditions

The boundaries chosen for the groundwater flow model describe mathematically how the simulated groundwater system interacts with the surrounding hydrologic system (Anderson and Woessner, 2002). Mathematical boundaries that are used to represent hydrologic boundaries include no-flow boundaries, specified-flux boundaries, and head-dependent flux boundaries. These boundaries define the physical limits of the simulated groundwater system and are also used to simulate recharge and discharge. No-flow boundaries are considered impermeable and no groundwater flow is simulated across them. Specified-flux boundaries allow a specified rate of water through the cell and are used to simulate all recharge, lateral inflow, and well withdrawals in this model. Head-dependent flux boundaries simulate flow across the boundary proportional to the difference in heads across the boundary and are used to simulate all discharge, except well withdrawals, in this model.

No-Flow Boundaries

Lateral no-flow boundaries (fig. 12) were defined on the basis of water-level data (Gardner and others, 2011), geologic data (Sweetkind and others, 2011b), and a larger numerical groundwater flow model developed for the eastern Great Basin (Lynette Brooks, U.S. Geological Survey, written commun., August 2010). No-flow boundaries simulated in the model include (1) the top of the Deep Creek, Snake, and Fortification Ranges, the top of the San Francisco and Cricket Mountains, and the southern boundaries of Snake, Pine, and Wah Wah Valleys where potentiometric contours indicate groundwater divides (Heilweil and Brooks, 2011) or where the relative likelihood of connection across the boundary is low based on geology (Sweetkind and others, 2011b); (2) parts of the western boundary in northern and southern Spring Valley where potentiometric contours indicate groundwater divides (Gardner and others, 2011; Heilweil and Brooks, 2011) and (or) where the larger numerical groundwater flow model indicated divergent flow (Lynette Brooks, U.S. Geological Survey, written commun., August 2010); and (3) the western and eastern parts of the northern boundary dividing Snake Valley and Fish Springs Flat from the Great Salt Lake Desert where either potentiometric contours indicate groundwater flow parallel to the boundary (Heilweil and Brooks, 2011) or the relative likelihood of connection across the boundary is low based on geology (Sweetkind and others, 2011b).

Recharge Boundaries

Recharge from infiltration of precipitation (including in-place recharge, recharge from runoff, infiltration of mountain stream base flow, and infiltration of unconsumed surface-water irrigation) and unconsumed irrigation from well withdrawals is simulated as a specified-flux boundary with the Recharge (RCH) Package (Harbaugh and others, 2000). Recharge is applied to the highest active cell (model layer 1) and defined using a multiplier array. The multiplier array represents the conceptual recharge rate at each cell in m/day (figs. 5 and 14). Parameters and zones were used to multiply the conceptual recharge rates by a constant value and were allowed to vary during calibration and parameter estimation.

In this model, BCM in-place recharge is simulated at the same location as it occurs in the BCM. The BCM, however, does not route runoff, so in this groundwater flow model, runoff that originated at higher altitudes was redistributed to cells along the mountain front that contained unconsolidated basin-fill material with a slope of 5 to 10 percent; in this way, recharge from upland runoff was accounted for where the streams enter the valleys. Recharge from mountain stream base flow was distributed to these same areas. Areal recharge of unconsumed irrigation from well withdrawals was distributed using an irrigated acreage database (Welborn and Moreo, 2007) to determine the area (or model cells) over which irrigation was applied. If there was no clear associated irrigated area for a specific well withdrawal indicated in the database, the recharge was applied to the cell in which the well was located.

Additionally, recharge from subsurface inflow was simulated across part of the eastern boundary using a specified-flux boundary by placing injection wells in all seven model layers along the boundary (fig. 15) using the Well (WEL) Package (Harbaugh and others, 2000). The specified flux applied to each of the wells was estimated using simulated groundwater flow amounts taken from a larger groundwater model that encompasses the Snake Valley area (Lynette Brooks, U.S. Geological Survey, written commun., August 2010). A parameter was used to multiply the specified-flux rate by a constant value and was allowed to vary during calibration and parameter estimation.

Discharge Boundaries

Discharge is simulated to evapotranspiration, springs, mountain streams, wells, and as subsurface outflow to the north (fig. 6). Discharge to evapotranspiration, springs,

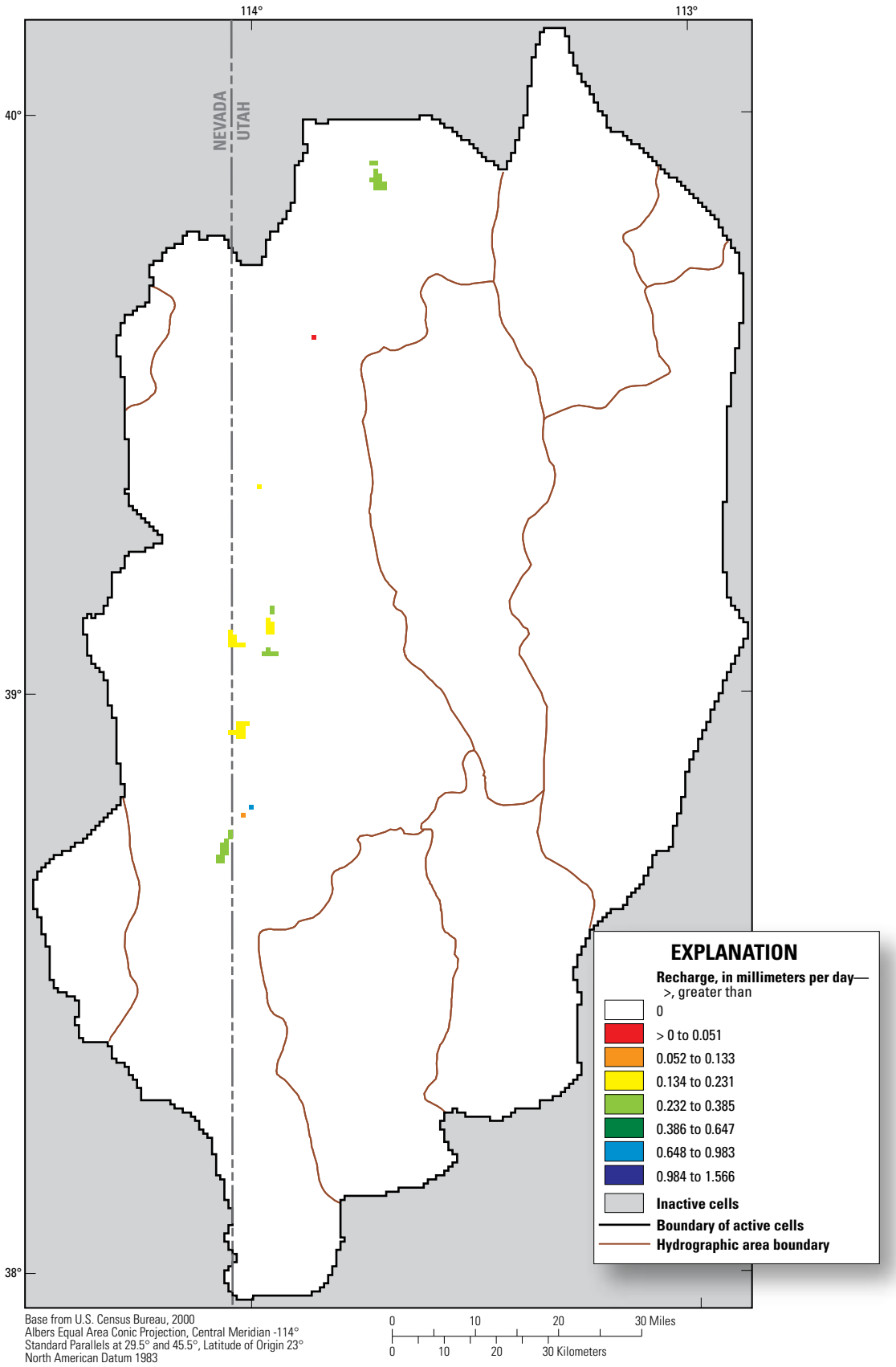

Figure 14. Conceptual rate and distribution of recharge from unconsumed irrigation from well withdrawals simulated in the Snake Valley area groundwater model.

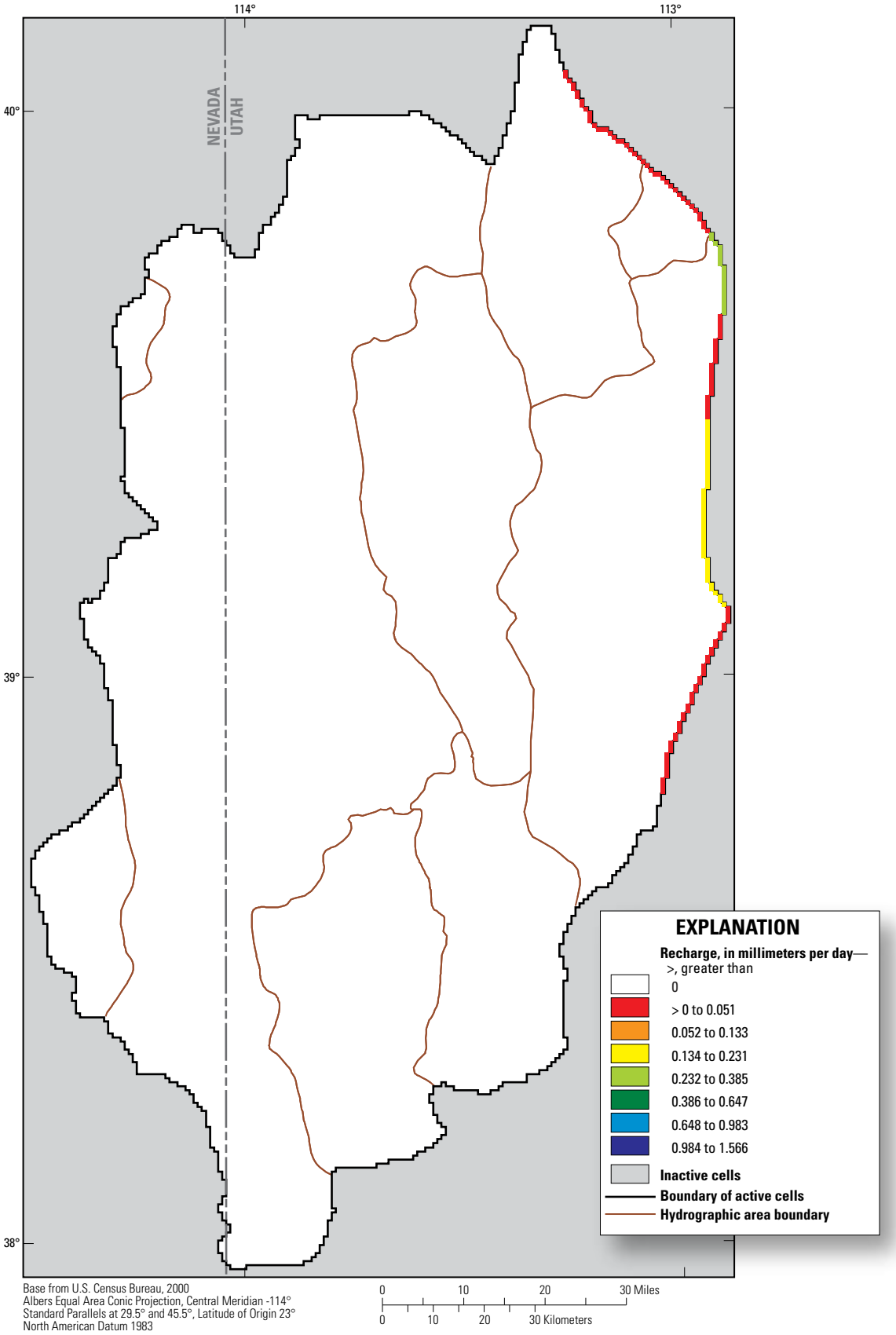

Figure 15. Conceptual rate of subsurface inflow from adjacent areas simulated in the Snake Valley area groundwater model.

mountain streams, and subsurface outflow is simulated using head-dependent flux boundaries, and well withdrawals are simulated using specified-flux boundaries.

Evapotranspiration

Groundwater discharge to evapotranspiration (ETg) is simulated in layer 1 (fig. 6) with the Evapotranspiration (EVT) Package (Harbaugh and others, 2000). Data required for the EVT Package are the altitude of the ETg surface, the extinction depth, and the maximum ETg rate. The simulated ETg rate varies linearly between the extremes of no ETg when the simulated water level is below the extinction depth, and the maximum ETg rate when the simulated water level is at or above the altitude of the ETg surface (Anderson and Woessner, 2002). The altitude of the ETg surface was estimated using the NED and was defined as the minimum land-surface altitude within each model cell. The minimum land-surface altitude was used to minimize vertical accuracy errors of the NED which average plus or minus 7 m. ETg studies in the area have shown that the maximum rooting depth of certain phreatophytes can be as much as 35 to 60 ft (Moreo and others, 2007). An extinction depth of 12 m (about 40 ft), therefore, was used for all areas of evapotranspiration.

Simulated ETg areas were defined using digital data from two regional scale studies (Smith and others, 2007; Buto, 2011; Masbruch and others, 2011). These studies used a combination of satellite and aerial photographic imagery, as well as field reconnaissance and mapping techniques, to define the outer extent of phreatophyte areas (based on plant species), including playas, where groundwater may be consumed by evapotranspiration (Masbruch and others, 2011). The maximum ETg rate for each area was calculated by dividing the estimated conceptual volumetric discharge of ETg by the size of the simulated ETg area and, therefore, is constant across each area. The maximum rate of ETg was assigned to each model cell using a multiplier array (fig. 16). Parameters and zones were used to multiply the maximum rate of evapotranspiration by a constant value and were allowed to vary during calibration and parameter estimation.

Springs

Discharge to 12 point springs and one area spring (fig. 6) within the model domain was simulated using the Drain (DRN) Package (Harbaugh and others, 2000). The DRN Package simulates a head-dependent flux boundary for each cell to which it is assigned, and discharge is a function of the simulated water level and drain conductance (McDonald and Harbaugh, 1988). Data required for the DRN Package are altitude and conductance of the drain. A parameter was used to define the conductance and was allowed to vary during model calibration and parameter estimation. The altitude of each drain was originally set at land surface and was varied to no more than 10 m below the minimum land-surface altitude within each cell during calibration to account for springs being located in land-surface depressions that are lower than would be evident in the top surface of the model. Additionally, drains were originally inserted into all layers within the model, and during calibration drains in the lower layers were removed at some of the springs.

This model simulates discharge to springs in the mountains. Previous studies have assumed that the regional water table is below the altitude of mountain springs and that discharge from those springs represents perched discharge from locally-derived recharge (Harrill and Bedinger, 2004). Discharge to mountain springs was simulated in the model for the following reasons: (1) the BCM is used to estimate recharge and ignoring the discharge of higher-altitude springs would require a reduction in recharge equal to the discharge from those springs; (2) although downward vertical gradients likely exist in mountain recharge areas, it is unlikely that all mountain springs are separate from the regional groundwater system; (3) ignoring discharge to mountain springs assumes that water levels in the mountains are about the same as water levels in the adjacent valleys and does not account for recharge mounds that probably occur beneath high-recharge areas in the mountains; and (4) simulating discharge to mountain springs provides sensitivity to model parameters within the mountain block.

Mountain Streams

Similar to mountain spring discharge, simulating rivers in the mountains provides sensitivity to model parameters within the mountain block, and ignoring the groundwater discharge to mountain streams does not account for recharge mounds that probably occur beneath high-recharge areas in the mountains. Discharge representing base flow to five mountain streams (fig. 6) in layer 1 was simulated using the River (RIV) Package (Harbaugh and others, 2000). The RIV Package simulates a head-dependent flux boundary for each cell to which it is assigned, and will allow recharge or discharge to a cell that is a function of the simulated water level and riverbed conductance, which accounts for the geometry of the river channel (Anderson and Woessner, 2002). Data required for the RIV Package are river stage, or hydraulic-head (water-level) altitude, conductivity of the riverbed, and the altitude of the bottom of the riverbed (Harbaugh and others, 2000). Only gaining portions of mountain streams are simulated in the model; losing portions of the streams contributing recharge to the aquifer were distributively simulated in cells along the mountain front that contained unconsolidated basin-fill material with a slope of 5 to 10 percent (see "Recharge Boundaries" section of this report). Because only gaining portions were simulated, the river stage and river bottom were both set at the minimum land-surface altitude within each cell. A parameter was used to define the conductance and was allowed to vary during model calibration and parameter estimation.

Well Withdrawals

Discharge to 63 irrigation wells (fig. 6) was simulated in layers 1 through 3 with the Well (WEL) Package (Harbaugh

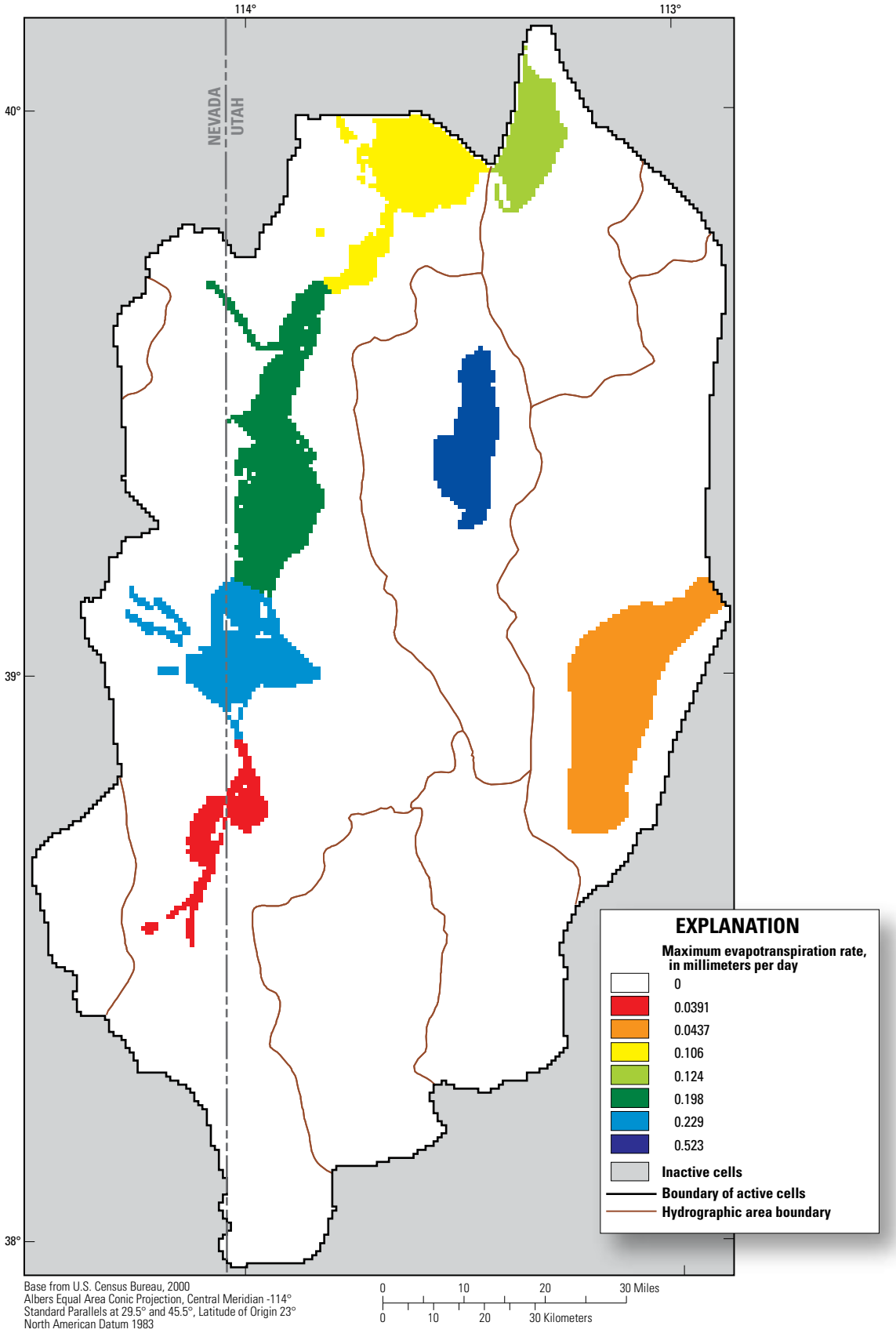

Figure 16. Maximum groundwater evapotranspiration rate simulated in the Snake Valley area groundwater model.

and others, 2000). The WEL Package simulates a specified-flux boundary in each cell to which a well is assigned. Data required for the WEL Package are the withdrawal rates in each layer. For the wells in which the withdrawals were estimated as part of the Utah statewide groundwater use monitoring program (Burden and others, 2011), the distribution of withdrawals among layers for each well was determined by multiplying the total withdrawal rate by the proportion of the open interval in each layer. For example, if 75 percent of the open interval of a well was in layer 1 and 25 percent of the open interval was in layer 2, the withdrawal rate assigned to the well in layer 1 was 75 percent of the total withdrawal for the well, with the remaining 25 percent of the withdrawal assigned as the withdrawal rate in layer 2. For the well withdrawals from the center pivots in the southern part of the study area east of Big Springs, 11 wells were inserted into layers 1 and 2 approximately at the center of each pivot, and the withdrawal rate for each well was split evenly between the two layers. A parameter was used to define a multiplier on the withdrawal rate for all of the wells and was allowed to vary during model calibration and parameter estimation.

Subsurface Outflow

Water levels and geology suggest that there may be some subsurface groundwater outflow from northern Snake Valley and western Fish Springs Flat towards the Great Salt Lake Desert (Heilweil and Brooks, 2011; Gardner and others, 2011). Previous estimates of this subsurface outflow, however, vary widely (Hood and Rush, 1965; Harrill and others, 1988; Welch and others, 2007). Because of the uncertainty in the amount of outflow, the center part of the northern boundary of the model was simulated as a head-dependent flux boundary (fig. 6) using the General-Head Boundary (GHB) Package (Harbaugh and others, 2000). The GHB was simulated where either potentiometric contours indicate groundwater flow perpendicular to the boundary (Heilweil and Brooks, 2011) or the relative likelihood of connection across the boundary was uncertain based on geology (Sweetkind and others, 2011b). The GHB Package takes as input the conductance between the aquifer cell and the boundary, and the water-level altitude at the boundary. The difference between this boundary water-level altitude and the simulated water-level altitude in the cell dictates whether water will enter or leave the model domain through this boundary. If the simulated water-level altitude is less than the boundary water-level altitude, water will enter the model through this boundary; if the simulated water-level altitude is greater than the boundary water-level altitude, water will leave the model through this boundary.

The conductance used in the GHB Package was based on the cross-sectional area for each cell across all seven layers. A parameter was used to define the conductance and was allowed to vary throughout model calibration and parameter estimation. The head at the boundary was set at 1,305 m (Heilweil and Brooks, 2011).

Heat Transport Model Boundary Conditions

The boundaries chosen for the heat transport model describe mathematically how the simulated groundwater system interacts with the surrounding thermal system. Mathematical boundaries that are used to represent thermal boundaries include no-flux boundaries, specified-flux boundaries, and specified-temperature boundaries. No-flux boundaries were used to represent the lateral boundaries of the model as it was assumed that no additional heat was crossing these boundaries. Specified-flux boundaries allow a specified rate of heat flow through the cell and are used to simulate heat flux across the base of the model. Specified-temperature boundaries are used to simulate the temperature across the top of the water table, as well as recharge temperatures in the model.

Basal Heat Flux

Basal heat flux, the amount of heat that is transferred conductively from the interior of the Earth across the base of the model, was simulated using the Source/Sink Mixing (SSM) Package in MT3DMS (Zheng and Wang, 1999). The SSM Package allows for point sources of heat to be defined that are independent of the flow solution by using the "mass-loading source" option, which was needed because the bottom boundary of the groundwater flow model was assigned as a no-flow boundary. The heat transport equivalent of this mass-loading source can be calculated using the following equation (Langevin and others, 2008):

$$\dot{M}_T = \frac{\dot{E}}{\rho_f c_{Pfluid}} \tag{1}$$

where

$\dot{M}_T$ is the mass-loading source for heat transport per model cell, in degrees Celsius cubic meters per second (°Cm^3/s),

$\dot{E}$ is the heat flux per cell, in watts (W),

ρ_f is the fluid (groundwater) density, and is equal to 1,000 kilograms per cubic meter (kg/m^3), and

c_{Pfluid} is the specific heat capacity of the fluid (groundwater), and is equal to 4,186 Joules per kilogram degrees Celsius (J/kg°C).

The heat flux for each cell across the base of the model was defined as a parameter and was allowed to vary during model calibration and parameter estimation.

Specified Temperature

The top layer of the model was simulated using a specified-temperature boundary condition (fig. 17) to allow for conduction of heat out of the top of the model, except at cells used to simulate spring discharge or the general-head boundary where advective heat loss through groundwater discharge dominates

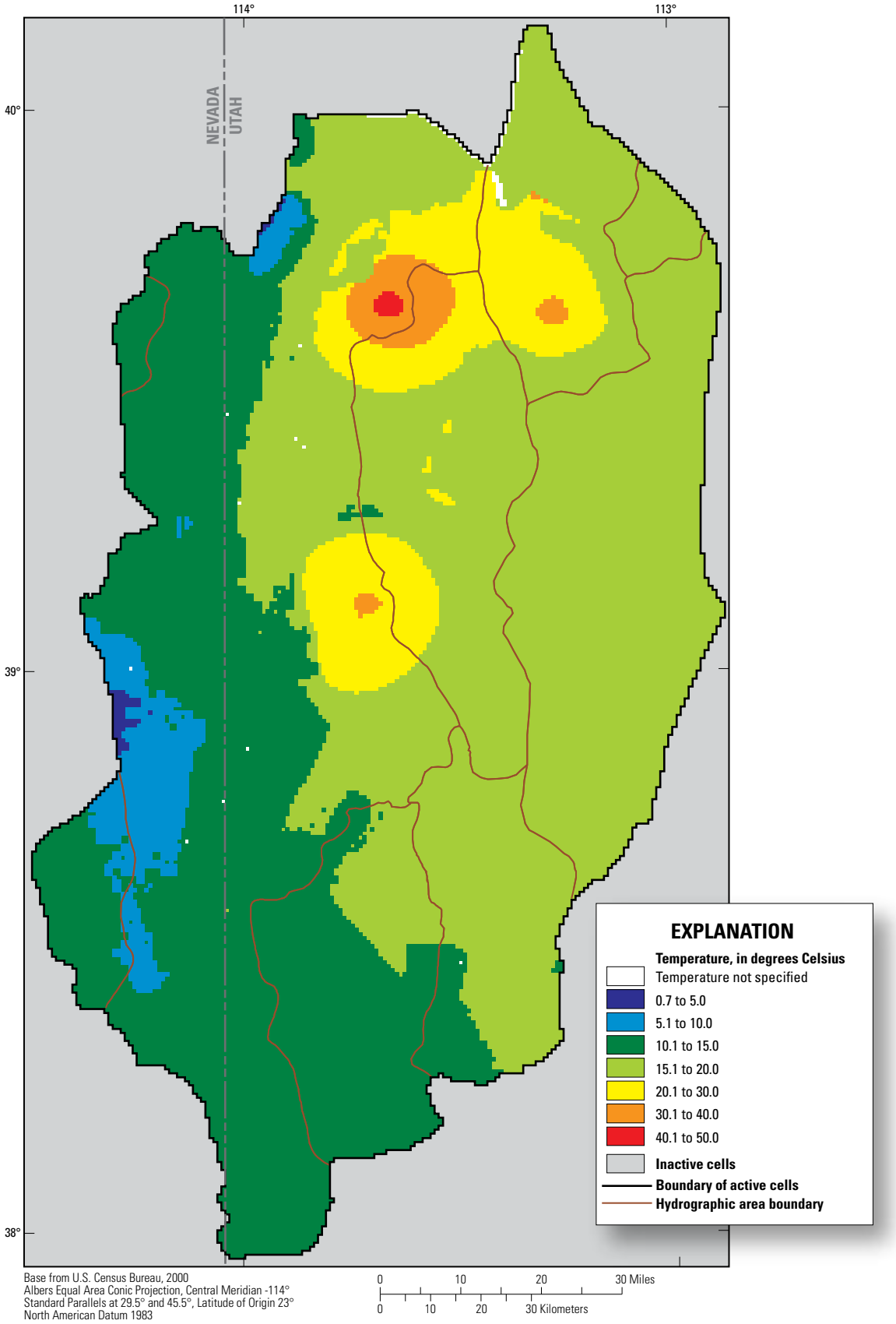

Figure 17. Distribution of specified temperatures assigned to layer 1 in the Snake Valley area groundwater model.

over conductive heat loss. In an early model simulation, groundwater temperatures in layer 1 were only specified in areas where no groundwater recharge or discharge occurred. This led to unreasonably warm simulated temperatures in both the recharge and discharge areas, by a factor of at least two and up to five, and resulted in model instability. A rough calculation showed that heat transport by groundwater advection through the top of the model in the groundwater recharge and ETg areas was diffuse enough to approximately equal heat transport by conduction calculated in adjacent areas with no advective flux out of the top of the model. By not specifying the temperature at the top of the model in the recharge and ETg areas and, thereby, not accounting for conductive heat transport through these cells, total heat transport across the top model boundary was not being correctly accounted for.

Because the top of the model represents the water table, three interpolated datasets were used to calculate the specified temperatures used to represent temperatures at the water table. The first dataset is a natural neighbor interpolation (fig. 18) using 23 measured water-table temperatures (Blackett, 2011) from the newly installed UGS wells and temperatures at 50 springs (National Water Information System database, accessed on October 28, 2010); this dataset was used to better represent the temperatures at the deeper water tables measured at a number of the UGS wells. The cooler temperatures from the springs in the House and Deep Creek Ranges were not used as it was assumed that these springs represent local perched water tables, based on noble gas recharge temperatures calculated for water from wells downgradient of these ranges (Gardner and Heilweil, 2014) and do not represent the regional system. The second dataset is a lapse curve (fig. 19*A*) derived from temperatures measured in 95 springs and shallow (less than 100-ft depth below land surface) wells (Pavelko, 2007; National Water Information System database, accessed on October 28, 2010; Blackett, 2011) throughout the study area; this relation was used to project water-table temperatures into the mountains. The third dataset is a lapse curve (fig. 19B) derived from noble gas recharge temperatures and altitudes calculated for water from several wells and springs in the study area (Gardner and Heilweil, 2014); this relation was used for water-table temperatures in the carbonates in the southern part of the Snake Range. Groundwater recharge temperatures were set equal to these same specified temperatures used in layer 1.

Hydraulic Properties

The nine hydrogeologic units (HGUs) described in Sweetkind and others (2011a) form the basis for assigning horizontal hydraulic conductivity and vertical anisotropy to the cells of the model grid using the Hydrogeologic-Unit Flow (HUF) Package (Anderman and Hill, 2000). Zone arrays in MODFLOW-2000 were used to account for variations in hydraulic properties within an HGU. The HUF Package was chosen because it easily facilitates the discretization of the complicated geometry of the HGUs within the model (Faunt and others, 2010). Hydrogeologic structures that act as barriers to groundwater flow were simulated using the Horizontal-Flow Barrier (HFB) Package (Harbaugh and others, 2000).

Hydrogeologic Units

The HUF Package (Anderman and Hill, 2000) takes as input the tops and thicknesses of each HGU, and allows the hydraulic conductivity of the HGUs to be defined through zones and parameters. The HGUs are assigned to model cells in the HUF Package. Some model cells are filled by a single HGU, while other model cells may contain multiple HGUs. The HUF Package calculates the effective hydraulic conductivity in both the vertical and horizontal directions for each cell based on the hydraulic properties and thicknesses of the HGUs present within the cell (Anderman and Hill, 2000).

Of the nine HGUs defined in the hydrogeologic framework developed for the GBCAAS (Sweetkind and others, 2011a), seven exist in the current study area (figs. 20 to 26) and are defined in the HUF package. Each of these HGUs are stratigraphically and structurally heterogeneous, and all but the USCU were further divided into a number of zones based on depositional and structural characteristics; these zones are defined in chapter B of the GBCAAS study (Sweetkind and others, 2011a). Many of these zones do not have independent measurements of hydraulic conductivity from aquifer tests, and the relative differences in hydraulic conductivity are defined on other hydrogeologic information (Sweetkind and others, 2011a). Initial HGU parameters defined for the model were based on these zones and were allowed to vary during calibration and parameter estimation.

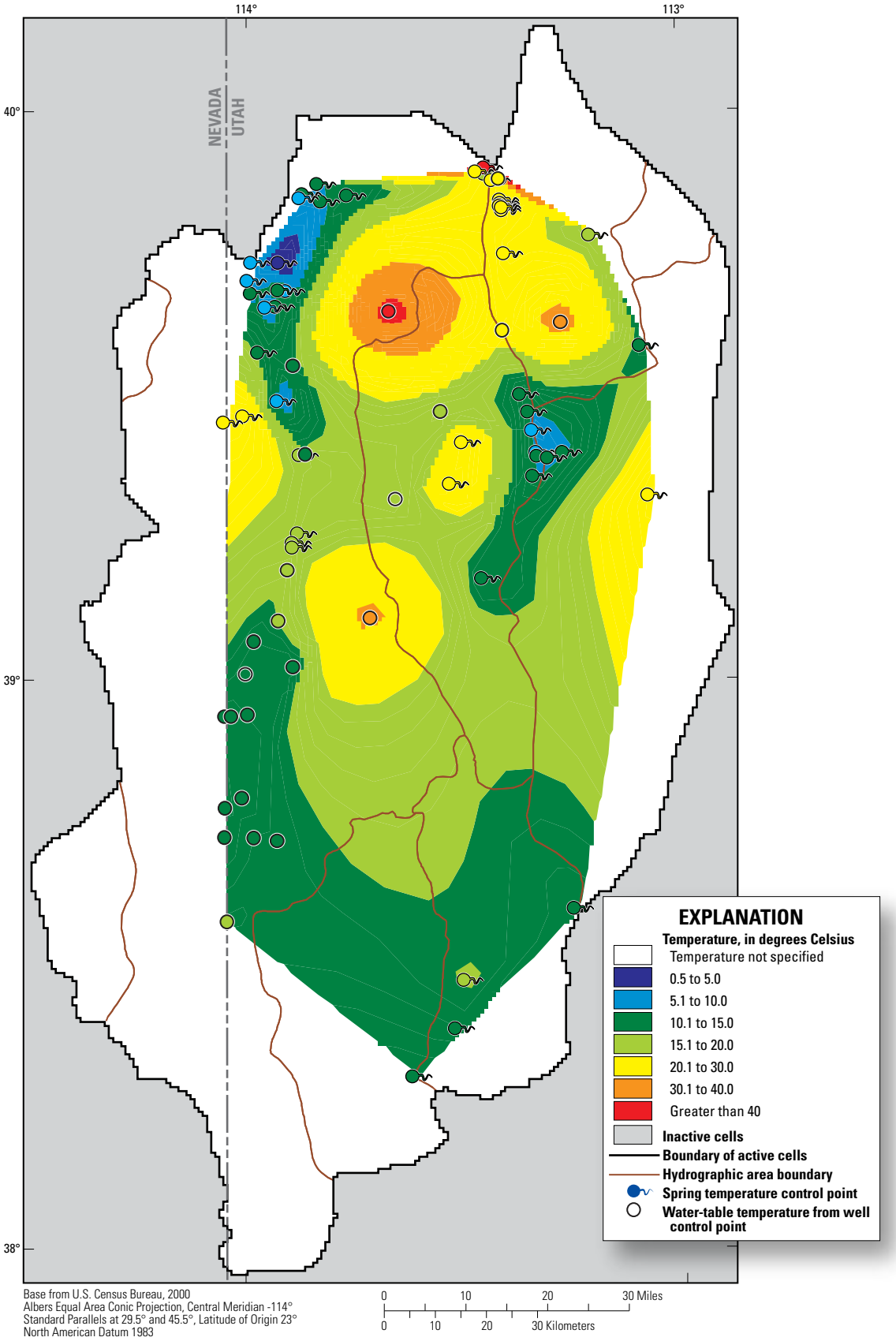

Figure 18. Water-table temperature control points and calculated water-table temperatures in the Snake Valley study area, Utah and Nevada, using natural neighbor interpolation.

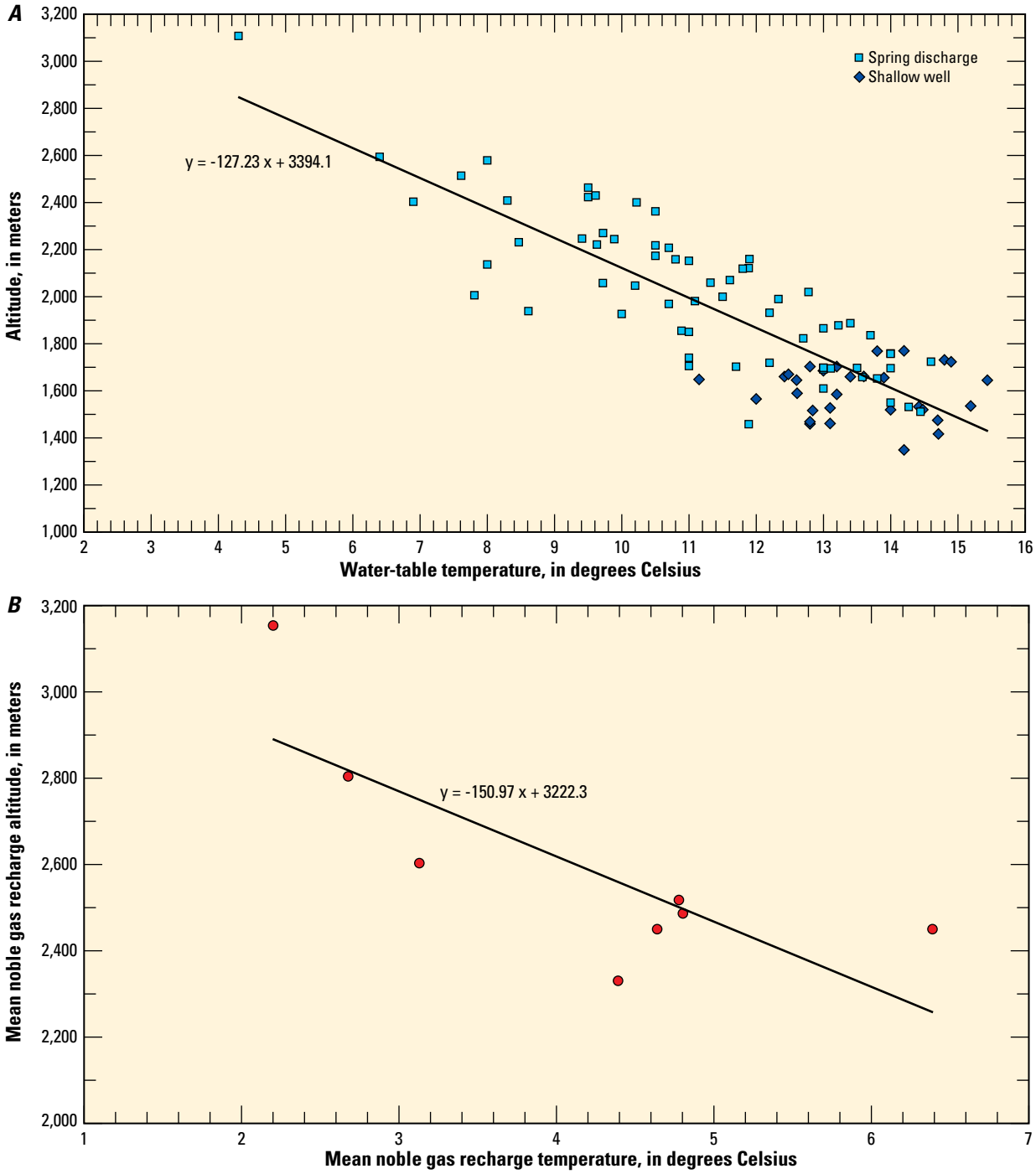

Figure 19. Derived lapse curves from *A*, springs and shallow wells, and *B*, noble gas recharge temperatures and altitudes from selected wells and springs in the Snake Valley study area, Utah and Nevada.

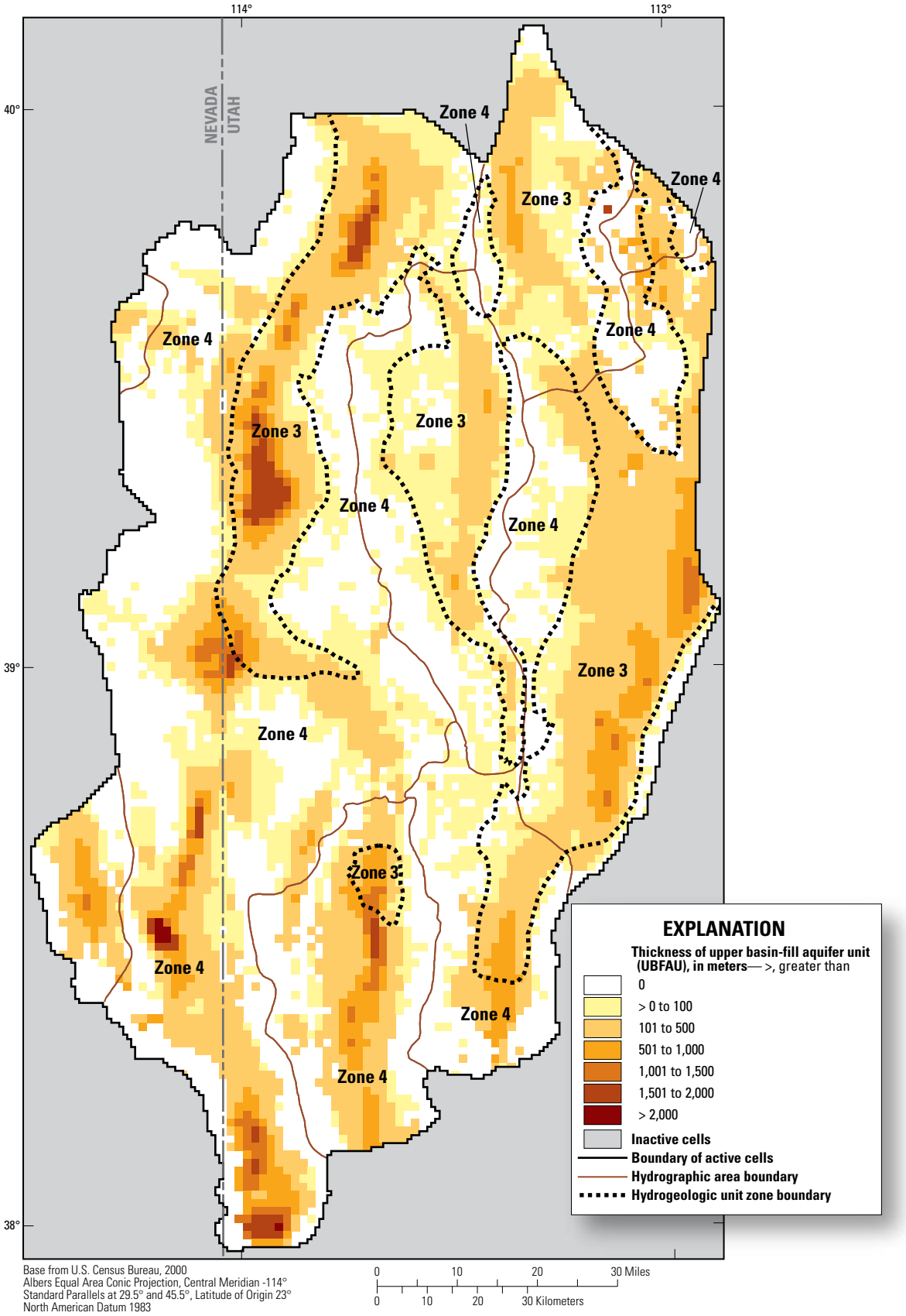

Figure 20. Simulated extent, thickness, and initial hydrogeologic unit zones of the upper basin-fill aquifer unit (UBFAU) in the Snake Valley area groundwater model.

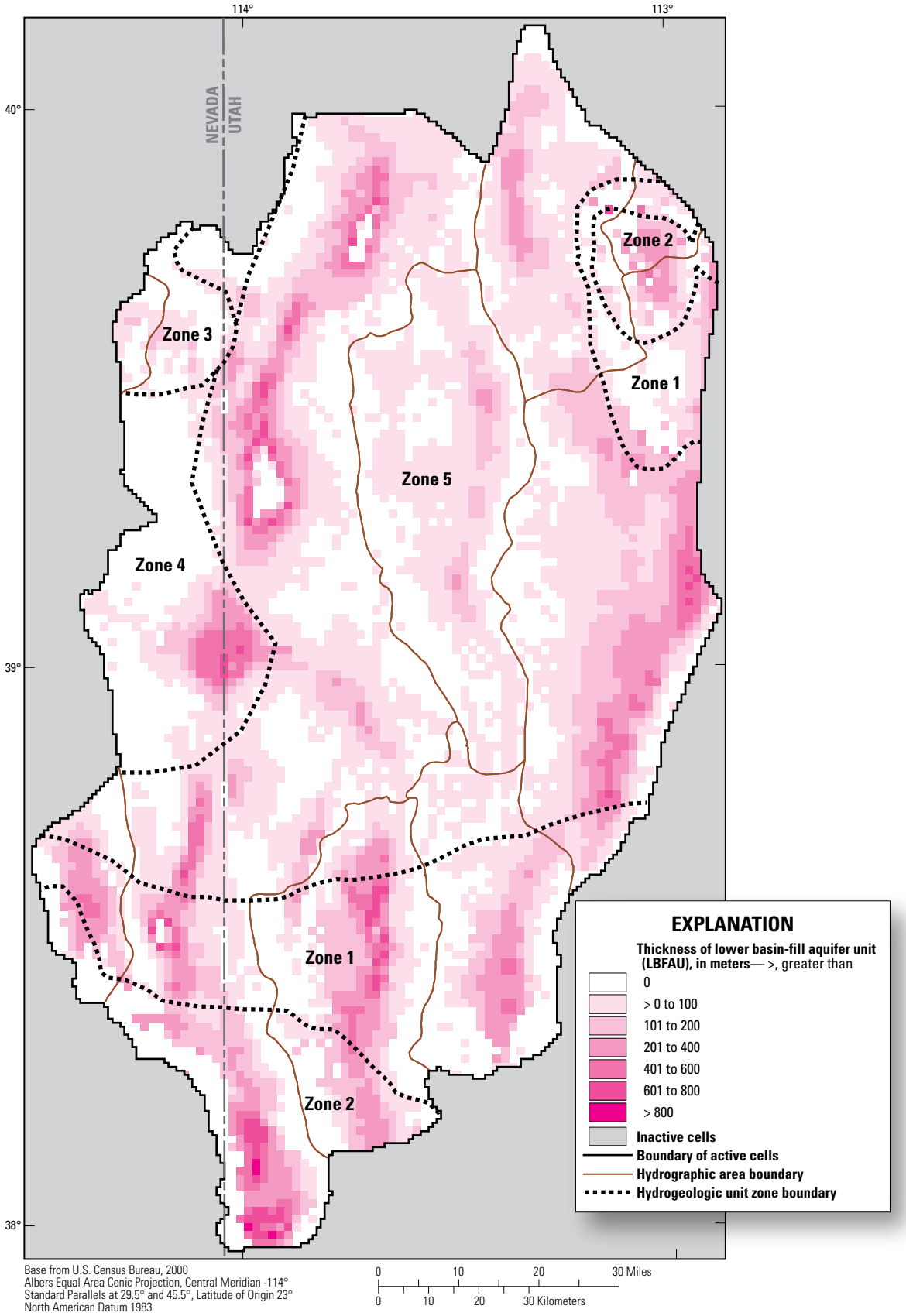

Figure 21. Simulated extent, thickness, and initial hydrogeologic unit zones of the lower basin-fill aquifer unit (LBFAU) in the Snake Valley area groundwater model.

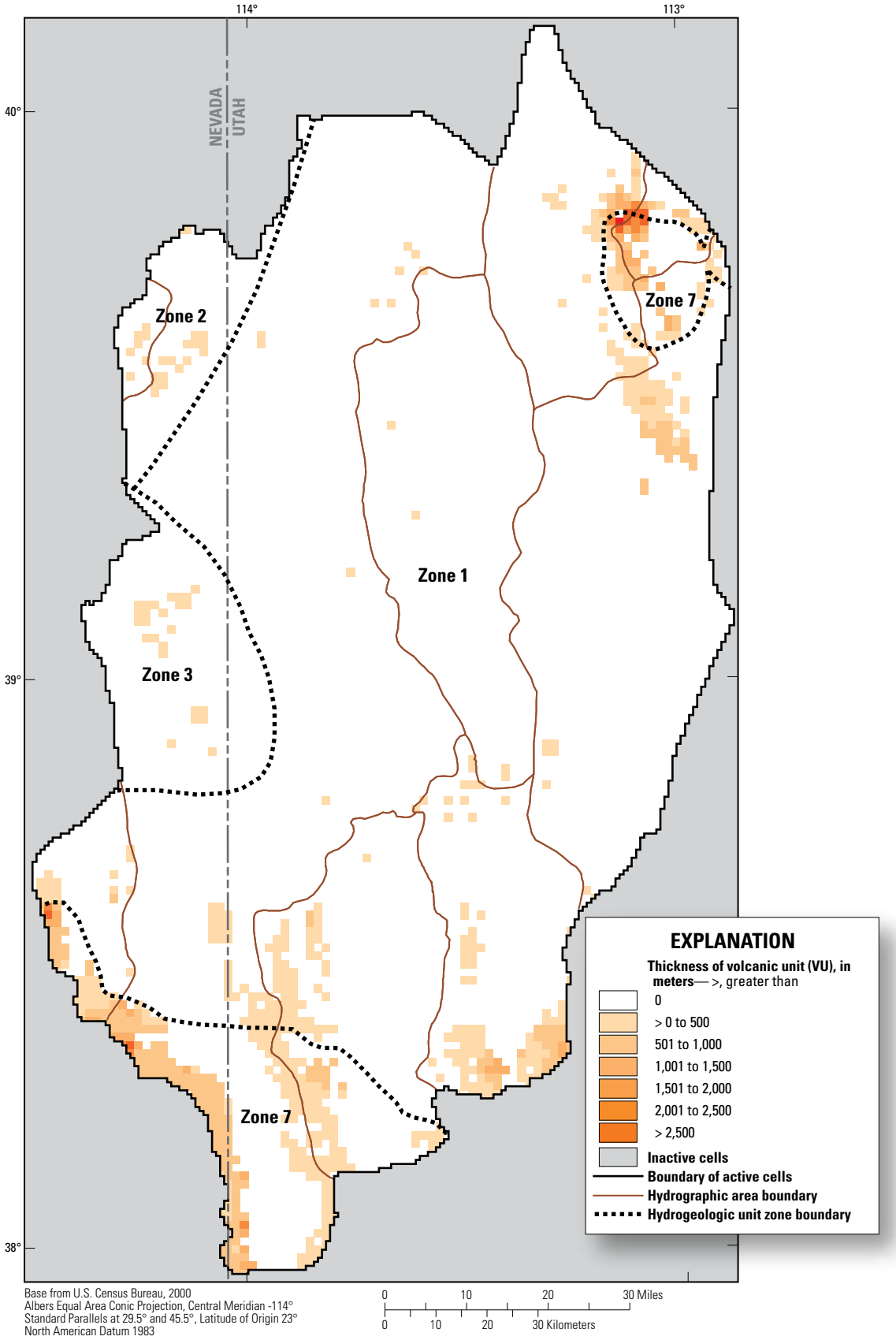

Figure 22. Simulated extent, thickness, and initial hydrogeologic unit zones of the volcanic unit (VU) in the Snake Valley area groundwater model.

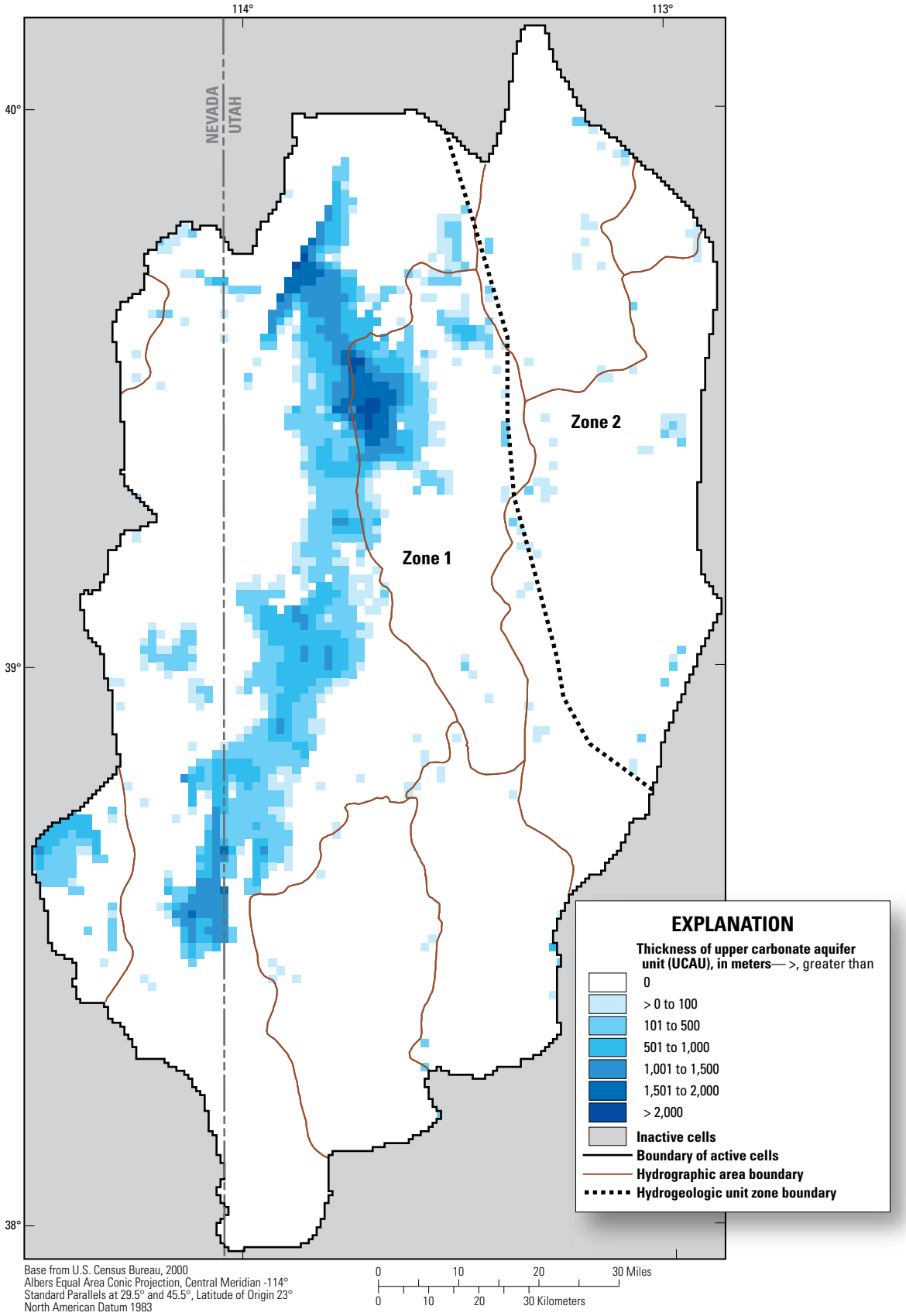

Figure 23. Simulated extent, thickness, and initial hydrogeologic unit zones of the upper carbonate aquifer unit (UCAU) in the Snake Valley area groundwater model.

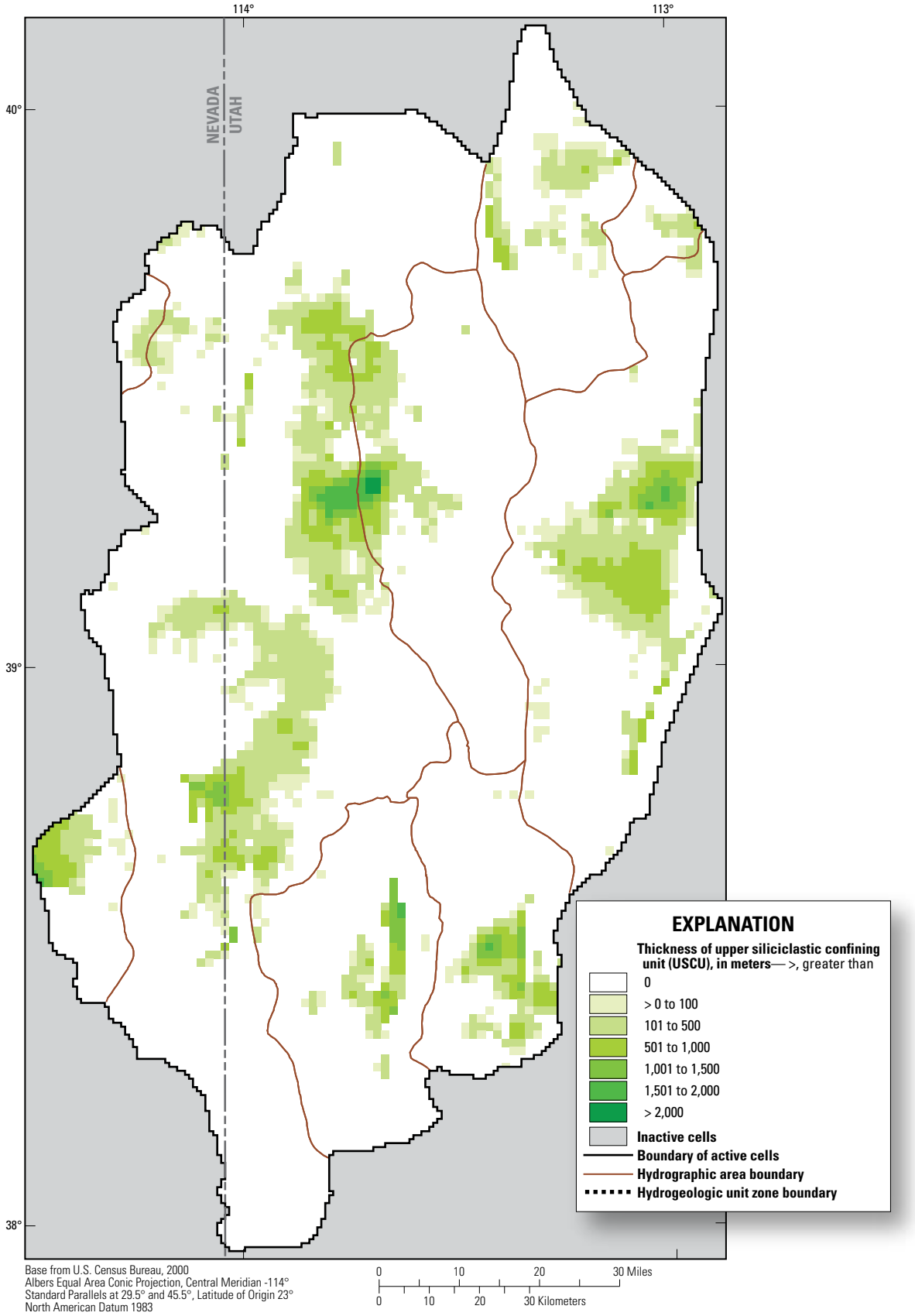

Figure 24. Simulated extent and thickness of the upper siliciclastic confining unit (USCU) in the Snake Valley area groundwater model.

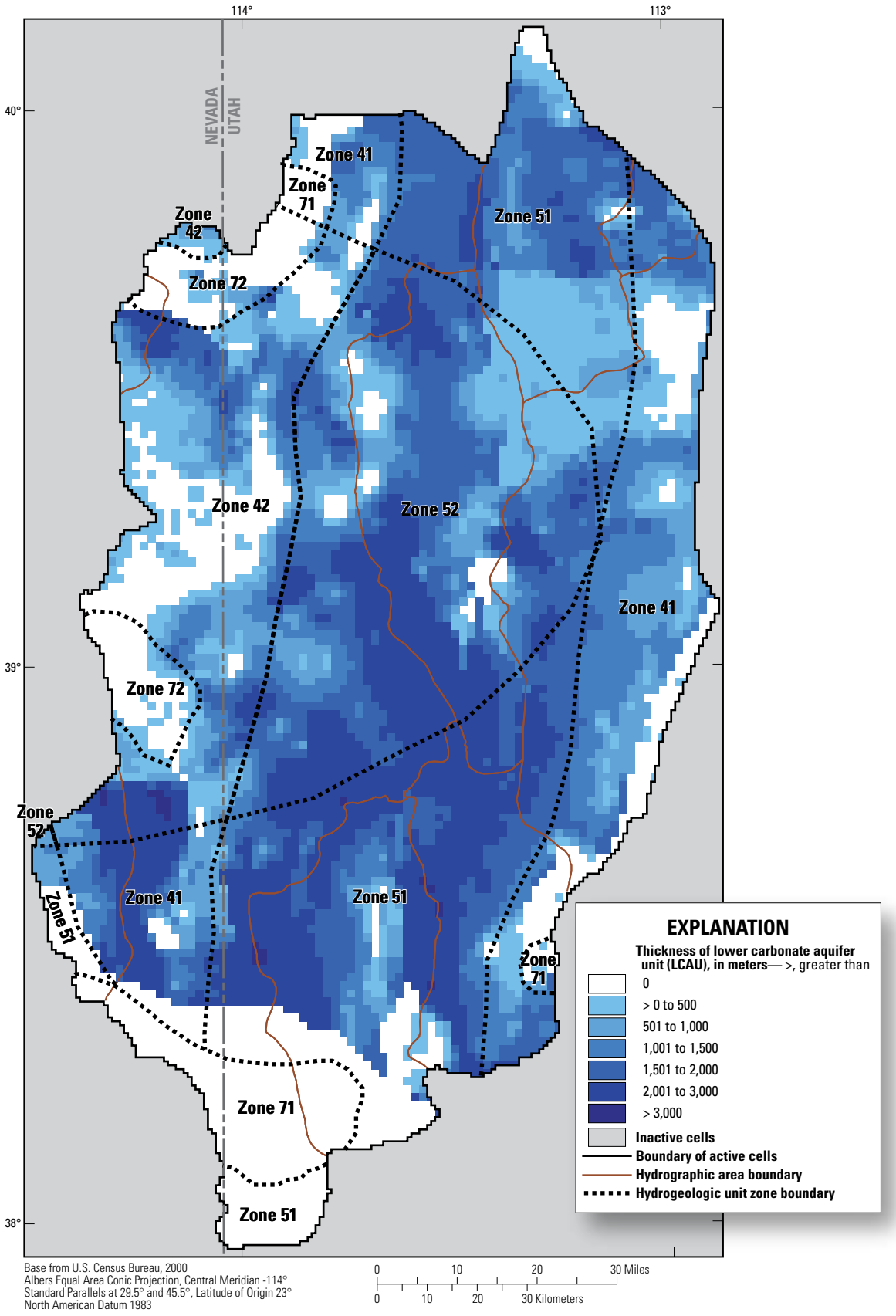

Figure 25. Simulated extent, thickness, and initial hydrogeologic unit zones of the lower carbonate aquifer unit (LCAU) in the Snake Valley area groundwater model.

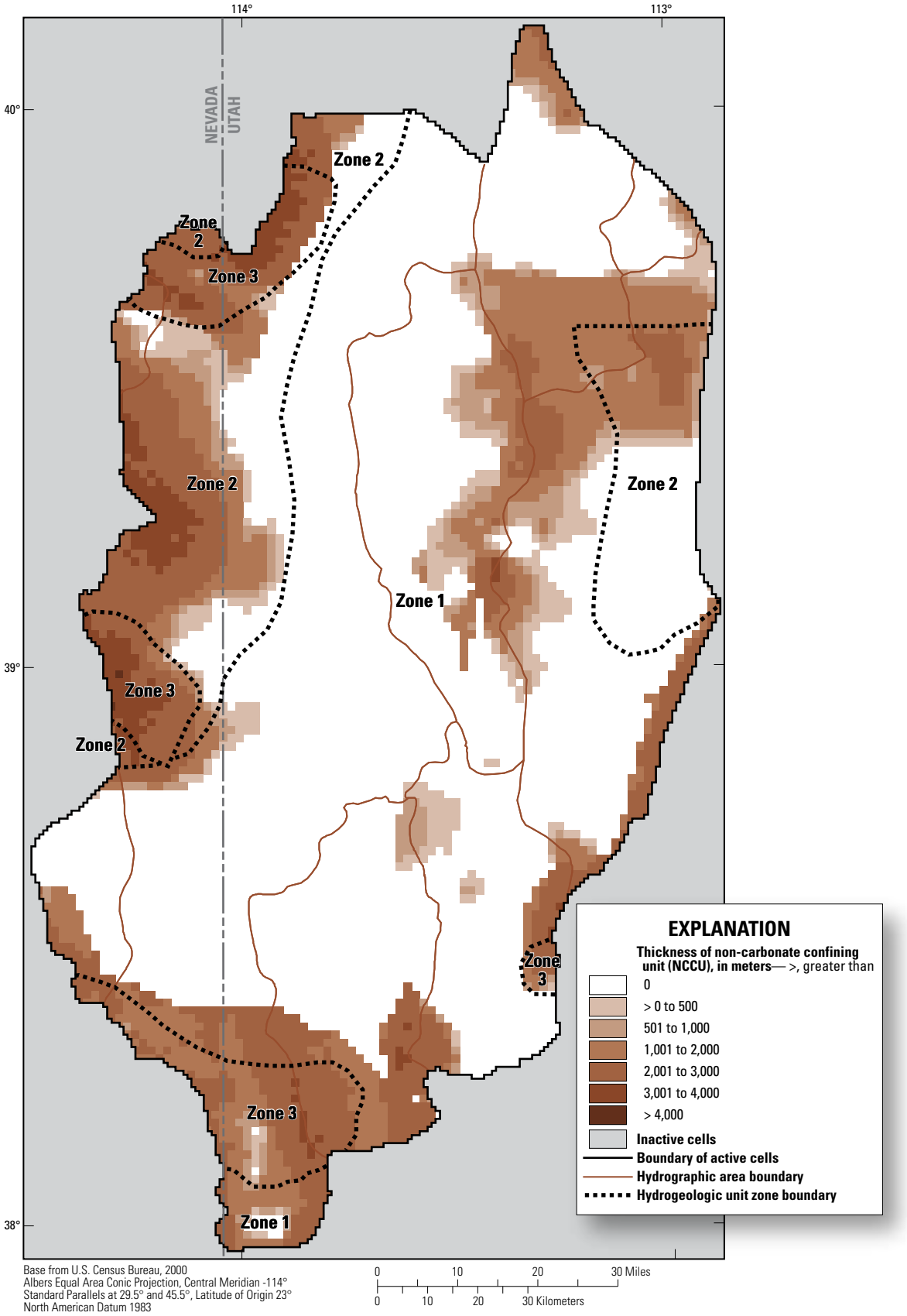

Figure 26. Simulated extent, thickness, and initial hydrogeologic unit zones of the non-carbonate confining unit (NCCU) in the Snake Valley area groundwater model.

Vertical Anisotropy

Vertical anisotropy, the ratio of horizontal hydraulic conductivity to vertical hydraulic conductivity, was defined for each HGU parameter by using the HUF package. Because of their layered nature, and the existence of playa and prehistoric Lake Bonneville deposits (Sweetkind and others, 2011a), the basin-fill HGUs are likely to have significant vertical anisotropy (Domenico and Schwartz, 1998). The carbonate and other consolidated-rock HGUs are likely to have relatively small vertical anisotropy due to the assumed presence of solution features and fractures, respectively (Faunt and others, 2010, table F-13). Parameters were defined to represent vertical anisotropy for different HGUs and were allowed to vary during model calibration and parameter estimation.

Horizontal-Flow Barriers

Observed water levels and the existence of some springs in the study area indicate distinct variability in the hydraulic gradient. Areas where the gradient steepens abruptly or where discharge from a spring occurs could not always be simulated using only changes in the hydraulic conductivity within model cells. In these areas, simulated horizontal-flow barriers using the HFB Package (Harbaugh and others, 2000) were used to reduce the hydraulic conductivity between model cells. The HFB Package takes as input the location of the horizontal-flow barrier and the hydraulic characteristic of the barrier, which is the hydraulic conductivity of the barrier divided by the width of the barrier. The HFB Package allows the value of the hydraulic characteristic of the barrier to be defined as a parameter. Simulated horizontal-flow barriers in the model are located along cell boundaries to approximate the location of the features. The horizontal-flow barrier between Snake Valley and Pine and Tule Valleys (B_SV_NS1) corresponds with a steeply, almost vertically dipping synclinal limb of the USCU (fig. 27); this HFB is simulated in all seven layers, except for a short section near the center of the length of the HFB where there is a slight break in the USCU. The horizontal-flow barriers near Gandy Warm Springs in northern Snake Valley (B_SV_GWS) and Wah Wah Springs in Wah Wah Valley (B_SV_WWS) correspond to mapped faults in the study area (fig. 27); these HFBs are simulated in all seven layers in the model. Parameters representing the hydraulic characteristic of the horizontal-flow barriers were defined and allowed to vary during model calibration and parameter estimation.

Thermal Properties

Five additional thermal properties that are required for the heat transport model are porosity, thermal diffusivity, dispersivity, bulk density, and the thermal distribution factor. These are assigned in MT3DMS in arrays that represent each model layer (Zheng and Wang, 1999). The equations that were used to calculate each of these parameters are shown in appendix 1.

Porosity

Porosity is defined as the percentage of rock that is void space (Domenico and Schwartz, 1998). It is needed in transport models to define the volume of water containing solute, in this case heat, in the bulk volume of the system. It is also needed to compute the bulk thermal conductivity and bulk density of the system (appendix 1).

Because a model cell may contain multiple HGUs, the porosity for each cell was calculated using a thickness weighted mean for each HGU within the cell (appendix 1). It was assumed that the UBFAU, LBFAU, and VU have a porosity of 0.3 (middle of range of porosities for sediments and basalts reported in Domenico and Schwartz, 1998); that the UCAU and LCAU have a porosity of 0.1 on the basis of the reported range for carbonates in the Great Basin (Harrill and Prudic, 1998); and that the USCU and NCCU have a porosity of 0.01 on the basis of a model using similar rock types (Manning and Solomon, 2005). Early simulations showed that the model was insensitive to porosity; these values were held constant and not included in sensitivity analysis or regression.

Thermal Diffusivity

Thermal diffusivity, which is analogous to molecular diffusion in solute transport (Langevin and others, 2008), is used to define the heat transport process of thermal conduction within the system. The thermal diffusivity is dependent on the bulk thermal conductivity of the aquifer (includes both the solid aquifer material and the fluid in the pore spaces, in this case groundwater), the porosity of the aquifer, the density of the groundwater, and the heat capacity of the groundwater (appendix 1).

Thermal diffusivity was initially set up with a parameter that was allowed to vary and that defined a multiplier on the diffusivity (DMCOEF) array in the Dispersion Package in MT3DMS where thermal diffusivity is assigned (Zheng and Wang, 1999; Langevin and others, 2008). This multiplier, however, was not allowed enough significant figures in MT3DMS for UCODE_2005 to determine any sensitivity on this parameter. Simple tests showed that small changes in thermal diffusivity had little effect on temperatures within the model. Thermal diffusivity, therefore, was held constant and not included in sensitivity analysis or regression.

Dispersivity

Dispersivity values are needed to calculate the dispersion coefficient term of the transport equation, which accounts for the apparent spreading of heat along flow paths due to small-scale variations in the groundwater velocity caused by small-scale heterogeneities in the aquifer. Values of dispersivity are highly scale dependent (Gelhar and others, 1992); dispersivity observed at a regional scale is much higher (up to several orders of magnitude) than dispersivity observed at a more local scale.

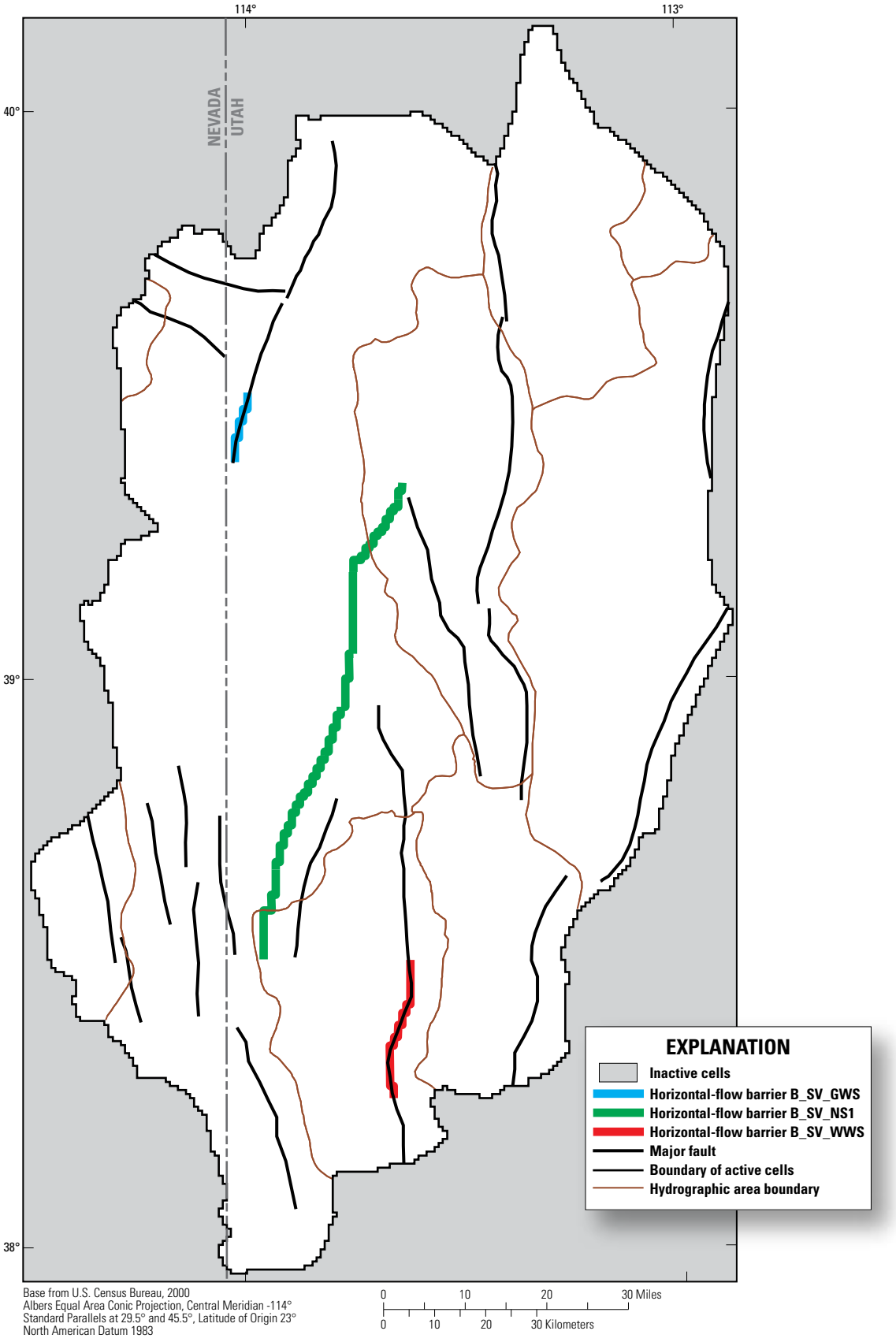

Figure 27. Location of faults and simulated horizontal-flow barriers in the Snake Valley study area, Utah and Nevada.

For a three-dimensional transport model, three types of dispersivity need to be considered: (1) longitudinal dispersivity, which describes the dispersive transport in the direction parallel to groundwater flow; (2) horizontal-transverse dispersivity, which describes the dispersive transport perpendicular to groundwater flow in the horizontal direction; and (3) vertical-transverse dispersivity, which describes the dispersive transport perpendicular to groundwater flow in the vertical direction (Zheng and Bennet, 2002). Without field data, Zheng and Bennett (2002) suggest that horizontal-transverse dispersivity should be one order of magnitude less than longitudinal dispersivity, and vertical-transverse dispersivity should be two orders of magnitude smaller than longitudinal dispersivity.

Longitudinal dispersivity and the ratios of horizontal- and vertical-transverse dispersivity to longitudinal dispersivity are assigned in the Dispersion Package in MT3DMS. Longitudinal dispersivity can be defined as being 5 to 10 percent of the scale of the system or length of the flow paths (Gelhar and others, 1992). In the current study area, possible flow path lengths can vary over two orders of magnitude, from less than 10 km to more than 100 km. Longitudinal dispersivity, therefore, was defined as a parameter and allowed to vary during model calibration and parameter estimation.

Bulk Density and Thermal Distribution Factor

The bulk density and thermal distribution factor, assigned in the Chemical Reaction Package in MT3DMS, are used to compute the thermal equilibration between the aquifer solids and fluid (groundwater). The bulk density is dependent on the density of the aquifer solids and the porosity of the aquifer (appendix 1). The thermal distribution factor depends on both the heat capacity of the aquifer solids and fluid (groundwater), and the density of the groundwater (appendix 1). Early simulations showed that the model was insensitive to the bulk density and thermal distribution factor, so these values were held constant and not included in sensitivity analysis or regression.

Observations Used in Model Calibration

Model observations are measured values of water levels, spring discharge, gain and loss in streams, and other measurable indicators of the groundwater system. The term "observation" is used to denote that model output will be compared to the measured value, and this comparison is part of calibration, sensitivity analysis, and parameter estimation. Observations used in model calibration include water-level altitudes; discharge measurements from springs, mountain streams, and evapotranspiration areas; and groundwater temperatures from wells. Additional measurements of spring and river water-level altitudes, and selected groundwater temperature measurements at springs were also included. For each set of observations, uncertainties, which are expressed as standard deviation (σ), variance (σ^2), or coefficient of variation (σ divided by the observation value), were calculated. These were then converted to variances that UCODE_2005 uses to define weights (which equal 1 divided by the variance) that are applied to the observations for sensitivity analysis and parameter estimation.

Water-Level Observations and Uncertainty

Water-level altitudes used for model calibration were measured in early spring 2009 from 123 wells in the Snake Valley study area (fig. 28). Only 27 wells within the study area had long-term records. At these wells the spring 2009 water-level measurements were found to be similar to long-term average water levels. Additionally, the spring 2009 water levels measured in wells without long-term records were similar to those with long-term records. The spring 2009 water-level measurements used as observations in the model, therefore, were assumed to represent steady-state conditions. Most water-level observations are from wells completed in the shallow part of the groundwater system. For wells open to more than one model layer, simulated water levels are a weighted average based on the proportion of the open interval of the well within each layer, which is calculated by the Hydraulic-Head Observation Process of MODFLOW-2000 (Hill and others, 2000).

The uncertainty determined for each water-level observation includes uncertainties related to errors in the well altitude and location, water-level measurement error, nonsimulated transient error, and model discretization. The error for each of these components was calculated following the procedure outlined by San Juan and others (2010) and Faunt and others (2010), and is presented in appendix 2.

The standard deviations of water-level observations range from 1.2 m to 7.7 m, and average 2.3 m. About 98 percent of the water-level observations have a standard deviation of less than 5 m, and about 41 percent have a standard deviation of less than 2 m. The contribution of individual sources of uncertainty to total water-level observation uncertainty varies. In general, the smaller uncertainties are dominated by nonsimulated transient and model discretization error, while the larger uncertainties are dominated by well altitude and model discretization error.

Water Levels at Discharge Locations

Water levels at selected discharge locations also were used as observations early in the process of model calibration because if simulated discharge to a head-dependent boundary is zero, the sensitivity of the discharge observation to all parameters is also zero; therefore, this does not create a signal to regression to change parameters that will cause discharge to occur at this location. Water levels at these locations, however, were sensitive, and if the simulated water level was below the observed level, regression would change parameters that would increase the water level and cause discharge to occur.

The altitude used for water-level observations at the springs was set at the minimum of either the reported spring altitude or 10 m below the minimum land-surface altitude within the cell. For mountain streams, two points were used as

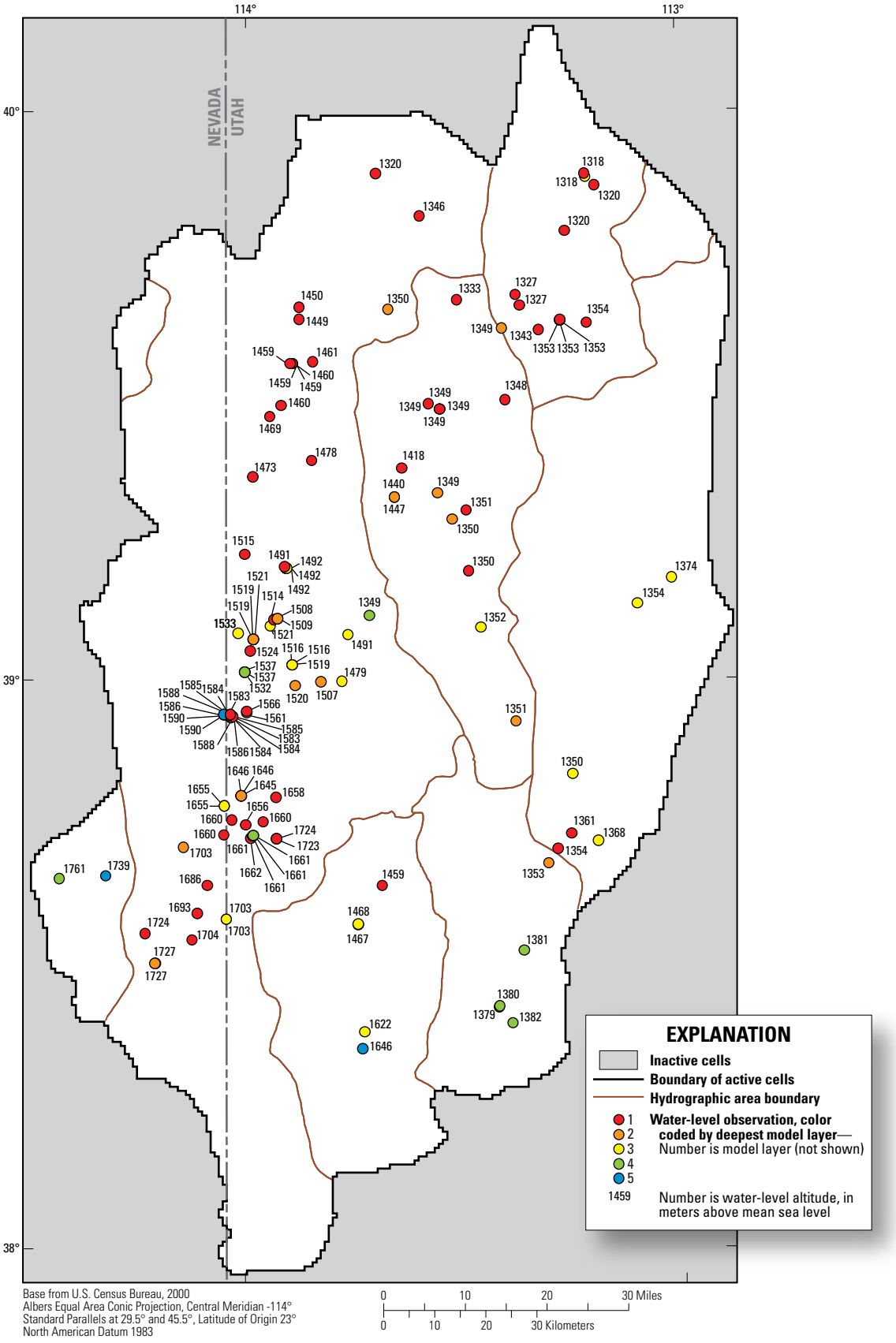

Figure 28. Spatial distribution of water-level observations and altitudes used in calibration of the Snake Valley area groundwater model.

water-level observations, one representing stream altitude at the point midway between the gage and the upper end of the stream, and one representing the stream altitude near the gage. The variance assigned to the altitude of the discharge points was 100 m^2. These water-level observations were removed from the model once discharge to the spring or stream began to occur, and the discharge observation became sensitive within the regression because the discharge observation may have a different sensitivity than the water level.

Water Levels Above Land Surface

During model calibration, the simulated water levels were frequently compared to land-surface altitude to ensure that abnormally high simulated water levels were not occurring. These comparisons were not formally included as observations and, therefore, did not influence the regressed values of parameters. Regressed values of the parameters, however, were modified manually if they created areas with water-level altitudes of more than 50 m above the mean land-surface altitude within the cell. Given the large area of the model, the relatively large cell size, and simulated water-level altitudes ranging over almost 2,000 m, an error of 50 m (2.5 percent of simulated range) in simulated water levels was considered acceptable.

Groundwater Discharge Observations and Uncertainty

Groundwater discharge observations used for model calibration include discharge to ETg, springs, and mountain streams (figs. 6 and 29). Uncertainties were calculated depending on the type of data available for each discharge observation and are discussed below.

During early model calibration, regression would often match water-level observations while ignoring discharge observations when using error-based weights. This is due to observations being clustered in the model because of the high number of water-level observations in relation to the number of discharge observations (Hill and Tiedeman, 2007, p. 285). All discharge observations, therefore, were given a weight multiplier of 5.0 to force the regression not to ignore these observations (Hill and Tiedeman, 2007, p. 285). In UCODE_2005, weight is the inverse of the variance, and variance is proportional to the square of the coefficient of variation (CV). Thus, the weight multiplier changes the CV on discharge observations from an average of 0.26 to $[0.26/5^{1/2}]$ or 0.11.

Evapotranspiration

Uncertainties on estimates of groundwater discharge to ETg were determined by assuming a CV of 0.3. This is similar to CVs in other areas of the Great Basin where ETg has been extensively studied. In the Death Valley region, CVs of ETg range from 0.1 to 0.71, and average about 0.31 (Faunt and others, 2010). In the BARCAS (Welch and others, 2007) study area, CVs of ETg range from 0.13 to 1.5, and average about 0.24 (Zhu and others, 2007).

Springs

Discharge observations and uncertainties for springs within the study area came from a variety of sources, and are summarized in table 5. At springs with more than one measurement, the discharge and variance were calculated directly from the measurements. If the spring only had one discharge measurement, the variance was assumed to equal the average of the variances of springs with similar amounts of discharge. Discharge observations from multiple springs were sometimes combined (summed) into one observation (fig. 29) because at the regional scale of the model minor variations of discharge in nearby cells is not as important as the total discharge in an area. When spring discharges were combined their variances were summed to determine the new total variance.

For springs monitored by the UGS (fig. 6; Clay, Dearden, Miller, Foote Reservoir, and Twin Springs), average discharge and variances were calculated directly from the discharge data (Lucy Jordan, Utah Geological Survey, written commun., August 2010). For Twin Springs, the north pool was monitored slightly longer than the south pool, so the average discharge was calculated as the sum of the averages for each pool, and the total variance was the sum of the variances for each of the pools. Average discharge and variances for Gandy Warm Springs, Rowland Springs, and Big Springs (fig. 6) were calculated from discharge data from the USGS NWIS database (accessed on July 26, 2010). For Spring Creek Spring (fig. 6), data from Elliott and others (2006) were used to determine the discharge and variance based on measurement uncertainty (plus or minus 8 percent) and seasonal fluctuations (difference between June and October measurements), and assuming that these represent with 95 percent confidence the error in the discharge measurement. Unnamed Spring and Wah Wah Springs (fig. 6) only had one reported discharge measurement. Variances for these two springs were determined by using the average variance for springs with similar discharge (1 to 3 ft^3/s). Discharge from Fish Springs (fig. 6) was taken from Bolke and Sumsion (1978) and was assumed to have a CV of 0.29 (Lynette Brooks, U.S. Geological Survey, written commun., August 2010).

Mountain Streams

Discharge of base flow (groundwater) to mountain streams and associated uncertainties were determined using a variety of sources and are summarized in table 6. Base flow to Granite and Trout Creeks (fig. 6) was determined by using the estimates of groundwater discharge to base flow given in Heilweil and Brooks (2011), whereby the annual groundwater discharge was estimated to be the minimum mean daily discharge at each gage for the period of record, as reported in the NWIS database, multiplied by 365 days per year. Uncertainty of

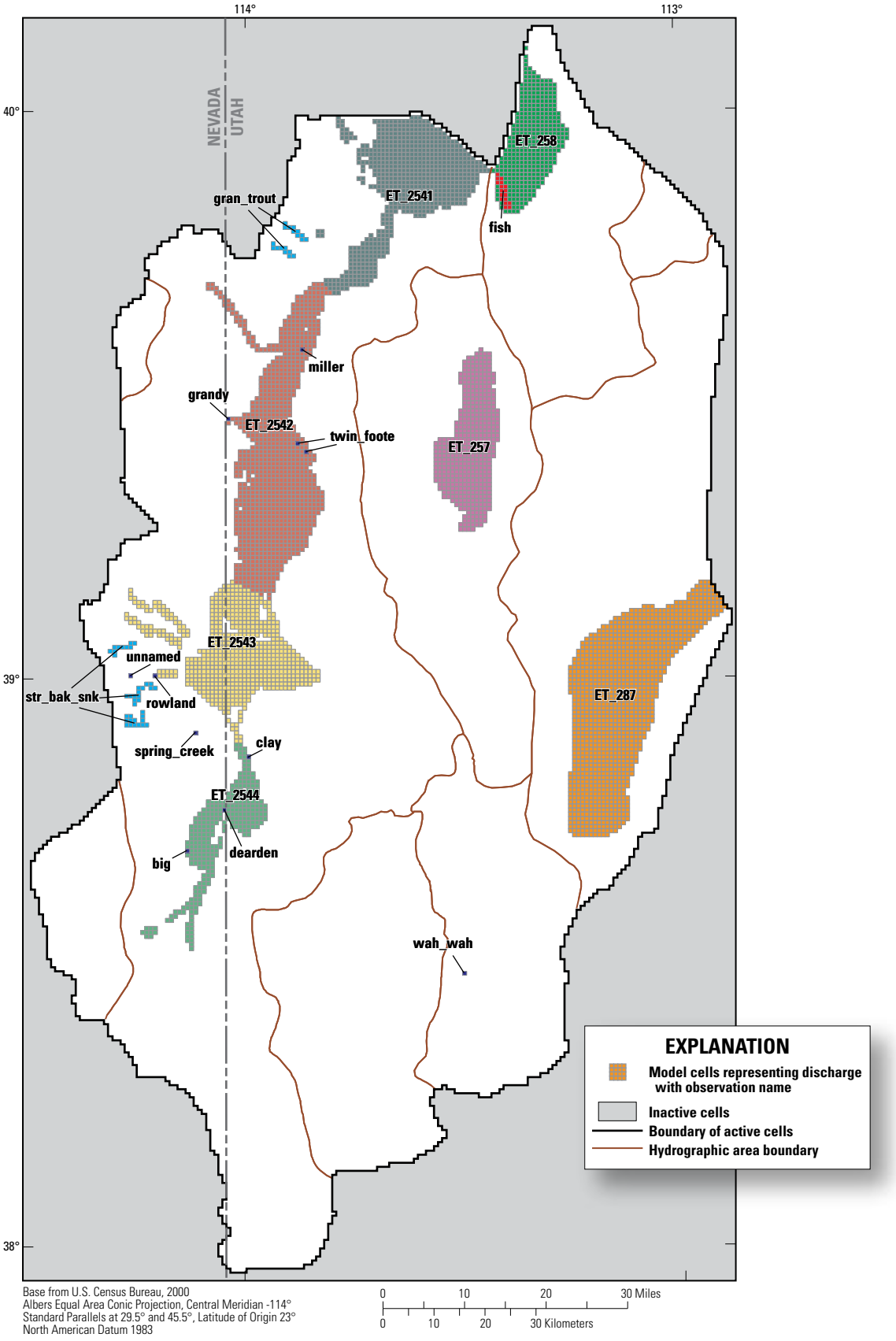

Figure 29. Spatial distribution of groundwater discharge observations used in calibration of the Snake Valley area groundwater model.

Table 5. Summary of discharge and coefficient of variation data for springs used as observations in the Snake Valley area groundwater model.

[**Abbreviations:** NWIS, National Water Information System; UGS, Utah Geological Survey; USGS, U.S. Geological Survey]

Spring name	Mean discharge (cubic meters per day)	Coefficient of variation	Period of record used	Discharge data source
Fish Springs	87,790	0.29	1970–1977	Bolke and Sumsion, 1978
Miller Spring	931	0.045	5/27/2010–8/2/2010	Lucy Jordan, UGS, written commun., August 2010
Gandy Warm Springs	36,830	0.11	10/1/2005–7/25/2010	NWIS, USGS site 10172860
Foote Reservoir Spring	6,968	0.072	6/7/2005–7/6/2010	Lucy Jordan, UGS, written commun., August 2010
Twin Springs (North and South)	6,274	0.017	1/2/2010–7/30/2010	Lucy Jordan, UGS, written commun., August 2010
Unnamed Spring	4,906	0.21	9/7/2007	NWIS, USGS site 390042114152601
Rowland Springs	5,576	0.35	10/1/2002–9/30/2004	NWIS, USGS site 10243265
Spring Creek Spring	4,648	0.051	6/10/2003–10/7/2003	Elliott and others, 2006, table 4, site Sn5
Clay Spring	868	0.023	9/21/2009–7/7/2010	Lucy Jordan, UGS, written commun., August 2010
Dearden Spring Group	16,320	0.11	9/25/2009–7/26/2010	Lucy Jordan, UGS, written commun., August 2010
Big Springs (North and South)	24,420	0.058	10/1/2005–7/26/2010	NWIS, USGS sites 102432241 and 10243224
Wah Wah Springs	2,725	0.37	10/12/1972	Stephens, 1974

Table 6. Summary of discharge and coefficient of variation data for streams used as observations in the Snake Valley area groundwater model.

Stream name	Mean discharge (cubic meters per day)	Coefficient of variation	Period of record used	Discharge data source
Granite Creek	709	0.25	6/21/2003–6/14/2007	Heilweil and Brooks, 2011, Auxiliary 3J
Trout Creek	4,052	0.25	12/1/1958–6/14/2007	Heilweil and Brooks, 2011, Auxiliary 3J
Strawberry Creek	612	5.9	6/10/2003–10/7/2003	Elliott and others, 2006, table 4, site St4
Baker Creek	4,697	0.19	6/10/2003–10/7/2003	Elliott and others, 2006, table 4, site B5
Snake Creek	2,251	3.5	6/10/2003–10/7/2003	Elliott and others, 2006, table 4, site Sn3

groundwater discharge to these streams was assumed to have a CV of 0.25 (Lynette Brooks, U.S. Geological Survey, written commun., August 2010). Base flow to Strawberry, Baker, and Snake Creeks (fig. 6) was determined using data from Elliott and others (2006) who performed seepage measurements on these creeks in 2003. The variances of these discharges were based on measurement uncertainty (plus or minus 8 percent) and seasonal fluctuations (difference between June and October measurements), and assuming that these represent with 95 percent confidence the error in the discharge measurement for Snake and Baker Creeks, and 90 percent confidence for Strawberry Creek. Because these measurements are based on the minimum mean daily discharge or are instantaneous low-flow measurements, they are considered to represent the minimum amount of groundwater discharge to mountain streams.

Discharge to mountain streams was combined in observations in two groups; Granite and Trout Creeks were combined into one observation (observation name gran_trout; fig. 29), and Strawberry, Baker, and Snake Creeks were combined into another observation (observation name str_bak_snk; fig. 29). The variances for each stream were added to determine the total variance for each observation.

Groundwater Temperature Observations and Uncertainty

Groundwater temperature observations used for model calibration are from groundwater temperature logs measured in 16 wells in the Snake Valley area (Blackett, 2011) as part of the UGS Snake Valley groundwater monitoring project, and groundwater temperature data for five springs from the NWIS database (fig. 30). Temperatures in the UGS wells were measured at intervals of 5 to 20 m at depths up to 500 m using a high-precision thermistor probe and temperature-logging equipment (Blackett, 2011). Only temperatures that were measured at or below the water table were used as observations in the groundwater model, and temperature observations from layer 1 were not used because temperatures in layer 1 were assigned as a specified-temperature boundary in most cells (see "Thermal Model Boundary Conditions" section of this report). This resulted in a total of 36 temperature observations in different model layers at 21 sites that were used for model calibration.

Temperature observations per each model layer for the wells were calculated as the mean of all temperature

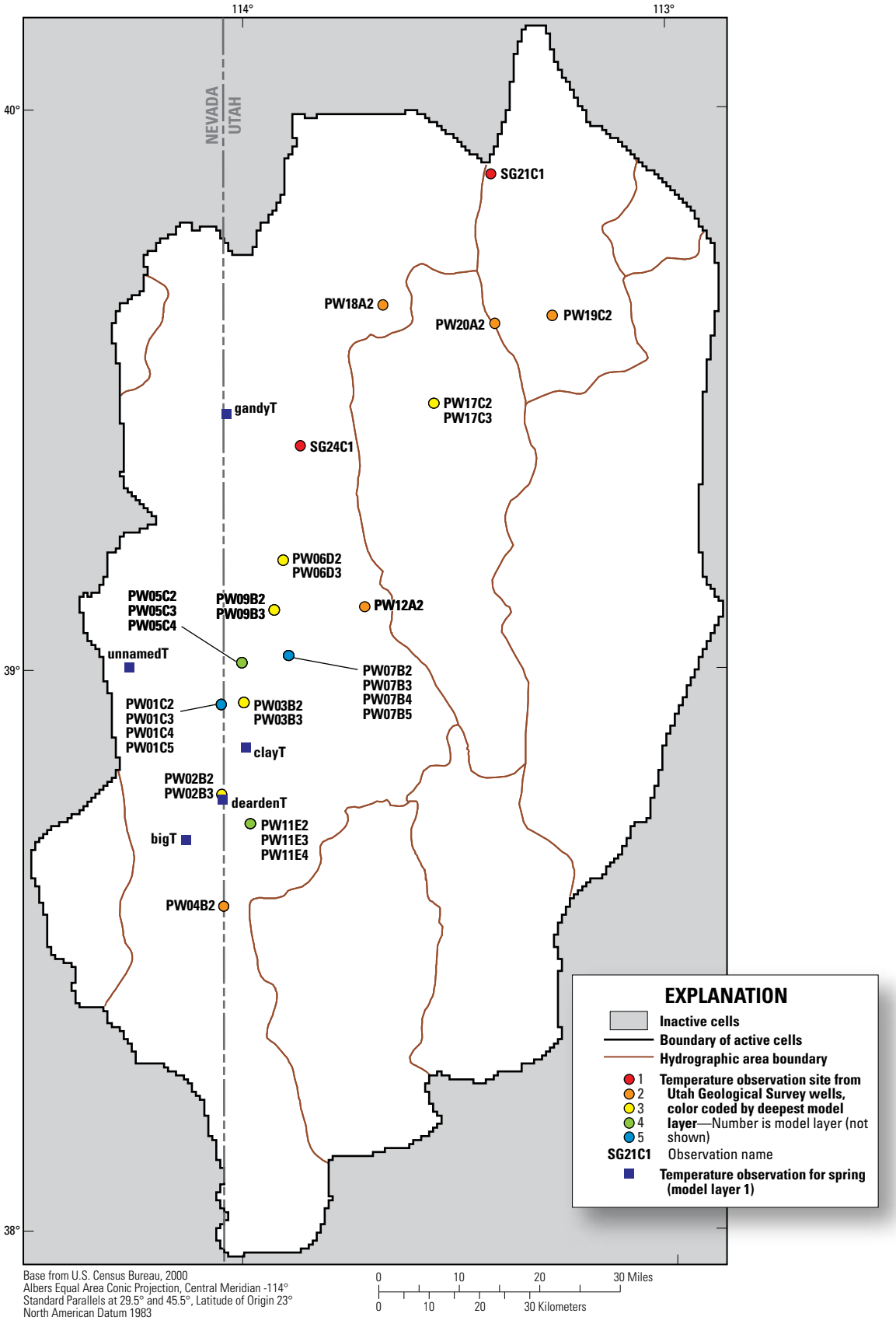

Figure 30. Spatial distribution of groundwater temperature observations for wells and springs used in calibration of the Snake Valley area groundwater model.

measurements across each model layer. If a well did not penetrate the entire layer, then the temperature observation was calculated as either (1) the observation that was closest to the altitude of the middle of the model layer, for wells that reached the middle of the layer; or (2) the temperature observation at the lowest altitude within the layer, for wells that did not reach the middle of the layer. Temperature observations for the springs were calculated as the mean temperature for the period of record and applied to model layer 1.

The uncertainty determined for each temperature observation includes uncertainties related to errors in the temperature measurement and model vertical discretization, which are discussed in appendix 3. The total standard deviations of temperature observations range from 0.0064 °C to 1.8 °C.

During early model calibration, regression would often match temperature observations while ignoring water-level and discharge observations. At the regional scale of the model, local processes that could affect temperature observations such as climatic effects, poor well construction, or local variations in geology or structures that can affect groundwater flow, could not be simulated and, therefore, were omitted. Because these errors cannot be quantified, they could not be directly included in the error-based weighting. As a result, the error-based weights on select temperature observations needed to be adjusted to reflect the expected error introduced by the omission of these local processes (Hill and Tiedeman, 2007, p. 286). The temperature observations were split into three groups and given a weight multiplier of 1.0, 0.5, or 0.05 depending on their variance. This weighting changed the average standard deviation of temperatures from 0.33 °C to 0.35 °C.

Model Calibration

Model calibration is the process by which the model input is changed in an attempt to match simulated and observed conditions, until the model reasonably represents groundwater recharge, movement, and discharge, and reasonably matches measured water levels and groundwater temperatures. Model calibration was accomplished by minimizing the sum of squared errors between simulated and observed data using UCODE_2005 (Poeter and others, 2005). During calibration, various aspects of the model were changed to minimize differences between simulated results and associated observations in order to make differences between simulated and observed water levels, groundwater temperatures, and groundwater flows acceptable for the intended use of the model. This model was developed to simulate general groundwater flow and heat transport throughout the Snake Valley study area. It was not developed to simulate local effects of withdrawals, water budgets, or heat transport on a cell-by-cell basis. To determine the value and distribution of hydraulic conductivity, drain and river conductance, horizontal-flow barriers, and heat transport properties, model parameters were adjusted to cause simulated conditions to more closely match steady-state conditions. Calibration was achieved through formal parameter-estimation (nonlinear regression) methods using UCODE_2005 (Poeter and others, 2005) and manual (trial and error) calibration.

Approach

Sensitivity analysis was used to evaluate the information provided by the observations for the estimation of all defined parameters, and nonlinear regression was used to estimate selected parameter values. For the Snake Valley area groundwater model, 47 parameters were used in sensitivity analyses and at least 43 were estimated at some point during the modeling process.

Uncertain aspects of the hydrogeology and thermal regime were evaluated by constructing models with different hydraulic property distributions, and different methods to simulate recharge, discharge, and boundary conditions. These models were evaluated through sensitivity analysis and nonlinear regression. These evaluation tools are discussed in the following sections, as well as how estimated parameter values considered unreasonable were used to detect model error. The linear confidence intervals used to evaluate the estimated parameter values also are discussed.

Sensitivity Analysis

Sensitivity analysis was used to assess the effects of different conceptual models (different model designs and parameter values) including (1) identifying and eliminating insensitive parameters from the regression and model, where possible; and (2) identifying areas where parameters could be further divided or combined. Changes in the conceptual model were assessed by evaluating the effects of parameter changes on model fit. Parameter sensitivities can be used to compare the importance of different observations to the estimation of a single parameter, or the importance of different parameters to the simulation of an observation (Hill, 1998).

Composite Scaled Sensitivities

The sensitivity of observations to parameters was used to aid in model calibration. Composite scaled sensitivities (CSS) are used to evaluate the overall sensitivity of a parameter and to evaluate whether available observations provide adequate information to estimate each parameter (Hill and others, 2000). CSS can also provide an overall view of the average amount that simulated values change given a 1-percent change in the parameter value (Hill and Tiedeman, 2007).

The relative size of CSS values can be used to assess whether additional parameters can be estimated. A relatively large CSS value indicates that observations contain enough information to represent that aspect of the system in more detail using additional parameters. A relatively small CSS value (about two orders of magnitude less than the largest CSS value) indicates that the observations provide insufficient information with which to estimate the parameter (Poeter and

others, 2005; Faunt and others, 2010). Parameters with small CSS values generally were either assigned a fixed value or were lumped with another parameter in the model.

Parameter Correlation Coefficients

Parameter correlation coefficients (PCC) indicate whether parameter values can be estimated uniquely and are calculated for each pair of parameters (Hill and Tiedeman, 2007). A PCC having an absolute value close to 1.00 indicates that the two parameters involved likely cannot be estimated uniquely. Generally, absolute values greater than 0.95 are cause for concern, but values as small as 0.85 can affect the uncertainty of parameter estimates. In this model, there were no PCC values greater than 0.85.

Influence Statistics

The RESIDUAL_ANALYSIS program (Poeter and others, 2005) calculates additional statistics useful in identifying observations that are influential in the regression, which aids in finding observation errors and model construction errors, and highlighting changes in model construction that may lead to more realistic values of model parameters. Two of the statistics calculated are the Cook's D and DFBETAS statistics. The Cook's D statistic identifies observations that, if omitted, would cause the greatest changes in estimated parameter values. The DFBETAS statistic identifies observations that are influential in the estimation of each parameter (Poeter and others, 2005). These statistics are used to make model changes if nonlinear regression leads to unreasonable parameter values, or if regression statistics indicate that a parameter change improves one part of the model but makes the fit worse in other areas.

Nonlinear Regression

Nonlinear regression (UCODE_2005) is used to find parameter values that produce simulations that best fit the observations. The fit between model simulated values and associated observations is quantified using a weighted least-squares objective function (Hill and Tiedeman, 2007). The weighting used in the objective function is based on the observation errors presented in the "Observations Used in Model Calibration" section of this report and is a diagonal weight matrix, which assumes that errors in the observations are uncorrelated.

Nonlinear regression adjusts parameter values to minimize the sum of squared weighted residuals. Weighted residuals are dimensionless quantities that reflect model fit in the context of the expected accuracy of the observations (Hill and Tiedeman, 2007). A weighted residual of 2.0, for example, indicates that the unweighted residual is twice the observation error, where the error is defined as standard deviation.

Evaluation of Parameter Estimates

An advantage to using regression to estimate parameter values is that the regression does not limit the parameter estimates to reasonable values (Faunt and others, 2010). If a model represents a physical system adequately, and the observations used in the regression provide substantial information about the parameters being estimated, estimated parameter values should be realistic. Unrealistic estimated parameter values can indicate model error (Hill and Tiedeman, 2007) and that model changes or further calibration are necessary.

Evaluating estimated parameter values requires that a reasonable range of the parameter values be determined from information other than the model simulation. Few estimates have been completed in the study area, and estimates of hydraulic and thermal properties are sparse. Sweetkind and others (2011a) present estimates of hydraulic properties (summarized in table 1 in this report) that were compiled from aquifer tests in the Death Valley regional groundwater flow system (DVRFS), and are considered representative of hydraulic properties over much of the eastern Great Basin because of similar rock types and HGUs. More detail for these hydraulic properties is given in Belcher and others (2002, table 1) that allows calculation of the standard deviation of the hydraulic conductivity as summarized in table 7.

Surficial heat-flow values in the study area, which are generally used as a proxy for basal heat flux, range from 50 to 100 mW/m^2 (Southern Methodist University Geothermal Laboratory, 2011). Although the surficial heat flow within the study area is likely largely affected by groundwater flow, it was assumed that the reasonable range of basal heat flux within the study area was similar to the range of surficial heat-flow values within the study area.

Parameter estimate uncertainty is measured using linear confidence intervals that are calculated by UCODE_2005 (Poeter and others, 2005). The size of the confidence interval is a measure of the amount of information the observations provide about the parameter; a smaller interval typically means that the observations provide more information to constrain the parameter. A linear 95-percent confidence interval on a parameter estimate that excludes reasonable values indicates model bias, misinterpreted data on the parameter or observation, or incorrect model construction (Hill and Tiedeman, 2007). An estimated parameter value that falls outside the range of reasonable values, but for which the confidence interval includes reasonable values may or may not indicate similar problems.

In addition to assessing possible model error, confidence intervals on estimated parameters also were used to assess whether all parameters were warranted (Hill and Tiedeman, 2007; Faunt and others, 2010). For example, if the confidence intervals for two parameters representing the hydraulic conductivity of rock types of similar hydraulic properties overlapped, the rocks were represented by a single hydraulic-conductivity parameter. If the simulation using fewer hydraulic-conductivity parameters yielded a similar model fit to the

Table 7. Horizontal hydraulic-conductivity estimates and statistics for hydrogeologic units in the Death Valley regional groundwater flow system and relation to hydrogeologic units used in the Snake Valley area groundwater model.

[Modified from Belcher and others, 2002, table 1. **Abbreviations:** DVRFS, Death Valley regional groundwater flow system; AA, alluvial aquifer; ACU, alluvial confining unit; LBFAU, lower basin-fill aquifer unit; LCA, lower carbonate aquifer; LCAU, lower carbaonte aquifer unit; LCCU, lower clastic confining unit; NCCU, non-carbonate confining unit; OVU, older volcanic rocks unit; TV, Tertiary volcanic rocks; UBFAU, upper basin-fill aquifer unit; UCA, upper carbonate aquifer; UCAU, upper carbonate aquifer unit; UCCU, upper clastic confining unit; USCU, upper siliciclastic confining unit; VSU, volcaniclastic and sedimentary rocks unit; VU, volcanic unit; YVU, younger volcanic rocks unit]

DVRFS hydrogeologic unit or subunit	Snake Valley area hydrogeologic unit	Horizontal hydraulic conductivity (meters per day)					Standard deviation of log values[1]	Number of measurements
		Geometric mean[1]	Arithmetic mean	Minimum	Maximum	95-percent confidence interval		
AA	UBFAU, non-playa	1.5	10.8	0.00006	130	0.005–430	1.26	52
ACU	UBFAU, playa	3.0	10.5	0.003	34	0.02–470	1.12	15
YVU/VSU	LBFAU	0.06	1.5	0.00004	6	0.00005–80	1.58	15
TV	VU	0.12	3.9	0.000002	180	0.0002–78	1.43	172
OVU	VU	0.004	0.07	0.000001	1	0.00002–5	1.38	46
UCA and LCA	UCAU and LCAU	2.5	90.0	0.0001	820	0.0008–7,700	1.78	53
UCCU and LCCU	USCU and NCCU	0.00002	0.2	0.00000003	5	0.0000000001–3	2.67	29

[1] Geometric mean and standard deviation are back-transformed from logarithmic values.

observations, the available observations were insufficient to distinguish between the two models. Thus, the model with more hydraulic-conductivity parameters represents a level of complexity that is not supported by the available data. If model fit deteriorated significantly, the parameters were not combined.

Use of Prior Information

To encourage understanding of the information that is available from observations, model parameters were not constrained during model construction and calibration, and prior information was not used to keep regressed values close to observed values. Because observations are more accurate than prior information on parameter values, observations should be emphasized in model calibration (Hill and Tiedeman, 2007). For final analysis of sensitivity, parameter correlation, parameter confidence intervals, and prediction uncertainty, prior information was used for parameters with very large calculated confidence intervals to simulate a reasonable degree of uncertainty in these parameters (Hill and Tiedeman, 2007). Nine out of the final 51 parameters required prior information.

Model Variations

During calibration, a number of models were evaluated. Evidence of model error or data problems was investigated after each model run, and the model fit to observations was analyzed. These analyses were used in conjunction with hydrogeologic and thermal data to modify and improve the existing conceptual model and observation data sets. Sensitivity and fit statistics were used to determine if model changes, such as rezoning hydraulic conductivity or recharge parameters, could lead to better model fit and if additional parameters were warranted on the basis of the information provided by the observations. Parameters could be divided, for example, if the CSS of a parameter was substantially greater than 1.0 and large compared to the CSS of other parameters (Hill and Tiedeman, 2007).

The initial model used the conceptual recharge from the BCM; conceptual groundwater ETg rates; one value of hydraulic conductivity (HK) for each of the HGU zones defined by Sweetkind and others (2011a; figs. 20 to 26 in this report); one value of vertical anisotropy (VANI) for the UBFAU and one value of VANI for all other units; one value of spring, river bed, and general-head boundary conductance; no horizontal-flow barriers; and one value each for basal heat flux and dispersivity. This model had 39 parameters. Nonlinear regression converged for this model, but took some parameters to unreasonable values, did not provide discharge to 7 of 20 discharge observations, and reduced the overall groundwater budget to about 79 percent of the estimated budget. This was not considered to be an acceptable representation of the groundwater system. The composite scaled sensitivities for the model indicated that the observations provide more information about the hydraulic conductivity of the UBFAU and LCAU HGUs than about any other hydraulic-conductivity parameter (fig. 31).

The first conceptual model described above indicated that more variety was needed in the parameters to achieve reasonable matches to water-level, discharge, and temperature observations. The methods discussed in the "Model Calibration Approach" section of this report were used to assign new parameter zones during calibration; nonlinear regression was then used to estimate the value of parameters using the new zonation. Multiple versions of the model were created using this method and only changes that improved model fit were retained from one model version to the next, until calibration was achieved; only the final calibrated model construction is discussed in the following sections.

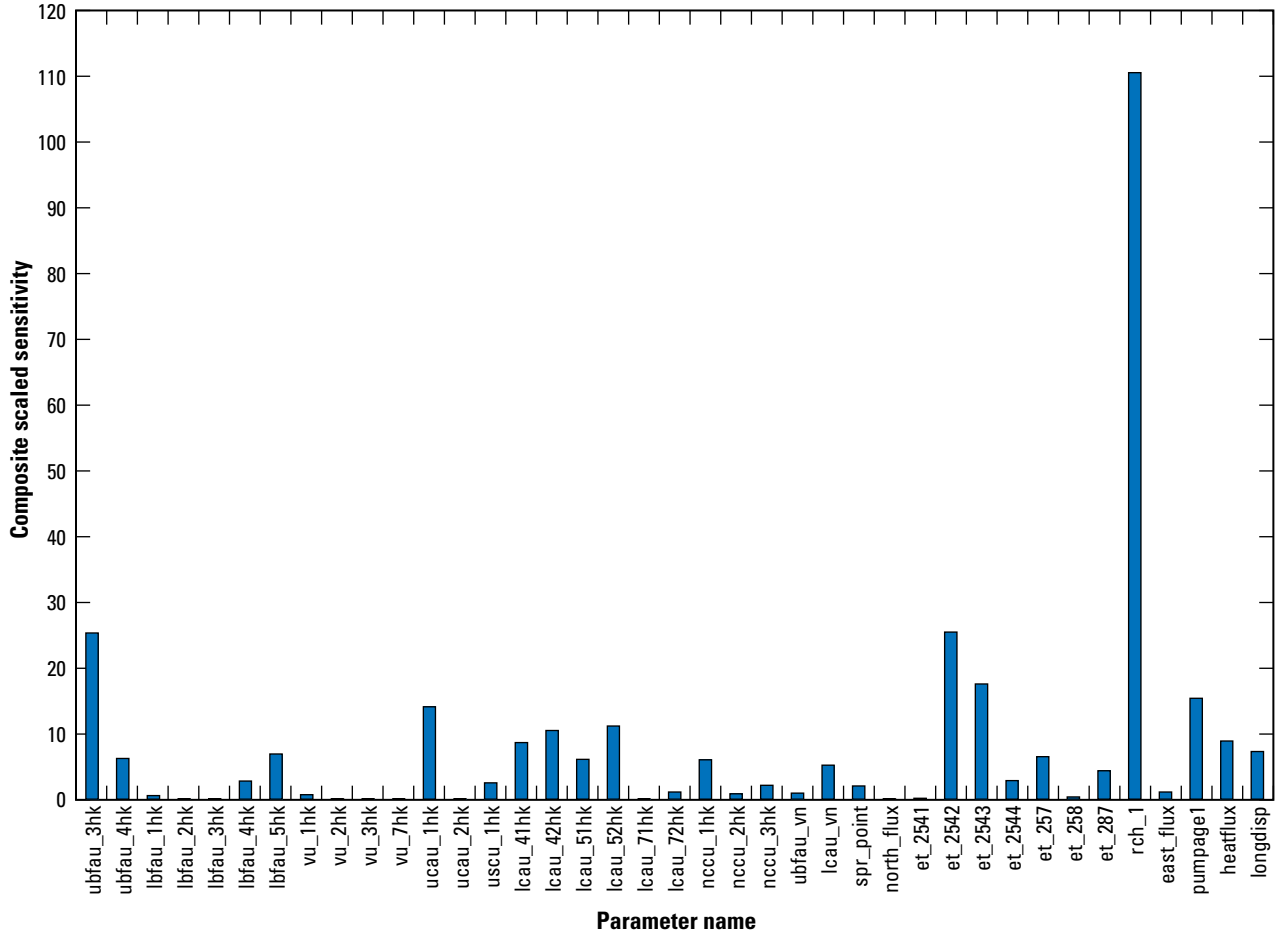

Figure 31. Composite scaled sensitivities for parameters used in the initial groundwater model definition of the Snake Valley study area, Utah and Nevada.

Final Calibrated Model

Of the numerous model variations, most differed in how recharge and hydraulic conductivity were represented. The relative likelihood of the different models was evaluated by considering how simulated water levels, discharges, and temperatures compared to the observations, and how the estimated parameters compared to reasonable ranges. The model that yielded the best fit with reasonable parameter values and a reasonable number of parameters was retained. Figure 32 shows the composite scaled sensitivities for the final parameter set, and figure 33 shows the calibrated parameter values and their associated 95-percent confidence intervals.

Recharge

Observations in the Snake Valley area groundwater model are highly sensitive to areal recharge parameters (fig. 32; parameters rch_1, rch_2, rch_3, rch_4, and rch_5). As a result, five zones were defined for areal recharge (fig. 34). Each recharge parameter refers to one recharge zone. During model calibration, zones were combined and divided on the basis of composite scaled sensitivities and parameter confidence intervals. The areal recharge parameter value is a multiplier on the conceptual recharge rate assigned in the model as explained in the "Boundary Conditions" section of this report. Generally, the recharge zones were delineated by surficial HGU type; this provides the recharge and variability needed to achieve calibration of this regional model, but should not be considered accurate at the cell-by-cell level. Final areal recharge rates ranged from 0 to 1.566 mm/d (fig. 35).

In the southwestern part of the study area, recharge over the volcanic units was reduced compared to the BCM with a multiplier of 0.55 to minimize flooding in these mountain blocks and to reduce water levels in southern Snake and Pine Valleys. Recharge was increased compared to the BCM with a multiplier of 1.3 in the southern Snake Range and in the Fortification Range in Spring Valley, which was indicated by both the temperature and groundwater discharge observations in this area. Recharge from unconsumed irrigation from well withdrawals was increased by a factor of 1.3 because well withdrawals were increased by a factor of 1.3 (see "Discharge" section below).

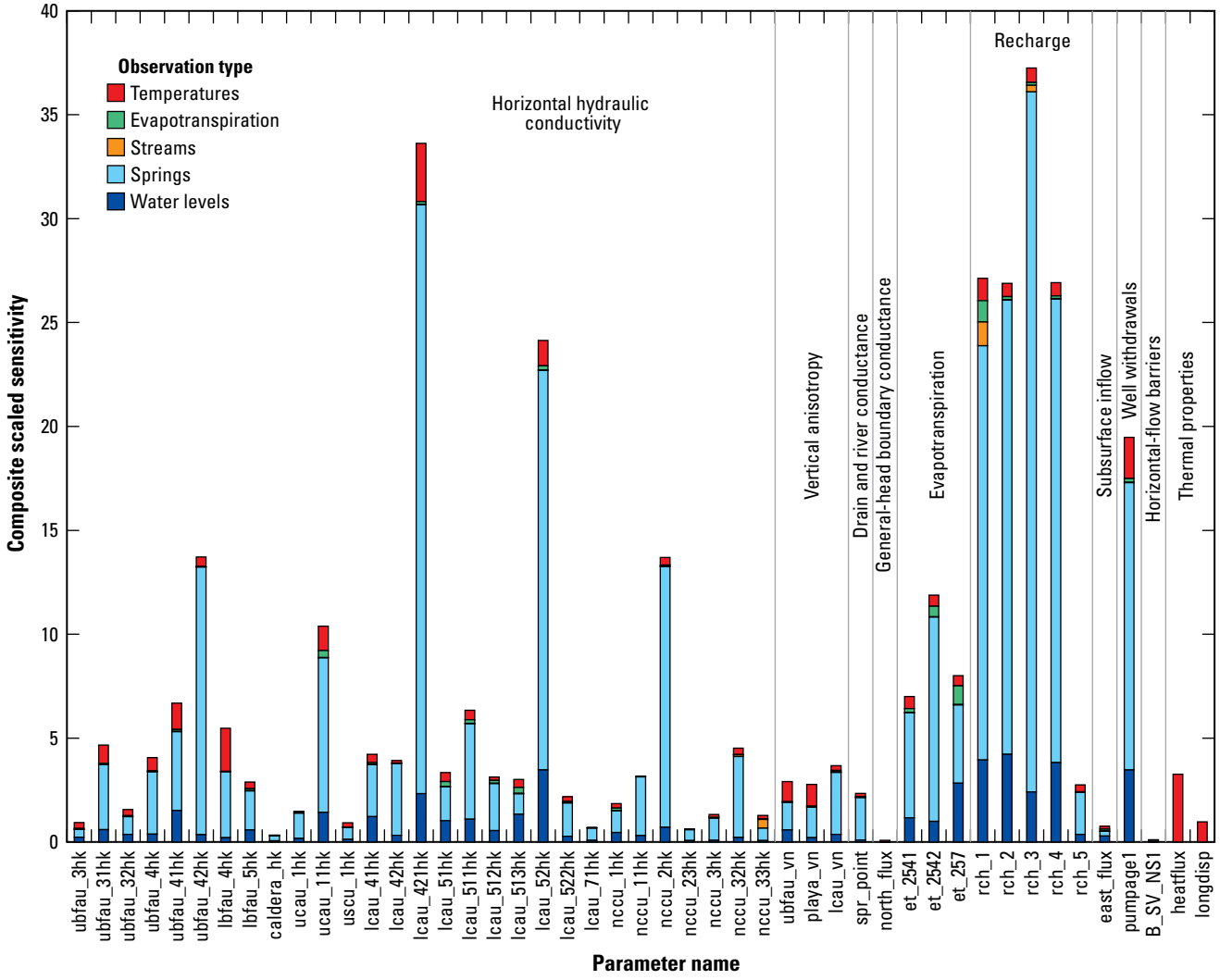

Figure 32. Composite scaled sensitivities for parameters used in the final calibrated groundwater model of the Snake Valley study area, Utah and Nevada.

Observations were insensitive to the parameter assigned to the subsurface inflow rates along the eastern boundary of the model (figs. 32 and 36; parameter east_flux). Because of this insensitivity, a standard deviation of 0.5 was applied to this parameter as prior information.

Discharge

The conductances of spring (drain), river, and general-head boundary cells, as well as multipliers on the ETg rate and well withdrawal rate were defined as parameters in the groundwater model. Spring, river, and general-head boundary conductances are defined by the conductance factor multiplied by the parameter value. The conductance factor for rivers is the length of river segment in a cell; width was not used because many of the rivers are mountain streams and have similar width. The conductance factor for all point springs is one-tenth of the cell area. The conductance factor for area springs (Fish Springs) is the area of the spring in each cell. Model observations were insensitive to the conductance on the rivers and area springs, but were somewhat sensitive to the conductance on the point springs (fig. 32). The conductances for rivers, area springs, and point springs were combined into one parameter (spr_point) in the final calibrated model.

The conductance factor for the general-head boundary cells that simulate flow out of the model boundary to the north was defined as the cross-sectional area of the cell face that is perpendicular to the direction of flow (cell width multiplied by the layer thickness). One parameter (north_flux) was used to define conductance for the general-head boundary. Model observations were insensitive to this parameter (fig. 32). Because of this insensitivity, and because conductance is dependent on hydraulic conductivity, a standard deviation of 2.67, the highest standard deviation for hydraulic conductivity (table 7), was applied to the log values of this parameter as prior information.

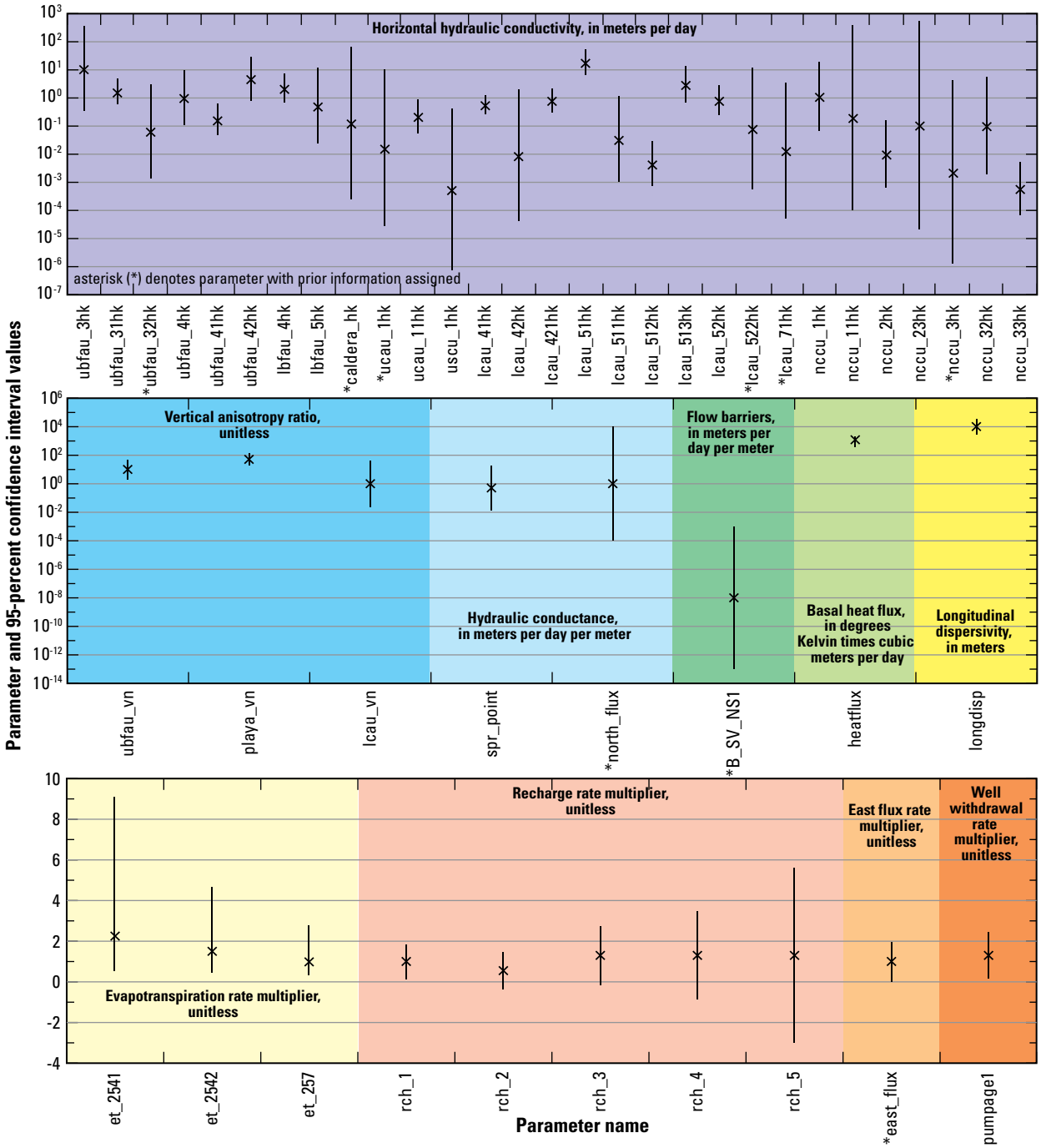

Figure 33. Calibrated values and linear 95-percent confidence intervals for parameters used in the groundwater model of the Snake Valley study area, Utah and Nevada.

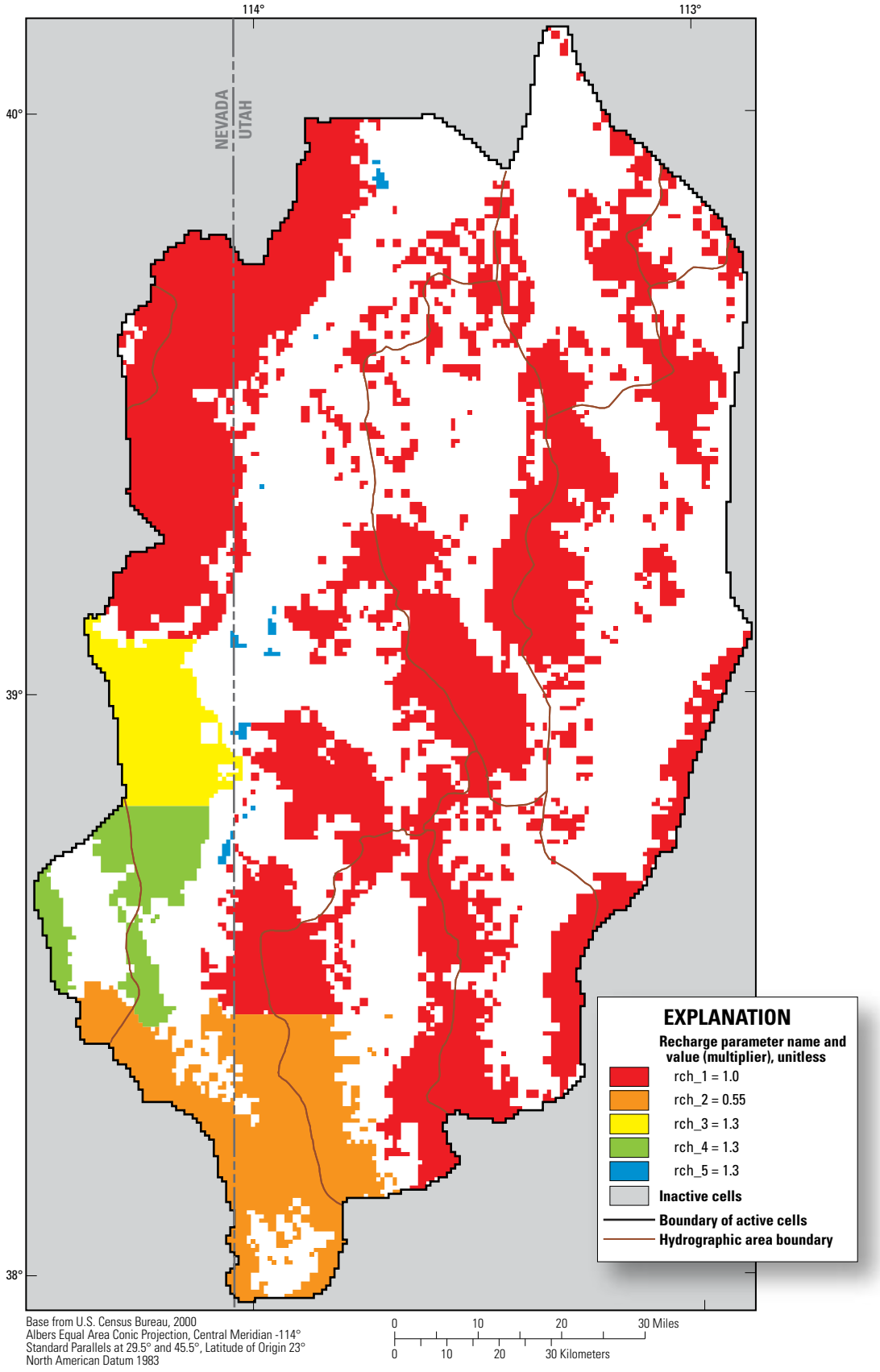

Figure 34. Distribution of areal recharge parameters and values (multipliers) in the Snake Valley area groundwater model.

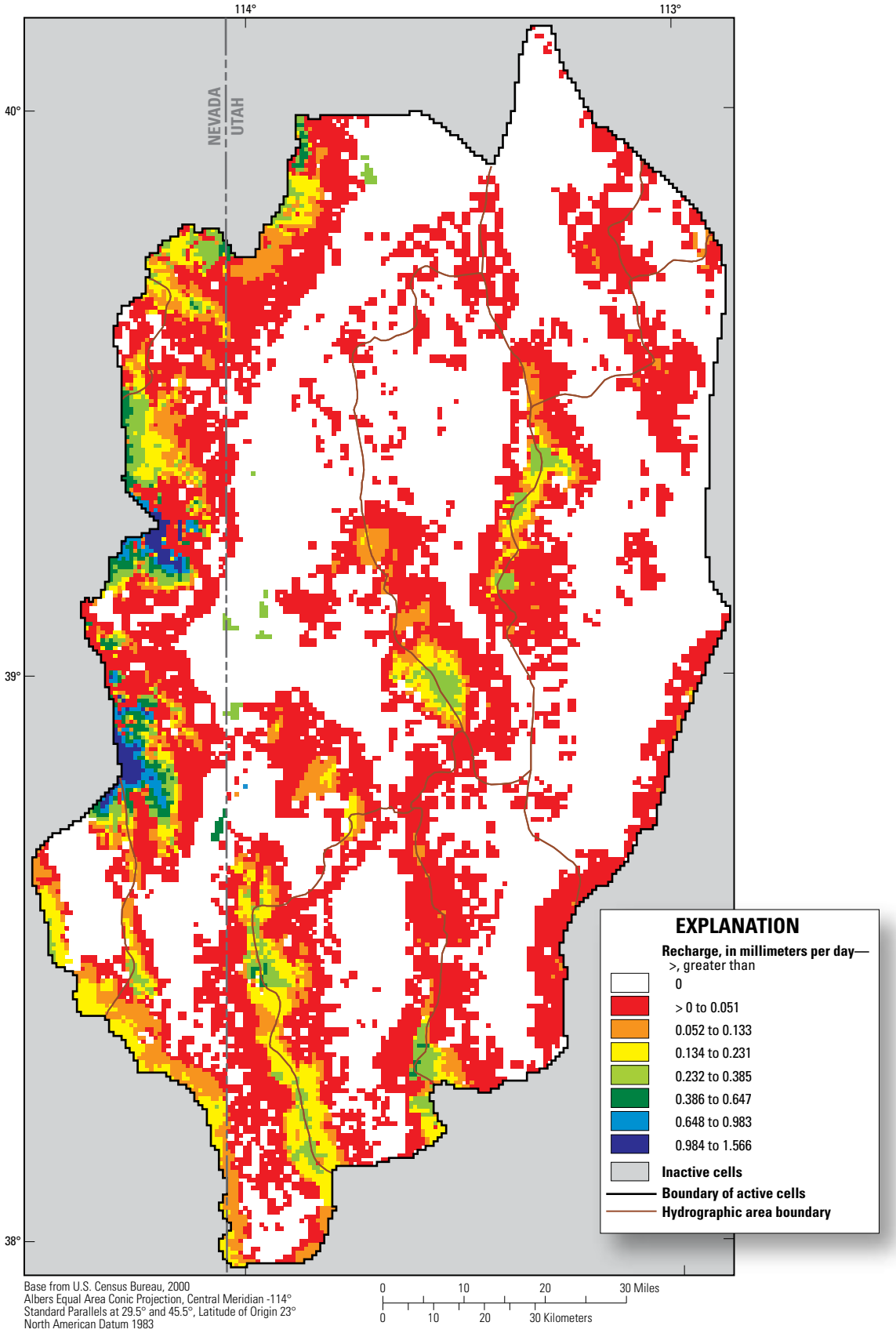

Figure 35. Total rate of recharge from precipitation, streams, and irrigation return flow simulated in the Snake Valley area groundwater model.

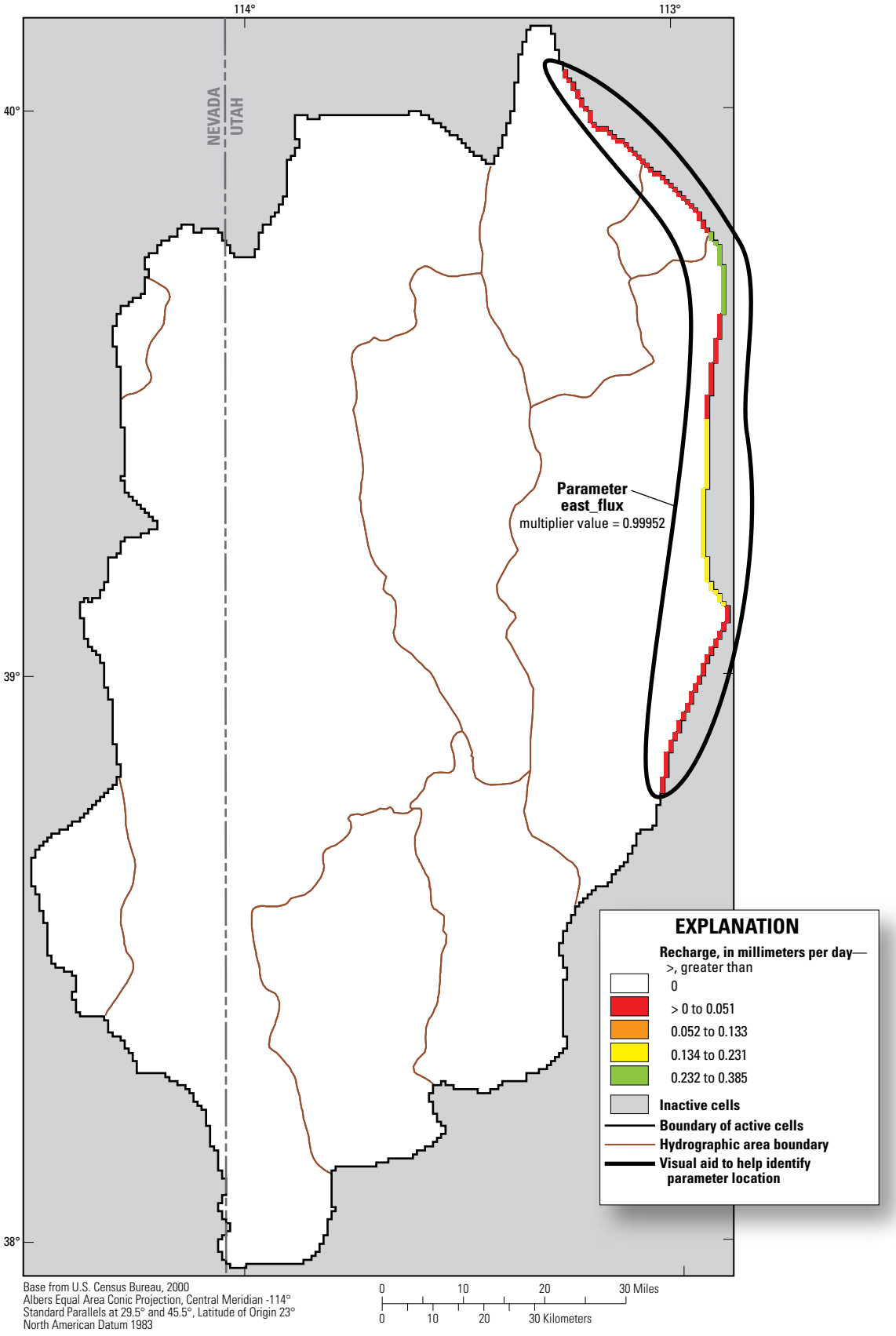

Figure 36. Subsurface inflow recharge parameter (multiplier) and recharge rate simulated in the Snake Valley area groundwater model.

Model observations were highly sensitive to the multiplier applied to the ETg rate (fig. 32). Similar to recharge, the parameter values were defined using zones, and early during the modeling process were generally defined at the HA or sub-HA level. During model calibration, zones were combined or divided on the basis of composite scaled sensitivities and parameter confidence intervals. In the final calibrated model, three parameters were defined to simulate discharge to ETg (fig. 37); this provides the variability needed to achieve calibration of this regional model, but should not be considered accurate at the cell-by-cell level. Final simulated ETg rates ranged from 0 to 0.515 mm/d (fig. 38).

Model observations were also greatly sensitive to the multiplier applied to the well withdrawal rate (fig. 32). One parameter (pumpage) was used to define this multiplier. The value of this parameter, 1.3, was determined by regression within reasonable limits as the uncertainty on the well withdrawal estimates, which were based on using power records to rate the wells, can be as high as 50 percent (Michael Enright, U.S. Geological Survey, oral commun., August 2010).

Horizontal Hydraulic Conductivity

Horizontal hydraulic-conductivity parameters were assigned using the zonation capability of the HUF package (Anderman and Hill, 2000). Model zones are used to define areas with the same simulated properties within individual HGUs. Hydrogeologic evidence was used initially to define model zones (figs. 20 to 26) of similar horizontal hydraulic conductivity within the HGUs (Sweetkind and others, 2011a). A parameter defining the horizontal hydraulic conductivity was associated with each model zone. During calibration, however, it became apparent that this zonation does not provide enough variability in hydraulic conductivity to achieve adequate matches to observations. Additional model zones and parameters were added to achieve calibration while minimizing the number of parameters. These additional model zones were delineated within the original 23 HGU zones described by Sweetkind and others (2011a; figs. 20 to 26 in this report) using the CSS and DFBETAS statistics. These statistics represented the ability and need to define additional model zones

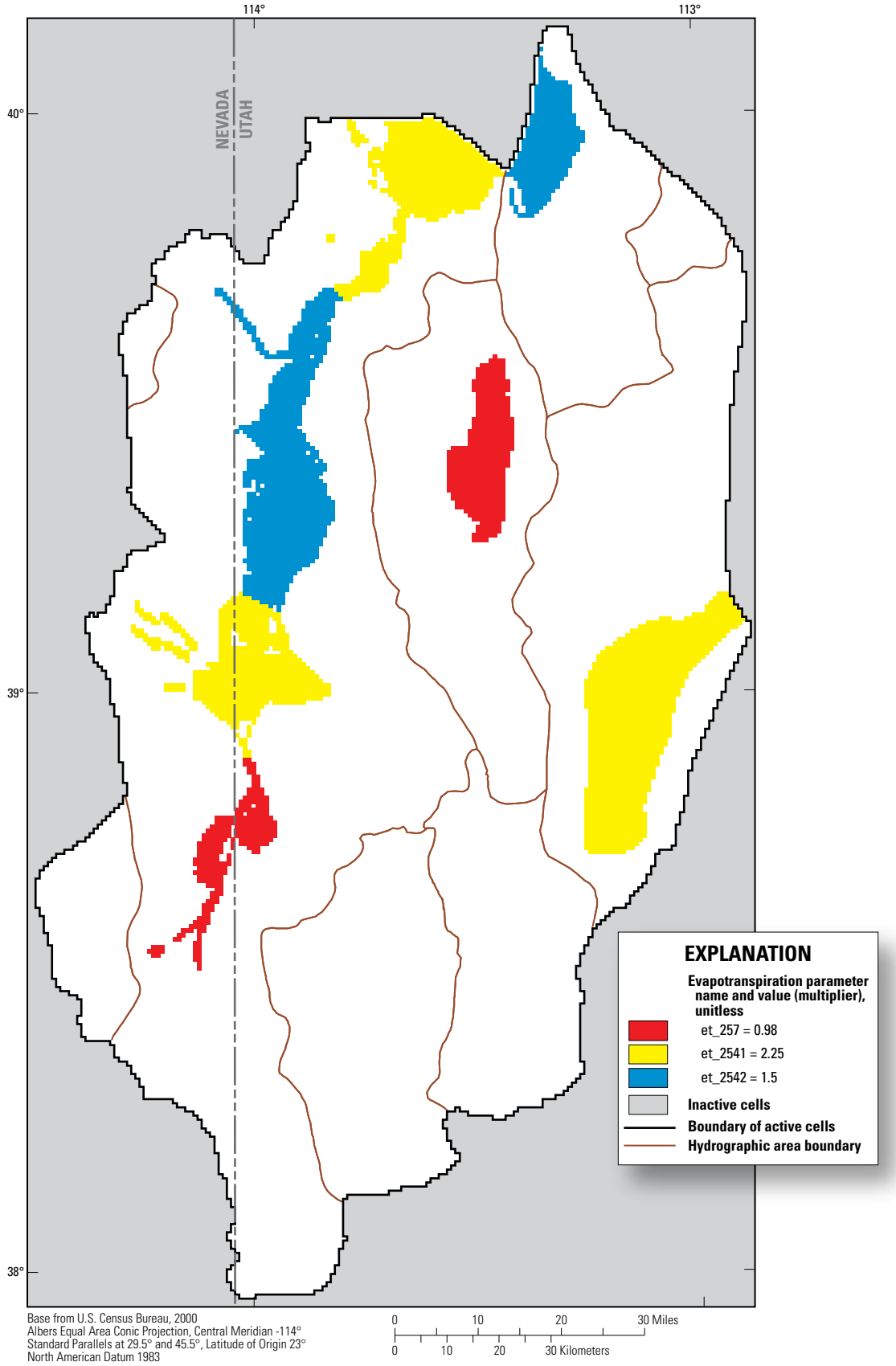

Figure 37. Distribution of evapotranspiration parameters and values (multipliers) in the Snake Valley area groundwater model.

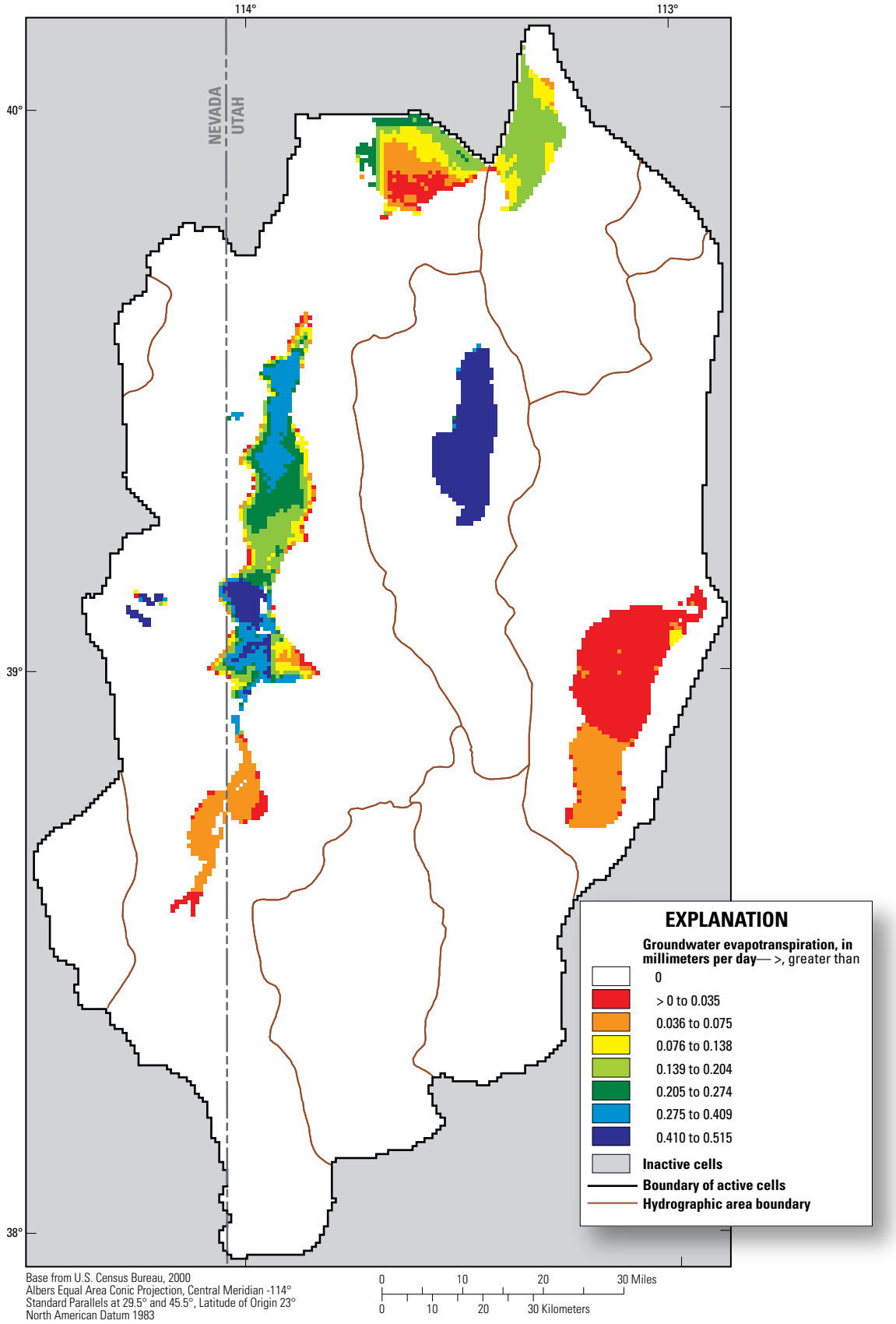

Figure 38. Total rate of groundwater evapotranspiration simulated in the Snake Valley area groundwater model.

Table 8. Calibrated horizontal hydraulic-conductivity values and statistics for parameters used in the Snake Valley area groundwater model.

[**Model zone:** zone number used in MODFLOW files. **Abbreviations:** LBFAU, lower basin-fill aquifer unit; LCAU, lower carbonate aquifer unit; NCCU, non-carbonate confining unit; UBFAU, upper basin-fill aquifer unit; UCAU, upper carbonate aquifer unit; USCU, upper siliciclastic confining unit; VU, volcanic unit; NA, not applied]

Parameter name	Hydrogeologic unit and zone (from Sweetkind and others, 2011a)	Model zone	Horizontal hydraulic conductivity (meters per day)		Standard deviation of log values	Prior information standard deviation of log values[1]
			Calibrated parameter value	95-percent confidence interval		
ubfau_3hk	UBFAU zone 3	ubfau zone 3	10	0.32–320	0.76	NA
ubfau_31hk	UBFAU zone 3	ubfau zone 31	1.5	0.54–4.2	0.23	NA
ubfau_32hk[2]	UBFAU zone 3	ubfau zone 32	0.060	0.013–2.7	0.84	1.12
ubfau_4hk	UBFAU zone 4	ubfau zone 4	0.94	0.10–8.7	0.49	NA
ubfau_41hk	UBFAU zone 4	ubfau zone 41	0.15	0.043–0.54	0.28	NA
ubfau_42hk	UBFAU zone 4	ubfau zone 42	4.4	0.75–26	0.39	NA
lbfau_4hk	LBFAU zone 4	lbfau zone 4	2.0	0.64–6.3	0.25	NA
lbfau_5hk	LBFAU zones 1, 3, and 5	lbfau zone 1, 3, and 5	0.47	0.022–10	0.68	NA
caldera_hk[2]	LBFAU zone 2; VU zones 1,2,3, and 7	lbfau zone 2; vu zones 1,2,3, and 7	0.12	0.00024–59	1.36	1.43
ucau_1hk[2]	UCAU zones 1 and 2	ucau zones 1 and 2	0.015	0.000025–8.9	1.40	1.78
ucau_11hk	UCAU zone 1	ucau zone 11	0.20	0.051–0.80	0.30	NA
uscu_1hk	USCU (zone 1)	uscu zone 1	0.00050	0.00000069–0.37	1.45	NA
lcau_41hk	LCAU zone 41;USCU (zone 1)	lcau zone 41; uscu zone 2	0.52	0.25–1.1	0.17	NA
lcau_42hk	LCAU zone 42	lcau zone 42	0.0081	0.000038–1.7	1.18	NA
lcau_421hk	LCAU zones 42 and 51	lcau zones 421 and 514	0.75	0.29–1.9	0.21	NA
lcau_51hk	LCAU zones 51 and 52	lcau zones 51 and 521	17	6.0–47	0.23	NA
lcau_511hk	LCAU zone 51	lcau zone 511	0.031	0.00096–0.98	0.76	NA
lcau_512hk	LCAU zone 51	lcau zone 512	0.0041	0.00068–0.025	0.39	NA
lcau_513hk	LCAU zone 51	lcau zone 513	2.8	0.63–12	0.32	NA
lcau_52hk	LCAU zone 52	lcau zone 52	0.75	0.23–2.4	0.26	NA
lcau_522hk[2]	LCAU zone 52	lcau zone 522	0.075	0.00053–11	1.09	1.78
lcau_71hk[2]	LCAU zones 71 and 72	lcau zones 71 and 72	0.012	0.000050–3.1	1.21	1.78
nccu_1hk	NCCU zone 1	nccu zone 1	1.0	0.064–17	0.61	NA
nccu_11hk	NCCU zone 1	nccu zone 11	0.18	0.000098–350	1.66	NA
nccu_2hk	NCCU zone 2	nccu zone 2	0.0093	0.00060–0.14	0.60	NA
nccu_23hk	NCCU zone 2	nccu zone 23	0.10	0.000020–490	1.87	NA
nccu_3hk[2]	NCCU zone 3	nccu zone 3	0.0021	0.0000012–3.7	1.64	2.67
nccu_32hk	NCCU zone 3	nccu zone 32	0.095	0.0018–5.0	0.87	NA
nccu_33hk	NCCU zone 3	nccu zone 33	0.00055	0.000064–0.0048	0.47	NA

[1]Values from table 7.

[2]Denotes parameter with prior information assigned.

and parameters to aid the calibration. For instance, a model zone may include a part of NCCU zone 1 (fig. 26), but does not include other parts of NCCU zone 1 or any part of NCCU zone 2.

A final set of 29 horizontal hydraulic-conductivity parameters was used to calibrate the model. During calibration, in order to reduce the number of parameters, relatively insensitive hydraulic-conductivity parameters were combined with parameters of similar hydraulic conductivity. As a result, in some cases the hierarchy described above was not maintained, and rocks from different HGUs and different geologic zones within these HGUs (as defined by Sweetkind and others, 2011a) were simulated using the same parameter and the naming convention modified. Calibrated horizontal hydraulic-conductivity parameters are listed in table 8; figures 39 to 45 show the distribution of simulated hydraulic conductivity in each HGU. The variability in hydraulic conductivity is adequate to achieve calibration of this regional model but should not be considered accurate at a cell-by-cell level. The zonation and parameter values may not be unique; it is possible that different zones and parameter values could achieve a comparable model fit.

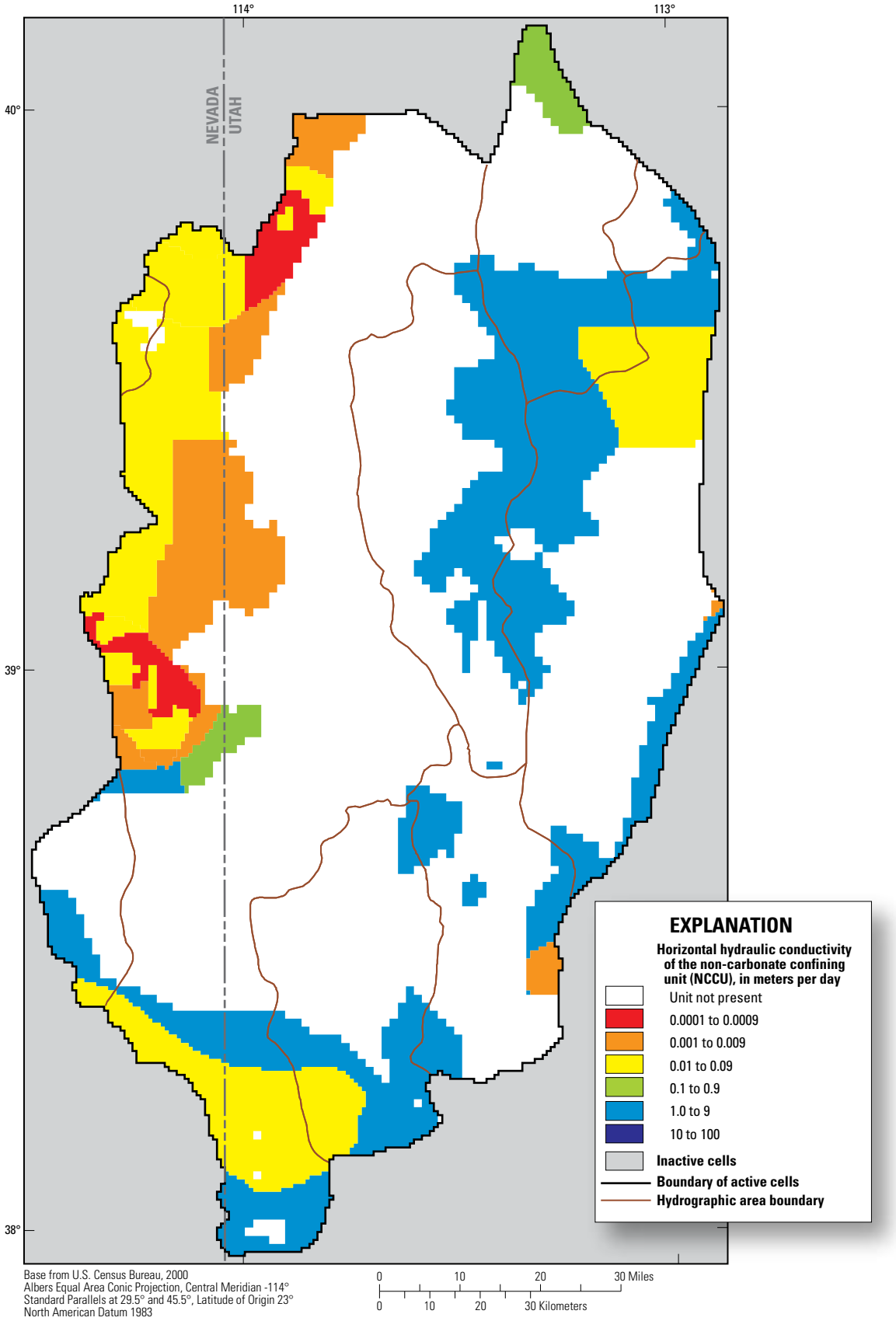

Figure 39. Distribution of simulated horizontal hydraulic conductivity of the non-carbonate confining unit (NCCU) in the Snake Valley area groundwater model.

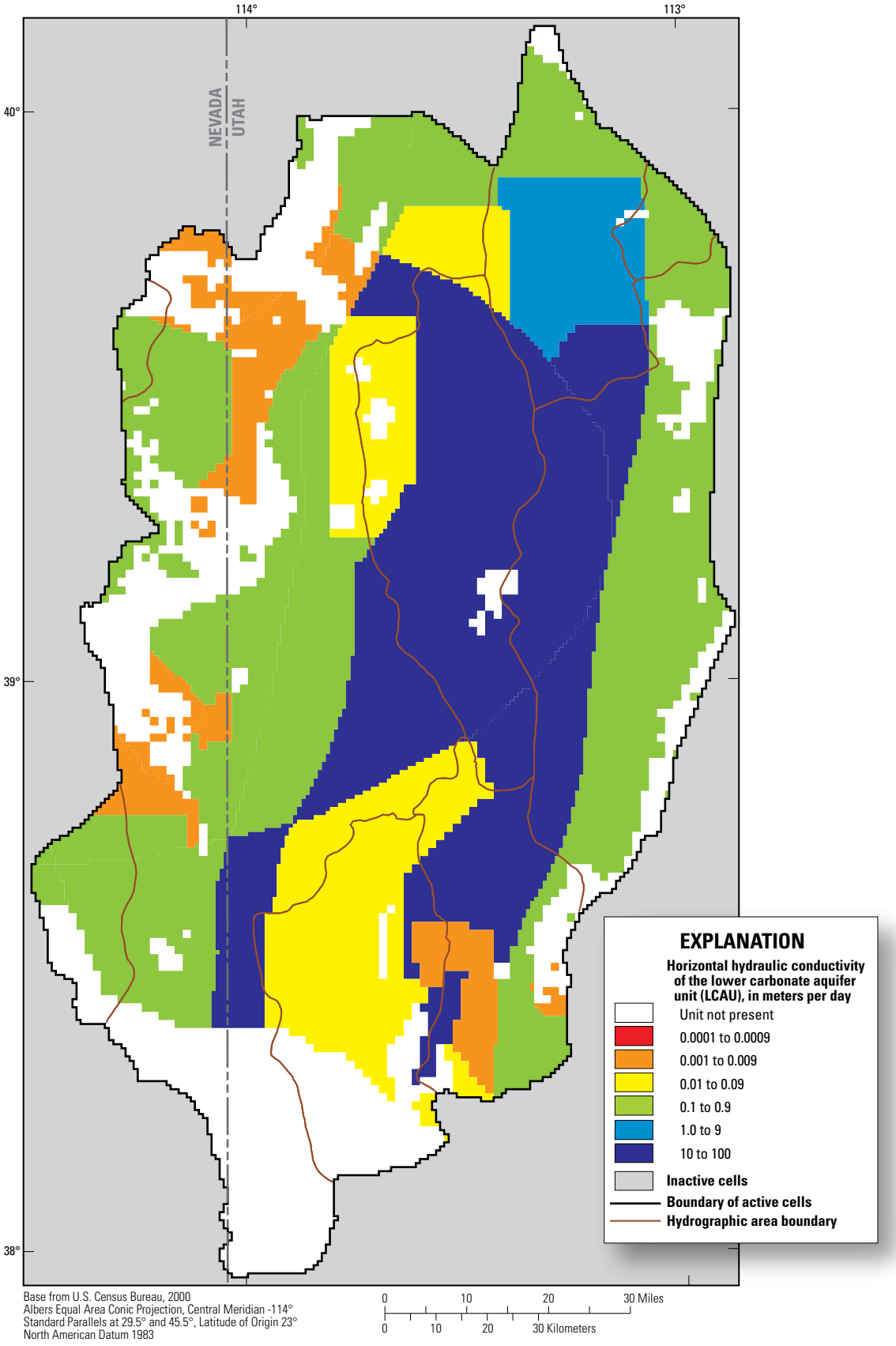

Figure 40. Distribution of simulated horizontal hydraulic conductivity of the lower carbonate aquifer unit (LCAU) in the Snake Valley area groundwater model.

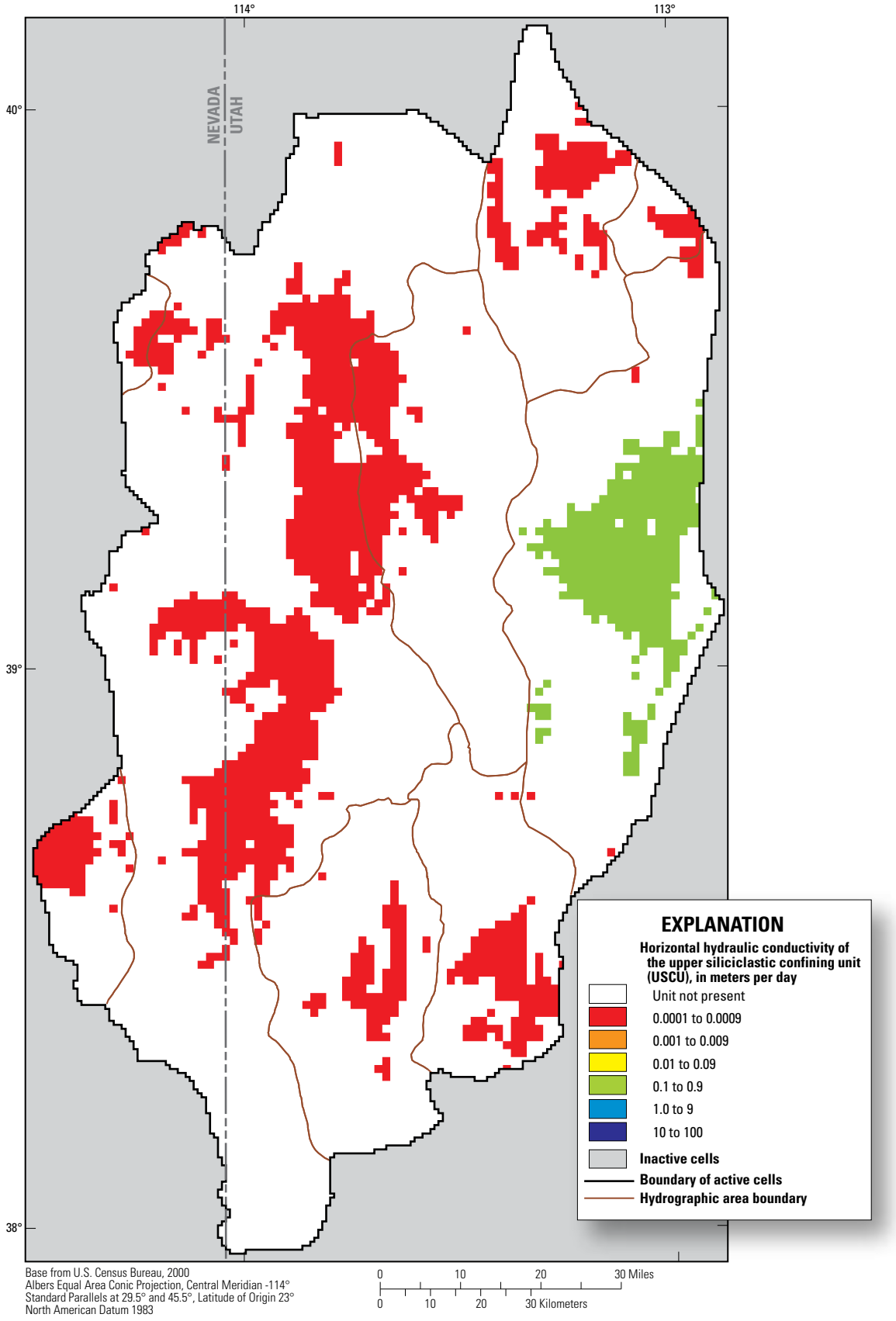

Figure 41. Distribution of simulated horizontal hydraulic conductivity of the upper siliciclastic confining unit (USCU) in the Snake Valley area groundwater model.

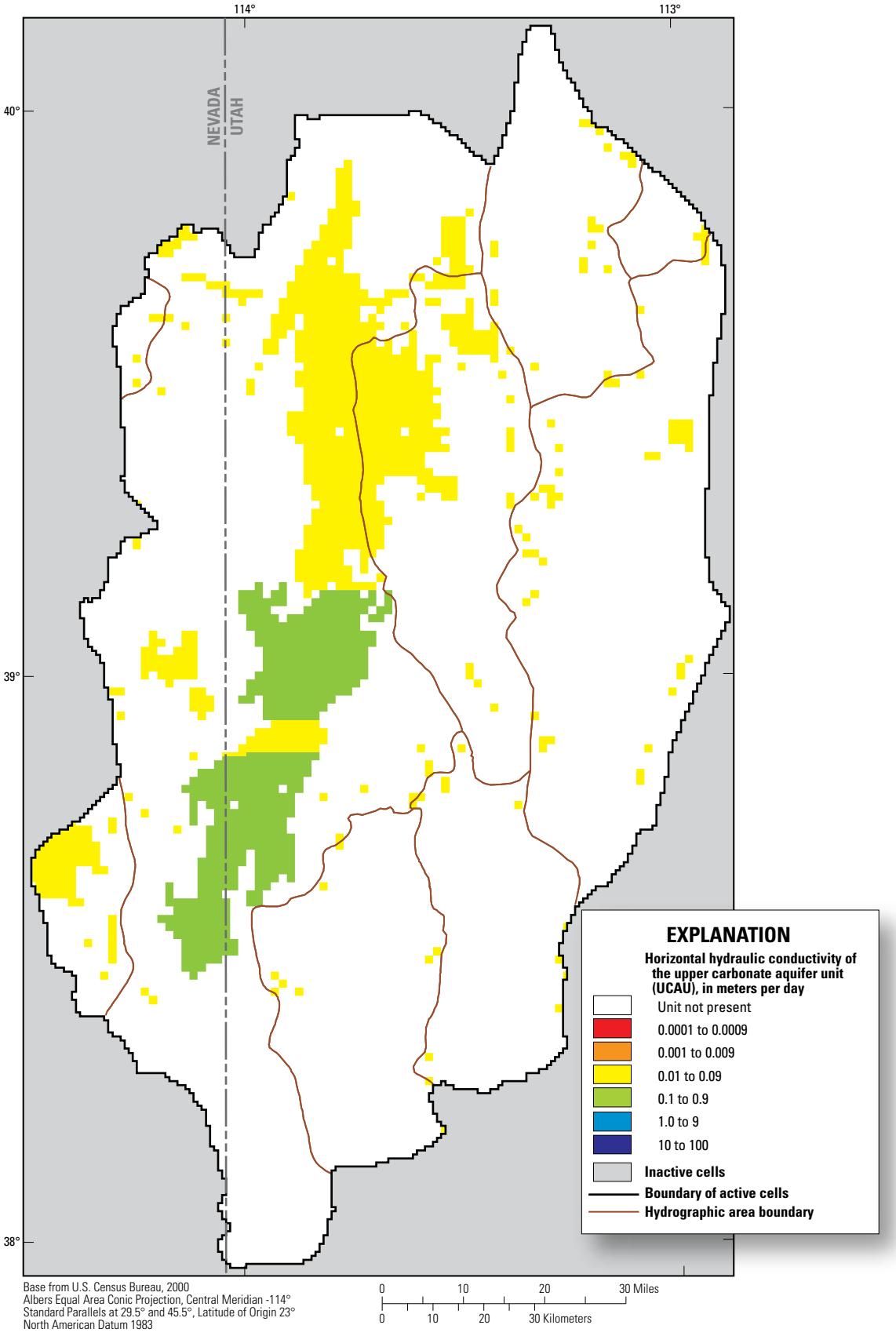

Figure 42. Distribution of simulated horizontal hydraulic conductivity of the upper carbonate aquifer unit (UCAU) in the Snake Valley area groundwater model.

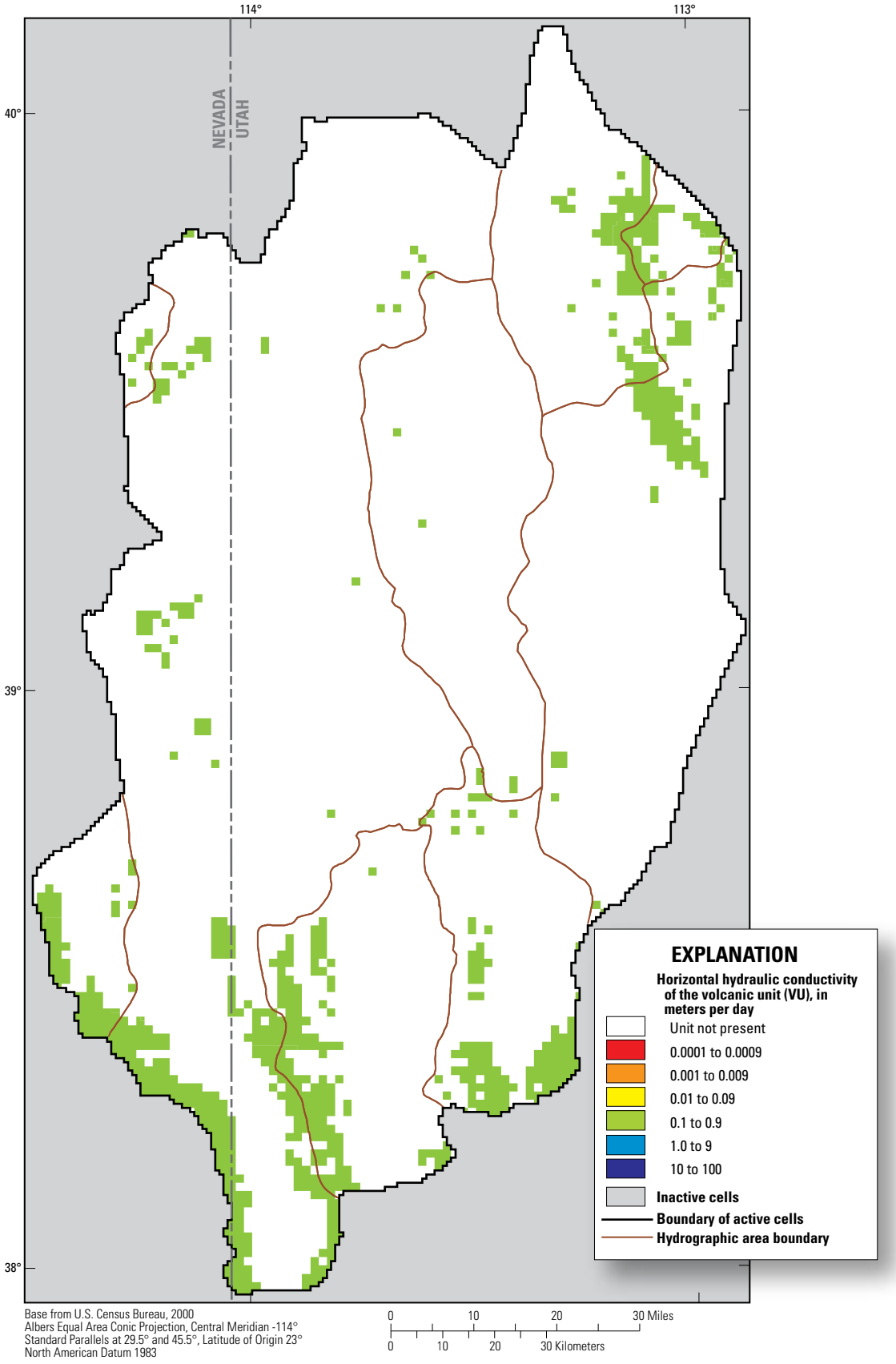

Figure 43. Distribution of simulated horizontal hydraulic conductivity of the volcanic unit (VU) in the Snake Valley area groundwater model.

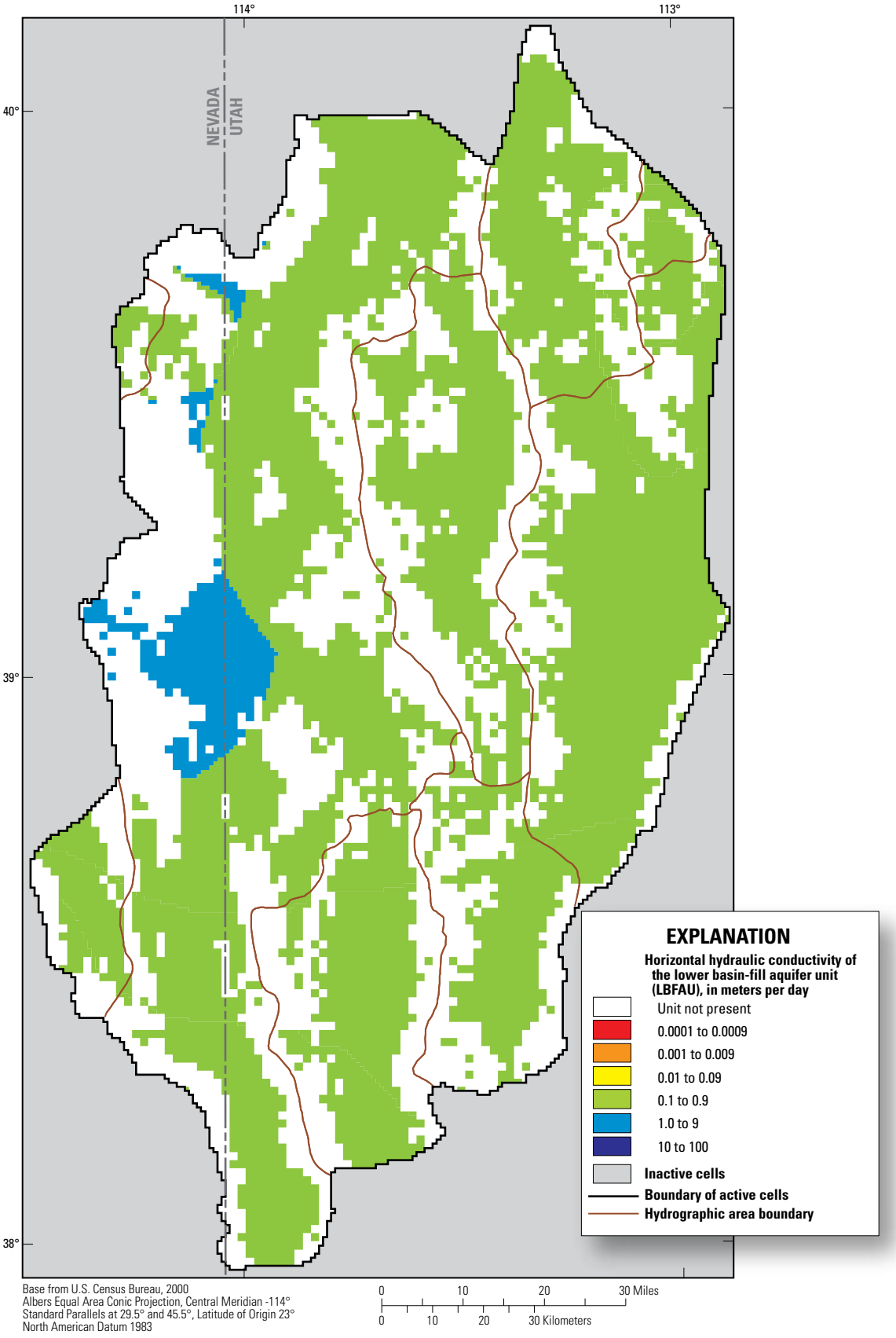

Figure 44. Distribution of simulated horizontal hydraulic conductivity of the lower basin-fill aquifer unit (LBFAU) in the Snake Valley area groundwater model.

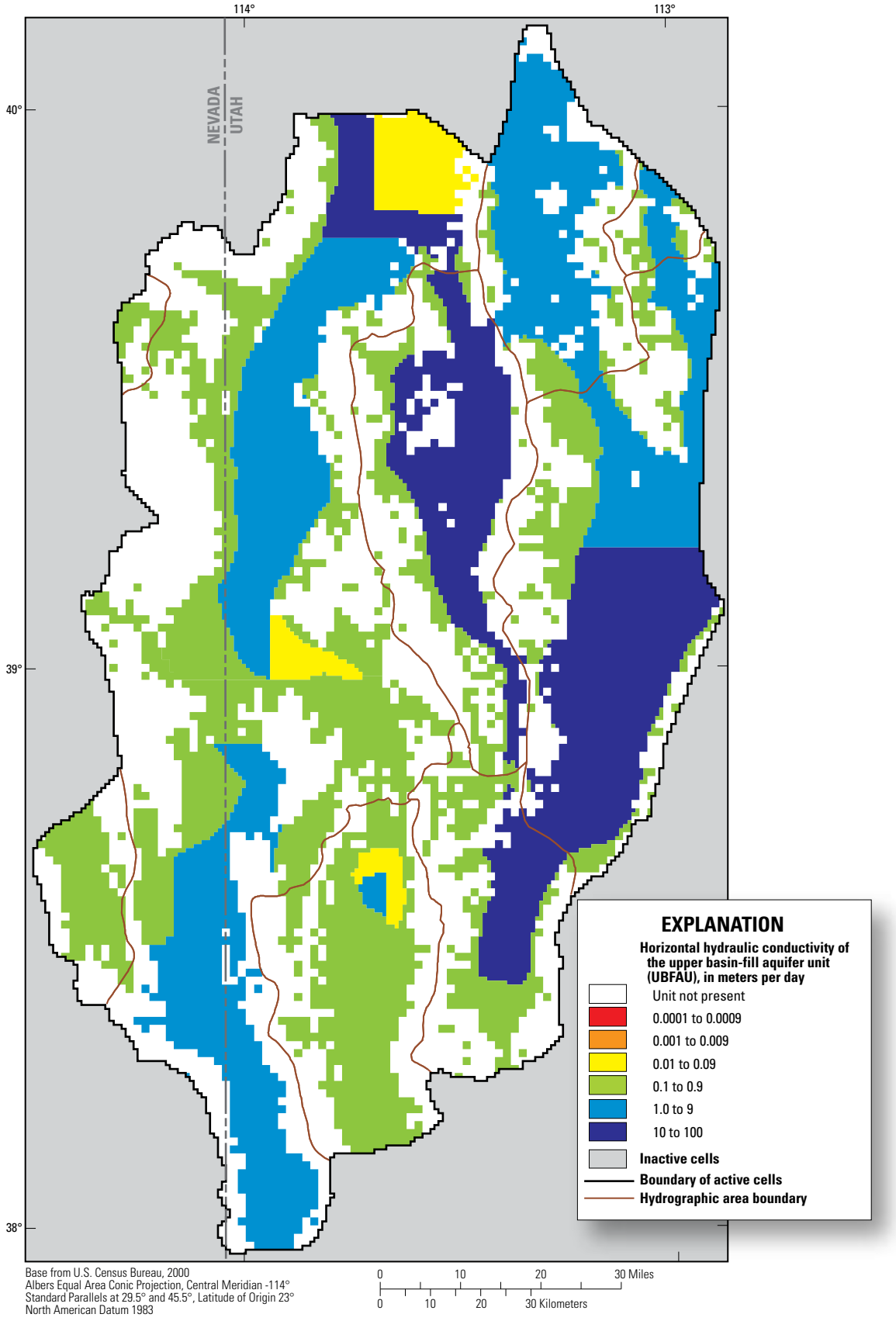

Figure 45. Distribution of simulated horizontal hydraulic conductivity of the upper basin-fill aquifer unit (UBFAU) in the Snake Valley area groundwater model.

Non-Carbonate Confining Unit (NCCU)

Model observations generally provide good information about the hydraulic conductivity of the NCCU (fig. 32), and seven parameters with values ranging from 0.00055 to 1.0 m/d define it in the model (fig. 39 and table 8). The estimated values of the parameters are within the expected hydraulic conductivity range reported for the NCCU (table 7), and all except one parameter (nccu_3hk) could be estimated with more certainty than the measured standard deviation of 2.67 on the log values of the parameters (table 7). The measured standard deviation of 2.67 was applied as prior information to parameter nccu_3hk.

Although hydraulic conductivities of 1 m/d are on the high end of conductivities for the NCCU (tables 7 and 8), this higher conductivity was needed to reduce water-level altitudes in Pine, Wah Wah, and Tule Valleys and Sevier Desert, and was needed to move water from these same HAs north towards Fish Springs (fig. 39). This higher conductivity is also supported by the fact that this zone (zone 1) of the NCCU is a quartzite that generally has a well-developed fracture network and is classified as having moderate permeability (Ludington and others, 1996; Hintze and others, 2000; Sweetkind and others, 2011a).

Lower Carbonate Aquifer Unit (LCAU)

Model observations provide good information about the hydraulic conductivity of the LCAU (fig. 32), and 10 parameters with values ranging from 0.0041 to 17 m/d define it in the model (fig. 40 and table 8). The estimated values of the parameters are within the expected hydraulic conductivity range reported for the LCAU (table 7), and all except two parameters (lcau_52hk and lcau_71hk) could be estimated with more certainty in the model than the measured standard deviation of 1.78 on the log values of the parameters. The measured standard deviation of 1.78 was applied as prior information on the two excepted parameters. Although the parameter with the lowest value (lcau_512hk) occurs in an area where the LCAU should have moderate permeability, it has limited area and was needed to simulate steep gradients and reduce discharge in downgradient areas.

Upper Siliciclastic Confining Unit (USCU)

The model observations provide little data about the hydraulic conductivity of the USCU (fig. 32), and only two parameters with values of 0.00050 and 0.52 m/d define it in the model (fig. 41 and table 8). The estimated values of the parameters are within the expected hydraulic conductivity range reported for the USCU (table 7) and can be estimated in the model with more certainty than the measured standard deviation of 2.67 on the log values of the parameters. The USCU zone with the higher hydraulic conductivity was simulated using an LCAU parameter (lcau_41hk) because during model calibration it was noticed that there was an error in the hydrogeologic framework in this part of the study area; the USCU units defined in this area of the framework do not exist and should have been defined as LCAU instead (Donald Sweetkind, U.S. Geological Survey, written commun., June 2012).

Upper Carbonate Aquifer Unit (UCAU)

Model observations generally provide good information about the hydraulic conductivity of the UCAU (fig. 32), and two parameters with values of 0.015 and 0.20 m/d define it in the model (fig. 42 and table 8). The estimated values of the parameters are within the expected hydraulic conductivity range reported for the UCAU (table 7), and one of the parameters (ucau_11hk) could be estimated with more certainty in the model than the measured standard deviation of 1.78 on the log values of the parameters. The measured standard deviation of 1.78 was applied as prior information on the other parameter (ucau_1hk).

Volcanic Unit (VU)

Model observations provide little information about the hydraulic conductivity of the VU (fig. 32), and only one parameter (caldera_hk) with a value of 0.12 m/d defines it in the model (fig. 43 and table 8). The estimated value of the parameter is within the expected hydraulic conductivity range reported for the VU (table 7); the parameter, however, could not be estimated with more certainty in the model than the measured standard deviation of 1.43 on the log values of the parameter. The measured standard deviation of 1.43 was applied as prior information on this parameter.

Lower Basin-Fill Aquifer Unit (LBFAU)

Model observations provide good information about the hydraulic conductivity of the LBFAU (fig. 32), and three parameters with values ranging from 0.12 to 2.0 m/d define it in the model (fig. 44 and table 8). Volcanic portions of the LBFAU were defined using the same parameter as the VU (caldera_hk). The estimated values of the parameters are within the expected hydraulic conductivity range reported for the LBFAU (table 7), and all parameters could be estimated with more certainty than the measured standard deviation of 1.58 on the log values of the parameters.

Upper Basin-Fill Aquifer Unit (UBFAU)

Most of the groundwater discharge in the study area and model occurs through this unit as ETg. Model observations generally provide good information about the hydraulic conductivity of the UBFAU (fig. 32), and six parameters with values ranging from 0.060 to 10 m/d define it in the model (fig. 45 and table 8). The estimated values of the parameters are within the expected hydraulic conductivity range reported for the UBFAU (table 7), and all parameters could be estimated with more certainty than the measured standard deviation of 1.26 on the log values of the parameters.

Vertical Anisotropy

Two vertical anisotropy parameters were initially defined, one for the UBFAU and one for all other HGUs. Initial sensitivity analysis indicated that the observations provide little information about these parameters (fig. 31). During calibration, however, vertical anisotropy in the UBFAU and LBFAU was sometimes important to simulate the observed discharge to evapotranspiration and groundwater temperatures. Two parameters (ubfau_vn and playa_vn) were defined to allow anisotropy in basin-fill units to vary. These units are the most likely to have stratification that would tend to decrease the vertical conductivity relative to the horizontal (anisotropy ratios greater than 1). An additional parameter (lcau_vn) was defined for the consolidated-rock HGUs. The calibrated values of all vertical anisotropy parameters were determined by regression, ranged from 1 to 51 (table 9), were within reasonable limits (Faunt and others, 2010), and had reasonable confidence intervals (fig. 33).

Horizontal-Flow Barriers

Most faults in the study area do not have enough data on either side to determine if they are barriers to groundwater flow. Two HFBs were simulated along selected faults, typically where HGU thickness changes dramatically across the fault and spring discharge observations could not be adequately simulated without the HFB (fig. 27). The HFB simulated between Snake Valley and Pine and Tule Valleys corresponds with a steeply, almost vertically dipping synclinal limb of the USCU (fig. 27) and is evidenced by distinctly different water levels on the east and west sides of this structure. One parameter (B_SV_NS1) representing the hydraulic characteristic of the barrier was defined for all HFBs simulated in the model and was estimated to be four orders of magnitude less than the lowest simulated horizontal hydraulic-conductivity parameter value. The value of this parameter was set to adequately simulate water levels or discharge without causing water levels to be above land surface on the upgradient side of the HFB. Composite scaled sensitivity to the HFB parameter is low (fig. 32), possibly because of its small value (Hill and Tiedeman, 2007). Because of this insensitivity, and because the hydraulic characteristic is dependent on hydraulic conductivity, a standard deviation of 2.67, the greatest standard deviation for hydraulic conductivity (table 7), was applied to the log values of this parameter as prior information.

Thermal Parameters

Two thermal properties, basal heat flux and longitudinal dispersivity, were defined using parameters (heatflux and longdisp, respectively) that could vary in the model. Model observations generally provide good information about the basal heat flux and slightly less information about the longitudinal dispersivity (fig. 32). The values of these parameters were determined by regression within reasonable limits and with reasonable confidence (fig. 33).

Model Evaluation

The calibrated model was evaluated to assess the accuracy of simulated results. An advantage of using nonlinear regression to calibrate the model is that a substantial methodology exists for model evaluation that facilitates a better understanding of model strengths and weaknesses (Hill and Tiedeman, 2007; Faunt and others, 2010). A protocol exists to evaluate the accuracy of simulated water-level altitudes, groundwater discharge, and groundwater temperatures; estimated and specified parameter values and associated sensitivities and confidence intervals; and other measures of parameter and prediction uncertainty. As part of the model evaluation, a comparison of simulated results to the conceptual regional water budget, previously published regional water-level contours, model fit

Table 9. Calibrated horizontal-to-vertical anisotropy values and statistics for parameters used in the Snake Valley area groundwater model.

[**Model zone:** zone number used in MODFLOW files. **Abbreviations:** LBFAU, lower basin-fill aquifer unit; LCAU, lower carbonate aquifer unit; NCCU, non-carbonate confining unit; UBFAU, upper basin-fill aquifer unit; UCAU, upper carbonate aquifer unit; USCU, upper siliciclastic confining unit; VU, volcanic unit]

Parameter name	Hydrogeologic unit	Model zone	Horizontal-to-vertical anisotropy (unitless)		Standard deviation of log values
			Calibrated parameter value	95-percent confidence interval	
ubfau_vn	UBFAU	ubfau zones 4, 41, and 42	9.9	2.0–49	0.35
	LBFAU	lbfau zones 1, 3, 4, and 5			
playa_vn	UBFAU	ubfau zones 3, 31, and 32	51	19–133	0.21
lcau_vn	LBFAU	lbfau zone 2	1.0	0.017–60	0.90
	VU	all vu zones			
	UCAU	all ucau zones			
	USCU	all uscu zones			
	LCAU	all lcau zones			
	NCCU	all nccu zones			

to observations, and values of parameter estimates and their associated sensitivities were evaluated. On the basis of this evaluation, as explained in the following sections, this model provides a reasonable representation of this regional groundwater system.

Model Fit to Observations

Model fit is evaluated using both unweighted and weighted residuals (the difference between observed and simulated values). Unweighted residuals have the same dimensions as the observations and are clearly understood, but they can be misleading because observations are measured with different accuracies. Two unweighted residuals that are of equal value may not indicate an equally satisfactory model fit. Given the large regional scale of this model, calibration attempts were concentrated to reduce unweighted residuals to 50 m for water levels, 30 percent of flow for discharge observations, and 2 °C for temperature observations. Weighted residuals are used in summary statistics and regression, and reflect model fit relative to the expected observation error, but are more difficult to interpret than unweighted residuals.

Summary statistics for model fit are listed in table 10. The square root of the sum of squared weighted residuals (SOSWR) divided by the number of observations (Nobs) is called the standard error of the regression and provides a measure of model fit relative to the weighting that can be compared for different types of observations (Hill and Tiedeman, 2007). A value of 1.0 indicates a match that is, overall, consistent with the observation error evaluation used to determine the weighting. The standard error of the regression can be used to multiply the average standard deviations and coefficients of variation to obtain dimensional values that reflect the fit of any group of observations (Hill and Tiedeman, 2007). The value of $[SOSWR/Nobs]^{1/2}$ of 6.62 for water-level observations from wells multiplied by the average standard deviation of observations from wells of 1.75 m indicates that the model has an overall fit to water levels in wells of 12 m, which is well within the 50 m considered adequate for this regional model. The model statistics for discharge include the weight multiplier that was used in UCODE_2005 to force regressions to match discharge more closely. The value of $[SOSWR/Nobs]^{1/2}$ of 2.98 for discharge observations indicates that the model has an overall fit to discharge observations of a coefficient of variation of 0.33, which is slightly greater than the estimated error in the discharge observations (see the "Groundwater Discharge Observations and Uncertainty" section of this report) but close to the 30 percent considered adequate for this regional model. Similar to discharge, the model statistics for groundwater temperature in wells include the weight multipliers used in UCODE_2005 to force regressions to match all types of observations equally, not just the temperatures with small variances. The value of $[SOSWR/Nobs]^{1/2}$ of 8.00 for temperature observations indicates that the model has an overall fit to temperature observations of 2.8 °C, which is only slightly above the 2 °C considered adequate for this regional model.

Water Levels

The fit of simulated to observed water levels is generally good; 98 percent of the simulated values of water levels in wells are within 30 m of the observation, and 58 percent of them are within 12 m (table 11). Weighted observations plotted against weighted simulated values generally fall on the 1 to 1 line (fig. 46*A*). Positive and negative water-level residuals are distributed randomly around the study area, indicating no systematic model error (fig. 47). Graphs of weighted water-level residuals and weighted simulated values (fig. 48*A*) also indicate little model bias; most of the weighted residuals vary randomly about a value of zero.

Comparison of the simulated water-level altitudes (fig. 49) with the potentiometric surface map of Gardner and others (2011) indicates that the groundwater model results adequately depict major features of the water-level altitude distribution and regional patterns of groundwater flow. In general, areas of nearly flat and steep hydraulic gradients are appropriately located.

Table 10. Summary statistics for measure of model fit for the Snake Valley area groundwater model.

[**Abbreviations:** SOSWR, sum of squared weighted residuals; Nobs, number of observations]

Type of observation	Number of observations	Average positive weighted residual	Average negative weighted residual	SOSWR	[SOSWR/Nobs]$^{1/2}$	Average standard deviation or coefficient of variation (with weighting)
Water levels in wells	123	4.25	-6.30	5,386	6.62	[1]1.75
Discharge	20	3.39	-1.07	178	2.98	[2]0.11
Groundwater temperatures in wells	31	6.79	-3.87	1,984	8.00	[3]0.35

[1]Standard deviation, in meters.
[2]Coefficient of variation.
[3]Standard deviation, in degrees Celsius.

Table 11. Summary of observed and simulated water-level altitudes for the Snake Valley area groundwater model.

[Values are rounded and may not exactly match model files. **Abbreviations:** USGS, U.S. Geological Survey]

Observation name	USGS site number	Altitude of well (meters)	Observed water-level altitude (meters)	Variance (square meters)	Simulated water-level altitude (meters)	Residual (observed minus simulated, in meters)
C281722dda1	382113113435401	1,761	1,646	11.12	1,686	-40
C281711cca1	382259113433701	1,733	1,622	21.26	1,660	-38
C281411abb1	382350113231901	1,585	1,382	43.61	1,411	-29
C271428ddd1	382535113251101	1,552	1,379	15.26	1,401	-22
C271428ddd2	382539113250601	1,551	1,380	13.16	1,400	-20
N086935CDDD1	383023114115301	1,775	1,727	5.23	1,721	6
N076902BABA2	383023114115302	1,781	1,727	6.68	1,721	6
C261425aad1	383131113214301	1,452	1,381	4.47	1,381	0
N087021AADA1	383252114075101	1,741	1,701	6.34	1,716	-15
N086915BCDD1	383325114134901	1,746	1,724	7.07	1,725	-1
C26173cdd1	383357113440601	1,600	1,467	8.98	1,480	-13
C26173cda1	383402113440601	1,601	1,468	9.07	1,479	-11
C26202aad1	383452114023401	1,884	1,703	1.63	1,709	-6
C26202aad2	383452114023402	1,884	1,703	1.64	1,709	-6
N097034DCDC1	383545114070101	1,727	1,693	3.85	1,714	-21
C251618bdd1	383825113410801	1,551	1,459	3.84	1,443	16
N097014DABD1	383826114051201	1,718	1,686	4.22	1,711	-25
N096711DBCD1	383907114253001	1,846	1,761	1.55	1,744	17
N096811BDBD1	383925114190801	1,887	1,739	1.74	1,734	5
C241334ccb1	384042113181601	1,417	1,353	4.08	1,376	-23
C241323ccd1	384215113165701	1,408	1,354	3.90	1,375	-21
N107028CBCB1	384227114082701	1,772	1,703	2.38	1,714	-11
C241215cdc1	384306113112601	1,393	1,368	1.69	1,374	-6
C241913cbd1	384324113554401	1,754	1,723	5.75	1,700	23
C241913cbd2	384324113554402	1,754	1,724	5.85	1,700	24
C241916cbb1	384327113591401	1,739	1,662	7.26	1,687	-25
C241916bdb2	384340113585701	1,727	1,661	7.57	1,686	-25
C241916bdb3	384340113585702	1,727	1,661	7.68	1,686	-25
C241916bdb4	384342113585401	1,725	1,661	7.93	1,686	-25
C241916bdb5	384342113585402	1,725	1,661	8.47	1,686	-25
C242014bbc1	384347114025601	1,685	1,660	1.61	1,676	-16
C241313aac1	384351113150501	1,389	1,361	1.51	1,375	-14
C24198baa1	384449113595401	1,677	1,656	7.59	1,678	-22
C24193dbc1	384510113573001	1,702	1,660	3.86	1,685	-25
C24201adc1	384521114014701	1,661	1,660	4.05	1,670	-10
C232025ccd1	384651114025101	1,664	1,655	3.94	1,666	-11
C232025ccd2	384651114025102	1,664	1,655	4.05	1,666	-11
C231924dcc1	384746113554701	1,766	1,658	15.30	1,667	-9
C231920cac1	384755114003301	1,651	1,645	4.03	1,631	14
C231920cac2	384755114003401	1,650	1,645	4.03	1,630	15
C231920cac3	384755114003402	1,650	1,646	1.47	1,639	7
C23126ccd1	385008113145301	1,413	1,350	10.82	1,374	-24
C22141cba1	385542113223601	1,458	1,351	2.72	1,373	-22
C22196bcc1	385607114015601	1,609	1,586	14.24	1,576	10
C22196bac2	385617114013801	1,603	1,584	6.74	1,571	13
C22201aba1	385623114021501	1,610	1,588	5.33	1,577	11

Table 11. Summary of observed and simulated water-level altitudes for the Snake Valley area groundwater model.—Continued

[Values are rounded and may not exactly match model files. **Abbreviations:** USGS, U.S. Geological Survey]

Observation name	USGS site number	Altitude of well (meters)	Observed water-level altitude (meters)	Variance (square meters)	Simulated water-level altitude (meters)	Residual (observed minus simulated, in meters)
C212036ccc1	385628114025701	1,619	1,590	11.49	1,580	10
C212036ccc2	385628114025702	1,619	1,590	13.01	1,585	5
C212036ccc3	385628114025703	1,619	1,586	14.50	1,583	3
C212036ddd2	385630114020201	1,604	1,584	2.15	1,576	8
C212036ddd3	385630114020202	1,604	1,583	2.17	1,579	4
C212036ddd1	385630114020301	1,604	1,585	4.70	1,577	8
C211932dad1	385643113594701	1,623	1,561	2.16	1,582	-21
C211932dad2	385643113594702	1,623	1,562	2.24	1,582	-20
C211932dad3	385649113594601	1,620	1,566	2.73	1,581	-15
C211817add1	385933113530801	1,538	1,520	7.62	1,529	-9
C211812ccd1	385958113493401	1,541	1,507	9.50	1,525	-18
C21178dcc1	390000113463701	1,547	1,479	13.38	1,489	-10
C201932ddd1	390059114000401	1,548	1,532	1.58	1,542	-10
C201932ddd2	390059114000402	1,548	1,537	1.59	1,543	-6
C201932ddd3	390059114000403	1,548	1,537	1.60	1,544	-7
C201832abd1	390141113532901	1,530	1,519	6.60	1,520	-1
C201832aba2	390143113533002	1,530	1,516	4.71	1,528	-12
C201832aba3	390143113533003	1,530	1,516	4.29	1,527	-11
C201921acc1	390312113591701	1,534	1,524	13.34	1,529	-5
C201916aaa1	390425113585201	1,527	1,519	4.57	1,523	-4
C201916aaa2	390426113585201	1,527	1,519	2.02	1,523	-4
C201916aaa3	390426113585202	1,527	1,521	2.04	1,524	-3
C20198bcb1	390503114005901	1,534	1,533	8.87	1,527	6
C20146dda2	390540113272301	1,379	1,352	10.73	1,371	-19
C20191bcc1	390549113562901	1,520	1,521	6.66	1,513	8
C191936cda1	390629113560301	1,537	1,514	5.13	1,511	3
C191936daa2	390637113553102	1,562	1,508	1.89	1,510	-2
C191936daa1	390637113553201	1,562	1,509	59.91	1,510	-1
C191736bcb1	390656113425101	1,784	1,349	41.35	1,371	-22
C191128bdb1	390803113054801	1,420	1,354	2.15	1,370	-16
C19107bda1	391050113010101	1,431	1,374	10.96	1,371	3
C181536cdd1	391136113290401	1,382	1,350	10.73	1,369	-19
C181832cbb1	391156113541901	1,524	1,491	1.45	1,489	2
C181832cbb2	391156113541902	1,524	1,492	1.45	1,489	3
C181832cbb3	391156113541903	1,524	1,492	1.45	1,489	3
C181832cbb4	391156113541904	1,524	1,492	1.45	1,489	3
C181831adb1	391205113543401	1,516	1,491	4.01	1,488	3
C181920ddd1	391322114000001	1,522	1,515	13.90	1,489	26
C171534cac1	391704113312001	1,359	1,350	2.03	1,365	-15
C171525cbb1	391801113292201	1,352	1,351	2.05	1,363	-12
C171616cdc1	391926113391801	1,605	1,440	6.74	1,423	17
C171616cdc2	391926113391802	1,605	1,447	6.81	1,423	24
C171517acc2	391951113331601	1,364	1,349	3.09	1,362	-13
C17194add2	392141113585601	1,487	1,473	4.73	1,473	0
C161634bcd2	392229113381701	1,462	1,418	14.89	1,381	37
C161826cba1	392317113504201	1,491	1,478	5.89	1,463	15

Table 11. Summary of observed and simulated water-level altitudes for the Snake Valley area groundwater model.—Continued

[Values are rounded and may not exactly match model files. **Abbreviations:** USGS, U.S. Geological Survey]

Observation name	USGS site number	Altitude of well (meters)	Observed water-level altitude (meters)	Variance (square meters)	Simulated water-level altitude (meters)	Residual (observed minus simulated, in meters)
C151936bca1	392756113563401	1,470	1,469	4.25	1,467	2
C151532aab3	392840113330401	1,374	1,349	1.63	1,360	-11
C151532aab2	392840113330402	1,374	1,349	1.62	1,360	-11
C151532aab1	392841113330401	1,374	1,349	1.62	1,360	-11
C151819dcc1	392906113550301	1,461	1,460	4.24	1,466	-6
C151630bdd1	392916113343301	1,393	1,349	1.55	1,359	-10
C151422ddd1	392924113235101	1,386	1,348	2.03	1,359	-11
C141832aaa1	393331113533001	1,460	1,459	4.04	1,459	0
C141832aaa2	393331113533002	1,460	1,459	4.04	1,459	0
C141832aaa3	393331113533003	1,460	1,460	1.48	1,459	1
C141832aba1	393331113534401	1,461	1,459	4.01	1,460	-1
C141826dbc1	393345113503201	1,513	1,461	14.60	1,453	8
C14139cba1	393701113191101	1,410	1,343	1.58	1,350	-7
C141410acb1	393714113242001	1,438	1,349	3.05	1,355	-6
C14124cbc1	393745113123001	1,467	1,354	1.49	1,347	7
C14132adb2	393803113161601	1,413	1,353	1.62	1,347	6
C14132adb3	393803113161602	1,413	1,353	1.62	1,347	6
C14132adb1	393806113161501	1,412	1,353	1.62	1,347	6
C131833ddc1	393814113522601	1,452	1,449	13.39	1,433	16
C131632abb1	393914113400701	1,580	1,350	1.67	1,356	-6
C131828dab1	393928113522601	1,458	1,450	14.85	1,427	23
C131425dac1	393933113214801	1,360	1,327	3.62	1,347	-20
C131523ccc1	394014113303301	1,494	1,333	10.85	1,356	-23
C131424baa1	394045113222501	1,383	1,327	2.13	1,344	-17
C121312caa1	394727113152901	1,376	1,320	3.79	1,326	-6
C111636cdb1	394905113354101	1,347	1,346	4.99	1,334	12
C111215bba1	395216113111801	1,397	1,320	10.75	1,322	-2
C11124ccd1	395310113123301	1,364	1,318	1.47	1,318	0
C11124cbc1	395331113123901	1,360	1,318	10.74	1,318	0
C11166cbc4	395355112423601	1,320	1,320	5.39	1,326	-6
C20179cad1	390453113454701	1,674	1,490	13.86	1,480	10

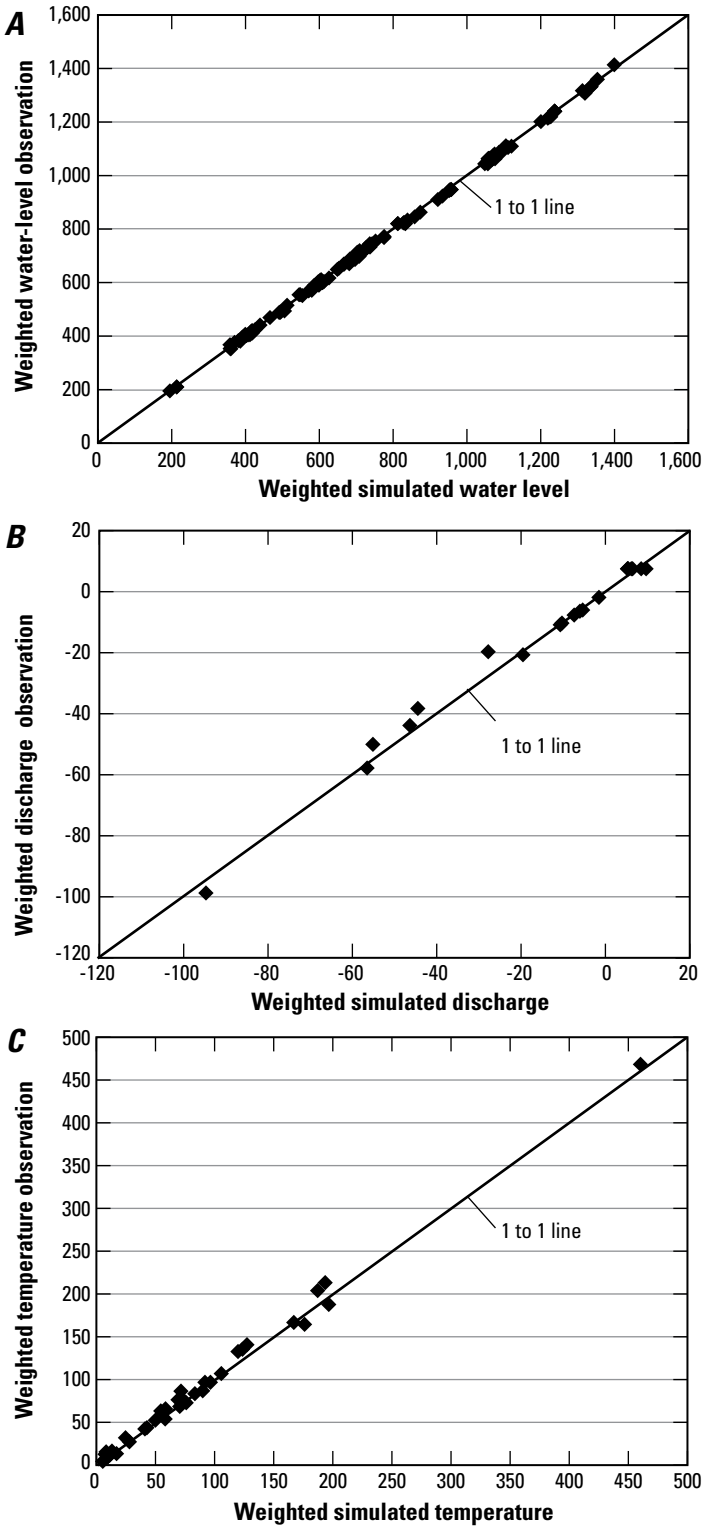

Figure 46. Weighted observations compared to weighted simulated values for *A*, water levels, *B*, discharge, and *C*, temperatures in the Snake Valley area groundwater model.

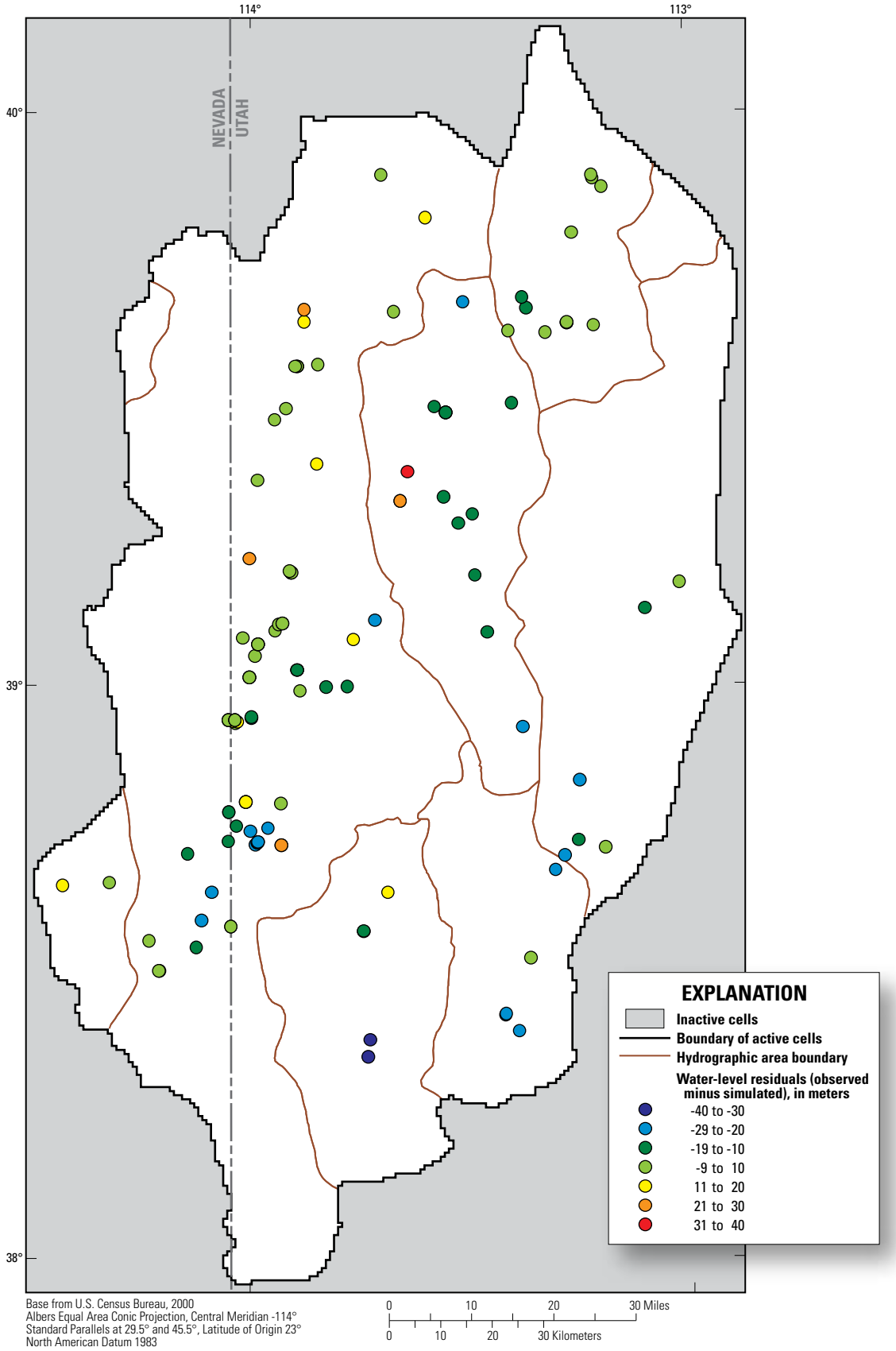

Figure 47. Distribution of water-level residuals (observed minus simulated) in the Snake Valley area groundwater model.

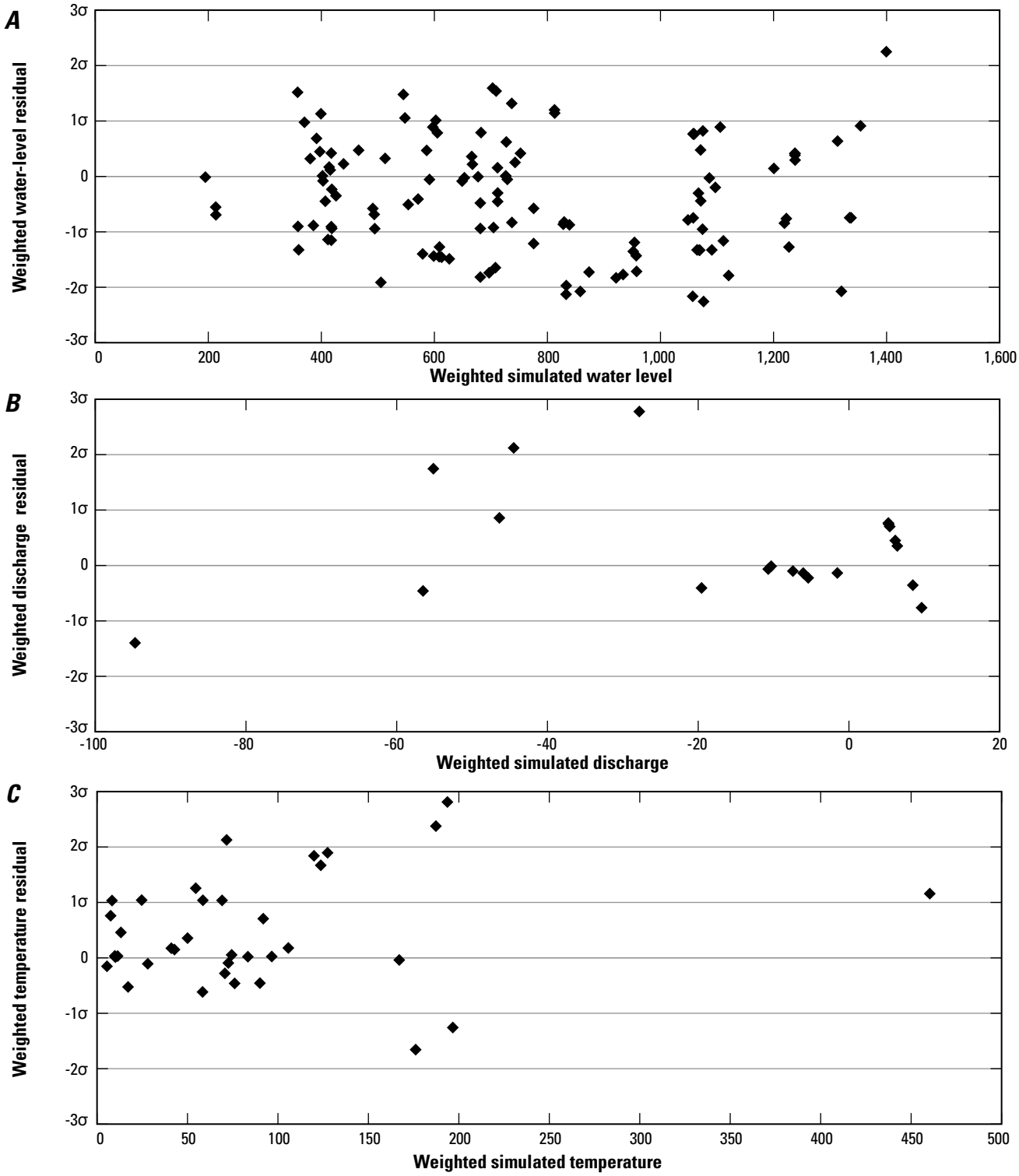

Figure 48. Weighted residuals compared to weighted simulated values for *A*, water levels, *B*, discharge, and *C*, temperatures in the Snake Valley area groundwater model. The standard deviations of the weighted residuals are used to define the grid lines.

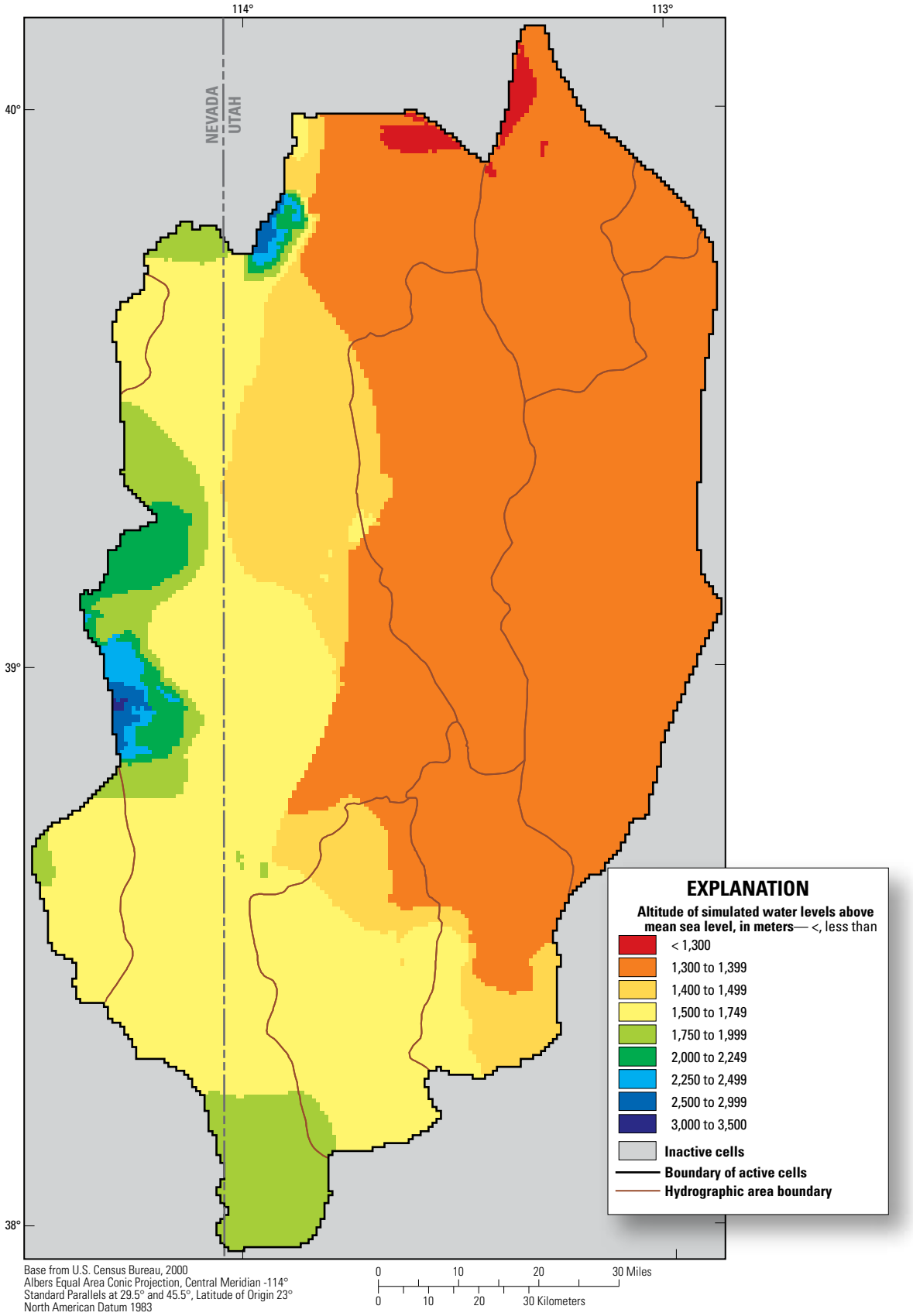

Figure 49. Distribution of simulated water-level altitudes in the Snake Valley area groundwater model.

Discharge

Calibration was focused on matching groundwater discharge to ETg, springs, and rivers more so than to matching individual water-level observations. Simulating accurate discharge was considered important in simulating the regional budget, in understanding regional sources of water to discharge areas, and in adequately simulating the complex regional aquifer system.

The fit of simulated to observed discharge is generally good; all simulated discharge with the exception of Dearden Spring Group is within 30 percent of the observed discharge (table 12). Dearden Spring Group is within 41 percent of the observed discharge. The discharge at Dearden Spring Group is difficult to measure; the springs discharge at diffuse areas along Big Springs Creek and cannot be measured directly. The streamflow measured at three flumes upstream and downstream of the springs was used to indirectly measure discharge from the springs. It is possible, therefore, that the observed discharge at Dearden Spring Group is in error. Weighted discharge observations plotted against weighted simulated values generally fall on the 1 to 1 line (fig. 46*B*). Positive and negative residuals are mostly evenly distributed throughout the study area (fig. 50), but a few trends are evident, most notably discharge to ETg. Simulated discharge to ETg is substantially more than observed discharge throughout the central part of the study area, and is less than observed in Snake Valley and Sevier Desert. Graphs of weighted discharge residuals and weighted simulated values (fig. 48*B*) also indicate little model bias; most of the weighted residuals vary randomly about a value of zero.

Table 12. Summary of observed and simulated discharge for the Snake Valley area groundwater model.

[**Abbreviations:** ETg, groundwater evapotranspiration; %, percent]

Groundwater discharge type	Observation name	Observed discharge (cubic meters per day)	Simulated discharge (cubic meters per day)	Simulated discharge as a percent of observed discharge
Snake Valley				
ETg				
North	ET_2541	45,755	32,493	71%
North-central	ET_2542	131,042	95,151	73%
South-central	ET_2543	96,827	83,516	86%
South	ET_2544	7,462	6,156	82%
Springs				
Miller Spring	miller	931	1,025	110%
Gandy Warm Springs	gandy	36,830	34,739	94%
Twin Springs and Foote Reservoir Spring	twin_foote	13,240	12,935	98%
Unnamed Spring	unnamed	4,906	4,820	98%
Rowland Springs	rowland	5,576	5,231	94%
Spring Creek Spring	spring_creek	4,648	4,912	106%
Clay Spring	clay	868	832	96%
Dearden Spring Group	dearden	16,320	22,985	141%
Big Springs	big	24,420	28,342	116%
Mountain streams				
Granite and Trout Creeks	gran_trout	4,761	4,743	100%
Strawberry, Baker, and Snake Creeks	str_bak_snk	7,560	6,005	79%
Wah Wah Valley				
Springs				
Wah Wah Springs	wah_wah	2,725	2,434	89%
Tule Valley				
ETg	ET_257	128,311	146,047	114%
Fish Springs Flat				
ETg	ET_258	27,013	35,019	130%
Springs				
Fish Springs	fish	87,790	84,447	96%
Sevier Desert				
ETg	ET_287	29,039	20,382	70%

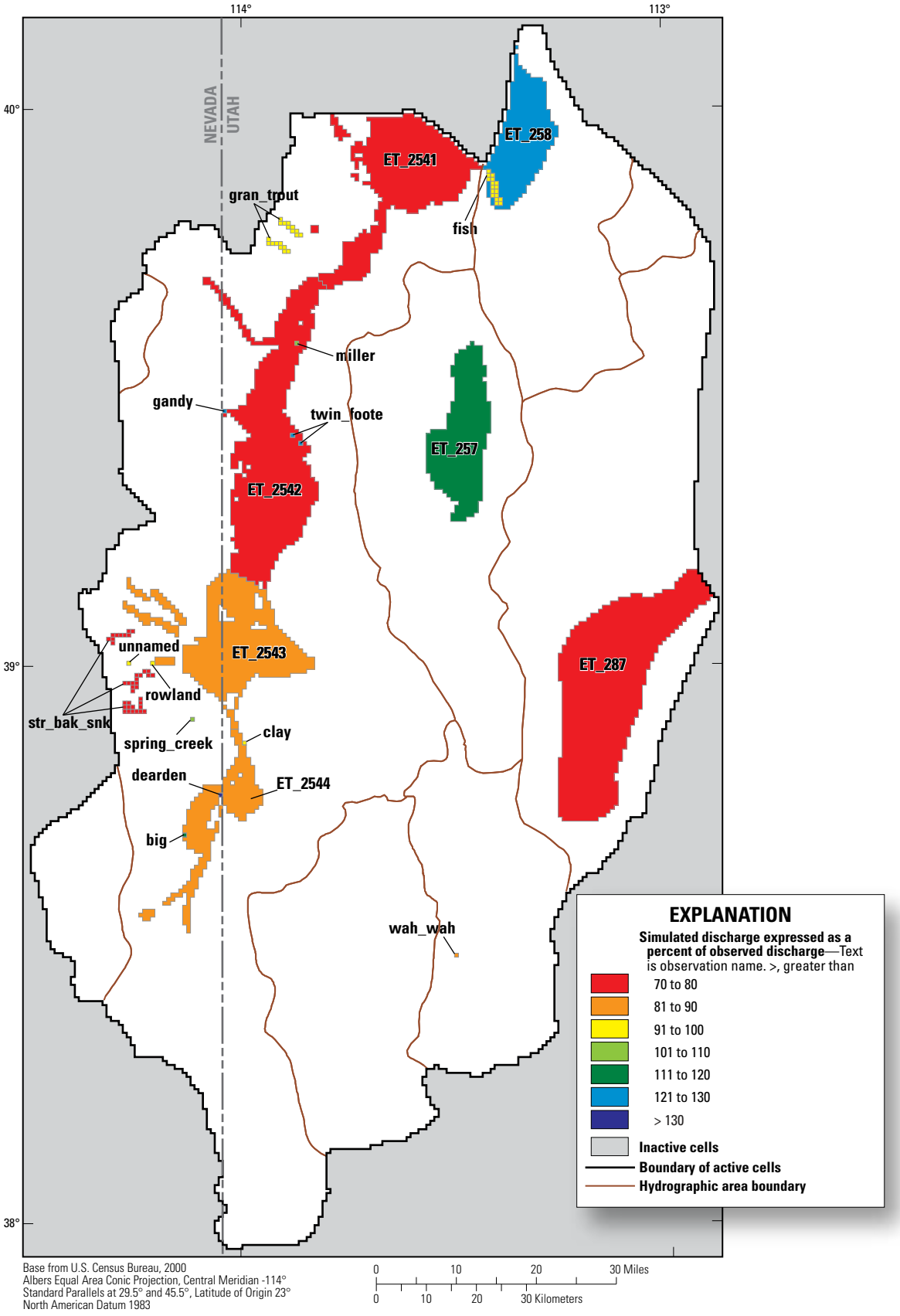

Figure 50. Simulated discharge as a percent of observed discharge in the Snake Valley area groundwater model.

Temperatures

The fit of simulated to observed temperatures is generally good; 81 percent of the simulated values of groundwater temperatures in wells are within 2 °C of the observation, and 55 percent of them are within 0.75 °C (table 13). The largest temperature residuals generally occur at or near springs. Simulated groundwater temperatures at Gandy Warm Springs (observation gandyT) and Big Springs (observation bigT) are cooler than the observed temperatures by 13 °C and 7.5 °C, respectively. It is possible that there are local effects leading to the warmer observed temperatures at these springs that could not be simulated in this larger regional model. Weighted temperature observations plotted against weighted simulated values generally fall on the 1 to 1 line, indicating good model fit (fig. 46*C*). Positive and negative temperature residuals are distributed randomly around the study area, indicating no systematic model error. Graphs of weighted temperature residuals and weighted simulated values (fig. 48*C*) also indicate little model bias; most of the weighted residuals vary randomly about a value of zero.

Table 13. Summary of observed and simulated groundwater temperatures for the Snake Valley area groundwater model.

Observation name	Observed temperature (degrees Celsius)	Simulated temperature (degrees Celsius)	Residual (observed minus simulated, in degrees Celsius)
PW01C2	12.7	13.6	-0.9
PW01C3	13.7	14.8	-1.1
PW01C4	15.6	14.9	0.7
PW01C5	19.1	15.3	3.8
PW02B2	14.8	13.4	1.4
PW02B3	16.7	12.8	3.9
PW03B2	13.2	13.2	0.0
PW03B3	13.3	13.1	0.2
PW04B2	15.7	14.2	1.5
PW05C2	13.8	14.5	-0.6
PW05C3	14.5	15.1	-0.5
PW05C4	15.8	15.5	0.4
PW06D2	18.2	16.4	1.8
PW06D3	18.6	16.0	2.6
PW07B2	13.5	13.5	0.0
PW07B3	14.4	14.9	-0.4
PW07B4	15.4	16.1	-0.7
PW07B5	17.0	17.5	-0.5
PW09B2	16.9	16.9	-0.0
PW09B3	18.0	18.2	-0.2
PW11E2	15.1	14.3	0.8
PW11E3	16.5	14.7	1.8
PW11E4	18.0	14.9	3.1
PW12A2	35.2	31.9	3.3
PW17C2	17.5	17.3	0.2
PW17C3	19.0	18.5	0.5
PW18A2	46.9	42.9	4.1
PW19C2	35.1	32.3	2.9
PW20A2	25.2	25.0	0.1
SG21C1	23.2	29.7	-6.6
SG24C1	16.4	16.1	0.3
clayT	13.6	13.3	0.3
deardenT	13.8	13.7	0.1
gandyT	27.2	14.2	13.0
bigT	17.5	10.0	7.5
unnamedT	5.6	7.1	-1.5

Estimated Parameter Values and Sensitivities

Most of the parameters estimated during model calibration are related to recharge, evapotranspiration, horizontal hydraulic conductivity, vertical anisotropy, well withdrawals, drain and river conductances, and thermal properties. Less sensitive parameters are related to general-head boundary conductances, hydraulic characteristics of HFBs, and subsurface flow across the eastern boundary (fig. 32). Of the 51 defined parameters, 40 were estimated using nonlinear regression, and 42 are within reasonable ranges. The other defined parameters were not estimated using regression because CSS values indicate that there is insufficient information to estimate them; most of these are horizontal hydraulic-conductivity parameters. These parameters are often important, however, in defining local flow patterns and gradients, especially in the mountain blocks. Compared to reported hydraulic-conductivity estimates (Sweetkind and others, 2011a), these non-regressed estimated hydraulic-conductivity parameter values fall within reasonable ranges (tables 7 and 8).

Reduction of Parameter Uncertainty with the Inclusion of Temperature Observations

Several previous studies (Woodbury and Smith, 1988; Bravo and others, 2002; Manning and Solomon, 2005; Heilweil and others, 2012) have shown that using temperature observations in numerical models reduces the uncertainty in model parameters more than using only water-level observations and (or) groundwater flow (discharge) observations. Most of these studies, however, are at the basin or sub-basin scale. This study represents one of the first regional modeling efforts to include calibration to groundwater temperature data.

UCODE_2005 was used to calculate the reduction in parameter uncertainties using groundwater temperature observations over using just water-level and (or) groundwater discharge observations. Figure 51 shows the 95-percent confidence intervals for model parameters using (1) only water-level observations (blue bars); (2) water-level plus discharge observations (green bars); and (3) water-level, discharge, and temperature observations (red bars). Although most parameters are highly sensitive to the spring discharge observations (fig. 32), the inclusion of temperature observations further reduces parameter uncertainty, in some cases quite significantly. For example, the 95-percent confidence interval for parameter lbfau_4hk (representing horizontal hydraulic conductivity) has a range spanning about 12 orders of magnitude when only water-level observations are used. This range is reduced to about six orders of magnitude with the addition of discharge observations, and is further reduced to about one order of magnitude with the addition of temperature observations.

Because groundwater temperatures are highly affected by the magnitude of groundwater flow, parameters controlling this aspect of the system were more constrained by temperature observations than water-level or groundwater discharge observations (fig. 51). These include parameters representing (1) the horizontal hydraulic conductivity of the basin-fill HGUs (UBFAU and LBFAU) and the carbonate HGUs (UCAU and LCAU); (2) the vertical anisotropy ratio, especially those of the basin-fill units (parameters ubfau_vn and playa_vn); (3) spring and river conductance; (4) recharge rate; and (5) well withdrawal rate.

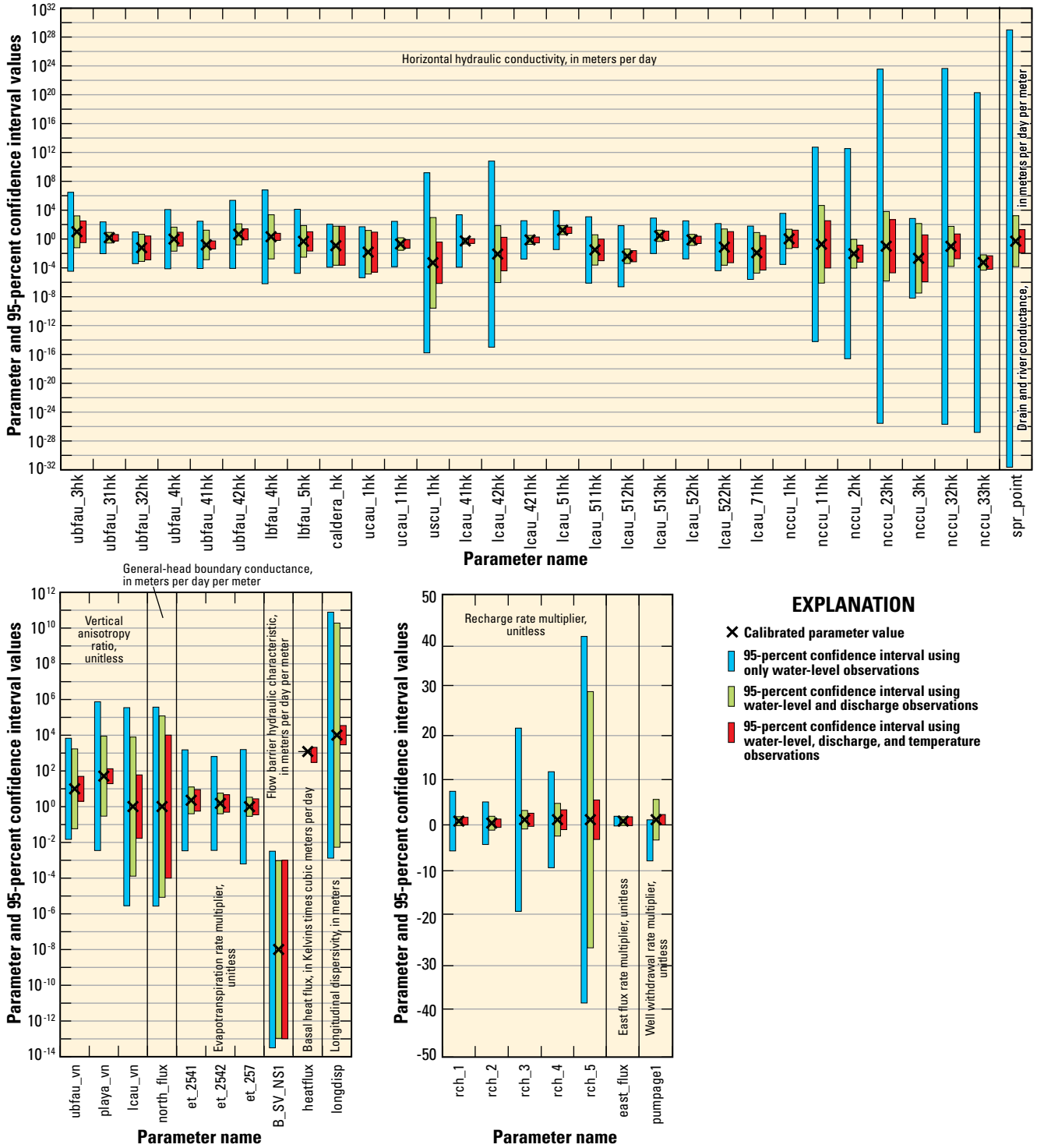

Figure 51. Calibrated model parameter values and 95-percent confidence intervals using only water-level observations, water-level plus discharge observations, and water-level plus discharge and temperature observations in the Snake Valley area groundwater model.

Regional Groundwater Budget

The conceptual and simulated water budgets for the entire study area and also for the eight individual HAs in the study area are listed in table 14. One calibration criterion for the model was to match conceptual recharge and discharge components to within plus or minus 30 percent, because the majority of the discharge measurements had uncertainties of about 30 percent. The model simulated recharge and discharge amounts to within plus or minus 30 percent of the conceptual recharge and discharge amounts with the exception of Pine Valley, where simulated areal recharge (in-place plus runoff plus unconsumed irrigation) is 68 percent of the conceptual recharge. This is because recharge was reduced in southern Spring, Snake, and Pine Valleys to minimize flooding in the mountain blocks and to reduce simulated water levels in

Table 14. Comparison of simulated, conceptual, and previously reported groundwater budget components for hydrographic areas and the Snake Valley study area, Utah and Nevada.

[All estimates in acre-feet per year rounded to two significant figures. **Abbrevations:** HA, hydrographic area; —, no data; NE, not estimated]

	Simulated	Conceptual	Previous studies
Spring Valley (HA 184)[1]			
Recharge			
Direct infiltration of precipitation (in-place recharge) + infiltration of runoff (including unconsumed surface-water irrigation) + infiltration of mountain stream base flow + unconsumed irrigation from well withdrawals	15,000	16,000	—
Subsurface inflow	0	NE	—
Discharge			
Groundwater evapotranspiration + springs	0	0	—
Mountain streams	0	0	—
Well withdrawals	0	0	—
Subsurface outflow	15,000	NE	[2,3,4,5,6,7,8]4,000 to 49,000
Northern Spring Valley to Snake Valley	2,200	NE	[5]16,000
Southern Spring Valley to Snake Valley	13,000	NE	[2,3,4,5,6,7,8]4,000 to 33,000
Snake Valley (HA 254)			
Recharge			
Direct infiltration of precipitation (in-place recharge) + infiltration of runoff (including unconsumed surface-water irrigation) + infiltration of mountain stream base flow + unconsumed irrigation from well withdrawals	160,000	160,000	[2,3,5,9,10]99,000 to 160,000
Subsurface inflow	15,000	NE	[2,3,4,5,6,7,8]4,000 to 49,000
From Northern Spring Valley	2,200	NE	[5]16,000
From Southern Spring Valley	13,000	NE	[2,3,4,5,6,7,8]4,000 to 33,000
Discharge			
Groundwater evapotranspiration + springs	100,000	120,000	[2,3,5,11]64,000 to 130,000
Mountain streams	3,300	3,600	[11]2,800
Well withdrawals	28,000	[12]22,000	[13,14]11,000
Subsurface outflow	44,000	NE	[2,3,4,5,7]25,000 to 43,000
To Pine Valley	2,000	NE	—
To Wah Wah Valley	23	NE	—
To Tule Valley	33,000	NE	[2,3,4]15,000 to 42,000
To Fish Springs Flat	790	NE	[4]0
To outside of study area	8,400	NE	[2,4,5]10,000 to 29,000
Pine Valley (HA 255)			
Recharge			
Direct infiltration of precipitation (in-place recharge) + infiltration of runoff (including unconsumed surface-water irrigation) + infiltration of mountain stream base flow + unconsumed irrigation from well withdrawals	18,000	27,000	[3,9,10,15]21,000 to 27,000
Subsurface inflow	2,000	NE	—
From Snake Valley	2,000	NE	—
Discharge			
Groundwater evapotranspiration + springs	0	0	[3,14,15]0
Mountain streams	0	0	[3,14,15]0
Well withdrawals	0	0	[16]5
Subsurface outflow	20,000	NE	[3,4,15,17]3,000 to 14,000
To Wah Wah Valley	20,000	NE	[4,15,17]3,000 to 14,000
To Tule Valley	0	NE	[3]14,000

southern Snake and Pine Valleys. The amount of reduction in recharge is approximately equal to the amount of previously reported groundwater discharge from perched areas to springs, streams, and ETg (Stephens, 1976), which would be disconnected from the larger regional flow system. Because the model did not simulate discharge from these perched areas, the reduction in recharge accounts for any groundwater that may have been discharged to these perched areas. Although simulated recharge was reduced in southern Spring and Snake Valleys, simulated areal recharge in Spring and Snake Valleys is more similar to conceptual amounts than in Pine Valley because simulated recharge was increased over conceptual recharge in other parts of these HAs, as indicated by both the temperature and groundwater discharge observations.

Table 14. Comparison of simulated, conceptual, and previously reported groundwater budget components for hydrographic areas and the Snake Valley study area, Utah and Nevada.—Continued

[All estimates in acre-feet per year rounded to two significant figures. **Abbrevations:** HA, hydrographic area; —, no data; NE, not estimated]

	Simulated	Conceptual	Previous studies
Wah Wah Valley (HA 256)			
Recharge			
Direct infiltration of precipitation (in-place recharge) + infiltration of runoff (including unconsumed surface-water irrigation) + infiltration of mountain stream base flow + unconsumed irrigation from well withdrawals	4,700	5,900	[3,9,10,18]6,000 to 7,000
Subsurface inflow	20,000	NE	[4,15,17]3,000 to 14,000
From Snake Valley	23	NE	—
From Pine Valley	20,000	NE	[4,15,17]3,000 to 14,000
Discharge			
Groundwater evapotranspiration + springs	710	740	[3,14,17]1,400 to 1,500
Mountain streams	0	0	[3,14,17]0
Well withdrawals	0	0	[19]110
Subsurface outflow	24,000	NE	[3,4]8,500
To Tule Valley	11,000	NE	[3,4]8,500
To Sevier Desert	13,000	NE	—
Tule Valley (HA 257)			
Recharge			
Direct infiltration of precipitation (in-place recharge) + infiltration of runoff (including unconsumed surface-water irrigation) + infiltration of mountain stream base flow + unconsumed irrigation from well withdrawals	14,000	13,000	[3,9,10,18]7,600 to 13,000
Subsurface inflow	44,000	NE	[2,3,4,18,20]15,000 to 50,000
From Snake Valley	33,000	NE	[2,3,4]15,000 to 42,000
From Wah Wah Valley	11,000	NE	[3,4,18]8,500 to 32,000
From Sevier Desert	2,000	NE	[4]9,000
Discharge			
Groundwater evapotranspiration + springs	44,000	39,000	[3,14,18]24,000 to 56,000
Mountain streams	0	0	[3,14,18]0
Well withdrawals	0	0	—
Subsurface outflow	16,000	NE	[4,21]27,000 to 31,000
To Fish Springs Flat	16,000	NE	[4]27,000
Fish Springs Flat (HA 258)			
Recharge			
Direct infiltration of precipitation (in-place recharge) + infiltration of runoff (including unconsumed surface-water irrigation) + infiltration of mountain stream base flow + unconsumed irrigation from well withdrawals	1,200	1,700	[3,9,10,21]1,600 to 4,000
Subsurface inflow	37,000	NE	[3,4,21]27,000 to 31,000
From Snake Valley	790	NE	[4]0
From Tule Valley	16,000	NE	[4]27,000
From Dugway-Government Creek Valley	5,100	NE	—
From Sevier Desert	15,000	NE	[4]0
From outside of study area	100	NE	—
Discharge			
Groundwater evapotranspiration + springs	35,000	34,000	[3,14,21]34,000 to 35,000
Mountain streams	0	0	[3,14,21]0
Well withdrawals	0	0	—
Subsurface outflow	2,400	NE	[3,4]100 to 1,000
To outside of study area	2,400	NE	[4]1,000

Simulated discharge matches conceptual discharge within the range of plus or minus 30 percent in all HAs. This indicates that the model reasonably represents the movement of water from recharge areas to discharge areas and water levels within the discharge areas.

Simulated subsurface flow between HAs and out of the study area, along with uncertainties (table 15), were also calculated for the model using the predictive capabilities of UCODE_2005 (Poeter and others, 2005). These subsurface flow estimates are HA based, and may include flow between

Table 14. Comparison of simulated, conceptual, and previously reported groundwater budget components for hydrographic areas and the Snake Valley study area, Utah and Nevada.—Continued

[All estimates in acre-feet per year rounded to two significant figures. **Abbrevations:** HA, hydrographic area; —, no data; NE, not estimated]

	Simulated	Conceptual	Previous studies
Dugway-Government Creek Valley (HA 259)[1]			
Recharge			
Direct infiltration of precipitation (in-place recharge) + infiltration of runoff (including unconsumed surface-water irrigation) + infiltration of mountain stream base flow + unconsumed irrigation from well withdrawals	230	300	—
Subsurface inflow	71	NE	—
From outside of study area	71	NE	—
Discharge			
Groundwater evapotranspiration + springs	0	0	—
Mountain streams	0	0	—
Well withdrawals	0	0	—
Subsurface outflow	5,000	NE	—
To Fish Springs Flat	5,000	NE	—
Sevier Desert (HA 287)[1]			
Recharge			
Direct infiltration of precipitation (in-place recharge) + infiltration of runoff (including unconsumed surface-water irrigation) + infiltration of mountain stream base flow + unconsumed irrigation from well withdrawals	8,900	10,000	—
Subsurface inflow	19,000	NE	—
From Wah Wah Valley	13,000	NE	—
From outside of study area	6,200	NE	—
Discharge			
Groundwater evapotranspiration + springs	6,200	8,600	[22]8,600
Mountain streams	0	0	—
Well withdrawals	0	0	—
Subsurface outflow	22,000	NE	[4,20]8,800 to 9,000
To Tule Valley	2,000	NE	[4]9,000
To Fish Srings Flat	15,000	NE	[4]0
To Dugway-Government Creek Valley	4,800	NE	—
Study area total			
Recharge			
Direct infiltration of precipitation (in-place recharge) + infiltration of runoff (including unconsumed surface-water irrigation) + infiltration of mountain stream base flow + unconsumed irrigation from well withdrawals	220,000	240,000	—
Subsurface inflow from outside of study area	6,400	NE	—
Discharge			
Groundwater evapotranspiration + springs	190,000	200,000	—
Mountain streams	3,300	3,600	—
Well withdrawals	28,000	22,000	—
Subsurface outflow to outside of study area	11,000	NE	—

[1]Partial HA; estimates only for portion of HA within study area.
[2]Hood and Rush, 1965.
[3]Gates and Kruer, 1981.
[4]Harrill and others, 1988.
[5]Welch and others, 2007.
[6]Rush and Kazmi, 1965.
[7]Scott and others, 1971.
[8]Nichols, 2000.
[9]Harrill and Prudic, 1998.
[10]Masbruch, 2011a.
[11]Masbruch, 2011c.
[12]Estimate for the year 2009.
[13]Estimate for the year 2000.
[14]Masbruch, 2011b.
[15]Stephens, 1976.
[16]Estimate for the year 1976.
[17]Stephens, 1974.
[18]Stephens, 1977.
[19]Estimate for the year 1974.
[20]Holmes, 1984.
[21]Bolke and Sumsion, 1978.
[22]Wilberg, 1991.

cells along the topographic divides; they are not just valley to valley flow as has been reported in previous studies. The magnitude of the uncertainties (shown as 95-percent confidence intervals in table 15) of the simulated flows is related to the uncertainty in the model parameters and the sensitivity of the simulated flows to the model parameters (Hill and Tiedeman, 2007). The uncertainties were calculated using simultaneous confidence intervals (Hill and Tiedeman, 2007) because no subsurface flow amounts within the study area are known with certainty. Methods used for determining simultaneous confidence intervals tend to produce larger intervals than exact intervals would be for a linear model with normally distributed residuals (Poeter and others, 2005). Additionally, the confidence intervals get larger as more intervals are calculated because the uncertainty of each individual subsurface flow amount is affected by the uncertainty of all the other subsurface flow amounts. The 95-percent simultaneous confidence intervals have a 95-percent probability of containing their respective true predicted values simultaneously (Hill and Tiedeman, 2007). The negative amounts shown on the lower end of the confidence intervals indicate that subsurface flow between HAs and across the model boundary could go in the opposite direction; no simulated boundary flow has 95-percent confidence in direction. Because the model developed in the current study takes into account the uncertainties of the parameters as well as the observations in calculating the uncertainties of the simulated subsurface flow amounts, these simulated subsurface flow estimates and uncertainties are considered a better quantification of subsurface flow than previously reported estimates.

Simulated subsurface flow estimates between HAs and across the study area boundary, along with their associated uncertainty, are within the range of previously reported estimates, except for subsurface flow from Spring Valley to Snake Valley north of the Snake Range; the simulated subsurface flow and associated uncertainty indicate that flow across this boundary is much less than has been estimated recently (Welch and others, 2007). Although simulated subsurface flow amounts are more than previously reported from Pine Valley to Wah Wah Valley, Wah Wah Valley to Tule Valley, Sevier Desert to Fish Springs Flat, and Fish Springs Flat to outside the model boundary, and are less than previously reported from Tule Valley to Fish Springs Flat, Sevier Desert to Tule Valley, and Snake Valley to outside the model boundary, their 95-percent confidence intervals encompass the range of previous estimates across these boundaries, indicating that the simulated subsurface flow is actually within the range of the previous estimates.

Table 15. Summary statistics of simulated subsurface flow between hydrographic areas and out of the study area in the Snake Valley groundwater model and comparison to previous estimates.

[All values in acre-feet per year. **Abbreviations:** NE, no estimate]

Direction of simulated subsurface net flow	Simulated net flow	95-percent confidence interval	Previous estimates of subsurface flow
Northern Spring Valley to Snake Valley	2,248	-471 to 4,967	[1]16,000
Southern Spring Valley to Snake Valley	13,052	-14,283 to 40,388	[1,2,3,4,5,6,7]4,000 to 33,000
Snake Valley to Pine Valley	1,955	-20,298 to 24,208	NE
Snake Valley to Wah Wah Valley	23	-353 to 399	NE
Snake Valley to Tule Valley	31,440	-18,217 to 81,097	[2,3,4]15,000 to 42,000
Snake Valley to Fish Springs Flat	787	-2,442 to 4,015	[4]0
Pine Valley to Wah Wah Valley	20,207	-8,425 to 48,839	[4,8,9]3,000 to 14,000
Wah Wah Valley to Tule Valley	11,302	-5,068 to 27,673	[3,4]8,500
Wah Wah Valley to Sevier Desert	13,017	-292 to 26,326	NE
Tule Valley to Fish Springs Flat	15,553	-20,140 to 51,246	[4]27,000
Dugway-Government Creek Valley to Fish Springs Flat	5,052	-3,647 to 13,752	NE
Sevier Desert to Tule Valley	2,026	-20,692 to 24,743	[4]9,000
Sevier Desert to Fish Springs Flat	15,157	-3,492 to 33,806	[4]0
Sevier Desert to Dugway-Government Creek Valley	4,754	-3,641 to 13,148	NE
Snake Valley to outside model boundary	8,378	-444,001 to 460,758	[1,2,4]10,000 to 29,000
Fish Springs Flat to outside model boundary	2,412	-261,298 to 266,121	[4]1,000

[1]Welch and others, 2007.
[2]Hood and Rush, 1965.
[3]Gates and Kruer, 1981.
[4]Harrill and others, 1988.
[5]Rush and Kazmi, 1965.
[6]Scott and others, 1971.
[7]Nichols, 2000.
[8]Stephens, 1976.
[9]Stephens, 1974.

Implications

The numerical model represents a more robust quantification of groundwater budget components than the previously reported conceptually developed budget estimates (table 14) because the model integrates all components of the groundwater budget. The numerical model represents and simulates the conceptual model of an interconnected groundwater system between consolidated rock and basin fill, and of recharge areas in the mountains connecting flow through the mountains to the basins and to the regional flow system, similar to the conceptual model presented in Heilweil and Brooks (2011) for the eastern Great Basin. The concept of the mountains and basins forming a continuous groundwater system provides a more detailed representation of groundwater budgets and flowpaths compared to previous studies that separated the flow and (or) groundwater budget components between the consolidated rock and basin fill (Prudic and others, 1995; Harrill and Prudic, 1998; Welch and others, 2007).

The numerical model is also an advancement over previous numerical models, specifically the RASA-GB model (Prudic and others, 1995; Halford and Plume, 2011), for several reasons: (1) the model incorporates a more detailed hydrogeologic framework whereas the RASA-GB model used two layers to represent shallower and deeper flow; (2) the model was calibrated using more observations including several new water-level altitudes from the recently installed UGS monitoring well network and other newer wells in the study area; several new measurements of spring discharge within Snake Valley, including Dearden Spring Group, Clay Spring, Twin Springs, Foote Reservoir, and Miller Spring; discharge to mountain springs and base flow to mountain streams; and temperature data from the UGS monitoring well network; and (3) the inclusion of calibration to temperature data resulted in a reduction of parameter uncertainty over using just water-level altitude and discharge observations, which is what was used to calibrate the Great Basin RASA model.

Uncertainty in the estimates of subsurface flow are less than those of previous studies because the model balanced recharge and discharge across the entire simulated area, not just in each HA, and because of the large dataset of observations (water-level altitudes, discharge, and temperatures) used to calibrate the model and the resulting transmissivity distribution. Previous estimates had uncertainty, but it was difficult to quantify and was seldom specified. Many of the previous estimates of subsurface flow (table 15) were made on the basis of whether estimated recharge exceeded estimated discharge, or the reverse, in a basin or HA. If estimated recharge was greater than estimated discharge within the basin, groundwater was assumed to leave the basin through one or more boundaries. The uncertainties associated with estimated recharge and discharge are additive in determining the uncertainty in the subsurface flow. For example, consider a basin where recharge is 100,000 acre-ft/yr with a 30-percent uncertainty, and discharge is 70,000 acre-ft/yr with a 30-percent uncertainty. It is possible that recharge could be as low as 70,000 acre-ft/yr and discharge could be as high as 91,000 acre-ft/yr, resulting in a deficit of 21,000 acre-ft/yr and, therefore, indicating that the basin receives subsurface inflow. It is also possible that recharge could be as high as 130,000 acre-ft/yr and discharge could be as low as 49,000 acre-ft/yr, resulting in an excess of 81,000 acre-ft/yr and, therefore, indicating that the excess water must leave the basin through subsurface outflow. In this example, both the amount and direction of subsurface flow varies by a substantial amount. If groundwater flow could move into or out of multiple adjacent basins, each subsurface flow amount is even more uncertain. A few of the previous estimates were made on the basis of Darcy's Law using estimates of transmissivity, length of the boundary, and hydraulic gradient across the boundary. Because of the paucity of data, these estimates seldom accounted for uncertainty in estimating transmissivity, the length of the permeable boundary, or the hydraulic gradient.

Because uncertainties in the subsurface HA flow represent uncertainties in many model parameters at one time, post-processing model statistical tools could be used to guide data collection that would help reduce uncertainty on model parameters. One example is OPR-PPR (Tonkin and others, 2007), a software program that can identify potential observations that would most reduce prediction uncertainty. For instance, OPR-PPR could be used to identify possible areas where additional observations would be useful for predicting the reduction of groundwater discharge to springs if increased well withdrawals were occurring.

Although the quantification of groundwater flow across HA boundaries in the model is important in understanding the occurrence and movement of groundwater in and through the study area, it should be noted that the effects of groundwater development on natural discharge are not dependent on the rate and direction of groundwater flow (Leake, 2011; Barlow and Leake, 2012). For example, the effects of groundwater withdrawals in southern Spring Valley on natural discharge in southern Snake Valley would be the same whether groundwater was moving from Spring Valley to Snake Valley or from Snake Valley to Spring Valley (fig. 52). As long as aquifer properties remain the same, groundwater withdrawals in southern Spring Valley could capture natural groundwater discharge in Snake Valley, such as at Big Springs or from ETg, regardless of the direction of the interbasin flow. Barlow and Leake (2012) show that the locations and timing of depletion and capture of natural groundwater discharge are affected by (1) aquifer properties, specifically the hydraulic diffusivity, which is the hydraulic transmissivity divided by the storage coefficient; and (2) system geometry, specifically the distance between pumping locations and connected groundwater discharge areas. The simulated transmissivity (fig. 53) across HA boundaries and the location of natural discharge (fig. 6), therefore, provide a better estimate of the effect of groundwater withdrawals on groundwater resources than does the amount and direction of subsurface flow between HAs.

The distribution of simulated transmissivity (fig. 53) includes many areas of high transmissivity within and between

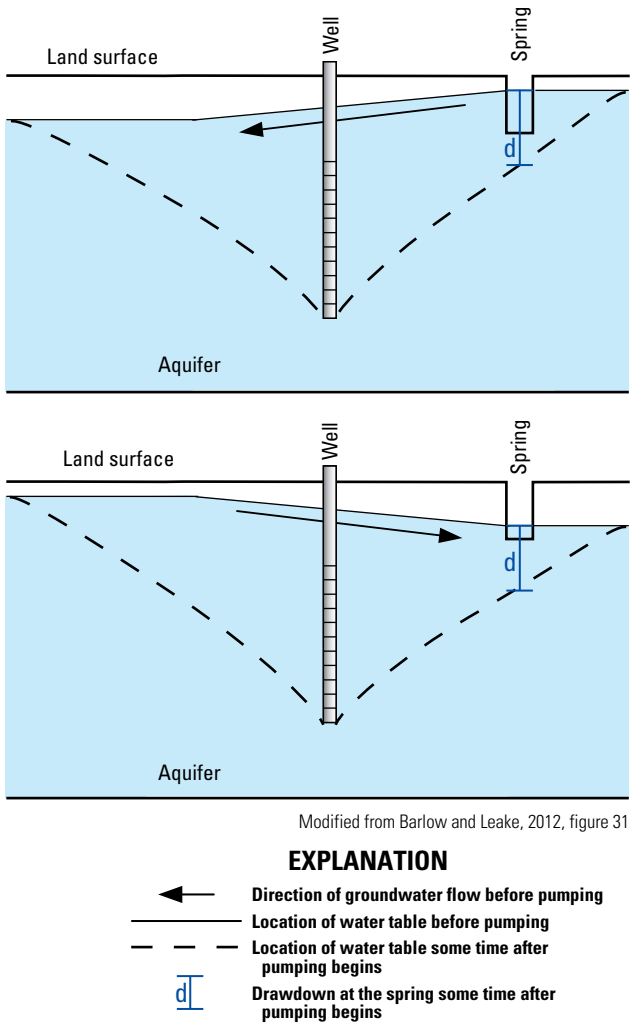

Figure 52. Position of a pumped well in relation to a spring with opposing directions of pre-pumping groundwater flow. As long as aquifer properties are the same in each case, the amount of drawdown (d) at the spring would be the same and, in the case shown, the spring would cease to flow.

HA boundaries. The highest transmissivity occurs in the middle section of the study area, extending from northern Wah Wah Valley through Tule Valley and parts of Sevier Desert and Snake Valley. This corresponds with an area where the LCAU is relatively thick (fig. 25). Other areas of high transmissivity between HAs occur between southern Spring Valley and southern Snake Valley, southern Snake Valley and southern Pine Valley, northeastern Tule Valley and Fish Springs Flat, northwestern Sevier Desert and Fish Springs Flat, and a small section between northern Spring Valley and Snake Valley. Most of these areas also correspond with thick sections of the LCAU. Well withdrawals from these areas of high transmissivity would likely affect natural groundwater discharge through a large part of the study area. For example, although the model simulates flow from Snake Valley to Pine Valley, the lack of natural discharge in Pine Valley, and the relatively large transmissivity between southern Pine Valley and Snake Valley, indicates that withdrawals in Pine Valley could cause drawdown in Snake Valley that could reduce natural discharge in southern Snake Valley. These reductions in natural discharge could occur at Big Springs, Dearden Spring Group, or from ETg in southern Snake Valley, or from all three discharge areas.

Conversely, there are a few areas where model calibration required zones of low transmissivity (fig. 53) in order to simulate discharge at springs. These include the areas between (1) northwestern Tule Valley and northeastern Snake Valley, which was needed to match discharge at Twin Springs, Foote Reservoir, Miller Spring, and Gandy Warm Springs; (2) northwestern and northern Pine Valley and Snake Valley, which was needed to match discharge at Clay Springs, Big Springs, and Dearden Spring Group; and (3) the area around Wah Wah Springs, which was needed to match discharge at Wah Wah Springs. Other areas of low transmissivity occur in the northern part of the southern Snake Range, the northern Snake Range, and the Deep Creek Range, and correspond with relatively thick sections of the lower permeability NCCU (fig. 26).

Appropriate Uses of the Model

The Snake Valley groundwater model was constructed to simulate regional-scale groundwater flow; thus, it can be used to answer questions regarding groundwater flow issues at this scale. The model can provide boundary conditions for local-scale models, but consistency between regional and local-scale models must be ensured. For example, using a regional model to determine boundary heads and then making extensive changes to hydraulic conductivity in a local model may allow more or less flow through the local model than would occur in the regional model. Programs such as Local Grid Refinement (Mehl and Hill, 2006) may be used derive boundary conditions for local-scale models that stay consistent with regional models.

The model can be used to evaluate alternative conceptualizations of the hydrogeology that are likely to have a regional effect. These might include the effects of decreased recharge caused by drought conditions, different interpretations of the extent or offset of faults, or other conceptual models of depositional environments that would affect the spatial variation of hydraulic properties.

Increased urbanization in the western United States necessitates the development of groundwater resources. Because this is a steady-state model, it can be used for examining the long-term effects of continued or increased groundwater withdrawals on the regional groundwater flow system and natural groundwater discharge, which can aid in effective management of groundwater resources.

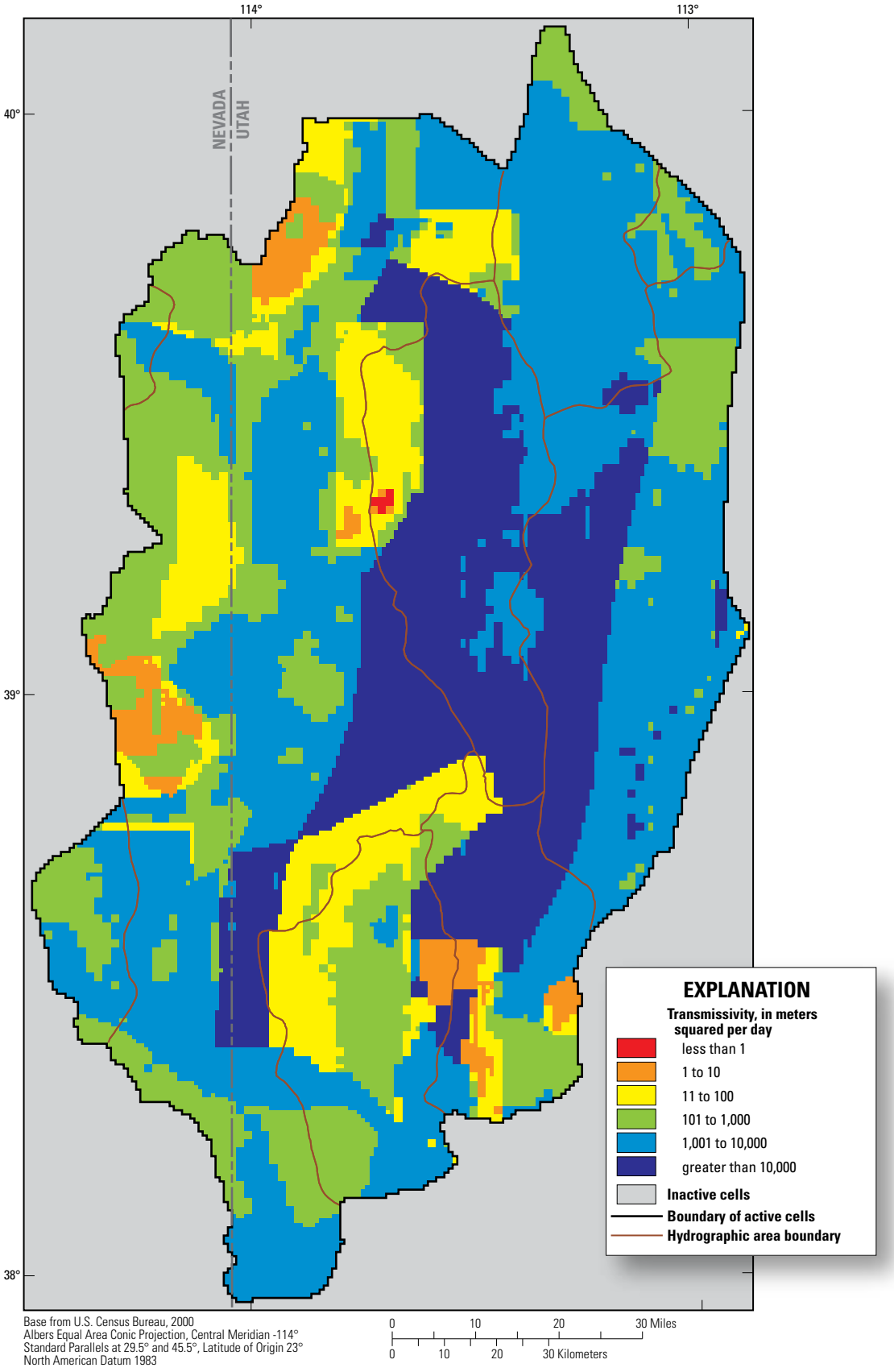

Figure 53. Simulated transmissivity in the Snake Valley area groundwater model.

Model Limitations

All models are based on a limited amount of data and, thus, are necessarily simplifications of actual systems. When creating a model of a large region it is necessary to make more simplifications than when creating models of smaller regions. Model limitations are a consequence of uncertainty in three basic aspects of the model, including inadequacies, inaccuracies, or simplifications in (1) observations used in the model, (2) representation of geologic complexity in the hydrogeologic framework, and (3) representation of the groundwater system in the model. It is important to understand how these characteristics limit the use of the model.

Observation Limitations

Observations of water levels, groundwater discharge, and temperatures constrain model calibration through parameter estimation (Faunt and others, 2010). Uncertainty in these observations introduces uncertainty in the results of model simulations. Although water-level, discharge, and temperature observations were analyzed prior to and throughout calibration, there was uncertainty regarding (1) the distribution and quality of the observation data, (2) appropriateness of the hydrogeologic interpretation, and (3) the representation of observations in the numerical model.

Distribution and Quality of Observations

The clustering of water-level and temperature observations limits the parameter estimation because it results in the overemphasis of observations in data-rich areas (Hill and Tiedeman, 2007). In the eastern (Sevier Desert) and southern (southern Snake Valley, and Pine and Wah Wah Valleys) parts of the study area, and in the mountain blocks, water-level and temperature data are sparse. A method of better distributing weights for these situations may reduce model uncertainty.

Some water-level observations used in the calibration may be affected by pumping. Only 27 wells within the study area had long-term water-level records. At these sites the spring 2009 water-level measurements were found to be similar to long-term average water levels. Additionally, the spring 2009 water levels measured in wells without long-term records were similar to those with long-term records. The spring 2009 water-level measurements used as observations in the model, therefore, were assumed to represent steady-state conditions. Without long-term water-level records, however, it is difficult to assess if the observations actually do represent steady-state conditions.

Errors in the estimates of groundwater flow across the model boundaries also affect the accuracy of the model. Any unknown and (or) unsimulated flow diminishes model accuracy. Improving estimates of flow across the boundaries can reduce model uncertainty.

Interpretation of Observations

It is difficult to assess whether certain water-level observations represent the regional saturated-zone flow system or more local-scale, perched water conditions. Areas of steep hydraulic gradient, which are important features in the regional groundwater flow system, also may be an artifact of perched water levels. Further evaluation of water levels in these areas may help reduce model uncertainty.

Evapotranspiration discharge observations were computed on the basis of vegetated areas and previously reported rates of evapotranspiration (Welch and others, 2007). These reports gave estimates of the amount of groundwater discharge that may have occurred prior to groundwater development. In Snake Valley, however, well withdrawals have increased and are assumed to have affected the amount of groundwater discharge available for ETg. Although adjustments were made to the observations to try to account for this decreased water availability, these adjustments were based on assumptions that have a great deal of associated uncertainty, namely the amount of recharge that occurs as irrigation return flow. The uncertainty in the discharge observations increases uncertainty in the flow model.

Representation of Observations

The altitude assigned to drains and ETg affects the ability of the model to simulate groundwater conditions accurately. The extinction-depth altitude used to simulate discharge through ETg likely approximates the extinction depth for all discharge areas, particularly in areas with highly variable plant root depth and discontinuous areas of capillary fringe. In areas with extensive capillary effects, such as in the fine-grained playas, observed heads may be lower than the drain altitudes or ETg extinction depth, and any drain or ETg cell will not discharge if the heads are simulated accurately.

Incised drainages and other focused discharge areas are difficult to simulate accurately at a grid resolution of 804.65 m (0.5 mi) because, in many cases, the hydraulic conductivity of the HGUs at the land surface controls the simulated discharge. Larger springs were often simulated as being in several layers in the model to minimize this effect and more closely mimic the probable high vertical conductance that occurs at these springs.

The representation of groundwater temperatures in the model was difficult given the large grid resolution and layer thicknesses. Local scale effects that may affect groundwater temperatures could not be simulated accurately at this grid resolution. Likewise, small changes in thermal gradients are difficult to capture given the layer thicknesses in the model. To better represent more local dynamics and gradients, smaller grid cells and layer thicknesses or local refinement of the model grid around selected features or in critical areas of the model domain would be required.

Hydrogeologic Framework Limitations

The accuracy of the groundwater model depends on the accuracy of the hydrogeologic conceptual model. Limitations exist in the groundwater flow model because of the difficulties inherent in the interpretation and representation of the complex geometry and spatial variability of hydrogeologic materials and structures in the hydrogeologic framework and in the application of that framework to a 804.65 m (0.5 mi) grid cell size. Abrupt changes in rock type and conductivity cannot be located at their exact positions, and small but important features may get missed completely at this scale.

The spatial variability of material properties of the HGUs and structures (Sweetkind and others, 2011a) is represented to some degree in the model. Incorporating these features in the groundwater model substantially improved the simulation, however, the model remains a significantly simplified version of reality. Detailed stratigraphy not represented in the hydrogeologic framework probably causes some of the mismatch between simulated and observed hydraulic gradients and water levels. In the groundwater model, the assumption of homogeneity within a given HGU or hydraulic-conductivity zone removes the potential effects of smaller scale variability.

Limitations of Model Representation of the Groundwater System

Three limitations of the groundwater model are inherent in its construction. These inaccuracies are in the representation of the physical framework, representation of the hydrologic conditions, and representation of thermal conditions.

Representation of Physical Framework

The 804.65 m (0.5 mi) resolution of the model grid is appropriate to represent regional conditions. A smaller grid cell size would improve simulation accuracy, especially in areas of geologic or thermal complexity. The large grid cells generalize important local-scale complexities that can affect regional flow paths and gradients, or the thermal regime within the system. To represent more local dynamics, smaller grid cells or local refinement of the model grid around selected features or in critical areas of the model domain would be required.

Representation of Hydrologic Conditions

The hydrologic conditions represented by the model are expressed as boundary conditions and include recharge; discharge from ETg, springs, and streams; and no-flow, specified-flux, and head-dependent flux boundaries at the edges of the model. Of these boundary conditions, the most significant is recharge. The main limitation in the representation of recharge is the uncertainties associated with the BCM (Flint and others, 2011; Masbruch and others, 2011). In addition to the possible errors discussed in Flint and others (2011, p. 158) and Masbruch and others (2011, p. 86–88), the BCM may overestimate recharge in parts of the model domain because it is assumed that all infiltrating water that passes the root zone ultimately reaches the water table. This assumption ignores the possibility that infiltrating water could be intercepted and perched by a lower permeability layer in the unsaturated zone.

Limitations in the definition of lateral boundary flow are the result of an incomplete understanding of natural conditions. Because very little data exist in the areas defined as lateral flow boundary segments, all aspects of the assigned boundary conditions are poorly known. Despite these uncertainties, the data used to characterize these boundary flows have been thoroughly analyzed for this model.

Representation of Thermal Conditions

Thermal conditions represented by the model are expressed as boundary conditions and thermal properties. The main limitation in the representation of boundary conditions is unknown variability in the basal heat flux across the model domain, and having to specify temperatures at the top of the model to account for conductive heat flux. Limitations associated with unknown variability in the basal heat flux are the result of highly limited to no basal heat flux data in the study area. Although several studies (Sass and others, 1971; Lachenbruch and Sass, 1977, 1978; Blackwell, 1983; Southern Methodist University Geothermal Laboratory, 2011) have identified variability in the surficial heat flow within the Great Basin and Snake Valley study area, it is likely that surficial heat flow in the Snake Valley study area is being highly affected by groundwater flow, which can mask variability in the basal heat flux. By assuming that the basal heat flux is the same across the model domain, there is associated uncertainty in the heat transport and energy balance throughout the model.

Limitations associated with applying specified temperatures across the top of the model domain are the result of uncertainty in the temperatures at the water table. Although there is a large amount of data and, therefore, good control on water table temperatures in Snake Valley, northern Tule Valley, and western Fish Springs Flat, little data exist in the southern and eastern parts of the study area and in the mountain blocks; consequently, water table temperatures in these areas are poorly known. Despite these uncertainties, the data used to characterize temperatures in these areas have been thoroughly analyzed for this model.

Limitations associated with applying a single (bulk) thermal conductivity value for an HGU are the result of limited source data (drill cuttings) to substantiate these values. Variability in these values within an HGU is highly likely at a local scale; at the resolution of the model grid, however, these variations would be difficult to quantify and represent. There is associated uncertainty, therefore, in the heat transport and energy balance throughout the model, assuming a single bulk thermal conductivity for each HGU.

Summary

The Southern Nevada Water Authority (SNWA) has proposed developing unappropriated groundwater resources in Snake Valley and adjacent basins in eastern Nevada in order to supply the growing urban population of Las Vegas, Nevada. A ruling was issued on March 22, 2012, granting SNWA water rights for 61,100 acre-ft/yr of groundwater from Spring Valley, located immediately to the west of Snake Valley. Furthermore, SNWA holds applications for approximately 50,700 acre-ft/yr of groundwater in Snake Valley.

Because of the magnitude of the SNWA groundwater development project and the interconnected nature of groundwater basins in the region, groundwater users and managers in Utah are concerned about declining groundwater levels and springflows in western Utah that could result from the proposed groundwater withdrawals. The objective of this study is focused on understanding the links between basin-fill and carbonate aquifer systems, groundwater flow paths, sources of water to springs, and the movement of groundwater between basins in the Snake Valley area. This study lays the foundation for future studies and will provide a baseline that can be used to assess the effects of future groundwater withdrawals on groundwater resources in the Snake Valley area.

This report describes the groundwater hydrology of Snake Valley and the surrounding areas and presents the construction, calibration, and results of a numerical simulation of the groundwater system developed to test the conceptual understanding of the groundwater system. Information from a number of previous and current investigations was compiled to conceptualize and quantify hydrologic and thermal components of the groundwater system, and to provide hydraulic and thermal properties and observation data used in the calibration of the numerical groundwater model. A more complete understanding of the groundwater system and budget can aid in effective management of groundwater resources.

It was beyond the scope of the current study to develop a transient groundwater model to simulate increased groundwater withdrawals within the study area. The groundwater model developed in this study, however, can be used as a tool in future studies to assess long-term effects of groundwater withdrawals and to guide the collection of additional data that will lead to better predictions of the reduction of groundwater discharge to springs and declining water levels if increased well withdrawals were occurring.

The Snake Valley area regional groundwater flow system was simulated using a three-dimensional model incorporating both groundwater flow and heat transport. The model was constructed with MODFLOW-2000, a version of the U.S. Geological Survey's groundwater flow model, and MT3DMS, a transport model that simulates advection, dispersion, and chemical reactions of solutes or heat in groundwater systems. Observations of groundwater discharge by evapotranspiration, springflow, mountain stream base flow, and well withdrawals; groundwater-level altitudes; and groundwater temperatures were used to calibrate the model. UCODE_2005 was used to perform sensitivity analysis, calibration (including parameter estimation through nonlinear regression), and uncertainty evaluation of the groundwater model. Parameter values estimated by regression were reasonable and within the range of expected values.

The model consists of seven layers, on a finite-difference grid of 310 rows and 175 columns, and uniform, square model cells with a dimension of 804.65 m (0.5 mi) on each side. Model layers were simulated under confined flow conditions, so that the top of each layer and its thickness are defined. Although the top of the actual flow system is unconfined, the model accurately simulates the position of the water table. The model was run as steady-state and, therefore, model parameters were temporally constant. Recharge into the model is from the simulation of infiltration of direct precipitation (in-place recharge), recharge from runoff, including mountain stream base flow and unconsumed irrigation from surface water, and from the simulation of subsurface groundwater inflow across the model boundary. The distribution of simulated recharge varies spatially. Groundwater discharge out of the model primarily is through simulated evapotranspiration, discharge at springs, mountain stream base flow, and well withdrawals and, to a lesser extent, by subsurface outflow across the model boundary. Several conceptual models were evaluated during calibration to test the validity of various interpretations about the flow system. The evaluation focused on testing alternative hypotheses concerning (1) the location and type of flow system boundaries (both hydrogeologic and thermal), (2) the definition of recharge areas, and (3) variations in interpretation of the hydrogeologic framework. For each conceptual model, a new set of parameters was estimated, and the resulting simulated water levels, groundwater discharges, and groundwater temperatures were compared to observed values. Only those conceptual model changes contributing to a significant improvement in model fit were retained in the final calibrated model.

This study represents one of the first regional modeling efforts to include calibration to groundwater temperature data. The inclusion of temperature observations reduced parameter uncertainty, in some cases quite significantly, over using just water-level and discharge observations. For instance, of the 39 parameters used to simulate horizontal hydraulic conductivity, uncertainty on 11 of these parameters was reduced to one order of magnitude or less. Because groundwater temperatures are highly affected by the magnitude of groundwater flow, parameters controlling this aspect of the system were more constrained by temperature observations than water-level or groundwater discharge observations. These include parameters representing (1) the horizontal hydraulic conductivity of the higher permeability basin-fill and carbonate hydrogeologic units, (2) the vertical anisotropy ratio, especially those of the basin-fill units, (3) spring and river conductance, (4) recharge rates, and (5) well withdrawal rates.

The model provides a good representation of the groundwater system; 98 percent of the simulated values of water-level altitudes in wells are within 30 m of observed water-level

altitudes, and 58 percent of them are within 12 m. Nineteen of 20 discharge observations are within 30 percent of observed discharge. Eighty-one percent of the simulated values of groundwater temperatures in wells are within 2 °C of the observed values, and 55 percent of them are within 0.75 °C.

The numerical model represents a more robust quantification of groundwater budget components than previous studies because the model integrates all components of the groundwater budget. The model also incorporates new data including (1) a detailed hydrogeologic framework, and (2) more observations, including several new water-level altitudes throughout the study area, several new measurements of spring discharge within Snake Valley, which previously had not been monitored, and groundwater temperature data. The numerical model represents and simulates the conceptual model of an interconnected groundwater system between consolidated rock and basin fill, and of recharge areas in the mountains connecting flow through the mountains to the basins and to the regional flow system. The concept of the mountains and basins forming a continuous groundwater system provides a more detailed representation of groundwater budgets and flow paths compared to previous studies that separated the flow and (or) groundwater budget components between the consolidated rock and basin fill. Uncertainty in the estimates of subsurface flow are less than those of previous studies because the model balanced recharge and discharge across the entire simulated area, not just in each hydrographic area (HA), and because of the large dataset of observations (water-level altitudes, discharge, and temperatures) used to calibrate the model and the resulting transmissivity distribution.

The model simulated recharge and discharge amounts to within plus or minus 30 percent of the conceptual recharge and discharge amounts, which are largely based on previous estimates, with one exception—Pine Valley has simulated areal recharge that is 68 percent of the conceptual recharge. This is because recharge was reduced in southern Spring, Snake, and Pine Valleys to minimize flooding in the mountain blocks and to reduce simulated water levels in southern Snake and Pine Valleys. The amount of reduction in recharge is approximately equal to the amount of previously reported groundwater discharge from perched areas to springs, streams, and evapotranspiration, which would be disconnected from the larger regional flow system. Because the model did not simulate discharge from these perched areas, the reduction in recharge accounts for any groundwater that may have been discharged to these perched areas. Although simulated recharge was reduced in southern Spring and Snake Valleys, simulated areal recharge in Spring and Snake Valleys was more similar to conceptual amounts than in Pine Valley because simulated recharge was increased over conceptual recharge in other parts of these HAs, as indicated by both the temperature and groundwater discharge observations. Simulated subsurface flow estimates between HAs along with their associated uncertainty are within the range of previously reported estimates, except for subsurface flow from Spring Valley to Snake Valley north of the Snake Range; the simulated subsurface flow and associated uncertainty indicate that flow across this boundary is much less than has been previously estimated.

Groundwater recharge from precipitation and unconsumed irrigation in Snake Valley is 160,000 acre-ft/yr, which is within the range of previous estimates. Subsurface inflow from southern Spring Valley to southern Snake Valley is 13,000 acre-ft/yr and also is within the range of previous estimates; subsurface inflow from Spring Valley to Snake Valley north of the Snake Range, however, is only 2,200 acre-ft/yr, much less than has been previously estimated. Groundwater discharge from groundwater evapotranspiration and springs is 100,000 acre-ft/yr, and discharge to mountain streams is 3,300 acre-ft/yr; these are within the range of previous estimates. Current well withdrawals are 28,000 acre-ft/yr. Subsurface outflow from Snake Valley moves into Pine Valley (2,000 acre-ft/yr), Wah Wah Valley (23 acre-ft/yr), Tule Valley (33,000 acre-ft/yr), Fish Springs Flat (790 acre-ft/yr), and outside of the study area towards Great Salt Lake Desert (8,400 acre-ft/yr); these outflows, totaling about 44,000 acre-ft/yr, are within the range of previous estimates.

Although the quantification of groundwater flow across HA boundaries in the model is important in understanding the occurrence and movement of groundwater in and through the study area, the effects of groundwater development on natural discharge are not dependent on the rate and direction of groundwater flow. The simulated transmissivity and the locations of natural discharge provide a better indication of the effect of groundwater withdrawals on groundwater resources than does the amount and direction of subsurface flow between HAs. The distribution of simulated transmissivity throughout the study area includes many areas of high transmissivity within and between HAs. Increased well withdrawals within these high transmissivity areas will likely affect a large part of the study area, resulting in declining groundwater levels, as well as leading to a decrease in natural discharge to springs and evapotranspiration.

Because this is a regional, steady-state model, it can be used for the evaluation of regional-scale processes including (1) determining boundary conditions for the development of local-scale models, (2) evaluating alternative conceptual models, (3) transport of contaminants and heat, and (4) analysis of long-term consequences of changed system stresses, such as those that would be imposed on the system by drought or increased groundwater withdrawals.

References Cited

Anderman, E.R., and Hill, M.C., 2000, MODFLOW-2000, the U.S. Geological Survey modular ground-water flow model—Documentation of the Hydrogeologic-Unit Flow (HUF) package: U.S. Geological Survey Open-File Report 00-342, 89 p.

Anderson, M.P., and Woessner, W.W., 2002, Boundaries, chap. 4 *of* Applied groundwater modeling: Simulation of flow and advective transport: San Diego, Elsevier, p. 97–145.

Barlow, P.M., and Leake, S.A., 2012, Streamflow depletion by wells—Understanding and managing the effects of groundwater pumping on streamflow: U.S. Geological Survey Circular 1376, 84 p.

Belcher, W.R., Elliott, P.E., and Geldon, A.L., 2001, Hydraulic-property estimates for use with a transient ground-water flow model of the Death Valley regional ground-water flow system, Nevada and California: U.S. Geological Survey Water-Resources Investigations Report 01-4210, 28 p.

Belcher, W.R., Sweetkind, D.S., and Elliott, P.E., 2002, Probability distributions of hydraulic conductivity for the hydrogeologic units of the Death Valley regional groundwater flow system, Nevada and California: U.S. Geological Survey Water-Resources Investigations Report 02-4212, 24 p.

Blackett, R.E., 2011, Temperature profiles of water monitoring wells in Snake Valley, Tule Valley, and Fish Springs Flat, Millard and Juab Counties, Utah: Utah Geological Survey Open-File Report 578, 13 p.

Blackwell, D.D., 1983, Heat flow in the northern Basin and Range province: Geothermal Resources Council Special Report No. 13, p. 81–92.

Bolke, E.L., and Sumsion, C.T., 1978, Hydrologic reconnaissance of the Fish Springs Flat area, Tooele, Juab, and Millard Counties, Utah: Utah Department of Natural Resources Technical Publication No. 64, 30 p.

Bravo, H.R., Jiang, Feng, and Hunt, R.J., 2002, Using groundwater temperature data to constrain parameter estimation in a groundwater flow model of a wetland system: Water Resources Research, v. 38, doi: 10.1029/2000WR000172.

Bredehoeft, J.D., and Papadopulos, I.S., 1965, Rates of vertical groundwater movement estimated from the earth's thermal profile: Water Resources Research, v. 1, p. 325–328.

Burden, C.B., and others, 2010, Groundwater conditions in Utah, spring of 2010: Utah Department of Natural Resources Cooperative Investigations Report No. 51, 135 p.

Burden, C.B., and others, 2011, Groundwater conditions in Utah, spring of 2011: Utah Department of Natural Resources Cooperative Investigations Report No. 52, 118 p.

Buto, S.G., 2011, Description of spatial datasets accompanying the conceptual model of the Great Basin carbonate and alluvial aquifer system, appendix 6 *of* Heilweil, V.M., and Brooks, L.E., eds., Conceptual model of the Great Basin carbonate and alluvial aquifer system: U.S. Geological Survey Scientific Investigations Report 2010-5193, p. 177–179.

Cartwright, K., 1970, Groundwater discharge in the Illinois Basin as suggested by temperature anomalies: Water Resources Research, v. 6, p. 912–918.

Cederberg, J.R., Sweetkind, D.S., Buto, S.G., and Masbruch, M.D., 2011, Three-dimensional hydrogeologic framework, appendix 1 *of* Heilweil, V.M., and Brooks, L.E., eds., Conceptual model of the Great Basin carbonate and alluvial aquifer system: U.S. Geological Survey Scientific Investigations Report 2010-5193, p. 127–141.

Clauser, Christoph, and Huenges, Ernst, 1995, Thermal conductivity of rocks and minerals, section (3-9) *of* Ahrens, T.J., ed., Rock physics and phase relations: A handbook of physical constants: Washington, D.C., American Geophysical Union, p. 105–126.

Cooper, H.H., and Jacob, C.E., 1946, A generalized graphical method for evaluating formation constants and summarizing well field history: American Geophysical Union Transactions, v. 27, p. 526–534.

Cunningham, W.L., and Schalk, C.W., comps., 2011, Groundwater technical procedures of the U.S. Geological Survey: U.S. Geological Survey Techniques and Methods 1–A1, 151 p.

Daly, C., Halbleib, M., Smith, J.I., Gibson, W.P., Doggett, M.K., Taylor, G.H., Curtis, J., and Pasteris, P.A., 2008, Physiographically-sensitive mapping of temperature and precipitation across the conterminous United States: International Journal of Climatology, v. 28, p. 1977–2087.

Daly, C., Neilson, R.P., and Phillips, D.L., 1994, A statistical-topographic model for mapping climatological precipitation over mountain terrain: Journal of Applied Meteorology, v. 33, p. 140–158.

Domenico, P.A., and Schwartz, P.A., 1998, The origin of porosity and permeability, chap. 2 *of* Physical and chemical hydrogeology (2): New York, John Wiley and Sons, Inc., p. 13–32.

Elliott, P.E., Beck, D.A., and Prudic, D.E., 2006, Characterization of surface-water resources in the Great Basin National Park area and their susceptibility to ground-water withdrawals in adjacent valleys, White Pine County, Nevada: U.S. Geological Survey Scientific Investigations Report 2006-5099, 156 p.

Faunt, C.G., Blainey, J.B., Hill, M.C., D′Agnese, F.A., and O′Brien, G.M., 2010, Transient numerical model, chap. F *of* Belcher, W.R., ed., Death Valley regional ground-water flow system, Nevada and California—Hydrogeologic framework and transient ground-water flow model: U.S. Geological Survey Professional Paper 1711, p. 257–344.

Faunt, C.G., Provost, A.M., Hill, M.C., and Belcher, W.R., 2011, Comment on "An unconfined groundwater model of the Death Valley Regional Flow System and a comparison to its confined predecessor", by Carroll, R.W.H., Pohll, G.M., and Hershey, R.L., [Journal of Hydrology v. 373, p. 316–328]: Journal of Hydrology, v. 397, p. 306–309.

Fenneman, N.M., 1931, Physiography of western United States: New York, McGraw-Hill, Inc., 534 p.

Flint, A.L., and Flint, L.E., 2007a, Application of the basin characterization model to estimate in-place recharge and runoff potential in the Basin and Range carbonate-rock aquifer system, White Pine County, Nevada, and adjacent areas in Nevada and Utah: U.S. Geological Survey Scientific Investigations Report 2007-5099, 20 p.

Flint, A.L., Flint, L.E., and Masbruch, M.D., 2011, Input, calibration, uncertainty, and limitations of the Basin Characterization Model, appendix 3 *of* Heilweil, V.M., and Brooks, L.E., eds., Conceptual model of the Great Basin carbonate and alluvial aquifer system: U.S. Geological Survey Scientific Investigations Report 2010-5193, p. 149–163.

Flint, L.E., and Flint, A.L., 2007b, Regional analysis of ground-water recharge, *in* Stonestrom, D.A., Constantz, J., Ferré, T.P.A., and Leake, S.A., eds., Ground-water recharge in the arid and semiarid southwestern United States: U.S. Geological Survey Professional Paper 1703, p. 29–59.

Gardner, P.M., and Heilweil, V.M., 2014, A multiple-tracer approach to understanding regional groundwater flow in the Snake Valley area of the eastern Great Basin, USA: Applied Geochemistry, v. 45, p. 33–49.

Gardner, P.M., Masbruch, M.D., Plume, R.W., and Buto, S.G., 2011, Regional potentiometric-surface map of the Great Basin carbonate and alluvial aquifer system in Snake Valley and surrounding areas, Juab, Millard, and Beaver Counties, Utah, and White Pine and Lincoln Counties, Nevada: U.S. Geological Survey Scientific Investigations Map 3193, 2 sheets.

Gates, J.S., 1987, Ground water in the Great Basin part of the Basin and Range Province, western Utah: Cenozoic geology of western Utah—Site for precious metal and hydrocarbon accumulations: Utah Geological Association Publication 16, p. 75–89.

Gates, J.S., and Kruer, S.A., 1981, Hydrologic reconnaissance of the southern Great Salt Lake Desert and summary of the hydrology of west-central Utah: Utah Department of Natural Resources Technical Publication No. 71, 55 p.

Gelhar, L.W., Welty, C., and Rehfeldt, K.W., 1992, A critical review of data on field-scale dispersion in aquifers: Water Resources Research, v. 28, p. 1955–1974.

Gilliam, T.M., and Morgan, I.L., 1987, Shale: Measurement of thermal properties: Oak Ridge National Laboratory TM-10499, 139 p., accessed on June 29, 2012 at *http://web.ornl.gov/info/reports/1987/3445602782148.pdf*.

Halford, K.J., and Plume, R.W., 2011, Potential effects of groundwater pumping on water levels, phreatophytes, and spring discharges in Spring and Snake Valleys, White Pine County, Nevada, and adjacent areas in Nevada and Utah: U.S. Geological Survey Scientific Investigations Report 2011-5032, 52 p.

Harbaugh, A.W., Banta, E.R., Hill, M.C., and McDonald, M.G., 2000, MODFLOW-2000, the U.S. Geological Survey modular ground-water model—User guide to modularization concepts and the ground-water flow process: U.S. Geological Survey Open-File Report 00-92, 121 p.

Harrill, J.R., and Bedinger, M.S., 2004, Estimated model boundary flows, appendix 2 *of* Belcher, W.R., ed., Death Valley regional ground-water flow system, Nevada and California—Hydrologic framework and transient ground-water flow model: U.S. Geological Survey Scientific Investigations Report 2004-5205, p. 376–408.

Harrill, J.R., Gates, J.S., and Thomas, J.M., 1988, Major ground-water flow systems in the Great Basin region of Nevada, Utah, and adjacent states: U.S. Geological Survey Hydrologic Investigations Atlas HA-694-C, 2 sheets, scale 1:1,000,000.

Harrill, J.R., and Prudic, D.E., 1998, Aquifer systems in the Great Basin region of Nevada, Utah, and adjacent states—Summary report: U.S. Geological Survey Professional Paper 1409-A, 66 p.

Heilweil, V.M., and Brooks, L.E., eds., 2011, Conceptual model of the Great Basin carbonate and alluvial aquifer system: U.S. Geological Survey Scientific Investigations Report 2010-5193, 191 p.

Heilweil, V.M., Healy, R.W., and Harris, R.N., 2012, Noble gases and coupled heat/fluid modeling for evaluating hydrogeologic conditions of volcanic island aquifers: Journal of Hydrology, v. 464–465, p. 309–327.

Heilweil, V.M., Sweetkind, D.S., and Susong, D.D., 2011, Introduction, chap. A *of* Heilweil, V.M., and Brooks, L.E., eds., Conceptual model of the Great Basin carbonate and alluvial aquifer system: U.S. Geological Survey Scientific Investigations Report 2010-5193, p. 3–14.

Hevesi, J.A., Flint, A.L., and Flint, L.E., 2003, Simulation of net infiltration and potential recharge using a distributed-parameter watershed model of the Death Valley region, Nevada and California: U.S. Geological Survey Water-Resources Investigations Report 03-4090, 161 p.

Hill, M.C., 1998, Methods and guidelines for effective model calibration: U.S. Geological Survey Water-Resources Investigations Report 03-4090, 90 p.

Hill, M.C., Banta, E.R., Harbaugh, A.W., and Anderman, E.R., 2000, MODFLOW-2000, the U.S. Geological Survey modular ground-water model—User guide to the observation, sensitivity, and parameter-estimation processes and three post-processing programs: U.S. Geological Survey Open-File Report 00-184, 209 p.

Hill, M.C., and Tiedeman, C.R., 2007, Effective groundwater model calibration with analysis of data, sensitivities, predictions, and uncertainty: Hoboken, New Jersey, John Wiley and Sons, Inc., 455 p.

Hintze, L.F., Willis, G.C., Laes, D.Y.M., Sprinkel, D.A., and Brown, K.D., 2000, Digital geologic map of Utah: Utah Geological Survey Map 179 DM, CD-ROM, scale 1:500,000.

Holmes, W.F., 1984, Ground-water hydrology and the projected effects of ground-water withdrawals in the Sevier Desert, Utah: State of Utah Department of Natural Resources Technical Publication 79, 54 p.

Hood, J.W., and Rush, F.E., 1965, Water-resources appraisal of the Snake Valley area, Utah and Nevada: Nevada Department of Conservation and Natural Resources Water Resources Reconnaissance Report 34, 43 p.

Kirby, S., and Hurlow, H., 2005, Hydrogeologic setting of the Snake Valley hydrologic basin, Millard County, Utah, and White Pine and Lincoln Counties, Nevada—Implications for possible effects of proposed water wells: Utah Geological Survey Report of Investigation 254, 22 p.

Lachenbruch, A.J., and Sass, J.H., 1977, Heat flow in the United States and the thermal regime of the crust, *in* Heacock, J.G., ed., The Earth's crust, its nature and physical properties: Geophysical Monograph 20, Washington, D.C., American Geophysical Union, p. 626–675.

Lachenbruch, A.J., and Sass, J.H., 1978, Models of extending lithosphere and heat flow in the Basin and Range province, *in* Smith, R.B., and Eaton, G.P., eds., Cenozoic tectonics and regional geophysics of the western Cordillera: Geological Society of America Memoir 152, p. 209–250.

Langevin, C.D., Thorne, D.T., Dausman, A.M., Sukop, M.C., and Guo, Weixing, 2008, SEAWAT Version 4: A computer program for simulation of multi-species solute and heat transport: U.S. Geological Survey Techniques and Methods 6-A22, 39 p.

Leake, S.A., 2011, Capture—Rates and directions of groundwater flow don't matter!: Ground Water, v. 49, p. 456–458.

Leavesley, G.H., Lichty, R.W., Troutman, B.M., and Saindon, L.G., 1983, Precipitation-runoff modeling system: User's manual: U.S. Geological Survey Water-Resources Investigations Report 83-4238, 207 p.

Ludington, Steve, Cox, D.P., Leonard, K.R., and Moring, B.C., 1996, Cenozoic volcanic geology of Nevada, chap. 5 *of* Singer, D.A., ed., An analysis of Nevada's metal-bearing mineral resources: Nevada Bureau of Mines and Geology Open-File Report 96-2, 10 p.

Manning, A.H., and Solomon, D.K., 2005, An integrated environmental tracer approach to characterizing groundwater circulation in a mountain block: Water Resources Research, v. 41, W12412, doi: 10.1029/2005WR004178.

Masbruch, M.D., 2011a, Current study groundwater recharge estimates for predevelopment conditions and ranges of previously reported estimates of groundwater recharge for each hydrographic area within the Great Basin carbonate and alluvial aquifer system study area, appendix 4 *of* Heilweil, V.M., and Brooks, L.E., eds., Conceptual model of the Great Basin carbonate and alluvial aquifer system: U.S. Geological Survey Scientific Investigations Report 2010-5193, p. 165–170.

Masbruch, M.D., 2011b, Comparison of predevelopment and recent (2000) groundwater budget estimates for each hydrographic area within the Great Basin carbonate and alluvial aquifer system study area, appendix 7 *of* Heilweil, V.M., and Brooks, L.E., eds., Conceptual model of the Great Basin carbonate and alluvial aquifer system: U.S. Geological Survey Scientific Investigations Report 2010-5193, p. 181–186.

Masbruch, M.D., 2011c, Current study groundwater discharge estimates for predevelopment conditions and ranges of previously reported estimates of groundwater discharge for each hydrographic area within the Great Basin carbonate and alluvial aquifer system study area, appendix 5 *of* Heilweil, V.M., and Brooks, L.E., eds., Conceptual model of the Great Basin carbonate and alluvial aquifer system: U.S. Geological Survey Scientific Investigations Report 2010-5193, p. 171–176.

Masbruch, M.D., Heilweil, V.M., Buto, S.G., Brooks, L.E., Susong, D.D., Flint, A.L., Flint, L.E., and Gardner, P.M., 2011, Estimated groundwater budgets, chap. D *of* Heilweil, V.M., and Brooks, L.E., eds., Conceptual model of the Great Basin carbonate and alluvial aquifer system: U.S. Geological Survey Scientific Investigations Report 2010-5193, p. 73–125.

Mathey, S.B., ed., 1998, National Water Information System (NWIS): U.S. Geological Survey Fact Sheet 027-98, 2 p.

Maxey, G.B., and Eakin, T.E., 1949, Ground water in White River Valley, White Pine, Nye, and Lincoln Counties, Nevada: Nevada Office of the State Engineer Water Resources Bulletin no. 8, 59 p.

McDonald, M.G., and Harbaugh, A.W., 1988, A modular three-dimensional finite-difference ground-water flow model: U.S. Geological Survey Techniques of Water-Resources Investigations 6-A1, variously paged.

Mehl, S.W., and Hill, M.C., 2006, MODFLOW-2005, the U.S. Geological Survey modular ground-water model—Documentation of shared node local grid refinement (LGR) and the boundary flow and head (BFH) package: U.S. Geological Survey Techniques and Methods 6-A12, 68 p.

Moreo, M.T., Laczniak, R.J., and Stannard, D.I., 2007, Evapotranspiration rate measurements of vegetation typical of ground-water discharge areas in the Basin and Range carbonate-rock aquifer system, Nevada and Utah, September 2005–August 2006: U.S. Geological Survey Scientific Investigations Report 2007-5078, 36 p.

Nichols, W.D., 2000, Regional ground-water evapotranspiration and ground-water budgets, Great Basin, Nevada, chap. C. *of* Regional ground-water budgets and ground-water flow, eastern Nevada: U.S. Geological Survey Professional Paper 1628, 82 p.

Pavelko, M.T., 2007, Spring database for the Basin and Range carbonate-rock aquifer system, White Pine County, Nevada, and adjacent areas in Nevada and Utah: U.S. Geological Survey Data Series 272, 10 p.

Plume, R.W., and Carlton, S.M., 1988, Hydrogeology of the Great Basin region of Nevada, Utah, and adjacent states: U.S. Geological Survey Hydrologic Investigations Atlas HA-694-A, 1 sheet, scale 1:1,000,000.

Poeter, E.P., Hill, M.C., Banta, E.R., Mehl, Steffen, and Christensen, Steen, 2005, UCODE_2005 and six other computer codes for universal sensitivity analysis, calibration, and uncertainty evaluation: U.S. Geological Survey Techniques and Methods 6-A11, 283 p.

Prudic, D.E., Harrill, J.R., and Burbey, T.J., 1995, Conceptual evaluation of regional ground-water flow in the carbonate rock province of the Great Basin, Nevada, Utah, and adjacent states: U.S. Geological Survey Professional Paper 1409-D, 102 p.

Rush, F.E., and Kazmi, S.A.T., 1965, Water resources appraisal of Spring Valley, White Pine and Lincoln Counties, Nevada: State of Nevada Department of Conservation and Natural Resources Water Resources Reconnaissance Report 33, 36 p.

San Juan, C.A., Belcher, W.R., Laczniak, R.J., and Putnam, H.M., 2010, Hydrologic components for model development, chap. C *of* Belcher, W.R., ed., Death Valley regional ground-water flow system, Nevada and California—Hydrogeologic framework and transient ground-water flow model: U.S. Geological Survey Professional Paper 1711, p. 99–132.

Sass, J.H., Lachenbruch, A.H., Munroe, R.J., Greene, G.W., and Moses, T.H., 1971, Heat flow in the western United States: Journal of Geophysical Research, v. 76, p. 6376–6412.

Scott, B.R., Smales, T.J., Rush, F.E., and Van Denburgh, A.S., 1971, Water for Nevada: Nevada Department of Conservation and Natural Resources Water Planning Report No. 3, 87 p.

Smith, J.L., Laczniak, R.J., Moreo, M.T., and Welborn, T.L., 2007, Mapping evapotranspiration units in the Basin and Range carbonate-rock aquifer system, White Pine County, Nevada, and adjacent areas in Nevada and Utah: U.S. Geological Survey Scientific Investigations Report 2007-5087, 20 p.

Smith, Leslie, and Chapman, D.S., 1983, On the thermal effects of groundwater flow systems: 1. Regional scale systems: Journal of Geophysical Research, v. 88, p. 593–608.

Southern Methodist University Geothermal Laboratory, 2011, The geothermal map of North America, 2011 update, accessed on May 21, 2012, at *http://www.smu.edu/Dedman/Academics/Programs/GeothermalLab.*

Southern Nevada Water Authority (SNWA), 2011, Southern Nevada Water Authority Clark, Lincoln, and White Pine Counties groundwater development project conceptual plan of development, 152 p., accessed on July 31, 2012, at *http://www.snwa.com/assets/pdf/ws_gdp_copd.pdf*.

Stephens, J.C., 1974, Hydrologic reconnaissance of the Wah Wah Valley drainage basin, Millard and Beaver Counties, Utah: Utah Department of Natural Resources Technical Publication No. 47, 53 p.

Stephens, J.C., 1976, Hydrologic reconnaissance of the Pine Valley drainage basin, Millard, Beaver, and Iron Counties, Utah: Utah Department of Natural Resources Technical Publication No. 51, 38 p.

Stephens, J.C., 1977, Hydrologic reconnaissance of the Tule Valley drainage basin, Juab and Millard Counties, Utah: Utah Department of Natural Resources Technical Publication No. 56, 37 p.

Stephens, J.C., and Sumsion, C.T., 1978, Hydrologic reconnaissance of the Dugway Valley-Government Creek area, west-central Utah: Utah Department of Natural Resources Technical Publication No. 59, 1978, 42 p.

Stonestrom, D.A., Prudic, D.E., Laczniak, R.J., Akstin, K.C., Boyd, R.A., and Henkelman, K.K., 2003, Estimates of deep percolation beneath native vegetation, irrigated fields, and the Amargosa River channel, Amargosa Desert, Nye County, Nevada: U.S. Geological Survey Open-File Report 03-104, 88 p.

Susong, D.D., 1995, Water budget and simulation of one-dimensional unsaturated flow for a flood- and sprinkler-irrigated field near Milford, Utah: U.S. Geological Survey Water-Resources Investigations Report 95-4072, 32 p.

Sweetkind, D.S., Cederberg, J.R., Masbruch, M.D., and Buto, S.G., 2011a, Hydrogeologic framework, chap. B *of* Heilweil, V.M., and Brooks, L.E., eds., Conceptual model of the Great Basin carbonate and alluvial aquifer system: U.S. Geological Survey Scientific Investigations Report 2010-5193, p. 15–50.

Sweetkind, D.S., Masbruch, M.D., Heilweil, V.M., and Buto, S.G., 2011b, Groundwater flow, chap. C *of* Heilweil, V.M., and Brooks, L.E., eds., Conceptual model of the Great Basin carbonate and alluvial aquifer system: U.S. Geological Survey Scientific Investigations Report 2010-5193, p. 51–72.

Thomas, J.M., Mason, J.L., and Crabtree, J.D., 1986, Groundwater levels in the Great Basin region of Nevada, Utah, and adjacent states: U.S. Geological Survey Hydrologic Investigations Atlas HA-694-B, 2 sheets, scale 1:1,000,000.

Thomas, J.M., Welch, A.H., and Dettinger, M.D., 1996, Geochemistry and isotope hydrology of representative aquifers in the Great Basin region of Nevada, Utah, and adjacent states: U.S. Geological Survey Professional Paper 1409-C, 100 p.

Tonkin, M.J., Tiedeman, C.R., Ely, D.M., and Hill, M.C., 2007, OPR-PPR, a computer program for assessing data importance to model predictions using linear statistics: U.S. Geological Survey Techniques and Methods Report TM-6E2, 115 p.

U.S. Geological Survey EROS Data Center, 1999, 1 arc-second (30-meter) National Elevation Dataset: U.S. Geological Survey dataset, accessed on September 15, 2008, at *http://ned.usgs.gov/*.

Utah Geological Survey, 2009, Snake Valley ground-water monitoring-well project: Snake Valley and adjacent areas, accessed on August 6, 2012, at *http://geology.utah.gov/esp/snake_valley_project/index.htm*.

Welborn, T.L., and Moreo, M.T., 2007, Irrigated acreage within the Basin and Range carbonate-rock aquifer system, White Pine County, Nevada, and adjacent areas in Nevada and Utah: U.S. Geological Survey Data Series 273, 18 p.

Welch, A.H., Bright, D.J., and Knochenmus, L.A., eds., 2007, Water resources of the Basin and Range carbonate-rock aquifer system, White Pine County, Nevada, and adjacent areas in Nevada and Utah: U.S. Geological Survey Scientific Investigations Report 2007-5261, 96 p.

Wilberg, D.E., 1991, Hydrologic reconnaissance of the Sevier Lake area, west-central Utah: Utah Department of Natural Resources Technical Publication No. 96, 51 p.

Wilkowske, C.D., Allen, D.V., and Phillips, J.V., 2003, Drought conditions in Utah during 1999–2002: A historical perspective: U.S. Geological Survey Fact Sheet 037-03, 6 p.

Woodbury, A.D., and Smith, Leslie, 1988, Simultaneous inversion of hydrogeologic and thermal data: 2. Incorporation of thermal data: Water Resources Research, v. 24, p. 356–372.

Zheng, Chunmiao, 2010, MT3DMS v 5.3: Supplemental user's guide: U.S. Army Engineer Research and Development Center Technical Report, 51 p.

Zheng, Chunmiao, and Bennett, G.D., 2002, Dispersive transport and mass transfer, chap. 3 *of* Applied contaminant transport modeling (2): New York, John Wiley and Sons, Inc., p. 34–77.

Zheng, Chunmiao, and Wang, P.P., 1999, MT3DMS: A modular three-dimensional multispecies transport model for simulation of advection, dispersion, and chemical reactions of contaminants in groundwater systems; documentation and user's guide: U.S. Army Engineer Research and Development Center Contract Report SERDP-99-1, 169 p.

Zhu, Jianting, Young, M.H., and Cablk, M.E., 2007, Uncertainty analysis of estimates of ground-water discharge by evapotranspiration for the BARCAS study area: Desert Research Institute, Division of Hydrologic Sciences Publication No. 41234, 28 p.

Appendix 1. Equations and Calculations of Thermal Properties Used for Model Input

Introduction

Input of thermal properties into the transport model code MT3DMS (Zheng and Wang, 1999) is done through arrays that represent each model layer. Because a model cell may contain multiple hydrogeologic units (HGUs) with differing properties of porosity and thermal conductivity, a system of thickness-weighted mean equations were developed to calculate arrays on a layer by layer basis. This appendix presents these equations.

Porosity

Porosity is entered into the Basic Transport Package of MT3DMS in arrays that represent each model layer (Zheng and Wang, 1999). It was assumed that the UBFAU, LBFAU, and VU have a porosity of 0.3 (middle of range of porosities for sediments and basalts reported in Domenico and Schwartz, 1998); the UCAU and LCAU have a porosity of 0.1 on the basis of the reported range for carbonates in the Great Basin (Harrill and Prudic, 1998); and that the USCU and NCCU have a porosity of 0.01 on the basis of a model using similar rock types (Manning and Solomon, 2005). Because a model cell may contain multiple HGUs, the porosity was calculated using a thickness-weighted mean for each HGU within the cell using the following equation:

$$por_n = \left[0.3\left(\frac{thk_{UBFAU_n} + thk_{LBFAU_n} + thk_{VU_n}}{dz_n}\right)\right] + \left[0.1\left(\frac{thk_{UCAU_n} + thk_{LCAU_n}}{dz_n}\right)\right] + \left[0.01\left(\frac{thk_{USCU_n} + thk_{NCCU_n}}{dz_n}\right)\right] \quad (1)$$

where

por_n is the total porosity for layer n of the model cell,
n is the layer number,
thk_{UBFAU_n} is the thickness of the UBFAU in layer n, in meters
thk_{LBFAU_n} is the thickness of the LBFAU in layer n, in meters
thk_{VU_n} is the thickness of the VU in layer n, in meters
dz_n is the thickness of layer n, in meters
thk_{UCAU_n} is the thickness of the UCAU in layer n, in meters
thk_{LCAU_n} is the thickness of the LCAU in layer n, in meters
thk_{USCU_n} is the thickness of the USCU in layer n, in meters, and
thk_{NCCU_n} is the thickness of the NCCU in layer n, in meters.

Thermal Conductivity and Thermal Diffusivity

Bulk thermal conductivity incorporates both the thermal conductivity of the aquifer solids, as well as the thermal conductivity of the fluid (groundwater) and is needed to calculate the thermal diffusivity, which accounts for the heat transport process of conduction. The thermal conductivity of the aquifer solids was measured at the University of Utah thermal laboratory (contact: David Chapman) from several rock cuttings from wells drilled in the study area. Summary statistics for these measurements are given in table A1-1. The measured samples did not include cuttings from the VU and USCU, or cuttings from NCCU zones 2 and 3, which are significantly different in lithology from the quartzites of NCCU zone 1 (Sweetkind and others, 2011a). It was assumed that the VU had the same aquifer solids thermal conductivity as the UBFAU and LBFAU (Clauser and Huenges, 1995). Thermal conductivity for the USCU was assumed to be 1.35 watts per meter per degree Kelvin ($Wm^{-1}K^{-1}$), which was the average of the range reported for shales in Gilliam and Morgan (1987).

Table A1-1. Summary statistics for measured aquifer solids thermal conductivity samples from the Snake Valley study area, Utah and Nevada.

[Thermal conductivity values are in units of watts per meter per Kelvin. **Abbreviations:** LBFAU, lower basin-fill aquifer unit; LCAU, lower carbonate aquifer unit; NCCU, non-carbonate confining unit; UBFAU, upper basin-fill aquifer unit; UCAU, upper carbonate aquifer unit]

Lithology	Hydrogeologic unit abbreviation	Number of samples	Thermal conductivity	
			Mean	Standard deviation
Basin-fill sediments	UBFAU, LBFAU	45	3.88	0.67
Carbonate rocks	UCAU, LCAU	16	4.36	0.60
Quartzite	NCCU (zone 1)	8	5.09	0.74

Thermal conductivity for NCCU zones 2 and 3 was assumed to be 3.00 $Wm^{-1}K^{-1}$, which was the average of the range reported for "poor in quartzite" metamorphic rocks in Clauser and Huenges (1995).

Similar to porosity, a cell may contain multiple HGUs that can have different aquifer solids thermal conductivities. The solid thermal conductivity for each cell per layer was calculated as a thickness-weighted mean by the following equation:

$$k_{Tsolid_n} = \left[k_{Tsed} \left(\frac{thk_{UBFAU_n} + thk_{LBFAU_n} + thk_{VU_n}}{dz_n} \right) \right] + \left[k_{Tcarb} \left(\frac{thk_{UCAU_n} + thk_{LCAU_n}}{dz_n} \right) \right] + \left[k_{Tshale} \left(\frac{thk_{USCU_n}}{dz_n} \right) \right] + \left[k_{Tmeta} \left(\frac{thk_{NCCU_n}}{dz_n} \right) \right] \quad (2)$$

where

k_{Tsolid_n} is the total aquifer solids thermal conductivity for layer n of the model cell, in $Wm^{-1}K^{-1}$,

n is the layer number,

k_{Tsed} is the aquifer solids thermal conductivity for the UBFAU, LBFAU, and VU (basin-fill sediments and volcanics), specified as a constant value of 3.88 $Wm^{-1}K^{-1}$,

thk_{UBFAU_n} is the thickness of the UBFAU in layer n, in meters,

thk_{LBFAU_n} is the thickness of the LBFAU in layer n, in meters,

thk_{VU_n} is the thickness of the VU in layer n, in meters,

dz_n is the thickness of layer n, in meters,

k_{Tcarb} is the aquifer solids thermal conductivity for both the UCAU and LCAU (carbonate rocks), specified as a constant value of 4.36 $Wm^{-1}K^{-1}$,

thk_{UCAU_n} is the thickness of the UCAU in layer n, in meters,

thk_{LCAU_n} is the thickness of the LCAU in layer n, in meters,

k_{Tshale} is the aquifer solids thermal conductivity for the USCU (shale), specified as a constant value of 1.35 $Wm^{-1}K^{-1}$,

thk_{USCU_n} is the thickness of the USCU in layer n, in meters,

k_{Tmeta} is the aquifer solids thermal conductivity for the NCCU (metamorphic rocks), specified as a constant value of 5.09 $Wm^{-1}K^{-1}$ for NCCU zone 1, and 3.00 $Wm^{-1}K^{-1}$ for NCCU zones 2 and 3, and

thk_{NCCU_n} is the thickness of the NCCU in layer n, in meters.

The bulk thermal conductivity for each layer is then calculated using the following equation:

$$k_{Tbulk_n} = k_{Tfluid}^{(por_n)} k_{Tsolid_n}^{(1-por_n)} \quad (3)$$

where

k_{Tbulk_n} is the bulk thermal conductivity of the aquifer for layer *n* of the model, in $Wm^{-1}K^{-1}$,

n is the layer number,

k_{Tfluid} is the thermal conductivity of the fluid (groundwater), specified as a constant value of 0.6 $Wm^{-1}K^{-1}$,

por_n is the total porosity for layer *n* of the model cell, and

k_{Tsolid_n} is the total aquifer solids thermal conductivity for layer *n* of the model cell, in $Wm^{-1}K^{-1}$.

Because the thermal diffusivity is entered into MT3DMS in arrays that represent each model layer (Zheng and Wang, 1999), and is dependent on both the bulk thermal conductivity and porosity, it is calculated using the following equation (Langevin and others, 2008):

$$Dmcoef_n = \frac{k_{Tbulk_n}}{por_n \rho_f c_{Pfluid}} \quad (4)$$

where

$Dmcoef_n$ is the thermal diffusivity for layer *n* of the model cell, in square meters per second (m^2/s),

n is the layer number,

k_{Tbulk_n} is the bulk thermal conductivity of the aquifer for layer *n* of the model, in $Wm^{-1}K^{-1}$,

por_n is the total porosity for layer *n* of the model cell,

ρ_f is the density of the fluid (groundwater), specified as a constant value of 1,000 kilograms per cubic meter (kg/m^3); although the density of water is temperature dependent, it would only vary up to 4 percent over the expected range of temperatures, and

c_{Pfluid} is the heat capacity of the fluid (groundwater), specified as a constant value of 4,186 Joules per kilogram Kelvin (J/kgK).

Bulk Density and Thermal Distribution Factor

Because the bulk density is entered into the Chemical Reaction Package of MT3DMS in arrays that represent each model layer (Zheng and Wang, 1999) and is dependent on porosity, the bulk density for each cell per layer was calculated using the following equation:

$$\rho_{bn} = \rho_s (1 - por_n) \quad (5)$$

where

ρ_{bn} is the bulk density for layer n of the model cell, in kg/m^3,

n is the layer number,

ρ_s is the density of the aquifer solids, specified as a constant value of 2,700 kg/m^3 in this simulation (average of densities of representative rock types reported in Langevin and others, 2008), and

por_n is the total porosity for layer n of the model cell.

The thermal distribution factor, which is also input to the Chemical Reaction Package in MT3DMS (Zheng and Wang, 1999) was calculated using the following equation (Langevin and others, 2008):

$$K_{d\_temp} = \frac{c_{Psolid}}{\rho_f c_{Pfluid}} \quad (6)$$

where

K_{d_temp} is the thermal distribution factor of the model cell, in cubic meters per kilogram (m^3/kg),

c_{Psolid} is the specific heat capacity of the aquifer solids, and is specified as a constant value of 840 J/kgK (Langevin and others, 2008),

ρ_f is fluid (groundwater) density, and is specified as a constant value of 1,000 kg/m^3, and

c_{Pfluid} is the specific heat capacity of the fluid (groundwater), and is specified as a constant value of 4,186 J/kgK.

Consequently, the thermal distribution factor is equal to 0.0002 m^3/kg for all cells in the model.

Appendix 2. Water-Level Observation Uncertainty Calculations

Introduction

The uncertainty determined for each water-level observation includes uncertainties related to errors in the well altitude and location, water-level measurement error, nonsimulated transient error, and model discretization. The error for each of these components presented in this appendix was calculated following the procedure outlined by San Juan and others (2010) and Faunt and others (2010).

Well Altitude Error

The well altitude error was computed from the altitude accuracy code given for each well in the USGS National Water Information System (NWIS) database. The altitude accuracy code is generally expressed as a plus or minus range related to the method by which the land-surface altitude is determined. In the study area, this ranges between plus or minus 0.003 meter(s) (m) for high-precision methods, such as differential global positioning system (GPS) surveys, and plus or minus 15 m for estimates determined from topographic maps having large (100 ft) contour intervals. The range defined by the altitude accuracy code is assumed to represent, with 95-percent confidence, the true well altitude uncertainty. Assuming that the water-level observation represents the mean value and that the error is normally distributed, the uncertainty of the water-level observation, with respect to the well altitude error, can be expressed as a standard deviation by the following equation:

$$sd_1 = \frac{AAC}{2} \tag{1}$$

where

sd_1 is the standard deviation of the well altitude error, in meters, and

AAC is the value of the NWIS altitude accuracy code, in meters.

Accordingly, the standard deviation for well altitude water-level error ranges from 0.0015 m to 7.5 m in the study area.

Well Location Error

The well location error was computed as the product of the hydraulic gradient at the well and the locational uncertainty distance determined from the latitude/longitude coordinate accuracy code values given in NWIS. The latitude/longitude coordinate accuracy code is generally expressed as a plus or minus range related to the method by which the latitude/longitude is determined. In the study area this ranges between plus or minus 0.01 seconds to plus or minus 60 seconds.

The uncertainty distance based on the latitude/longitude accuracy code was calculated using the following formula (which assumes that the Earth is a perfect sphere):

$$DA = (LLAC)(30.9)\cos\left(\frac{\pi Lat}{180}\right) \tag{2}$$

where

DA is the distance accuracy, in meters,

$LLAC$ is the value of the NWIS latitude/longitude accuracy code, in seconds,

30.9 is the distance, in meters, of one second at the equator, and

$\cos\left(\frac{\pi Lat}{180}\right)$ is the cosine of the latitude (in decimal degrees) of the well.

Accordingly, the distance accuracy within the study area ranges from plus or minus 0.24 m to plus or minus 1,422 m.

The hydraulic gradient at the well was estimated from a regional potentiometric-surface map developed by Gardner and others (2011) for the study area. The gradient ranges between 0.01 percent and 1.2 percent within the study area.

To determine the well location error, the range defined by the value of the coordinate accuracy is assumed to represent, with 95-percent confidence, the true error in the water-level observation as related to well location uncertainty. Assuming that the water-level observation represents the mean value and that the error is normally distributed, the uncertainty of the water-level observation, with respect to the well location error, can be expressed as a standard deviation by the following equation:

$$sd_2 = \left(\frac{DA}{2}\right)HG \tag{3}$$

where

sd_2 is the standard deviation of the well location error, in meters,

DA is the distance accuracy, in meters, and

HG is the hydraulic gradient, in percent slope divided by 100.

Accordingly, the standard deviation for well location water-level error ranges from 0.00028 m to 0.61 m for the study area.

Measurement Error

Measurement errors result from inaccuracies in the measurement of depth to water and depend primarily on the device used to make the measurement. For the study area, a general

value of plus or minus 0.003 m was assumed to represent the measurement accuracy (Cunningham and Schalk, 2011).

To determine the measurement error, the range defined by the measurement accuracy is assumed to represent, with 95-percent confidence, the true error in the water-level observation as related to measurement uncertainty. Assuming that the water-level observation represents the mean value and the error is normally distributed, the uncertainty of the water-level observation, with respect to the measurement error, can be expressed as a standard deviation by the following equation:

$$sd_3 = \frac{MA}{2} \quad (4)$$

where

sd_3 is the standard deviation of the measurement error, in meters, and

MA is the measurement accuracy, in meters.

Accordingly, the standard deviation for the measurement water-level error is 0.0015 m for the study area.

Nonsimulated Transient Error

Nonsimulated transient errors result from uncertainty in the magnitude of water-level response caused by stresses not simulated in the groundwater model, which are typically seasonal and long-term climate changes. Seasonal fluctuations in wells in Spring and Snake Valleys with known open intervals of less than 30.5 m depth below land surface can be as high as 2.9 m, with an average of about 1 m; seasonal fluctuations in wells with known open intervals of less than 30.5 m below land surface outside these valleys only averages approximately 0.2 m. For wells with known open intervals greater than 30.5 m below land surface, average seasonal fluctuations in wells in Spring and Snake Valleys and wells outside of these valleys were 0.15 m and 0.25 m, respectively.

On the basis of the above seasonal water-level fluctuation analysis, seasonal fluctuations were assigned in the following manner:

1. For wells with known open interval depths of less than 30.5 m (about 100 ft) below land surface in Spring and Snake Valleys, seasonal fluctuations of 1 m were assigned.
2. For wells with known open interval depths of less than 30.5 m below land surface outside of Spring and Snake Valley, seasonal fluctuations of 0.2 m were assigned.
3. For wells with known open interval depths of greater than 30.5 m below land surface, an average value for seasonal fluctuations of 0.2 m was assigned for all HAs within the study area.
4. For wells with no open interval data, it was assumed that wells with a total depth of less than 45 m below land surface could possibly have open interval depths of less than 30.5 m below land surface. Wells with a total depth of more than 45 m were assumed to have open interval depths of greater than 30.5 m below land surface. Seasonal fluctuations for wells with total depths of less than 45 m and more than 45 m were assigned as above depending on their location.

On the basis of analysis of available water-level data from wells outside of pumping areas, long-term (greater than 30 years) climate response is relatively small, on average less than 1.2 m, within the study area. The potential error associated with long-term climatic response at each well was not calculated independently as very few wells have long-term water-level data. Instead, it was accounted for by adding 1 m to the seasonal fluctuation assigned to each well.

The range defined by this sum is assumed to represent, with 95-percent confidence, the true error in the water-level observation as related to nonsimulated transient uncertainty. Assuming that the water-level observation represents the mean value and the error is normally distributed, the uncertainty of the water-level observation, with respect to the nonsimulated transient error, can be expressed as a standard deviation by the following equation:

$$sd_4 = \frac{\left(SF + LTF\right)}{4} \quad (5)$$

where

sd_4 is the standard deviation of the nonsimulated transient error, in meters,

SF is the seasonal fluctuation, in meters, and

LTF is the long-term fluctuation, and is equal to 1 m.

Accordingly, the standard deviation for nonsimulated transient water-level error for wells outside of Spring and Snake Valleys is 0.3 m; the standard deviation for wells inside Spring and Snake Valleys is 0.5 m for wells having an open interval within 30.5 m of land surface, and 0.3 m for deeper wells.

Model Discretization Error

Model discretization error results from inaccuracies in the geometric representation of HGUs and major structural features in the model (Hill and Tiedeman, 2007). The magnitude of these errors is assumed to be a function of

1. Nodal width—larger widths result in a less accurate representation of the geometry of HGUs and major structural features relative to well location.
2. Hydraulic gradient—inaccurate geometric representations tend to shift the location of local hydraulic gradients.
3. Well open interval depth—there is a decrease in knowledge of HGUs and structures with depth.

Model discretization error is the product of the nodal width, hydraulic gradient, and a scalar representing the error associated with the well open interval depth. The nodal width used in the model is 804.65 m (0.5 mi). The hydraulic gradient at the well was estimated from a regional potentiometric-surface map developed for the study area (Gardner and others, 2011), and ranges between 0.01 percent and 1.2 percent. The

potential error attributed to a decrease in geologic certainty with depth is calculated using a scalar that is a function of the well open interval depth. The scalar is calculated as 2 plus the quotient of the depth of the top of the open interval and the approximate thickness of the aquifer material in the model (assumed to be 1,450 m on the basis of the average thickness of basin fill, and volcanic and Paleozoic carbonate rocks in the model).

The range defined by this product is assumed to represent, with 95-percent confidence, the true error in the water-level observation as related to model discretization error. Assuming that the water-level observation represents the mean value and the error is normally distributed, the uncertainty of the water-level observation, with respect to model discretization error, can be expressed as a standard deviation by the following equation:

$$sd_5 = \frac{(NW)(HG)\left[\frac{TOPUPOPEN}{MT} + 2\right]}{4} \qquad (6)$$

where

sd_5 is the standard deviation of the model discretization error, in meters,

NW is the nodal width, and is equal to 804.65 m,

HG is the hydraulic gradient, in percent slope divided by 100,

$TOPUPOPEN$ is the top of the upper well opening, in meters below land surface, and

MT is the approximate thickness of aquifer material in the model, specified as 1,450 m for this study.

Accordingly, the standard deviation for the model discretization water-level error ranges from 0.045 m to 5.5 m for the study area.

Total Water-Level Observation Error

The total uncertainty associated with each water-level observation is the composite of all errors contributed by the different components. This uncertainty can be expressed as a standard deviation by the following equation:

$$sd_h = \sqrt{\left(sd_1^2 + sd_2^2 + sd_3^2 + sd_4^2 + sd_5^2\right)} \qquad (7)$$

where

sd_h is the total standard deviation for each water-level observation, in meters,

sd_1 is the standard deviation of the well altitude error, in meters,

sd_2 is the standard deviation of the well location error, in meters,

sd_3 is the standard deviation of the measurement error, in meters,

sd_4 is the standard deviation of the nonsimulated transient error, in meters, and

sd_5 is the standard deviation of the model discretization error.

Accordingly, the total standard deviations of water-level observations range from 1.2 m to 7.7 m, and average 2.3 m.

Appendix 3. Groundwater Temperature Observation Uncertainty Calculations

Introduction

The uncertainty determined for each temperature observation includes uncertainties related to errors in the temperature measurement error and model vertical discretization error, and are discussed below.

Measurement Error

Measurement errors result from inaccuracies in the measurement of temperature and depend primarily on the device used to make the measurement. For the temperatures measured in the Utah Geological Survey (UGS) wells, the instrument used had a measurement precision of 0.01 °C (Blackett, 2011). For spring temperature data reported in NWIS, it was assumed that these measurements had a precision of 0.5 °C.

To determine the measurement error, the range defined by the measurement accuracy is assumed to represent, with 95-percent confidence, the true error in the temperature as related to measurement uncertainty. Assuming that the temperature represents the mean value and that the error is normally distributed, the uncertainty of the temperature, with respect to the measurement error, can be expressed as a standard deviation by the following equation:

$$sd_1 = \frac{MA}{2} \quad (1)$$

where

sd_1 is the standard deviation of the measurement error, in °C, and

MA is the measurement accuracy, and is equal to either 0.01 °C or 0.5 °C.

Accordingly, the standard deviation for the measurement error is 0.005 °C for groundwater temperatures measured in wells in the study area, and 0.25 °C for temperatures measured in springs in the study area.

Model Vertical Discretization Error

Model vertical discretization error results from model layer thickness discretization. The magnitude of this error is assumed to be a function of model layer thickness and the thermal gradient (temperature vs. depth) within each layer.

For UGS wells (except for those adjacent to springs) penetrating the entire model layer, the model discretization error was calculated as the standard deviation of all temperature measurements made within that layer.

For UGS wells that do not penetrate the entire layer, including those adjacent to springs, the gradient across the entire layer could not be accounted for, and the following assumptions were made:

1. For wells that reach the middle of the layer and are not adjacent to a spring, the thermal gradient for the upper part of the layer was assumed to extend to the bottom of the layer.
2. For wells that do not reach the middle of the layer and are not adjacent to a spring, the thermal gradient was assumed to be the same as the thermal gradient for the layer above.
3. For wells that are adjacent to springs, because the thermal gradient changes dramatically across the depth of the well, the gradient was calculated using the highest and lowest temperature measurements within the well.

The model vertical discretization error for these wells is calculated as the product of the layer thickness and the thermal gradient across the layer. The range defined by this product is assumed to represent, with 95-percent confidence, the true error in the temperature observation as related to model vertical discretization error. Assuming that the temperature observation represents the mean value and the error is normally distributed, the uncertainty of the temperature observation, with respect to model vertical discretization error, can be expressed as a standard deviation by the following equation:

$$sd_2 = \frac{(dz)(gradT)}{4} \quad (2)$$

where

sd_2 is the standard deviation of the model vertical discretization error, in °C,

dz is the layer thickness, in meters, and

$gradT$ is the thermal gradient across the layer, in °C per meter.

For spring temperature data from the NWIS database, the model vertical discretization error was calculated as follows:

1. For Dearden Spring Group, and Clay, Unnamed, and Big Springs, the error was calculated as the mean of the error calculated for UGS wells SG24C and SG25C (Blackett, 2011), which were assumed to be representative of thermal gradients at cold springs within the study area.
2. For Gandy Warm Springs, the error was assumed to be the same as the error calculated for UGS well SG21C (Blackett, 2011) as this site was assumed to be most representative of thermal gradients at warm springs within the study area.

Accordingly, the standard deviation for the model vertical discretization error ranges from 0.0039 to 1.8 °C within the study area.

Total Temperature Observation Error

The total uncertainty associated with each temperature observation is the composite of all errors contributed by the different components. This uncertainty can be expressed as a standard deviation by the following equation:

$$sd_T = \sqrt{\left(sd_1^2 + sd_2^2\right)} \tag{3}$$

where

sd_T is the total standard deviation for each temperature observation, in °C,

sd_1 is the standard deviation of the measurement error, in °C, and

sd_2 is the standard deviation of the model vertical discretization error, in °C.

Accordingly, the total standard deviations of temperature observations range from 0.0064 °C to 1.8 °C.

ISSN 2328-0328 (online)
http://dx.doi.org/10.3133/sir20145103